Viruses of hyperthermophilic archaea : entry and egress from the host cell

Emmanuelle Quemin

Université Pierre et Marie Curie – Paris VI
Ecole doctorale Complexité du Vivant ED515
7, quai Saint-Bernard, case 32
75252 Paris Cedex 05

Unité de Biologie Moléculaire du Gène chez les Extrêmophiles
Département de Microbiologie - Institut Pasteur
25, rue du Dr. Roux
75015 Paris

THESE DE DOCTORAT DE L'UNIVERSITE PIERRE ET MARIE CURIE
Spécialité : *Microbiologie*

Pour obtenir le grade de
DOCTEUR DE L'UNIVERSITE PIERRE ET MARIE CURIE

VIRUSES OF HYPERTHERMOPHILIC ARCHAEA: ENTRY INTO AND EGRESS FROM THE HOST CELL

Présentée par
M. Emmanuelle Quemin

Soutenue le 28 Septembre 2015 devant le jury composé de :

Prof. Guennadi Sezonov	*Président du jury*
Prof. Christa Schleper	*Rapporteur de thèse*
Dr. Paulo Tavares	*Rapporteur de thèse*
Dr. Claire Geslin	*Examinateur*
Dr. Jacomine Krijnse-Locker	*Examinateur*
Dr. David Prangishvili	*Directeur de thèse*
Dr. Mart Krupovic	*Superviseur de thèse*

VIRUSES OF HYPERTHERMOPHILIC ARCHAEA: ENTRY INTO AND EGRESS FROM THE HOST CELL

A mes parents,

A ma grand-mère,

Viruses Of Hyperthermophilic Archaea: Entry Into And Egress From The Host Cell

RESUME **1**

ABSTRACT **3**
Key words 3

INTRODUCTION **9**
The third domain of life. 9
Highly diversified archaea. 11
Unique archaeal virosphere. 12
Sulfolobus, a model for hyperthermophilic archaea. 17
Cell surface characteristics. 18
Cell surface appendages. 19
Insights into the biology of hyperthermophilic archaeal viruses. 22
SSV1. 23
SIRV2. 24
Virus-host interactions in Archaea: state-of-the-art. 25

CHAPTER 1 ..... **31**
Insights into the biology of archaeal viruses by high-throughput approaches 31

CHAPTER 2 ..... **37**
Virus-host interactions in Archaea - the best is yet to come. 37

CHAPTER 3 ..... **49**
Unique spindle-shaped viruses in Archaea. 49

CHAPTER 4 ..... **57**
One update on the architecture of SSV1 virions. 57

CHAPTER 5 ..... **85**
The egress of SSV1 or how to bud from an archaeon. 85

CHAPTER 6 ..... **107**
Unravelling the early stages of SIRV2 infection. 107

DISCUSSION **119**
Successful spindle-shaped archaeal viruses. 119
Architecture of spindle-shaped virions: the case-study of SSV1. 120
SSV1 as a model for lipid-containing viruses infecting archaea. 121
SIRV2 as a model for non-enveloped viruses infecting archaea. 127
Concluding remarks and future perspectives. 130

REFERENCES **133**

ACKNOWLEDGMENTS **145**

MEMBERS OF THE JURY **147**

RESUME

Les archées sont principalement connues pour leur capacité à croître et survivre dans des conditions extrêmes de température, pression, pH, etc. qui sont hostiles à l'homme. Néanmoins, il est désormais clair que les archées sont aussi présentes de manière ubiquitaire dans divers environnements. L'étude détaillée des différents aspects de la biologie de ces microorganismes a amené à des découvertes pour le moins inattendues comme celle de la virosphère associée aux archées qui est unique. En effet, plusieurs virus infectant les archées ont été isolés et présentent une incroyable diversité tant au niveau morphologique que génomique et ne ressemblent aucunement aux virus connus de bactéries ou d'eucaryotes. Récemment, l'analyse en détails du cycle viral a mis à jour de nouveaux mécanismes d'interactions avec la cellule hôte. Au cours de mes travaux de thèse, nous nous sommes intéressés aux systèmes virus-hôtes présents dans les milieux hyperthermiques et acidophiles en sélectionnant les virus fusiforme et filamenteux SSV1 et SIRV2 en tant que modèles d'étude. Tout d'abord, nous avons défini une nouvelle classification des virus fusiformes basée sur l'analyse comparative des protéines structurales et des génomes viraux. L'ensemble des virus considérés forme un réseau global malgré le fait qu'ils ont été isolés dans des environnements distincts ; qu'ils infectent des hôtes qui sont distant phylogénétiquement parlant et que certains de leurs virions présentent une certaine pléomorphicité. Ensuite, la caractérisation en détails de l'architecture des virions fusiformes de SSV1 a révélé qu'ils étaient enveloppés, composés de protéines de capside glycosylées et contenaient le complexe nucléoprotéique. Finalement, nous nous sommes concentrés sur la manière dont les virus d'archées interagissent avec la cellule hôte. Alors que les virions de SIRV2 semblent utiliser une stratégie pour l'entrée qui est similaire aux bactériophages dits flagellotrophiques ; on observe que les virions de SSV1 emploient un mécanisme de sortie qui rappelle le bourgeonnement des virus eucaryotes enveloppés. L'ensemble de ces recherches participent à une meilleure compréhension de la biologie des archées ainsi que de leurs virus et permettent de définir des cibles intéressantes pour de futures études.

ABSTRACT

Although, archaea were initially regarded as exotic microorganisms capable of growing in conditions which are hostile to humans, it became clear that they are ubiquitous and abundant in various environments. Detailed studies focusing on different aspects of archaeal biology have led to many unexpected discoveries, including the unique virosphere associated with archaea. Indeed, highly diverse viruses characterized by uncommon virion shapes and mysterious genomic contents have been isolated that typically do not resemble viruses of either bacteria or eukaryotes. Recent analysis of the sequential events of the viral cycle resulted in major breakthroughs in the field. In the framework of my PhD studies, I have focused on two model hyperthermo-acidophilic virus-host systems, the spindle-shaped SSV1 and rod-shaped SIRV2, both infecting organisms of the genus *Sulfolobus*. Initially, we defined structure-based lineages for all known spindle-shaped viruses isolated from highly divergent hosts and residing in very different environments. Then, we provided insights into the architecture of spindle-shaped viruses by showing that SSV1 virions are composed of glycosylated structural proteins and contain a lipid envelope. Finally, we focused on virus-host interplay. Whereas SIRV2 virions appear to use a similar entry strategy as flagellotrophic bacteriophages, SSV1 virions employ an exit mechanism reminiscent of the budding of eukaryotic enveloped viruses. Collectively, these studies shed light on the biology of archaeal viruses and help to define interesting targets that should be the focus of intensive research in the next future.

Key words

archaea – hyperthermohpiles – spindle-shaped viruses – rod-shaped viruses – viral entry – viral egress.

INTRODUCTION

INTRODUCTION

The third domain of life.

The classification of living organisms into three cellular domains, namely the Bacteria, the Archaea and the Eukarya, was initially proposed by Carl R. Woese based on ribosomal RNA gene sequences (Woese and Fox, 1977). This phylogenetic approach also indicated that the third domain of life, the Archaea, could be subdivided into two kingdoms: the *Euryarchaeota* and the *Crenarchaeota* (Woese et al., 1990). Although *Euryarchaeota* encompass methanogens, extreme halophiles, thermoacidophiles and a few hyperthermophiles; *Crenarchaeota* exclusively include thermophiles and hyperthermophiles. Subsequently, the possibility to sequence uncultivated organisms by high-throughput methods led to the proposal of other phyla (Figure 1). Historically, the first additional division was called *Korarchaeota* and included a large group of deep-branching unclassified archaea. These microorganisms have been detected in several geographically isolated terrestrial or marine thermal environments and remain uncultured (Barns et al., 1994; Barns et al., 1996; Elkins et al., 2008). Members of the *Thaumarchaeota* were initially classified as mesophilic crenarchaea and later on, their ecological importance together with peculiar genomic features were recognized (Brochier-Armanet et al., 2008). Indeed, thaumarchaea are highly diversified and widely distributed in oceans and soils where they are abundant and significantly contribute to the global cycles of carbon (Thauer, 2011) and nitrogen (Pester et al., 2011). The unprecedented parasitic lifestyle of *Nanoarchaeum equitans* argued in favor of a novel and early-diverging archaeal phylum, the '*Nanoarchaeota*' (Huber et al., 2000). Alternatively, *Nanoarchaeum equitans*, the obligate symbiot of *Ignicoccus hospitalis*, might also be part of a fast-evolving lineage within the *Euryarchaeota* (Brochier et al., 2005). '*Candidatus caldiarchaeum subterraneum*' has as well been proposed to represent a separate phylum tentatively named '*Aigarchaeota*' based upon specific genomic characteristics (Nunoura et al., 2010). Interestingly, the *Thaumarachaeota*, '*Aigarchaeota*', *Crenarchaeota* and *Korarchaeota* have a common set of genes involved in cytokinesis, membrane remodeling, cell shape determination and protein recycling. The fact that these genes are also shared with eukaryotes led to the hypothesis that they are related to, and even emerged from, the so-called 'TACK' superphylum (Guy and Ettema, 2011). In-depth phylogenetic analyses and tree reconstruction even placed Eukarya as a sister group of the 'TACK' superphylum (Raymann et al., 2015). In support of this hypothesis, phylogenomic analyses of recently

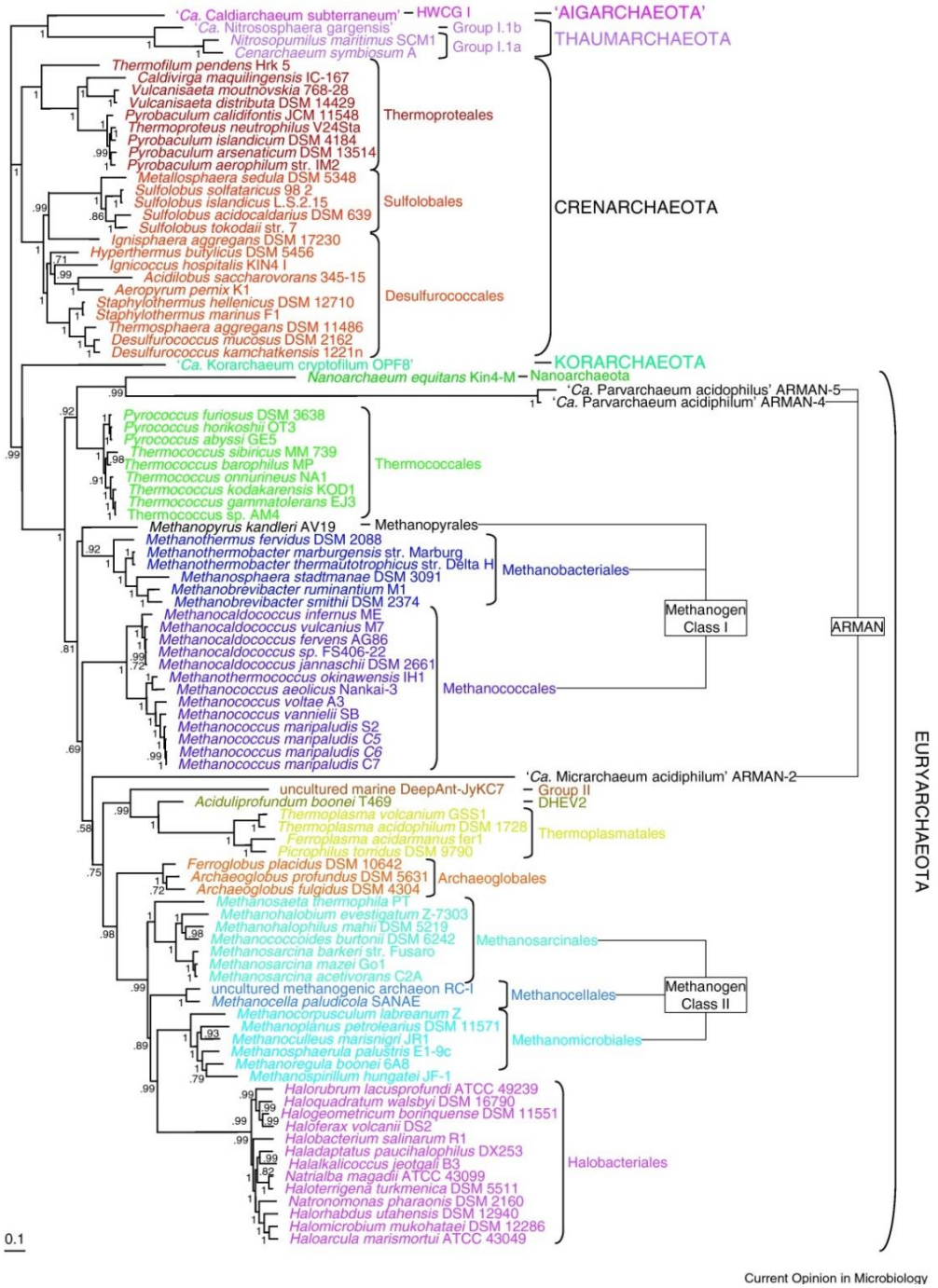

Figure 1: Unrooted Bayesian tree of the archaeal domain based on a concatenation of 57 ribosomal proteins present in at least 89 of 99 genomes (5838 unambiguously aligned amino acid positions); for details on the procedure for dataset assembly see [3•]. We used Phylobayes 3.3 [56] to recode the alignment according to the Dayhoff-6 amino acid categories and to infer a tree with the CAT+Γ model to take into account evolutionary rate site variations among sites. The scale bar indicates the average number of substitutions per site. Numbers at branches represent posterior probabilities as inferred by Phylobayes 3.3. Most relationships are well supported, but some need further investigation, in particular (i) the monophyly of Desulfurococcales, (ii) the relationships among Class I methanogens, (iii) the relationships among Class II methanogens and their link with Halobacteriales, (iv) the phylogenetic position of ARMAN (in particular the grouping of some of them with Nanoarchaeum equitans) and (v) the relationship among main archaeal phyla.

described '*Lokiarchaeota*' concluded to a common ancestry between eukaryotes and this deeply-rooting clade of the 'TACK' superphylum. The genomes reported, although only partially assembled, stem from the most abundant and uncultured organisms found in deep marine biosphere (Spang et al., 2015). Future research is likely to provide significant insights into the classification and biology of the closest relative to eukaryotes known to date.

Highly diversified archaea.

Metagenomic approaches have proven to be powerful in identifying and characterizing novel lineages of uncultivated archaea thereby increasing our comprehension of the diversity of life on our planet. Environmental surveys revealed that archaea are ubiquitous and present in almost all ecosystems examined until now including humans. Although archaea have never been shown to cause any disease, several reports described human-associated species from the gut (Miller et al., 1982), vagina (Belay et al., 1990), oral cavity (Kulik et al., 2001; Lepp et al., 2004) and skin (Probst et al., 2013). The potential activation of innate and adaptive immune systems by archaea as well as the overall impact of the human microbiome have been the focus of recent studies (Dridi et al., 2011; Bang and Schmitz, 2015). Various environments around the world have been sampled by scientists and sequences of genomes isolated from very different ecosystems are now available. The massive amount of data generated by metagenomic methods revealed that archaea are globally distributed. Prokaryotes form a significant fraction of the total biomass and in subsurface sediments archaea represent up to 87% of the biomarkers used to assess the presence of living cells (Lipp et al., 2008). In fact, the relative abundance of prokaryotes in soil and freshwater is known to vary depending on locations (Simon et al., 2000; Keough et al., 2003; Ochsenreiter et al., 2003; Tringe et al., 2005; Jorgensen et al., 2012; Jorgensen et al., 2013; Urich et al., 2014). In oceans, up to 20% of total microbiota is made of ammonia-oxidizing archaea and bacteria involved in the process of nitrification (Pester et al., 2011). Importantly, the copy number of archaeal amoA genes – encoding a subunit of the key ammonia monooxygenase enzyme – from crenarchaea was found to be 3,000 times more abundant than their bacterial homologues (Leininger et al., 2006). Activities of methanogens have been extensively investigated in deep-sea marine sediments (DeLong, 2005), hot spots of anaerobic oxidation of methane (Knittel et al., 2005), peatland ecosystems (Galand et al., 2005) or even petroleum hydrocarbon-contaminated aquifer (Kleikemper et al., 2005). Interestingly, methanogenic archaea are the only organisms capable of methanogenesis identified so far and other non-

classical energy metabolisms have been detected in metagenomes (Pester et al., 2011). Hence, members of the third domain of life significantly contribute to Nitrification and Carbon cycles (Offre et al., 2013). The predominance of archaea in marine plankton might also have a major impact in the global biogeochemistry of Earth, especially in the deep Ocean and cold marine water (DeLong et al., 1994). In addition, several species have been described as alkalophiles, acidophiles, halophiles, barophiles, hyperthermophiles or psycrophiles depending on optimal growth requirements. They are found in habitats with high or low pH, salinity close to saturation, high atmospheric pressure, and temperature above 80°C or down to -20°C. Although such ecological niches were initially regarded as sterile, they are now known to be almost exclusively inhabited by archaea (Alves et al., 2013; Eme et al., 2013; Gittel et al., 2014; Jaakkola et al., 2014). It has also become clear that archaea cannot only be seen as extremophiles but are highly diversified microorganisms in terms of metabolism and incredibly successful in colonizing almost all environments possible.

Unique archaeal virosphere.

Archaeal viruses belong to 15 families or equivalent groups and infect members of 16 archaeal genera, nearly exclusively hyperthermophiles and extreme halophiles. In comparison, bacterial viruses belong to 11 families and infect members of 179 bacterial genera (Ackermann and Prangishvili, 2012). A certain proportion of the viruses infecting archaea which have been described up to date resemble bacteriophages: (i) head-tail viruses belong to the well-studied families *Myoviridae*, *Siphoviridae* and *Podoviridae* from the order *Caudovirales*, (ii) icosahedral viruses with internal envelope structures are part of the *Sphaerolipoviridae* and *Turrivirdae* (*Tectiviridae* and *Corticoviridae* in bacteria) and (iii) pleomorphic viruses form the *Pleolipoviridae* (*Plasmaviridae* in bacteria). Direct observations suggested that the majority of virus-like particles (VLPs) found in hypersaline environments are non-tailed (Santos et al., 2012; Brum et al., 2013), however geographical and temporal screens for viral diversity in liquid and solid samples came to opposite conclusions (Atanasova et al., 2012; Atanasova et al., 2015). Indeed, all early isolated haloarchaeal viruses were similar to tailed bacteriophages (Reiter et al., 1988) and this holds true for the great majority of haloviruses characterized so far (Dyall-Smith et al., 2003; Kukkaro and Bamford, 2009). Beside the predominant myo-, sipho- and podoviruses, the first archaeal virus with ssDNA genome displayed enveloped, pleomorphic virions with protein spikes extending from the membrane surface (DeLong et al., 1994; Pietila et al., 2009; Pietila et al., 2010).

Halorubrum pleomorphic virus 1 (HRPV1) represented a novel viral group together with all lipid-containing, pleomorphic viruses: the '*Pleolipoviridae'* family (Roine et al., 2010; Pietila et al., 2012). For example, a detailed biochemical characterization indicated that His2 is a pleolipovirus (Pietila et al., 2012) although it had been initially assigned to the floating 'Salterprovirus' genus with the spindle-shaped virus His1 (Bath et al., 2006). Another family, the *Sphaerolipoviridae*, comprises tail-less, icosahedral viruses with a selectively acquired lipid membrane underneath the outer protein capsid. On top of the original members, the haloarchaeal viruses SH1, PH1, *Haloarchaea hispanica* icosahedral virus 2 (HHIV-2) and SNJ1, the family was expanded to include bacteriophages P23-77 and IN93 which infect *Thermus thermophiles.* Beside an overall similar virion morphology and structure of capsid, all members share a conserved block of core genes arranged in the same order, i.e. a gene for a putative genome packaging ATPase in close proximity to the genes encoding the small and the large MCPs (Pawlowski et al., 2014).

There are considerably fewer viruses characterized for methanogenic archaea: PG (Bertani and Baresi, 1987), φF1, φF3 (Nolling et al., 1993), ψM1 (Jordan et al., 1989), its deletion variant ψM2 (Pfister et al., 1998) and the prophage ψM100 (Luo et al., 2001). All the viruses listed above, except defective ψM100, have virions which display the typical morphology of siphoviruses. Notably, a VLP with morphology similar to fuselloviruses (see below) was found in cultures of *Methanococcus voltae* A3 (Wood et al., 1989). Further analyses of the diversity of VLPs in natural environments that contain predominantly archaea, i.e. extreme geothermal ecosystems, revealed that head-tail viruses are rather rare (Prangishvili et al., 2013). Electron microscopy on enrichment cultures from two hot springs of Yellowstone National Park shed light on the unexpected diversity reporting 12 different morphotypes (Rachel et al., 2002). Surveys in various locations – Iceland, Japan, USA – provided insights into the exceptional diversity of viruses infecting hyperthermophilic members (Rice et al., 2001; Rachel et al., 2002; Geslin et al., 2003; Bize et al., 2008; Garrett et al., 2010; Mochizuki et al., 2010; Quax et al., 2010). In fact, cultured archaeal viruses isolated from geothermal environments exhibit unique morphologies described hereinafter (Figure 2). They all, except two with single-stranded (ss) DNA, contain double-stranded (ds) DNA genomes and infect members of the genera *Pyrococcus, Thermococcus*, *Thermoproteus*, *Pyrobaculum*, *Aeropyrum, Sulfolobus* and *Acidianus* (Pina et al., 2011; Prangishvili, 2015).

Viruses with fusiform virions, either tail-less, tailed or two-tailed, are common in archaea-dominated environments and constitute a large fraction of described archaeal viruses. Within

the family *Fuselloviridae*, members share a unique spindle-shaped morphology with spindle- or lemon-shaped particles (60x100 nm) decorated by sticky terminal fibres at one of the two pointed ends (Wiedenheft et al., 2004). Exceptions are viruses *Sulfolobus* spindle-shaped virus 6 (SSV6) and *Acidianus* spindle-shaped virus 1 (ASV1), whose virions tend to be more pleomorphic resembling a thin cigar or a pear, respectively (Redder et al., 2009). In addition, they seem to differ from the other fuselloviruses in the presence of three or four thicker and slightly curved fibres at one pole (Redder et al., 2009). *Pyrococcus abyssi virus 1* (PAV1) and

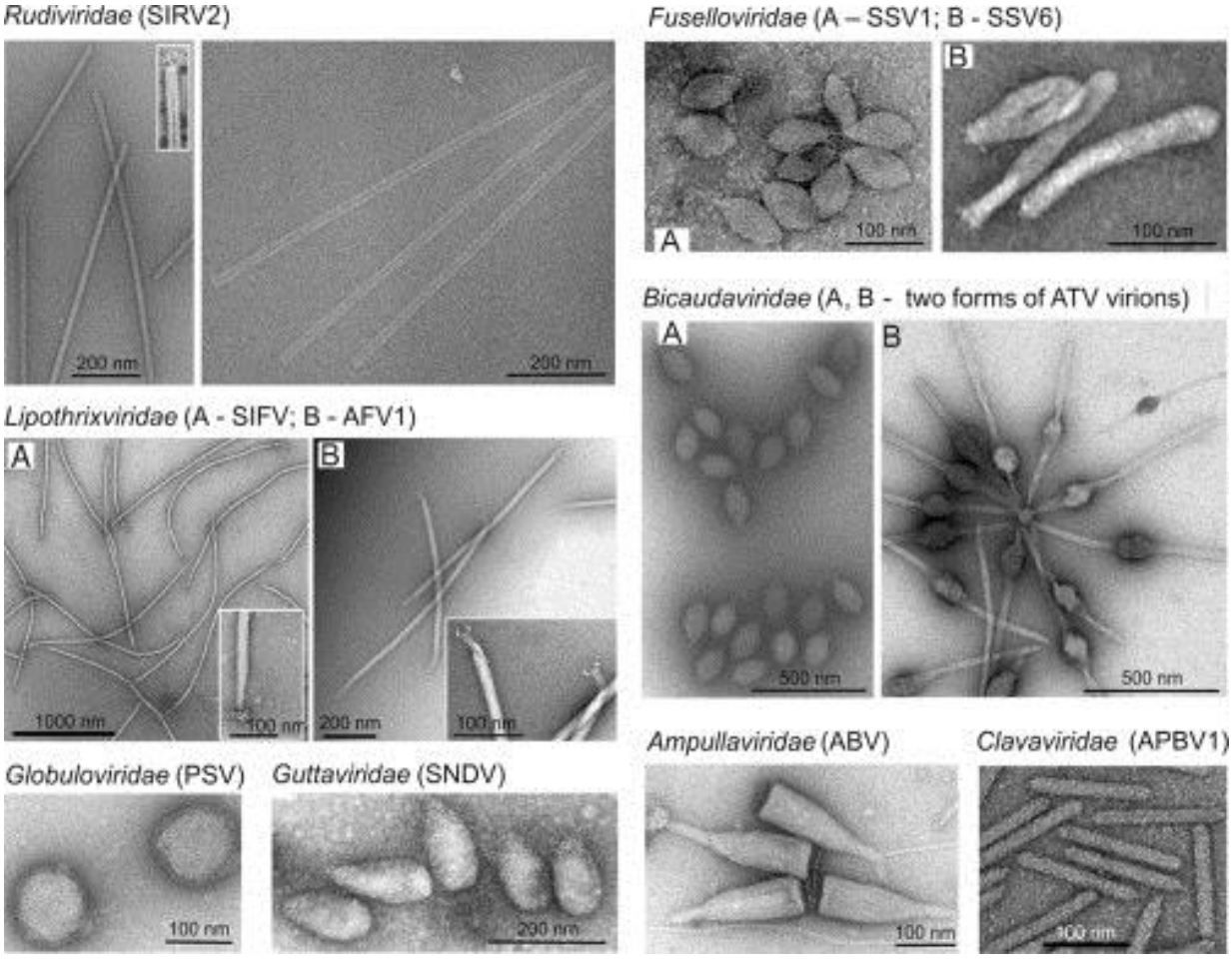

Figure 2: Transmission electron micrographs of representative members of eight families of viruses of the Crenarchaeota.

Reproduced with permission from Krupovic et al., 2012: *Chapter 2 – Postcards from the Edge: Structural Genomics of Archaeal Viruses*.

Thermococcus prieuri virus 1 (TPV1) infect hyperthermophilic euryarchaea and also produce enveloped, lemon-shaped particles with a tail-like protrusion terminated by fibres (Geslin et al., 2003; Gorlas et al., 2012). Single-tailed fusiform viruses, *Sulfolobus tengchongensis* spindle-shaped virus 1 (STSV1) and STSV2 discovered in China are distantly related to the *Bicaudaviridae* (Xiang et al., 2005; Erdmann et al., 2014). This family has been established

based on one known representative, *Acidianus* two-tailed virus (ATV) (Prangishvili et al., 2006). Notably, the two-tailed fusiform virions are extruded from host cells as tail-less particles and in conditions close to natural habitat, i.e. 85°C, two long tails are being developed from the spindle-shaped body. At the two identical ends, tubes are formed with a thin periodic filament inside and terminate in an anchor-like structure (Haring et al., 2005c).

Exclusive to archaea, fusiform viruses comprise several isolates which remained unclassified for a long time. They are associated with a broad range of hosts which are highly diverse in terms of metabolism and belong to phylogenetically distant groups. Using structural markers, we defined that the two viral lineages: the *Bicaudaviridae* or *Fuselloviridae* families depend on the unique helix-bundle fold in the major capsid protein (MCP) or the presence of two hydrophobic domains, respectively. Importantly, we show that most of the isolates display the hallmark of the *Fuselloviridae* making it the most prominent and evolutionary successful family among the viral groups which have been described in Archaea up to now (Krupovic et al., 2012). The results of our in-depth comparative analysis have been published and can be found in the **Chapter 3** of the manuscript.

In environments dominated by archaea, linear viruses are also very abundant and all of them have dsDNA genomes, a property not previously observed for any linear virus. They are part of the *Ligamenvirales* order which includes the two families *Rudiviridae* and *Lipothrixviridae* (Prangishvili and Krupovic, 2012). The discrimination between the rudiviruses and lipothrixviruses was initially claimed based on different principles of virion architecture and is now supported by comparative genomic data. Rudiviruses have non-enveloped virions with a length proportional to the size of the linear genomes (23x610-900 nm). They contain a superhelix formed by dsDNA genome and copies of a single glycosylated, basic DNA-binding protein. At the two ends of the tube-like structure are anchored three short tail fibres made of a minor structural protein of 100 kDa (Prangishvili et al., 2013). Members of the *Lipothrixiviridae* exhibit a variety of terminal appendages. In particular, there can be up to six terminal filaments forming the terminal appendage in the case of *Sulfolobus islandicus* filamentous virus (SIFV) (Arnold et al., 2000) or even synthesis of complex structures such as ‘claws’ in the case of *Acidianus* filamentous virus 1 (AFV1) (Bettstetter et al., 2003) or ‘bottle brush’ for AFV2 (Haring et al., 2005b). Consistently, they significantly differ in the structures of virion core, genomic properties and replication mechanisms sustaining a classification into four different genera (Pina et al., 2011). Historically, *Thermoproteus tenax* virus 1 (TTV1), TTV2, TTV3 were the first studied and belong to the α-lipothrixviruses (Reiter et al., 1988).

Other morphotypes are completely atypical and their unique characteristics justified the establishment of novel viral families by the International Committee for the Taxonomy of Viruses (ICTV). *Acidianus* bottle-shaped virus (ABV) is the only representative of the *Ampullaviridae* family and virions exhibit a complex architecture. The viral particles resemble a bottle with three structural elements: the 'stopper' or pointed end, the nucleoprotein core and the inner core. The dsDNA-containing nucleoprotein is folded into a cone-shaped core that is further encased in an envelope. There is a narrow, pointed end and a broad end with 20 short, thick filaments which insert into a disc and are also interconnected at their bases (Haring et al., 2005a). Members of the *Guttaviridae* are *Sulfolobus neozealandicus* droplet-shaped virus (SNDV) and *Aeropyrum pernix* ovoid virus 1 (APOV1). Virions of SNDV display a droplet-shaped body (90x180 nm) made of a core surrounded by a 7-nm-thick coat. Despite an overall droplet form, the surface seems to be helically ribbed and appears 'bearded' by multiple, long, thin fibres covering about half of the particles from the apex (Arnold et al., 2000). Interestingly, virions of APOV1 (70x55 nm) are about 1.5 times smaller than SNDV particles and do not exhibit any attached fibre (Mochizuki et al., 2011). The *Globuloviridae* includes *Pyrobaculum* spherical virus (PSV) and *Thermoproteus tenax* spherical virus 1 (TTSV1) infecting anaerobic and hyperthermophilic archaea of the genera *Pyrobaculum* and *Thermoproteus* (Haring et al., 2004; Ahn et al., 2006). The spherical virion (100 nm) of PSV contains multimers of a CP and host derived lipids enclosing a superhelical nucleoprotein (Haring et al., 2004). The first virus to be isolated from the order *Desulfurococcales* was *Aeropyrum pernix* bacilliform virus 1 (APBV1), family *Clavaviridae*. Viral particles have a rigid bacilliform topology (140x20 nm) with one end pointing and the other, round (Mochizuki et al., 2010). In the *Spiraviridae*, the ssDNA is bound by several copies of MCP folding into a superhelix with two levels of organization. Indeed, the non-enveloped, hollow, cylindrical virions of *Aeropyrym* coil-shaped virus (ACV) have appendages at both ends and are based on a rope-like fiber of two intertwined halves of a single nucleoprotein complex (Mochizuki et al., 2012). *Sulfolobus* turreted icosahedral virus (STIV) was the first icosahedral virus with an archaeal host identified. Viral particles are composed of circular dsDNA genome enclosed within an internal membrane and have been classified in the *Turriviridae* family (Rice et al., 2004; Maaty et al., 2006). Another icosahedrally symmetric, membrane-containing archaeal virus has been isolated, STIV2 for which the host-attachment structures are significantly different (Happonen et al., 2010).

To conclude, archaea, and hyperthermophilic members in particular, are infected by a range of viruses with unique morphotypes. The unexpected and unprecedented diversity of reported particle shapes is linked with unique aspects of the cellular biology of archaea (Prangishvili, 2015). Fusiform and filamentous viruses are the most abundant VLPs found in hyperthermic and hypersaline environments where archaea outnumber bacteria and thus have been quite extensively studied in comparison with the rest of the archaea-specific virosphere. The fusellovirus *Sulfolobus* spindle-shaped virus 1 (SSV1) and rudivirus *Sulfolobus islandicus* rod-shaped virus 2 (SIRV2) infect hosts of the genus *Sulfolobus* and have become model systems to study the biology of viruses infecting archaea.

Sulfolobus, a model for hyperthermophilic archaea.

One of the most impressive features of archaea is their capacity to sustain temperatures up to 122°C (Kashefi and Lovley, 2003). Thermophiles and hyperthermophiles have been the focus of pioneering research from Wolfman Zillig's laboratory (Albers et al., 2013). Numerous sampling campaigns provided insights into the diversity of archaeal species — often associated with various genetic elements — present in major solfataric fields, i.e. acidic springs, water and mud holes (Zillig et al., 1993). The members of the genus *Sulfolobus* are characterized by: (i) an overall spherical shape of cells with lobes; (ii) facultative autotrophy and growth on sulfur or simple organic compounds; (iii) non-classical cell wall structure devoid of peptidoglycan; (iv) pH requirement ranging from 0.9 to 5.8; (v) conditions of temperature between 55 and 80°C (Brock et al., 1972). Several species and strains have been isolated from different geographical locations including Naples, Italy; Kamchatka, Russia; Lassen Volvanic National Park and Yellowstone National Park, USA (Guo et al., 2011). Interestingly, the structure of populations showed intra-species diversification and local adaptation without any correlation with temperature or pH (Whitaker et al., 2003; Grogan et al., 2008). Comparative analyses of genomes from all *Sulfolobus islandicus* strains available concluded that there is a strong conservation of gene synteny with distinguishable biogeographical patterns of differentiation (Jaubert et al., 2013). In general, members of the *Sulfolobus* have been extensively studied and several aspects of their biology are now well understood (Stetter, 1999; Urbieta et al., 2014). For example *S. solfataricus* and *S. acidocaldarius* were used to conduct the first studies on the cell cycle in Archaea (Bernander and Poplawski, 1997; Hjort and Bernander, 1999). Detailed characterization has recently revealed that homologues to the endosomal sorting complex required for transport (ESCRT)

in Eukayotes are involved in cell division in Archaea as well (Samson et al., 2008; Lindas and Bernander, 2013). *Sulfolobus* species are relatively easy to cultivate under laboratory conditions, in comparison with other archaeal members, and have emerged as a model of choice for investigating adaptation to geothermal environments.

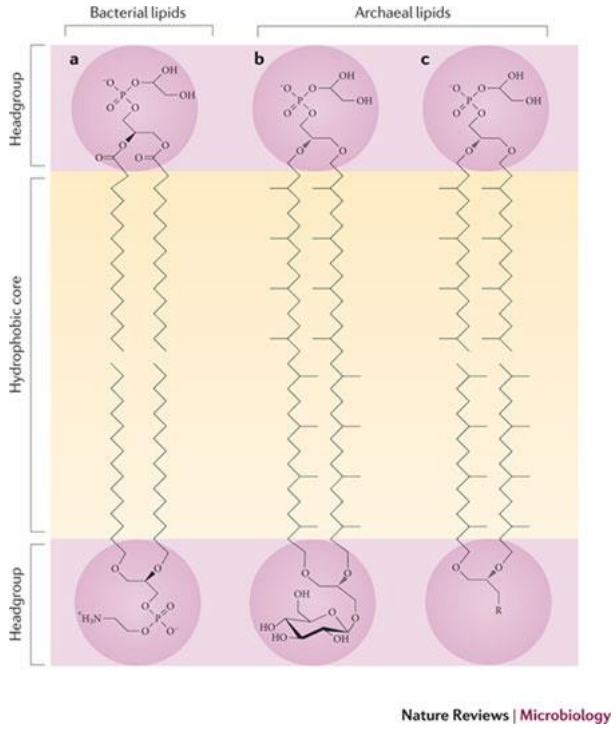

Figure 3: The lipids found in the archaeal membrane are fundamentally different from those found in eukaryotic and bacterial membranes. In eukaryotes and bacteria, the glycerol moiety is ester-linked to an sn-glycerol-3-phosphate backbone, whereas in archaea the isoprenoid side chains are ether-linked to an sn-glycerol-1-phosphate moiety. The sn1 stereochemistry of the glycerol backbone is a truly archaeal feature, as ether lipids occur in minor amounts in eukaryotes and bacteria. The common bilayer-forming lipids in bacteria are phophatidylglycerol (upper lipid) and phosphatidylethanolamine (lower lipid) (see the figure, part a). Part b of the figure shows the structure of monolayer-forming tetraether lipids; for example, the glycophospholipid from the thermoacidophilic archaeon Thermoplasma acidophilum, in which the hydrophobic core consists of C40C40 caldarchaeol. Part c of the figure shows a bilayer formed of archaeal diether lipids, which can be found, for example, in Halobacteriales. The hydrophobic core consists of C20C20 archaeol isoprenoids. The headgroups of phospholipids can be a range of polar compounds — for example, glycerol, serine, inosine, ethanolamine, myo-inositol or aminopentanetetrols. Glycolipids also exhibit a range of sugar residues — for example, glucose, mannose, galactose, gulose, N-acetylglucosamine or combinations thereof.

Reproduced with permition from Albers and Meyer, 2011: *The archaeal cell envelope*.

Cell surface characteristics. It was realized very early that the cell surface of archaea and bacteria differ substantially. The first noticeable characteristic is the presence of polar lipids composed of hydrocarbon chains of 20 to 40 carbons in length and usually saturated (Figure 3). The isoprenoid moieties are ether-linked to the glycerol-1-phosphate (G-1-P) backbone. By contrast, in bacteria and eukaryotes the fatty acid derived chains are ester-linked to G-3-P

(De Rosa et al., 1986; De Rosa and Gambacorta, 1988; Leininger et al., 2006). Notably, *Sulfolobus* cells were shown to almost exclusively contain glycerol dialkyl glycerol tetraether (GDGT) lipids organized in a covalently-bound bilayer resembling a monolayer (Langworthy et al., 1974; 1976; Langworthy, 1977; Chong, 2010). In nature, a variety of archaeal lipid species is found (Koga and Morii, 2005) and their biosynthesis pathways are just starting to be investigated (Jain et al., 2014; Villanueva et al., 2014). The polar head groups are identical between the three domains and it is generally assumed that the bipolar lipids found in archaea play an important role in the survival and adaptation of these microorganisms to extreme environments (Chong, 2010). On the basis that they are more chemically stable than their bacterial and eukaryotic lipids, archaeosomes, i.e. liposomes made of archaeal lipids, are being developed as potential next-generation adjuvants and drug delivery systems (Krishnan and Sprott, 2008). *In vivo*, the monolayer-like membrane is involved in the maintenance of cell homeostasis in combination with specific properties of the cell wall. Indeed, only a subgroup of archaea contains pseudomurein and the cytoplasmic membrane is normally surrounded by a proteinaceous, quasi-crystalline surface (S-) layer (Figure 4). In *Sulfolobus*, the cell wall is composed of two conserved polypeptides instead of one-component systems found in many other groups (Albers and Meyer, 2011). The outer layer assumes a three-fold symmetry based on dimers of the large protein SlaA and is anchored by membrane-bound stalks made of small peptide SlaB (Veith et al., 2009). The S-layer is proposed to contribute to cell shape, osmotic balance and protection from harsh environmental conditions. S-layer proteins (Peyfoon et al., 2010), as well as other surface-exposed proteins, undergo extensive post-translational modification by the N- and O-glycosylation pathways (Meyer and Albers, 2013; Jarrell et al., 2014).

Cell surface appendages. Several appendages and membrane-associated components have been identified at the surface of *Sulfolobus*, like flagella and pili which, at first glance, appear similar to their bacterial counterparts (Figure 5). However, detailed studies showed that the archaeal flagella, the archaella (Albers and Meyer, 2011), resemble bacterial flagella only in terms of function. A single locus is responsible for 'flagellation' in the vast majority of species; the *fla* operon contains seven genes which are conserved and essential for biosynthesis and function of the apparatus (Lassak et al., 2012a). FlaB encodes archaellins, subunit components homologous to bacterial pilins which maturate through proteolytic

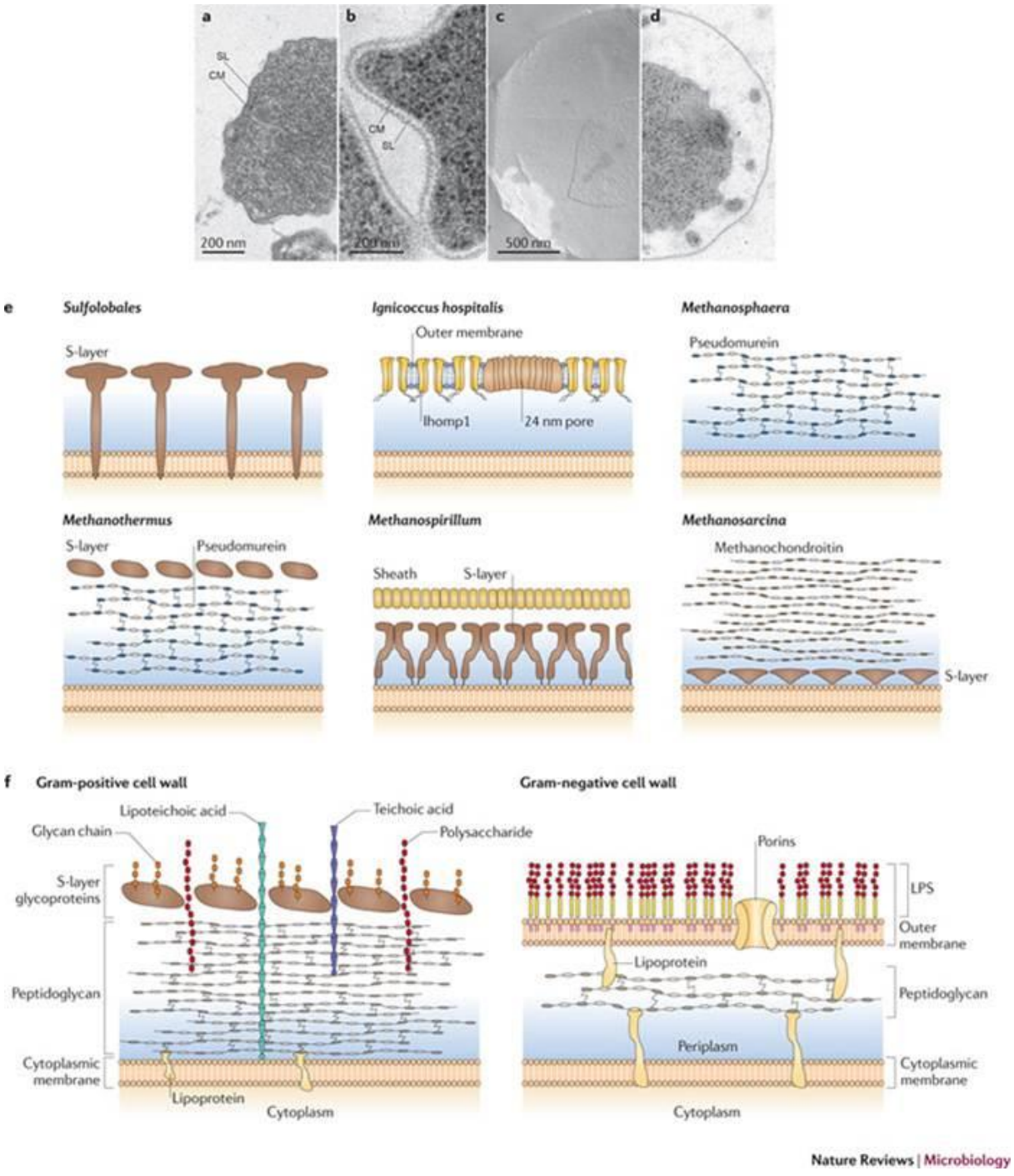

Figure 4: a,b | Electron micrographs of ultra-thin sections of the euryarchaeote Methanocaldococcus villosus (a) and the crenarchaeote Metallosphaera prunae (b). c,d | Electron micrographs of a freeze-etched cell (c) and a thin-section cell (d) of Ignicoccus hospitalis144. e | Schematic side view of cell wall profiles from different archaea. Pseudoperiplasmic space is shown in blue. f | Schematic of bacterial cell walls. Gram-positive bacteria have a thick, amorphous, multilayered coat of peptidoglycan, teichonic and lipoteichonic acid as their cell wall and in some cases have surface-layer (S-layer) glycoproteins as the outermost layer above the peptidoglycan (also known as murein), for example, in Bacillus stearothermophilus20, 21. Gram-negative bacteria have an outer asymmetric bilayer membrane composed of two leaflets, an outer one containing lipopolysaccharides (LPSs), and an inner one containing mainly phospholipids, a gel-like periplasm containing peptidoglycan and the cytoplasmic membrane. CM, cytoplasmic membrane; SL, S-layer.

Reproduced with permition from Albers and Meyer, 2011: *The archaeal cell envelope*.

cleavage. FlaG and FlaF are membrane proteins of unknown function and FlaH is an ATP-binding protein. In addition, FlaI (Reindl et al., 2013) and FlaJ are homologous to PilB and PilC, which correspond to the motor ATPase and basal membrane protein of the type IV pili in bacteria, respectively. Another key component is FlaX, the central protein required as a priming subunit during assembly in *S. acidocaldarius* (Banerjee et al., 2012). Structures of archaella from *Halorubrum salinarium* and *S. shibatae* are overall similar and display a thin filament with a right-handed helix around a central core (Cohen-Krausz and Trachtenberg, 2008). Given the assembly model and the structural characteristics, the archaellum is more

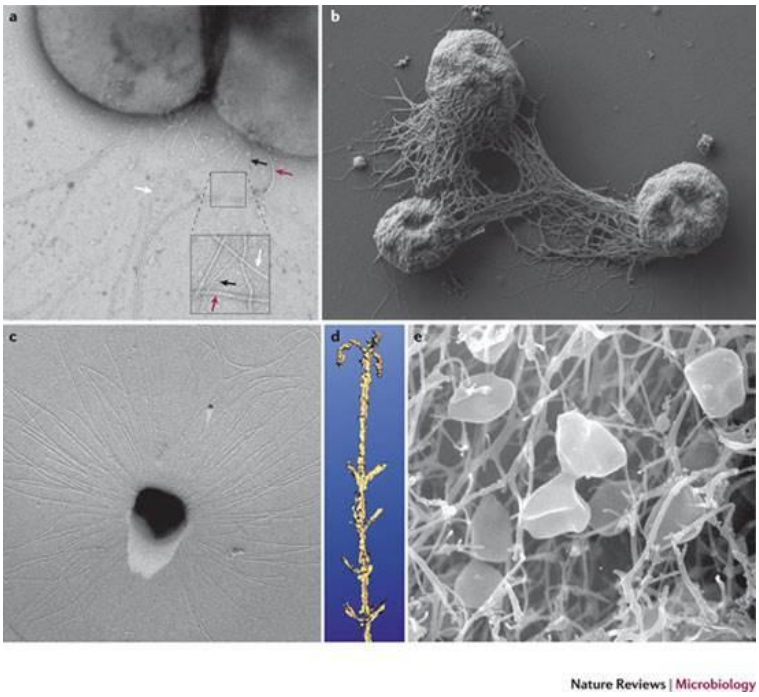

Figure 5: a | A transmission electron micrograph of negatively stained of Sulfolobales acidocaldarius cells showing flagella (~14 nm in diameter, red arrows) pili (~10–12 nm, white arrows) and threads (~5 nm, black arrows). b | A scanning electron micrograph of Methanocaldococcus villosus157 cells grown on a surface, exhibiting bundles of flagella that act in cell–cell connections and surface adherence. c | Electron micrograph of a platinum-shadowed SM1 euryarchaeal coccus. d | Three-dimensional model of the hamus structure as visualized by surface rendering of a de-noised data set, obtained by cryo-electron tomography. The hook is 60 nm in width. e | Scanning electron micrograph of Pyrodictium spp. cells growing in a net of cannulae.

Reproduced with permition from Albers and Meyer, 2011: *The archaeal cell envelope*.

related to bacterial type IV pili as opposed to flagella, despite the fact that they play the same role in motility, attachment to surface and biofilm formation (Ellen et al., 2010). In bacteria, the type IV pili are key structures mediating a variety of biological processes including adhesion to surface, cell-cell interactions, conjugation, twitching motility, and pathogenicity (Craig et al., 2004). In archaea, thin, flexible 10-nm filaments of variable lengths have also

been observed and resemble pili in their appearance (Ng et al., 2008; Ajon et al., 2011). For example, the UV-pilus is encoded by the *ups* operon and is strongly induced by UV irradiation. Its biosynthesis involves the potential secretion ATPase, two pre-pilins, a putative transmembrane protein and a protein of unknown function (Frols et al., 2008). Another operon critical for surface adhesion has also been identified: the *aap* operon (Lassak et al., 2012a). Notably, archaeal homologues to the ATPase PilB which provides the energy necessary for pilus assembly in bacteria has been characterized. However, no ATPase involved in retraction could be identified by *in silico* approaches, suggesting that pili and flagella are unable to retract in Archaea. Other reported structures seem to be unique to the third domain of life (Figure 5). In *S. solfataricus*, a large number of sugar binding proteins have been identified with a class III signal peptide. These proteins require the *bas* operon for their functional surface localization. It has been proposed that BasEF would form the core of the assembly machinery at the membrane while BasABC would participate in cleavage of pilin signal peptides and correct assembly of binding proteins into a macromolecular complex (Zolghadr et al., 2007). The 'bindosome' would serve as a platform dedicated for sugar uptake from the environment in addition to pore-like openings of S-layer which are suggested to only permit passage of nutrients and other small molecules (Ellen et al., 2010). Although never reported for *Sulfolobus*, cannulae and hamus are fascinating appendages associated with surface. Cannulae of hyperthermophilic *Pyrodictium abyssi* are hollow tubes with a diameter of ~25 nm and associate in a network facilitating intercellular communication, nutrient exchange or transport of genetic material (Rieger et al., 1995). Hamus found at the surface of the psychrophilic archaeon SM1 plays a role in surface attachment, biofilm formation and anchoring; the filaments are 7-8 nm in diameter forming a complex helix with three hooks present every 4 nm (Moissl et al., 2005).

Insights into the biology of hyperthermophilic archaeal viruses.

Fusiform and filamentous VLPs are highly abundant and widely distributed in archaea-dominated habitats. The two groups of viruses are represented by fusellovirus SSV1 and rudivirus SIRV2 which have been among the first archaeal viruses to be isolated from geothermal environments where they can infect *Sulfolobus* cells. SSV1 has a rather broad host range (Schleper et al., 1992), whereas SIRV2 can only infect a limited number of strains of *S. islandicus* (Bize et al., 2009). The two viruses serve as model systems for the study of hyperthermophilic archaeal viruses.

SSV1. The genome of SSV1 was shown to be present in *S. shibatae* B12 in two forms: as a linear form within the host chromosome and as free, circular episomal copies in the cytoplasm (Yeats et al., 1982). UV irradiation is a strong stimulus to enhance the production of lemon-shaped particles encasing the circular form of the viral genome (Martin et al., 1984). SSV1 was initially called SAV-1 due to misclassification of its natural host as a strain of *S. acidocaldarius*. It is a temperate virus and infection results in a lysogenic cycle leading to growth recovery of cultures even after stimulation (Schleper et al., 1992). The capacity to integrate into the cellular genome at a specific site within a tRNA-Arginine gene (Reiter et al., 1989) has been used to establish one of the first genetic systems in Archaea (Schleper et al., 1992). As a result, the viral tyrosine recombinase has been extensively studied (Muskhelishvili et al., 1993; Serre et al., 2002; Letzelter et al., 2004; Zhan et al., 2012). Development of genetic tools has also allowed systematic analysis of the functions of viral open reading frames (ORFs) and effects of their deletions on virus fitness (Stedman et al., 1999; Iverson and Stedman, 2012). In particular, the integrase gene has been shown to be non-essential for infection (Clore and Stedman, 2007). Interestingly, unlike the situation found in bacteriophages, upon viral genome integration, the integrase gene is partitioned in two fragments (Reiter et al., 1989). Several isolates are now known to be similar to SSV1 in morphology, genomic content, replication strategy, etc. (Stedman et al., 2003; Wiedenheft et al., 2004; Redder et al., 2009); nevertheless, SSV1 remains to be a model to understand the biology of spindle-shaped viruses. Using genome-wide microarray, it was shown that there is a tight regulation of gene expression timing, reminiscent of bacteriophages and eukaryotic viruses. The transcription starts with a small UV-specific transcript and continues with early and late transcripts towards the end of the viral cycle (Frols et al., 2007a; Fusco et al., 2013). Interestingly, there was no marked difference detected in the transcriptome of the host *S. solfataricus*, in line with the postulated egress of SSV1 by budding through the cytoplasmic membrane without lysis of the host (Martin et al., 1984). Most of the particles released are uniform in size (60x100 nm) although up to 1% of viral population can be larger, the maximum length being about 300 nm (Reiter et al., 1988). Recently, the structure of SSV1 was examined by cryo-electron microscopy (cryo-EM) and 3D image reconstruction. A model of SSV1 structure has been proposed despite the fact that resolution was severely limited by particle size, lack of global symmetry, structural heterogeneity, and a small number of particles considered (Stedman et al., 2015). In particular, the presence of an actual lipid

membrane encasing the virion body could not be verified and remained controversial up to now. Thus, one of the main objectives of my PhD was to perform a comprehensive biochemical characterization of SSV1 virions which is described in the **Chapter 4**. Briefly, we showed that SSV1 is a lipid-containing virus composed of glycrosylated proteins and host-derived lipids encasing the nucleoprotein filament (Quemin et al., 2015). These findings provide insights into the architecture of unique archaeal viruses and are used as a foundation for ongoing studies targeting the interactions of SSV1 with its host *Sulfolobus* (Quemin et al., in preparation). We recently obtained significant insights into the assembly and release strategy utilized by SSV1 virions which are presented in the **Chapter 5**.

SIRV2. The non-enveloped, linear dsDNA virus SIRV2 is the type-species of the *Rudiviridae* family. The stiff, rod-shaped particles (950x26 nm) were observed for the first time in the culture of *S. islandicus* strain KVEM10H3 (Zillig et al., 1993). There is a central cavity of 6 nm in diameter and three 28-nm-short appendages protruding from both ends. The viral particles consist of a tube-like superhelix which length correlates with the genome size, i.e. SIRV1 virions are 70 nm shorter than those of SIRV2 and have genomes of 32.3 versus 35.8 kbp in SIRV2. Recently, the structure of SIRV2 virions using cryo-EM and 3D image reconstruction became available and revealed a unique DNA topology in the A-form which has only been previously observed in bacterial spores and *in vitro* (DiMaio et al., 2015). Interestingly, SIRV1 is also known to have a very high mutation rate of 3.10^{-3} substitutions per nucleotide per replication cycle, whereas SIRV2 is considered to be invariant (Prangishvili et al., 1999). The genome of SIRV2 is covalently closed at the termini and carries inverted terminal repeats. It contains 54 ORFs (Peng et al., 2001). Transcription of the viral genome has been shown to start simultaneously at multiple sites and spread over the two strands in a uniform pattern through the course of infection (Kessler et al., 2004). Microarray analysis (Okutan et al., 2013) and RNA-seq approach (Quax et al., 2013) revealed that transcription is limited to the two distal termini of the viral genome immediately after infection and then spreads over the totality of ORFs within 2 hours. The host cell machinery is extensively reprogrammed with more than half of host genes having a different level of expression. The genes involved in cell division, chromosome maintenance, and stress response were down-regulated while anti-viral defense mechanisms, i.e Clustered Regularly Interspaced Short Palindromic Repeats (CRISPR) – CRISPR associated proteins (Cas) and toxin/antitoxin systems, were massively activated (Quax et al., 2013). The results on

transcription are consistent with the lytic cycle of SIRV2. Indeed, the virus orchestrates an elaborated mechanism leading to degradation of host chromosome and remodeling of the surface which results in cell death. The progeny is assembled in the cytoplasm occupying the entire space and released after formation and opening of specific virus-associated pyramids (VAPs) which are anchored in the plasma membrane and protrude through the S-layer (Bize et al., 2009; Quax et al., 2011; Daum et al., 2014). As opposed to the egress mechanism of SIRV2, prior to the advent of my PhD project literally nothing was known about the early stages of the infection cycle, i.e. adsorption to the host cell surface and entry of the viral genome into the cell interior. In order to gain insights into the entry of SIRV2 virions, we have utilized a number of different assays to assess the binding kinetics, reversible and irreversible adsorption, receptor saturation, etc. as well as transmission electron microscopy and whole-cell electron tomography (Quemin et al., 2013). The recently published article is included in my PhD thesis and reported in the **Chapter 6**.

The cases of SSV1 and SIRV2 exemplify the uniqueness of the virosphere specific to Archaea. Not only they display morphotypes which have never been associated with bacteria or eukaryotes but also reveal uncommon principles for virus biology and infection. Although, data have been accumulating on the diverse architectures of virions (Prangishvili et al., 2013) and original genomic content (Krupovic et al., 2012), the exploration of virus-host interactions in the third domain of life is still in its infancy. The aim of the work performed during the course of my PhD was to provide insights into the infection cycle of archaeal viruses. The global strategies employed for entry, assembly and egress have been investigated by a combination of electron microscopy approaches, biochemistry, cellular and molecular biology techniques. The data presented here on the molecular mechanisms of virus-host interactions for both lipid-containing, fusiform SSV1 and non-enveloped, filamentous SIRV2 allows comparison with bacterial and eukaryotic virus-host systems.

Virus-host interactions in Archaea: state-of-the-art.

Members of the third domain of life, the archaea, were initially regarded as exotic microorganisms capable of growing in conditions which are hostile to humans. Among other intriguing features, they are now known to host unique viruses classified into exclusive viral families. Several studies have permitted the isolation of highly diverse viruses characterized by atypical virion shapes and mysterious genomic contents. The research undertaken in the

past thirty years has improved our appreciation of the virosphere associated with archaea. However, the study of archaeal viruses imposes serious constraints and the collection of virus-host systems found in laboratories is far from representing the situation observed in natural environments. The isolation and characterization are indeed limited due to the need of culturing cells under extreme conditions of temperature, pH, salinity, pressure, etc. which are complicated to set up in laboratory. Another restriction comes from the viruses themselves which tend to be produced in low titers rendering analysis by classical techniques often challenging.

Using high-throughput approaches, one can neglect some of these factors and overcome the major difficulties linked to the research on archaeal viruses. In the **Chapter 1**, the editorial outlines the recent insights that have been obtained on the infection cycle of hyperthermo-acidophilic virus-host models, namely SSV1, SIRV2, and STIV (Quemin et al., 2014). We put a particular emphasis on data covering structural genomics, whole-genome microarrays or RNA-sequencing, as well as large-scale proteomic analysis of infected cells. In fact, comparative genomics defined the structure and/or function of more than 10% of the ORFs identified in viral genomes. Additional insights came from screens for interactions or whole-transcriptome analyses in the case of SIRV2. Viral and host gene expression through the course of infection varies and a tight timing of transcription has been described for SSV1 with early, middle and late genes. Considering the proteome, STIV infection was shown to induce significant differences in protein levels and, more importantly, in post-translational modification profiles. Together these studies highlight the rapid development of high-throughput methods in the field of archaeal viruses and help to define interesting targets that should be the focus of intensive research in the near future.

Moreover, recent studies trying to decipher the sequential events of the viral life cycle have led to major breakthroughs in the field. The review proposed in the **Chapter 2** has been written during the framework of my PhD. It summarizes the available information concerning the virus-host interplay in Archaea with a focus on hyperthermo-acidophilic virus-host systems (Quemin and Quax, 2015). We discuss the possibility that appendages, which are observed to decorate virion termini in various families and can even form complex structures, are required during the entry process of these viruses. In the same line, novel strategies employed for egress have been recently described and are reported in great detail. The molecular mechanisms of virus-host interactions in archaea are also compared to the ways bacterial and eukaryotic viruses interact with their respective hosts. Together with the harsh

environmental conditions, the characteristics of archaeal cell surface, i.e. cytoplasmic membrane and S-layer, might render the delivery of viral nucleic acids and the release of viral progeny quite difficult. Therefore, the host specificities in terms of ecology and biology could have compelled viruses to adapt and employ uncommon strategies that we are just starting to discover and understand.

RESULTS

CHAPTER 1

Insights into the biology of archaeal viruses by high-throughput approaches.

Future VIROLOGY

EDITORIAL

Hard out there: understanding archaeal virus biology



Emmanuelle RJ Quemin[1], David Prangishvili[1] & Mart Krupovic*[,1]

Each of the three domains of life, Archaea, Bacteria and Eukarya, is associated with a specific virosphere. Despite the fact that archaeal viruses represent only a minute portion of the characterized virosphere, they have recently gained wider attention, mainly due to the unexpected morphological properties of their virions and the unprecedented molecular mechanisms employed throughout their life cycles. Archaeal viruses are currently classified into 15 different families [1,2]. Especially remarkable are the viruses of the hyperthermohilic archaea; these viruses are extremely diverse morphologically and include members with lemon-shaped, droplet-shaped and bottle-shaped virions [1]. Furthermore, the viral genomes encode proteins with little to no significant similarity to proteins in public databases and often possess unique structural folds [3]. Although classical biochemical and genomic studies have yielded important information on the architectures of several hyperthermophilic archaeal viruses, as well as on the functions of some viral proteins, the molecular mechanisms underlying different aspects of the infection cycle remain poorly understood for most of these viruses.

Studies on bacterial and eukaryotic viruses have benefited from the availability of well-established genetic tools that have been developed for the respective hosts and, more generally, from the broad knowledge base on the host biology. This, unfortunately, has not been the case for most of the archaeal virus–host systems. The assays that are considered trivial when thinking about bacterial or eukaryotic viruses (e.g., the plaque test used for virus particle enumeration) present difficulties in the case of hyperthermophilic archaeal viruses. Indeed, the cultivation of hyperthermophilic acidophiles, such as *Sulfolobus*, which, for optimal growth, requires 80°C and pH 2–3, might be challenging. Similarly, live-cell imaging at physiological temperatures, which is widely used to investigate virus–host interaction in eukaryotes, is normally also off the table when dealing with hyperthermophiles. Consequently, the scientific inquiries into the properties of hyperthermophilic archaeal viruses have been, for a long time, limited by the lack of adequate tools.

KEYWORDS
• Archaea • hyperthermophiles • *Sulfolobus* rod-shaped virus 2 • virus evolution • virus–host interactions

[1]Institut Pasteur, Unité Biologie Moléculaire du Gène chez les Extrêmophiles, Département de Microbiologie, 75015 Paris, France
*Author for correspondence: krupovic@pasteur.fr

Future Medicine part of fsg

Given all of these difficulties, one might wonder why anyone would bother with studying archaeal viruses in the first place. The major incentives are the following. First, the morphological diversity of hyperthermophilic archaeal viruses is astonishing [1]. Whereas sampling of the bacterial virosphere seems to have reached convergence (i.e., no truly new morphotypes of bacterial viruses have been discovered for decades), virions with unique, previously unseen morphologies are constantly being discovered in the Archaea. It has been suggested that the archaeal virosphere more closely reflects the ancient diversity of viruses on our planet [1]. Consequently, exploration of the archaeal virus diversity provides an exclusive opportunity to learn about the ancient viral architectures that might not have been retained in other cellular domains. Second, the molecular mechanisms underlying virus–host interactions in Archaea combine components that are specific to archaeal viruses with those that are shared with viruses infecting other cellular domains. Thus, in addition to uncovering new Archaea-specific features that are sometimes breathtakingly elegant (as in the case of the recently discovered pyramidal egress structures [4,5]), these studies allow us to better understand the origin and evolution of the mechanisms underlying the infection processes of viruses infecting eukaryotic hosts (see below). Third, due to their ability to withstand harsh environmental conditions, hyperthermophilic archaeal viruses contain considerable appeal for developing various bio- and nano-technological applications. Furthermore, the enzymes encoded by these viruses can be potentially employed for molecular biology applications.

"...exploration of the archaeal virus diversity provides an exclusive opportunity to learn about the ancient viral architectures that might not have been retained in other cellular domains."

During the past few years, many modern high-throughput techniques have been adapted for studying archaeal viruses, and new genetic tools have been developed for an increasing number of archaeal hosts and their viruses [6–8]. These newly developed/adapted approaches and genetic tools, in combination with the more classical biochemical techniques, have recently yielded valuable information on the biology of some archaeal viruses. Two hyperthermophilic viruses infecting *Sulfolobus* species have been investigated from different perspectives and served as models for understanding the biology of archaeal viruses. These include *Sulfolobus* turreted icosahedral virus (STIV) and *Sulfolobus islandicus* rod-shaped virus 2 (SIRV2). These two viruses fundamentally differ from each other in virion morphology, genomic content and viral cycle [1]. STIV is a prototype member of the family *Turriviridae*. The STIV virion consists of an icosahedral protein capsid that covers the lipid membrane vesicle enclosing the circular dsDNA genome [9]. Such a virion architecture is commonly found in bacterial and eukaryotic viruses [10]. SIRV2 is the type organism of the family *Rudiviridae*, which comprises viruses with elongated rod-shaped particles containing linear dsDNA genomes [11]. The termini of SIRV2 virions are decorated with terminal protein fibers that mediate the attachment of the viral particles to the pili-like appendages at the host cell surface [12]. Interestingly, despite profound morphological and genomic differences, both STIV and SIRV2 utilize a unique virion release mechanism involving the formation and opening of large pyramidal structures at the surface of the host cell [4,5].

Even though high-throughput approaches generate impressive amounts of data, the comprehensive picture of the viral infection cycle can only be unraveled using a combination of different high-throughput and more classical techniques targeted at particular aspects of the infection cycle and specific viral proteins. Indeed, clues obtained in the course of high-throughput studies have proved to be instrumental for identifying prominent players in the viral life cycles and designing targeted studies in order to understand the functions of these proteins. For example, RNA sequencing analysis of SIRV2-infected cells has revealed that *ORF83a/b* transcripts are dominant, starting within the first minutes of infection and remaining abundant throughout the infection [13], predicting an important role for P83a/b. The x-ray structure of the P83a/b homolog from rudivirus SIRV1, which was solved during the structural genomics project, revealed a helix-turn-helix DNA-binding motif, suggesting that the protein might be involved in the processing of viral DNA [3]. Subsequent yeast two-hybrid analysis has showed that P83a/b interacts with the subunit of the host-encoded PCNA, a processivity factor for DNA polymerase [14]. These results indicate that P83a/b might be responsible for recruiting the PCNA for viral genome replication. Consequently, the complementary results

obtained from different studies illuminated a key role of P83a/b in SIRV2 propagation, providing a framework for further inquiries into the molecular mechanisms of its action.

An important step forward in understanding the biology of archaeal viruses has also been obtained for the example of STIV by the combination of different approaches. In this case, large-scale proteomic analysis of infected cells by 1D and 2D differential gel electrophoresis coupled with protein identification by mass spectrometry and activity-based protein profiling has been used to investigate the interaction between STIV and two *Sulfolobus solfataricus* strains (P2 and P2-2-12) that significantly differ with respect to their susceptibility to STIV [15,16]. In the highly susceptible P2-2-12 strain, only ten cellular proteins were changed in abundance. By contrast, 71 host proteins representing 33 different cellular pathways were affected during the infection of the poorly susceptible P2 strain [15,16], shedding some light on the basis of the different susceptibilities to infection of closely related *Sulfolobus* strains. Most notably, among the highly upregulated proteins were components of the antiviral CRISPR-Cas system and cell division proteins that are homologous to the eukaryotic endosomal sorting complexes required for transport (ESCRT) machinery [17,18], suggesting that the latter proteins play an important role in the STIV infection cycle. In eukaryotes, the ESCRT machinery is employed as the major escape route for many enveloped viruses, including important human pathogens, such as retroviruses, filoviruses, paramyxoviruses and herpesviruses [19]. Importantly, a recent study has confirmed a critical role of the archaeal ESCRT proteins during the late stages of STIV infection, specifically during the maturation of the virion membrane and possibly the opening of pyramidal portals located at the host cell envelope and involved in the release of viral progeny [20].

To conclude, a combination of different high-throughput approaches with more conventional biochemical and microscopic techniques has helped us to uncover the secrets of the enigmatic archaeal viruses. Even though studies on viruses thriving in extreme environments remain challenging, they are also highly rewarding. We have learned a great deal about the inventiveness of these viruses and new surprises are certainly expected in the future. The detailed understanding of archaeal viruses and their interactions with their hosts will enable comparisons with the bacterial and eukaryal virus–host systems, which should eventually reveal the general tendencies underlying the functioning of the virosphere.

"The detailed understanding of archaeal viruses and their interactions with their hosts will enable comparisons with the bacterial and eukaryal virus–host systems…"

Financial & competing interests disclosure

The authors have no relevant affiliations or financial involvement with any organization or entity with a financial interest in or financial conflict with the subject matter or materials discussed in the manuscript. This includes employment, consultancies, honoraria, stock ownership or options, expert testimony, grants or patents received or pending, or royalties.

No writing assistance was utilized in the production of this manuscript.

References

1 Prangishvili D. The wonderful world of archaeal viruses. *Annu. Rev. Microbiol.* 67, 565–585 (2013).

2 Pawlowski A, Rissanen I, Bamford JK, Krupovic M, Jalasvuori M. *Gammasphaerolipovirus*, a newly proposed bacteriophage genus, unifies viruses of halophilic archaea and thermophilic bacteria within the novel family Sphaerolipoviridae. *Arch. Virol.* 159, 1541–1554 (2014).

3 Krupovic M, White MF, Forterre P, Prangishvili D. Postcards from the edge: structural genomics of archaeal viruses. *Adv. Virus Res.* 82, 33–62 (2012).

4 Bize A, Karlsson EA, Ekefjard K *et al.* A unique virus release mechanism in the Archaea. *Proc. Natl Acad. Sci. USA* 106, 11306–11311 (2009).

5 Brumfield SK, Ortmann AC, Ruigrok V *et al.* Particle assembly and ultrastructural features associated with replication of the lytic archaeal virus *Sulfolobus* turreted icosahedral virus. *J. Virol.* 83, 5964–5970 (2009).

6 Iverson E, Stedman K. A genetic study of SSV1, the prototypical fusellovirus. *Front. Microbiol.* 3, 200 (2012).

7 Jaubert C, Danioux C, Oberto J *et al.* Genomics and genetics of *Sulfolobus islandicus* LAL14/1, a model hyperthermophilic archaeon. *Open Biol.* 3, 130010 (2013).

8 Wirth JF, Snyder JC, Hochstein RA *et al.* Development of a genetic system for the archaeal virus *Sulfolobus* turreted icosahedral virus (STIV). *Virology* 415, 6–11 (2011).

9 Veesler D, Ng TS, Sendamarai AK *et al.* Atomic structure of the 75 MDa extremophile *Sulfolobus* turreted icosahedral virus determined by CryoEM and x-ray crystallography. *Proc. Natl Acad. Sci. USA* 110, 5504–5509 (2013).

10 Krupovic M, Bamford DH. Double-stranded DNA viruses: 20 families and only five different architectural principles for virion assembly. *Curr. Opin. Virol.* 1, 118–124 (2011).

11 Prangishvili D, Koonin EV, Krupovic M. Genomics and biology of rudiviruses, a model for the study of virus–host interactions in Archaea. *Biochem. Soc. Trans.* 41, 443–450 (2013).

12 Quemin ER, Lucas S, Daum B *et al.* First insights into the entry process of hyperthermophilic archaeal viruses. *J. Virol.* 87, 13379–13385 (2013).

13 Quax TE, Voet M, Sismeiro O *et al.* Massive activation of archaeal defense genes during viral infection. *J. Virol.* 87, 8419–8428 (2013).

14 Gardner AF, Bell SD, White MF, Prangishvili D, Krupovic M. Protein–protein interactions leading to recruitment of the host DNA sliding clamp by the hyperthermophilic *Sulfolobus islandicus* rod-shaped virus 2. *J. Virol.* 88, 7105–7108 (2014).

15 Maaty WS, Selvig K, Ryder S *et al.* Proteomic analysis of *Sulfolobus solfataricus* during *Sulfolobus* turreted icosahedral virus infection. *J. Proteome Res.* 11, 1420–1432 (2012).

16 Maaty WS, Steffens JD, Heinemann J *et al.* Global analysis of viral infection in an archaeal model system. *Front. Microbiol.* 3, 411 (2012).

17 Moriscot C, Gribaldo S, Jault JM *et al.* Crenarchaeal CdvA forms double-helical filaments containing DNA and interacts with ESCRT-III-like CdvB. *PLoS ONE* 6, e21921 (2011).

18 Samson RY, Obita T, Freund SM, Williams RL, Bell SD. A role for the ESCRT system in cell division in archaea. *Science* 322, 1710–1713 (2008).

19 Votteler J, Sundquist WI. Virus budding and the ESCRT pathway. *Cell Host Microbe* 14, 232–241 (2013).

20 Snyder JC, Samson RY, Brumfield SK, Bell SD, Young MJ. Functional interplay between a virus and the ESCRT machinery in archaea. *Proc. Natl Acad. Sci. USA* 110, 10783–10787 (2013).

CHAPTER 2

Virus-host interactions in Archaea - the best is yet to come.

frontiers in Microbiology

REVIEW
published: 05 June 2015
doi: 10.3389/fmicb.2015.00552

Archaeal viruses at the cell envelope: entry and egress

Emmanuelle R. J. Quemin[1] *and Tessa E. F. Quax*[2]*

[1] Department of Microbiology, Institut Pasteur, Paris, France, [2] Molecular Biology of Archaea, Institute for Biology II - Microbiology, University of Freiburg, Freiburg, Germany

The cell envelope represents the main line of host defense that viruses encounter on their way from one cell to another. The cytoplasmic membrane in general is a physical barrier that needs to be crossed both upon viral entry and exit. Therefore, viruses from the three domains of life employ a wide range of strategies for perforation of the cell membrane, each adapted to the cell surface environment of their host. Here, we review recent insights on entry and egress mechanisms of viruses infecting archaea. Due to the unique nature of the archaeal cell envelope, these particular viruses exhibit novel and unexpected mechanisms to traverse the cellular membrane.

Keywords: archaea, archaeal virus, bacterial virus, virion entry, virion egress, archaeal membrane, pili, lysis

OPEN ACCESS

Edited by:
Mechthild Pohlschroder, University of Pennsylvania, USA

Reviewed by:
Jason W. Cooley, University of Missouri, USA
Jerry Eichler, Ben Gurion University of the Negev, Israel

***Correspondence:**
Tessa E. F. Quax, Molecular Biology of Archaea, Institute for Biology II - Microbiology, University of Freiburg, Schänzlestrasse 1, 79104 Freiburg, Germany
tessa.quax@biologie.uni-freiburg.de

Specialty section:
This article was submitted to Microbial Physiology and Metabolism, a section of the journal Frontiers in Microbiology

Received: *07 January 2015*
Accepted: *19 May 2015*
Published: *05 June 2015*

Citation:
Quemin ERJ and Quax TEF (2015) Archaeal viruses at the cell envelope: entry and egress. Front. Microbiol. 6:552. doi: 10.3389/fmicb.2015.00552

Introduction

Members of the three domains of life, Archaea, Bacteria and Eukarya, are all subject to viral infections. Viruses have been isolated from various environments, where they are often abundant, outnumbering prokaryotic cells by a factor of 10 (Bergh et al., 1989; Borsheim et al., 1990; Suttle, 2007). Viruses infecting archaea tend to display high morphological and genetic diversity compared to viruses of bacteria and eukaryotes (Pina et al., 2011). Several archaeal viral families have members, which display unique shapes that are not found amongst other viruses, such as a bottle, droplet or spiral (Prangishvili, 2013).

The cell envelope represents a major barrier for all viruses. In fact, the cell membrane has to be traversed twice by viruses to establish successful infection, first upon entry and secondly during exit. In order to cross the cell envelope, viruses have developed various strategies, each adapted to the membrane environment of their host.

The combination of high-throughput approaches with more classical techniques has shed light on the process of viral entry and release in some archaeal virus-host model systems. However, the detailed molecular mechanisms underlying the various stages of the viral life cycle remain poorly understood in archaea in general (Quemin et al., 2014). Recently, a few studies have focused on the adsorption at the surface of the archaeal host cell before viral entry and release of viral particles at the end of the infection cycle (Bize et al., 2009; Brumfield et al., 2009; Ceballos et al., 2012; Quemin et al., 2013; Deng et al., 2014). This has delivered the very first insights into the fashion in which viruses interact with the archaeal membrane.

The cell surface of archaea is fundamentally different from bacteria (Albers and Meyer, 2011). Archaeal membranes have an alternative lipid composition and generally lack a cell wall of peptidoglycan. In addition, the motility structures present at the surface of archaea are constructed from different building blocks than their bacterial counterparts (Pohlschroder et al., 2011). Gram positive bacteria contain a lipid bilayer covered by a thick peptidoglycan cell wall and gram negative cells are surrounded by two membranes with a thinner peptidoglycan in the periplasmic space in between. While bacteria typically contain a cell wall polymer of peptidoglycan (Typas et al., 2012),

peptidoglycan cell walls are absent from archaea. Instead, most archaea are surrounded by a thin proteinaceous surface layer (S-layer) that consists of glycosylated proteins, which are anchored in the cell membrane. In contrast to the peptidoglycan, which has a molecular composition that can be very similar from one species to another, S-layer proteins show a great diversity (Fagan and Fairweather, 2014). Hence, archaea exhibit specific features, in particular at the cell surface, which are not shared with bacteria and influence the mechanisms at play in the course of infection.

The first studies on archaeal viral entry and egress have shown that some archaeal viruses employ entry strategies that superficially resemble those of bacterial viruses (Quemin et al., 2013; Deng et al., 2014), while others utilize surprisingly novel exit mechanisms (Brumfield et al., 2009; Quax et al., 2011). Here we will give an overview of the first studies reporting viral interaction with the archaeal cell envelope, focusing on hyperthermophilic crenarchaeal viruses. Furthermore, current research permits comparison with corresponding mechanisms taking place during the viral cycle of bacterial viruses. We will discuss how features of cell surfaces compel viruses to employ specific strategies for entry and egress.

Viral Entry

A virus is able to infect only a few strains or species. Such specificity in interaction of viruses with their host is determined by the characteristics of entry, which in turn rely on the nature and structural peculiarities of the cell envelope. Adsorption as the first key step of the viral cycle is one of the most restrictive in terms of host range, depending on the accessibility and number of receptors present at the cell surface (Poranen et al., 2002). Structural proteins are found within the viral particle in metastable conformation and it is the interaction with the host cell, which leads to a more stable, lower-energy conformation of these proteins (Dimitrov, 2004). Indeed, virus entry and genome uncoating are energy-dependent processes and irreversible conformational change of the capsid proteins (CP) during adsorption triggers the release of the genome from the extracellular virions (Molineux and Panja, 2013). As a general rule, entry can be subdivided in two steps. For the well-studied viruses infecting bacteria, the first contact with the host is reversible and then, viruses attach irreversibly to a specific, saturable cell envelope receptor. Primary and secondary adsorptions can take place with the same receptor or, more frequently involve different players. Common cellular determinants in bacteria are peptidoglycan, lipopolysaccharide S (LPS), or cellular appendages (Poranen et al., 2002). Subsequently, delivery of the viral genome into the cellular cytoplasm happens through the cell wall and bacterial membrane. Indeed, the nature of the host cell wall has a great influence on the viral entry mechanism and different cell types expose diverse external envelope structures. Three main entry strategies have been reported for viral entry in bacteria: genome release through an icosahedral vertex; dissociation of virion at the cell envelope; and virion penetration via membrane fusion (Poranen et al., 2002). Thus far insights into the mechanisms of entry by archaeal viruses have been based on coincidental observations. However, more recently a few detailed analyses have provided a better understanding of the molecular mechanisms at play in archaeal virus-host systems from geothermal environments.

Interaction with Cellular Appendages

Filamentous, flexible viruses of the *Lipothrixviridae* family have been classified into four different genera partly based on the virion core and terminal structures. Indeed, the exposed filaments can vary in number from one (AFV9, *Acidianus* filamentous virus 9) to six (SIFV, *Sulfolobus islandicus* filamentous virus) or even form complex structures like claws (AFV1) or brushes (AFV2; Arnold et al., 2000; Bettstetter et al., 2003; Haring et al., 2005b; Bize et al., 2008). The high diversity of terminal structures observed in this particular family strongly suggests their involvement in cellular adsorption processes. Indeed, AFV1 particles terminate with claws that mediate attachment to cellular pili (Bettstetter et al., 2003). In the case of AFV2, the "bottle brush," a complex collar termini with two sets of filaments, should be able to interact with the surface of host cells directly since its specific host doesn't show any extracellular appendages (Haring et al., 2005b). In addition, SIFV virions display mop-like structures found in open or closed conformations (Arnold et al., 2000). Hence, lipothrixviruses are decorated with diverse and unique terminal structures that play a major role in recognition and interaction with the host cell.

In a similar manner, the stiff, filamentous rudivirus SIRV2 (*Sulfolobus islandicus* rod-shaped virus 2) was also shown to bind host pili by the three terminal fibers of virions. SIRV2 is one of the more appealing models to study virus-host interactions in archaea (Prangishvili et al., 2013). Recently published analyses concluded that adsorption occurs within the first minute of infection, much more efficiently than in halophilic archaeal systems for which binding requires several hours (Kukkaro and Bamford, 2009). The particles of SIRV2 specifically attach to the tip of host pili-like structures leading to a strong and irreversible interaction between the viral and cellular determinants (**Figure 1A**). Subsequently, viruses are found on the side of the appendages indicating a progression toward the cell surface where DNA entry is concomitant with virion disassembly (Quemin et al., 2013; **Figures 1C,D**). Thus, the three fibers located at the virion termini represent the viral anti-receptors involved in recognition of host cells and are responsible for the primary adsorption (**Figure 1B**). It is noteworthy that both ends of the virions have an equal binding capacity as previously noticed for the lipothrixvirus AFV1 (Bettstetter et al., 2003). The families *Lipothrixviridae* and *Rudiviridae* belong to the order *Ligamenvirales* and are known to attach to extracellular filaments (Prangishvili and Krupovic, 2012). Although AFV1 is capable of binding the side of host pili, a feature shared with bacterial leviviruses, cystoviruses and some tailed bacteriophages (Poranen et al., 2002), the interaction of SIRV2 with *Sulfolobus* filaments occurs initially via the tip. This resembles more closely the primary adsorption observed in the inoviruses (Rakonjac et al., 2011). All these data suggest that linear archaeal viruses employ a common strategy for the initiation of infection although

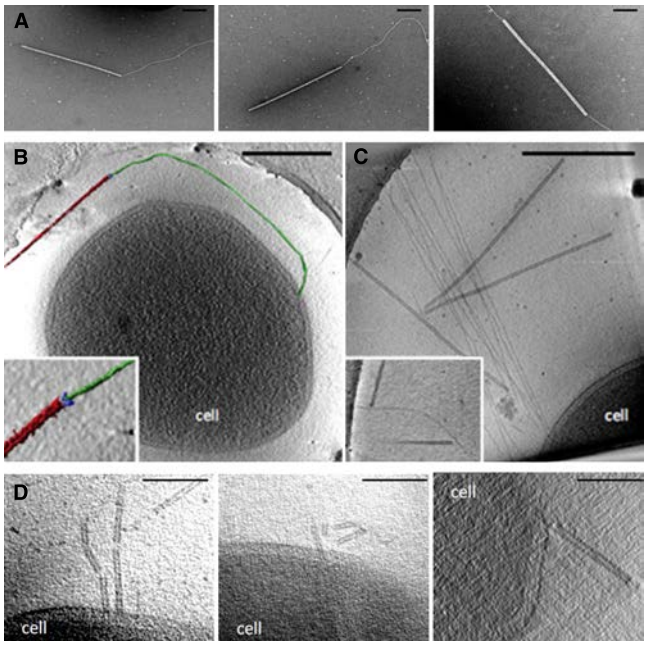

FIGURE 1 | Entry of SIRV2 in *S. islandicus* LAL14/1 cells.
(A) Transmission electron micrographs showing that SIRV2 virions interact with purified cellular filaments. Stained with 2% uranyl acetate for 2 min. Scale bar, 200 nm. Electron micrographs of SIRV2 interaction with *S. islandicus* LAL14/1 cells. Samples were collected 1 min post-infection and flash-frozen for electron cryotomography (cryo-ET). The virions interact both at the filament tips **(B)** and along the length of the filaments **(C)**. The lower left panel **(B)** also shows a segmented tomographic volume of the SIRV2 virion (red) attached to the tip of an *S. islandicus* filament (green). The three terminal virion fibers that appear to mediate the interaction are shown in blue (the inset depicts a magnified view of the interaction between the virion fibers and the tip of the filament). The inset in the lower right panel **(C)** depicts two virions bound to the sides of a single filament. Scale bars, 500 nm. **(D)** Tomographic slices through *S. islandicus* LAL14/1 cells at 1 min after infection with SIRV2 reveals partially disassembled SIRV2 virions at the cell surface. Adapted from (Quemin et al., 2013). Scale bar, 100 nm.

the molecular mechanisms involved are most likely to be distinct.

Interaction with Cell Surface

As a general rule, viral entry implies direct or indirect binding to the cell surface depending on whether a primary adsorption step is required. In the case of SIRV2, analysis of virus-resistant strains provided interesting candidates for the receptors of SIRV2 virions at the cell surface. In fact, two operons were identified: sso2386-2387 and sso3139-3141 (Deng et al., 2014). The former encodes proteins homologous to components of type IV pili and the latter presumably a membrane-associated cell surface complex. In *S. acidocaldarius*, the assembly ATPase, AapE, and the central membrane protein, AapF, homologous to Sso2386 and Sso2387, respectively, are both essential for the assembly of the type IV adhesive pilus (Henche et al., 2012). The sso3139-3141 operon is thought to encode a membrane bound complex, which could function as a secondary receptor for SIRV2 (Deng et al., 2014).

While entry of rudiviruses, and filamentous archaeal viruses in general, relies on two coordinated adsorption steps, other systems interact spontaneously with the cell surface. As far back as 1984, SSV1 (*Sulfolobus* spindle-shaped virus 1) was reported to exist in different states: isolated particles, incorporated in typical rosette-like aggregates or even bound to cell-derived membrane (Martin et al., 1984). The best known member of the *Fuselloviridae* family displays a lemon-shaped morphotype with terminal fibers at one of the two pointed ends (Stedman et al., 2015). The set of short, thin filaments of the α-fuselloviruses are involved in viral attachment and association with host-derived structures in general. However, the β-fuselloviruses, SSV6 and ASV1 (*Acidianus* spindle-shaped virus 1), exhibit more pleomorphic virions with three or four thick, slightly curved fibers (Krupovic et al., 2014). Although these appendages do not interact with each other as observed for SSV1, some genomic features strongly suggest that the fibers are composed of host-attachment proteins (Redder et al., 2009). Notably, one gene common to all family members (SSV1_C792) and two genes in β-fuselloviruses (SSV6_C213 and SSV6_B1232) encode for the protein responsible for terminal fibers. This protein shares a similar fold with the adsorption protein P2 of bacteriophage PRD1 (Grahn et al., 2002; Redder et al., 2009). In addition, the pointed end of the enveloped virus ABV (*Acidianus* bottle-shaped virus), from the *Ampullaviridae* family, is involved in attachment to membrane vesicles and formation of virion aggregates (Haring et al., 2005a). Therefore, even if data are still scarce, interaction with cellular membranes appears to be a common feature of hyperthermophilic archaeal viruses that contain a lipidic envelope. This particularly interesting feature merits further investigation.

Release of Viral Genome

Receptor recognition and binding typically induce a cascade of events that start with structural reorganization of the virions and lead to viral genome penetration through the cell envelope (Dimitrov, 2004). Non-enveloped viruses either inject the genome into the cell interior while leaving the empty capsid associated with the cell envelope or deliver the nucleic acids concomitantly with disassembly of the virion at the cell surface. Superficially, the entry of SIRV2 is similar to that of Ff inoviruses or flagellotrophic phages, which bind F-pili and flagella respectively (Guerrero-Ferreira et al., 2011; Rakonjac et al., 2011). First, the interaction with host pili-like structures has been shown and secondly, partially broken particles have been observed at the cellular membrane (Quemin et al., 2013; **Figure 1**). Notably, no archaeal retraction pili has been identified so far and flagella (called archaella in archaea) of *Sulfolobus* are considerably thicker than the filaments to which SIRV2 binds (Lassak et al., 2012). Additional experiments are needed in order to determine whether the mechanisms of SIRV2 translocation and genome delivery are related to those employed by Ff inoviruses and flagellotrophic bacteriophages, or are completely novel.

Lipid-containing viruses display unusual virion architecture and appear to make direct contact with the plasma membrane. It is reasonable to assume that enveloped viruses rely on a fundamentally different entry mechanism to that employed by non-enveloped filamentous viruses, such as rudiviruses. They might deliver their genetic material into the cell interior by fusion between the cytoplasmic membrane and the viral

envelope in a similar fashion to the eukaryotic enveloped viruses (Vaney and Rey, 2011). ATV (*Acidianus* two-tailed virus) resembles fuselloviruses with virions extruded from host cells as lemon-shaped. However, ATV has been classified within the *Bicaudaviridae* partly due to its peculiar life cycle (Haring et al., 2005c). Surprisingly, at temperatures close to that of its natural habitat (85°C), the released tail-less particles show the formation of two long tails protruding from the pointed ends. These extracellular developed tubes contain a thin filament inside and terminate in an anchor-like structure, not observed in the tail-less progeny. The two virion forms, tail-less and two-tailed, were reported to be infectious, thereby indicating that the termini are not involved in the initial stages of infection (Prangishvili et al., 2006b). However, genomic analysis as well as molecular studies highlighted some viral encoded proteins that could be important during infection. For example, the three largest open reading frames (ORFs) and one of the CPs have putative coiled-coil domains, which are usually associated with specific protein–protein interactions and protein complex formation. Moreover, two other proteins carry proline-rich regions (ORF567 and ORF1940) similar to the protein TPX and are abundant during infection by lipothrixvirus TTV1 (*Thermoproteus tenax* virus 1; Neumann and Zillig, 1990). Notably, in particular the motif TPTP has been implicated in host protein recognition for the African swine fever virus (Kay-Jackson, 2004). Finally, pull-down experiments provided evidence for a strong interaction between the ATV protein P529 and OppAss as well as cellular Sso1273, encoding a viral AAA ATPase. The cellular OppAss, an N-linked glycoprotein, is most likely part of the binding components of the ABC transporter system. It is encoded within the same operon and could serve as a receptor. It has also been proposed that the AAA ATPase would trigger ATV host cell receptor recognition. This is based on the hypothetical requirement of its endonuclease activity for the cleavage of the circular viral DNA prior to entry in the cell (Erdmann et al., 2011).

The case of the bottle-shaped virus ABV is also particularly intriguing. The enveloped particles display an elaborate organization with a funnel-shaped body composed of the "stopper," the nucleoprotein core and the inner core. Presumably, the so-called "stopper" takes part in binding to the cellular receptor and is the only component to which the viral genome is directly attached. Therefore, it has been suggested that the "stopper" could play the role of an "injection needle" in a manner similar to that found in bacterial viruses. Actually, it is well known that head-tail bacteriophages belonging to the *Caudovirales* order use this transmembrane pathway for channeling and delivery of nucleic acids (Poranen et al., 2002). The inner core of ABV virions is the most labile part and could undergo structural changes that would facilitate the release of viral DNA (Haring et al., 2005a). Whether the energy accumulated in the structure after packaging of the supercoiled nucleoprotein is sufficient to transport the whole genetic material into the cytoplasm is unclear. However, relaxation of the nucleoprotein filament, wound up as an inverse cone, concomitantly with its funneling into the cell could be an efficient way of utilizing the energy stored during packaging for DNA injection as previously observed in bacteria (Poranen et al., 2002).

How archaeal viruses interact with the cell surface and deliver the viral genome into the host cytoplasm is still puzzling. Some systems, rudiviruses and lipothrixviruses, show similarities to their bacterial counterparts while others, fuselloviruses, bicaudavirus and ampullavirus, could be related to eukaryotic viruses. Identification of the pathways utilized by both filamentous and unique lipid-containing viruses represents a great challenge and one of the main issues that should be tackled in the near future. It is noteworthy that the S-layer is generally composed of heavily glycosylated proteins and many archaeal viruses exhibit glycosylated capsid proteins. The fact that several glycosyltransferases are encoded in viral genomes (Krupovic et al., 2012) is particularly intriguing. Indeed, protein glycosylation is an important process, which could be involved in virion stability and/or interaction with the host cell (Markine-Goriaynoff et al., 2004; Meyer and Albers, 2013).

Strategies for Viral Escape from the Host Cell

The last and essential step of the viral infection cycle is escape of viral particles from the host cell. So far, the egress mechanism has been analyzed for only a small subset of archaeal viruses (Torsvik and Dundas, 1974; Bize et al., 2009; Brumfield et al., 2009; Snyder et al., 2013a). Some viruses are completely lytic, while others are apparently stably produced without causing evident cell lysis (Bettstetter et al., 2003). In addition, there are temperate archaeal viruses with a lysogenic life cycle for which induction of virion production in some cases leads to cell disruption (Janekovic et al., 1983; Schleper et al., 1992; Prangishvili et al., 2006b).

The release mechanisms utilized by archaeal viruses can be divided in two categories: those for which the cell membrane is disrupted and those where the membrane integrity remains intact. The strategy for egress is linked with the assembly mechanism of new virions. Some archaeal viruses are known to mature inside the cell cytoplasm and provoke lysis, such as STIV1 (*Sulfolobus* turreted icosahedral virus) and SIRV2 (Bize et al., 2009; Brumfield et al., 2009; Fu et al., 2010). However, most non-lytic viruses undergo final maturation concomitantly with passage through the cell membrane (Roine and Bamford, 2012) or even in the extracellular environment, as observed for ATV (Haring et al., 2005c).

Cell Membrane Disruption

Lysis by Complete Membrane Disruption

Disruption of cell membranes can be caused by lytic or temperate viruses. In case of temperate viruses the cell lysis occurs typically after induction of virus replication and virion formation. Virion production of lysogenic viruses can be induced by various stimuli such as; UV radiation, addition of mitomycin C, starvation or shift from aerobic to anaerobic growth (Janekovic et al., 1983; Schleper et al., 1992; Prangishvili et al., 2006b; Mochizuki et al., 2011).

The first archaeal viruses were isolated from hypersaline environments long before archaea were recognized as a separate domain of life (Torsvik and Dundas, 1974; Wais et al., 1975). These viruses infect halophiles, which belong to the phylum

Euryarchaeota. The viral particles exhibit a head-and-tail morphology classical for bacterial viruses. Infection with these viruses resulted in complete lysis of the cells, suggested by a decrease in culture turbidity. Later on, more euryarchaeal viruses were isolated from hypersaline or anaerobic environments, and several of these viruses displayed non-head-tail morphologies such as icosahedral or spindle shapes. Again, in some cases, optical density diminishes with time after viral infection, indicating that a part of these viruses initiate cell lysis (Bath and Dyall-Smith, 1998; Porter et al., 2005; Jaakkola et al., 2012). However, several euryarchaeal viruses apparently do not cause cell lysis.

Amongst hyperthermophilic crenarchaeal viruses there has only been a single report of a decrease in the turbidity of infected cultures (Prangishvili et al., 2006a). In this case, induction of virion production of the lysogenic viruses TTV1-3 led to cell lysis, which was measured by decreasing turbidity (Janekovic et al., 1983). Lysis induced by archaeal viruses can either be coupled with virion production (Jaakkola et al., 2012), or take place after the largest virion burst, therefore raising the possibility of an additional release mechanism in such systems (Bath and Dyall-Smith, 1998; Porter et al., 2005, 2013). Although measurement of optical density is a classical method for the characterization of viral cycles and decrease in turbidity has been observed for several archaeal viruses, no molecular mechanism to achieve complete membrane disruption in archaea has been proposed as yet.

Bacterial virus-host systems are widely studied and as a result the mechanism of lysis used by bacterial viruses is better understood. Bacterial viruses typically induce cell lysis by degradation of the cell wall, which is achieved by muralytic endolysins (Young, 2013). In addition, most bacterial viruses encode small proteins named holins (Bernhardt et al., 2001a,b; Catalao et al., 2013). Holins usually accumulate harmlessly in the bacterial cell membrane until a critical concentration is reached and nucleation occurs. Nucleation results in formation of two dimensional aggregates, "holin rafts," that rapidly expand and create pores in lipid layers through which the endolysins can reach the cell wall (Young, 2013). In gram negative bacteria the presence of an outer membrane requires additional virus-encoded proteins, spanins, which are suggested to induce fusion of the inner and outer membrane (Berry et al., 2012). After an initial degradation of the peptidoglycan cell wall, the cells burst due to osmotic pressure, explaining total loss of turbidity observed for infected bacterial cultures (Berry et al., 2012). Accurate timing of lysis is essential for successful virus reproduction and is achieved by regulation of holin expression (Young, 2013). Since archaea lack a peptidoglycan cell wall, endolysin-holin egress systems are not effective in archaea. Only a few archaeal species contain a peptidoglycan-like cell wall consisting of pseudomurein polymers (Albers and Meyer, 2011). The oligosaccharide backbone and amino acid interbridges of murein and pseudomurein are different, rendering bacterial endolysins ineffective to pseudomurein (Visweswaran et al., 2011). However, pseudomurein degrading enzymes are encoded by a few archaeal viruses infecting methanogens; the integrated provirus ψM100 from *Methanothermobacter wolfeii* and the virus ψM1 infecting *M. marburgensis* (Luo et al., 2001). How these intracellularly produced viral endolysis traverse the archaeal cell membrane in order to degrade the pseudomurein cell wall is not clear, since the mandatory pore forming holins have not been identified in the genomes of these viruses. The possible presence of archaeal holins could be currently overlooked, as genes encoding holins share generally very little sequence similarity, making it difficult to predict their presence in genomes (Saier and Reddy, 2015).

The large majority of archaea lack a pseudomurein cell wall. Therefore instead of a endolysin-holin system, a fundamentally different lysis mechanism would be required for release of virions from these cell wall lacking archaea. One hypothesis is that archaeal viruses employ holins to disrupt the cell membrane, possibly combined with proteolytic enzymes in order to degrade the S-layer. To date there are about a dozen holin homologs identified in archaeal genomes based on sequence similarity (Reddy and Saier, 2013), but none of the predicted proteins have been tested *in vivo*. Moreover, not a single holin-encoding gene has been identified in the genomes of currently isolated archaeal viruses (Reddy and Saier, 2013; Saier and Reddy, 2015). In addition, specific enzymes capable of S-layer degradation are currently unknown and S-layer proteins and sugars display a large diversity in different species (Albers and Meyer, 2011). Thus in contrast to bacterial endolysins that degrade peptidoglycan cell walls of virtually all bacteria, specific tailor made proteases would be required to degrade archaeal S-layers of different species.

Lysis by Formation of Defined Apertures

The egress mechanism of only two archaeal viruses (STIV1 and SIRV2) has been studied in high molecular detail. Both employ a release mechanism that relies on the formation of pyramidal shaped egress structures, which are unique to archaeal systems (Bize et al., 2009; Brumfield et al., 2009; Quax et al., 2011; Snyder et al., 2011). At first glance, both viruses were regarded as non-lytic viruses, since a decrease in cell culture turbidity was never observed (Prangishvili et al., 1999; Rice et al., 2004). However, the use of several electron microscopy techniques clearly showed that the two viruses induced cell lysis (Bize et al., 2009; Brumfield et al., 2009). Their particular lysis mechanism yields empty cell ghosts explaining the maintenance of culture turbidity.

Infection by SIRV2 and STIV1 leads to formation of several pyramidal shaped structures on the cell membrane of *S. islandicus* and *S. solfataricus* respectively (Bize et al., 2009; Brumfield et al., 2009; Prangishvili and Quax, 2011; **Figure 2A**). These virus-associated pyramids (VAPs) exhibit sevenfold rotational symmetry and protrude trough the S-layer (Quax et al., 2011; Snyder et al., 2011; **Figures 2B–D**). At the end of the infection cycle, the seven facets of the VAPs open outward, generating large apertures through which assembled virions exit from the cell (Fu et al., 2010; Quax et al., 2011; Daum et al., 2014; **Figure 2B**). The baseless VAP consist of multiple copies of a 10 kDa viral encoded protein, PVAP (STIV1_C92/SIRV2_P98) (Quax et al., 2010; Snyder et al., 2013a). This protein contains a transmembrane domain, but lacks a signal sequence and seems to be inserting in membranes based on hydrophobicity of its transmembrane domain (Quax et al., 2010; Daum et al., 2014). PVAP has the remarkable property to form pyramidal structures in virtually all biological membranes, as was demonstrated by heterologos

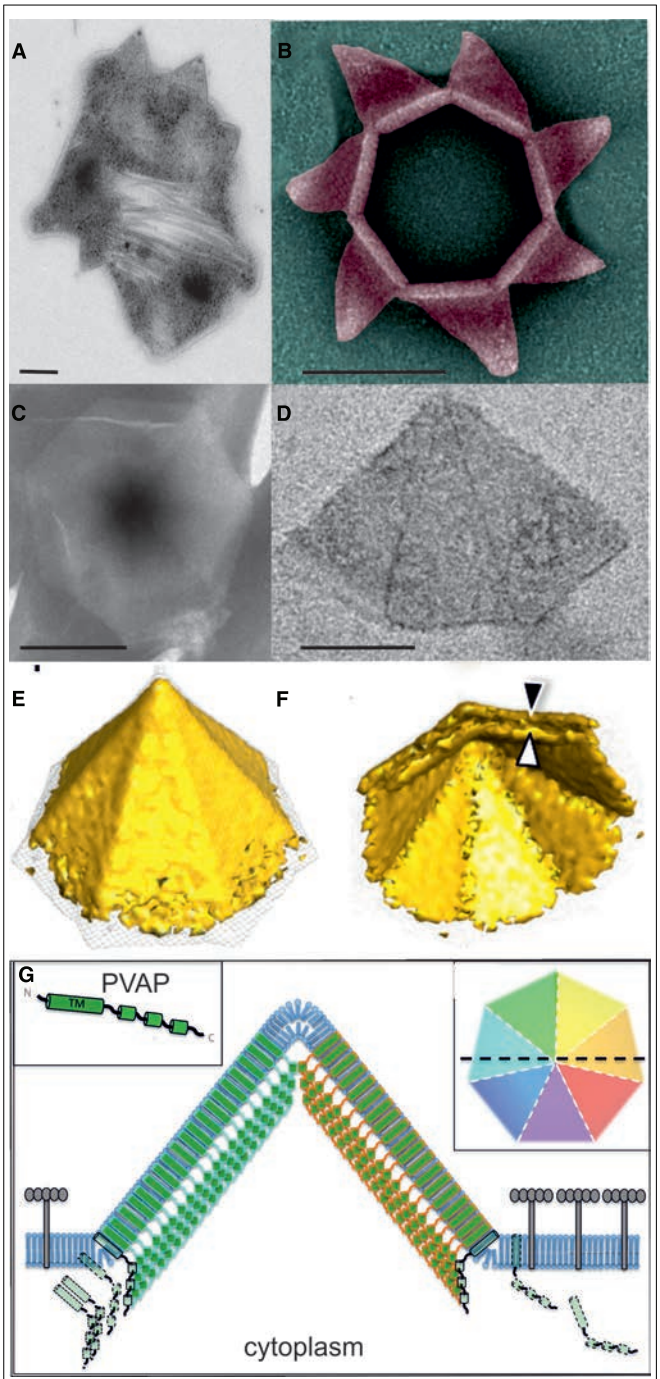

FIGURE 2 | Remarkable archaeal virion egress structure. (A) Scanning electron micrograph of an SIRV2 infected *S. islandicus* cell displaying several VAPs. **(B)** Transmission electron micrographs of isolated VAPs in closed and **(C)** open conformation. **(D)** Solid representation of VAP obtained by subtomogram averaging displaying the **(E)** outside and **(F)** interior. **(G)** Model of VAP formation. Adapted from (Bize et al., 2009; Quax et al., 2011; Daum et al., 2014). Scale bar, 100 nm.

expression of PVAP in archaea, bacteria and eukaryotes (Quax et al., 2011; Snyder et al., 2013a; Daum et al., 2014).

Nucleation of the PVAP-induced structure starts on the cell membrane, most likely with the formation of a heptamer of PVAP subunits (Daum et al., 2014). The structures develop by the outward expansion of their seven triangular facets. They reach sizes of up to 200 nm in diameter, both in natural and heterologous systems (Quax et al., 2011; Daum et al., 2014). In contrast to bacterial holin rafts, the formation of VAPs is not a sudden process depending on a critical protein concentration. PVAP transcripts steadily increase throughout the infection cycle and PVAP integrates in the membrane until late stages of infection (Quax et al., 2010, 2013; Maaty et al., 2012). Although VAPs are slowly formed, their actual opening is quite rapid (Bize et al., 2009; Brumfield et al., 2009; Snyder et al., 2011; Daum et al., 2014). The nature of the signal triggering this opening has not been identified yet. VAPs, formed after heterologous PVAP expression, in bacteria and eukaryotes were never observed in open conformation, suggesting that an archaeal specific factor is required (Daum et al., 2014). It has been proposed that the archaeal ESCRT (Endosomal Sorting Complex Required for Transport) machinery could be involved in the STIV1 VAP-based exit (Snyder et al., 2013b). Considering that genes encoding ESCRT machinery are specifically down regulated during SIRV2 infection (Quax et al., 2013), and that STIV1 contains in contrast to SIRV2 an inner lipid layer (Veesler et al., 2013), STIV1 requirement of the ESCRT system might be independent from VAP-induced lysis.

The ultrastructure of VAPs of SIRV2 was studied by whole cell cryo-tomography and subtomogram averaging. This revealed the presence of two layers, of which the outer one is continuous with the cell membrane and presumably formed by the N-terminal transmembrane domain (Daum et al., 2014; **Figures 2E,F**). The inner layer represents a protein sheet formed by tight protein–protein interactions of the C-terminal domain of the protein (Daum et al., 2014). The strong interactions between PVAP monomers are suggested to exclude most lipids and membrane proteins from the VAP assembly site, in a similar fashion as holin raft formation (White et al., 2011; **Figure 2G**). S-layer proteins are anchored in the membrane, and consequently will be excluded from the VAP assembly site, providing a strategy for VAP protrusion through the S-layer.

The described VAP-based egress mechanism is archaeal specific. Homologues of PVAP are only found amongst some archaeal viruses (Quax et al., 2010). However, the majority of archaeal viruses lack PVAP, suggesting that they rely on a different and as yet unknown mechanism for egress.

Viral Extrusion without Membrane Disruption

While the first isolated archaeal viruses were lytic, subsequent characterization of more viruses revealed that the large majority do not cause lysis of the host cell. To date, lytic viruses make up half of the viruses infecting euryarchaeota, and only three in crenarchaea (Torsvik and Dundas, 1974; Wais et al., 1975; Janekovic et al., 1983; Bize et al., 2009; Brumfield et al., 2009; Pina et al., 2011). In addition, some studies indicate that free virions can be observed before disruption of archaeal cells, suggesting that another egress mechanism exists, which preserves cell membrane integrity. It might be possible that some lytic archaeal viruses have been currently overlooked due to special characteristics of their lysis mechanism, as was the case for STIV1 and SIRV2 (Prangishvili et al., 1999; Rice et al., 2004). Nevertheless, the low

number of lytic archaeal viruses contrasts with the situation in bacteria, for which lytic viruses are very common. The majority of archaeal viruses are thought to be continuously produced without integrating into the host genome or killing their hosts (Pina et al., 2014). This equilibrium between viruses and cells is referred to as a "stable carrier state" (Bettstetter et al., 2003; Prangishvili and Garrett, 2005; Prangishvili et al., 2006a). The nature of this stable carrier state and the mechanisms by which virions are extruded from archaea without causing cell lysis, remain poorly understood.

In contrast to the situation in archaea, the majority of bacterial viruses are lytic. Almost all bacterial viruses exit via the holin based mechanism described above. However, an exception to the rule are the bacterial filamentous viruses belonging to the *Inoviridae* that egress without causing cell lysis (Rakonjac et al., 2011). The majority of the inoviruses infect gram negative bacteria. Assembly of inoviruses is finalized during particle extrusion. The interaction between the packaging signal of the viral genome and the cellular membrane initiates the exit step (Russel and Model, 1989). Virally encoded proteins are thought to form pores in the inner membrane through which the DNA is extruded. Multiple copies of the major CP accumulate in the inner membrane and associate with the ssDNA viral genome while it is passing through the virus-induced pores (Rakonjac et al., 1999). A barrel-like structure in the outer membrane permits the release of progeny and is composed of multiple copies of a virus-encoded protein with homology to proteins of type II secretion systems and type IV pili (Marciano et al., 2001). Alternatively, other inoviruses use the host secretion machinery to traverse the outer membrane (Davis et al., 2000; Bille et al., 2005). Even though replication of the viral genome and constituents might burden the cell, the infection of inoviruses does not lead to cell death and is a continuous process. There are several archaeal filamentous viruses known. However, filamentous archaeal viruses are not related to the bacterial inoviruses, nor encode homologs of the secretion-like proteins involved in egress of inoviruses (Janekovic et al., 1983; Bize et al., 2009; Quax et al., 2010; Pina et al., 2014). Therefore the filamentous archaeal viruses must rely on an alternative mechanism for viral extrusion from the cell.

Interestingly, lipid-containing archaeal viruses are quite common (Roine and Bamford, 2012). There are some archaeal icosahedral viruses that possess an inner membrane, such as STIV and SH1 (Bamford et al., 2005; Khayat et al., 2005; Porter et al., 2005). In addition, the filamentous lipothrixviruses (Janekovic et al., 1983; Arnold et al., 2000; Bettstetter et al., 2003), the spherical virus PSV (*Pyrobaculum* spherical virus; Haring et al., 2004) and the pleiomorphic euryarchaeal viruses (Pietila et al., 2009, 2013) all contain an external lipid envelope. The lipids are typically derived from the host cell. Several eukaryotic viruses contain a membrane that is usually obtained during "budding," a process by which particles egress without disturbing the membrane integrity. Eukaryotic enveloped viruses either encode their own scission proteins, or hijack vesicle formation machinery of their host (Rossman and Lamb, 2013). Archaea are also reported to produce vesicles (Soler et al., 2008; Ellen et al., 2011), and the machinery responsible for vesicle production might be utilized by lipid envelope containing viruses in archaea as well. In particular, the pleiomorphic viruses infecting euryarchaea are likely to be released through budding as their envelope has the same lipid composition as the host they infect (Pietila et al., 2009; Roine et al., 2010).

The most common scission machinery employed by eukaryotic viruses is the ESCRT system (Votteler and Sundquist, 2013). In eukaryotes these proteins are responsible for endosomal sorting in the multi vesicular body. Well-characterized viruses such as Ebola and human immunodeficiency virus (HIV) use the ESCRT proteins during egress (Harty et al., 2000; Weissenhorn et al., 2013). Interestingly, proteins homologous to ESCRT components have been identified in several archaea, where they are involved in cell division (Lindas et al., 2008; Samson et al., 2008; Makarova et al., 2010; Pelve et al., 2011). These proteins represent potential players in budding-like extrusion processes in archaea. The mechanism underlying the release of temperate archaeal viruses remains largely unexplored and represents an appealing area of research that should shed light on original and unconventional strategies.

Concluding Remarks

The last few years have shown a steady increase in an understanding of archaeal virus-host interactions, therefore revealing the first insights into viral interactions with the archaeal membrane. Viruses have developed various strategies to cross the membrane. These strategies are adapted to the nature of the cell envelope of their host. Some archaeal viruses employ fascinating novel mechanisms, while others appear to rely on processes that at first sight are analogous to their bacterial counterparts. Additional research will help to determine to which extent bacterial, eukaryotic and archaeal virospheres are evolutionary related. The uniqueness of the archaeal cell surface, and the diversity of the currently described archaeal entry and egress mechanisms, argue in favor of future discovery of more innovative and surprising molecular mechanisms.

Acknowledgments

We thank Dr. D. Prangishvili and Dr. S. Gill for critical reading of the manuscript, useful suggestions and comments. This work was supported by l'Agence Nationale de la Recherche, project "EXAVIR," by a FWO Pegasus Marie Curie fellowship to TQ. and by a grant from the French government and the Université Pierre et Marie Curie, Paris VI to EQ.

References

Albers, S. V., and Meyer, B. H. (2011). The archaeal cell envelope. *Nat. Rev. Microbiol.* 9, 414–426. doi: 10.1038/nrmicro2576

Arnold, H. P., Zillig, W., Ziese, U., Holz, I., Crosby, M., Utterback, T., et al. (2000). A novel lipothrixvirus, SIFV, of the extremely thermophilic crenarchaeon *Sulfolobus*. *Virology* 267, 252–266. doi: 10.1006/viro.1999.0105

Bamford, D. H., Ravantti, J. J., Ronnholm, G., Laurinavicius, S., Kukkaro, P., Dyall-Smith, M., et al. (2005). Constituents of SH1, a novel lipid-containing virus infecting the halophilic euryarchaeon *Haloarcula hispanica*. *J. Virol.* 79, 9097–9107. doi: 10.1128/jvi.79.14.9097-9107.2005

Bath, C., and Dyall-Smith, M. L. (1998). His1, an archaeal virus of the Fuselloviridae family that infects *Haloarcula hispanica*. *J. Virol.* 72, 9392–9395.

Bergh, O., Borsheim, K. Y., Bratbak, G., and Heldal, M. (1989). High abundance of viruses found in aquatic environments. *Nature* 340, 467–468. doi: 10.1038/340467a0

Bernhardt, T. G., Struck, D. K., and Young, R. (2001a). The lysis protein E of phi X174 is a specific inhibitor of the MraY-catalyzed step in peptidoglycan synthesis. *J. Biol. Chem.* 276, 6093–6097. doi: 10.1074/jbc.M00763 8200

Bernhardt, T. G., Wang, I. N., Struck, D. K., and Young, R. (2001b). A protein antibiotic in the phage Qbeta virion: diversity in lysis targets. *Science* 292, 2326–2329. doi: 10.1126/science.1058289

Berry, J., Rajaure, M., Pang, T., and Young, R. (2012). The spanin complex is essential for lambda lysis. *J. Bacteriol.* 194, 5667–5674. doi: 10.1128/JB.01245-12

Bettstetter, M., Peng, X., Garrett, R. A., and Prangishvili, D. (2003). AFV1, a novel virus infecting hyperthermophilic archaea of the genus *Acidianus*. *Virology* 315, 68–79. doi: 10.1016/S0042-6822(03)00481-1

Bille, E., Zahar, J. R., Perrin, A., Morelle, S., Kriz, P., Jolley, K. A., et al. (2005). A chromosomally integrated bacteriophage in invasive meningococci. *J. Exp. Med.* 201, 1905–1913. doi: 10.1084/jem.20050112

Bize, A., Karlsson, E. A., Ekefjard, K., Quax, T. E., Pina, M., Prevost, M. C., et al. (2009). A unique virus release mechanism in the Archaea. *Proc. Natl. Acad. Sci. U.S.A.* 106, 11306–11311. doi: 10.1073/pnas.0901238106

Bize, A., Peng, X., Prokofeva, M., Maclellan, K., Lucas, S., Forterre, P., et al. (2008). Viruses in acidic geothermal environments of the Kamchatka Peninsula. *Res. Microbiol.* 159, 358–366. doi: 10.1016/j.resmic.2008.04.009

Borsheim, K. Y., Bratbak, G., and Heldal, M. (1990). Enumeration and biomass estimation of planktonic bacteria and viruses by transmission electron microscopy. *Appl. Environ. Microbiol.* 56, 352–356.

Brumfield, S. K., Ortmann, A. C., Ruigrok, V., Suci, P., Douglas, T., and Young, M. J. (2009). Particle assembly and ultrastructural features associated with replication of the lytic archaeal virus *Sulfolobus* turreted icosahedral virus. *J. Virol.* 83, 5964–5970. doi: 10.1128/jvi.02668-08

Catalao, M. J., Gil, F., Moniz-Pereira, J., Sao-Jose, C., and Pimentel, M. (2013). Diversity in bacterial lysis systems: bacteriophages show the way. *FEMS Microbiol. Rev.* 37, 554–571. doi: 10.1111/1574-6976.12006

Ceballos, R. M., Marceau, C. D., Marceau, J. O., Morris, S., Clore, A. J., and Stedman, K. M. (2012). Differential virus host-ranges of the Fuselloviridae of hyperthermophilic Archaea: implications for evolution in extreme environments. *Front. Microbiol.* 3:295. doi: 10.3389/fmicb.2012.00295

Daum, B., Quax, T. E., Sachse, M., Mills, D. J., Reimann, J., Yildiz, O., et al. (2014). Self-assembly of the general membrane-remodeling protein PVAP into sevenfold virus-associated pyramids. *Proc. Natl. Acad. Sci. U.S.A.* 111, 3829–3834. doi: 10.1073/pnas.1319245111

Davis, B. M., Lawson, E. H., Sandkvist, M., Ali, A., Sozhamannan, S., and Waldor, M. K. (2000). Convergence of the secretory pathways for cholera toxin and the filamentous phage, CTXphi. *Science* 288, 333–335. doi: 10.1126/science.288.5464.333

Deng, L., He, F., Bhoobalan-Chitty, Y., Martinez-Alvarez, L., Guo, Y., and Peng, X. (2014). Unveiling cell surface and type IV secretion proteins responsible for archaeal *Rudivirus* entry. *J. Virol.* 88, 10264–10268. doi: 10.1128/jvi.01495-14

Dimitrov, D. S. (2004). Virus entry: molecular mechanisms and biomedical applications. *Nat. Rev. Microbiol.* 2, 109–122. doi: 10.1038/nrmicro817

Ellen, A. F., Rohulya, O. V., Fusetti, F., Wagner, M., Albers, S. V., and Driessen, A. J. (2011). The sulfolobicin genes of *Sulfolobus acidocaldarius* encode novel antimicrobial proteins. *J. Bacteriol.* 193, 4380–4387. doi: 10.1128/jb.05028-11

Erdmann, S., Scheele, U., and Garrett, R. A. (2011). AAA ATPase p529 of *Acidianus* two-tailed virus ATV and host receptor recognition. *Virology* 421, 61–66. doi: 10.1016/j.virol.2011.08.029

Fagan, R. P., and Fairweather, N. F. (2014). Biogenesis and functions of bacterial S-layers. *Nat. Rev. Microbiol.* 12, 211–222. doi: 10.1038/nrmicro3213

Fu, C. Y., Wang, K., Gan, L., Lanman, J., Khayat, R., Young, M. J., et al. (2010). *In vivo* assembly of an archaeal virus studied with whole-cell electron cryotomography. *Structure* 18, 1579–1586. doi: 10.1016/j.str.2010.10.005

Grahn, A. M., Daugelavicius, R., and Bamford, D. H. (2002). The small viral membrane associated protein P32 is involved in bacteriophage PRD1 DNA entry. *J. Virol.* 76, 4866–4872. doi: 10.1128/jvi.76.10.4866-4872.2002

Guerrero-Ferreira, R. C., Viollier, P. H., Ely, B., Poindexter, J. S., Georgieva, M., Jensen, G. J., et al. (2011). Alternative mechanism for bacteriophage adsorption to the motile bacterium *Caulobacter crescentus*. *Proc. Natl. Acad. Sci. U.S.A.* 108, 9963–9968. doi: 10.1073/pnas.1012388108

Haring, M., Peng, X., Brugger, K., Rachel, R., Stetter, K. O., Garrett, R. A., et al. (2004). Morphology and genome organization of the virus PSV of the hyperthermophilic archaeal genera *Pyrobaculum* and *Thermoproteus*: a novel virus family, the Globuloviridae. *Virology* 323, 233–242. doi: 10.1016/j.virol.2004.03.002

Haring, M., Rachel, R., Peng, X., Garrett, R. A., and Prangishvili, D. (2005a). Viral diversity in hot springs of Pozzuoli, Italy, and characterization of a unique archaeal virus, *Acidianus* bottle-shaped virus, from a new family, the Ampullaviridae. *J. Virol.* 79, 9904–9911. doi: 10.1128/JVI.79.15.9904-9911.2005

Haring, M., Vestergaard, G., Brugger, K., Rachel, R., Garrett, R. A., and Prangishvili, D. (2005b). Structure and genome organization of AFV2, a novel archaeal lipothrixvirus with unusual terminal and core structures. *J. Bacteriol.* 187, 3855–3858. doi: 10.1128/JB.187.11.3855-3858.2005

Haring, M., Vestergaard, G., Rachel, R., Chen, L., Garrett, R. A., and Prangishvili, D. (2005c). Virology: independent virus development outside a host. *Nature* 436, 1101–1102. doi: 10.1038/4361101a

Harty, R. N., Brown, M. E., Wang, G., Huibregtse, J., and Hayes, F. P. (2000). A PPxY motif within the VP40 protein of Ebola virus interacts physically and functionally with a ubiquitin ligase: implications for filovirus budding. *Proc. Natl. Acad. Sci. U.S.A.* 97, 13871–13876. doi: 10.1073/pnas.250277297

Henche, A. L., Ghosh, A., Yu, X., Jeske, T., Egelman, E., and Albers, S. V. (2012). Structure and function of the adhesive type IV pilus of *Sulfolobus acidocaldarius*. *Environ. Microbiol.* 14, 3188–3202. doi: 10.1111/j.1462-2920.2012.02898.x

Jaakkola, S. T., Penttinen, R. K., Vilen, S. T., Jalasvuori, M., Ronnholm, G., Bamford, J. K., et al. (2012). Closely related archaeal *Haloarcula hispanica* icosahedral viruses HHIV-2 and SH1 have nonhomologous genes encoding host recognition functions. *J. Virol.* 86, 4734–4742. doi: 10.1128/jvi.06666-11

Janekovic, D., Wunderl, S., Holz, I., Zillig, W., Gierl, A., and Neumann, H. (1983). TTV1, TTV2 and TTV3, a family of viruses of the extremely thermophilic, anaerobic, sulfur reducing archaebacterium *Thermoproteus tenax*. *Mol. Gen. Genet.* 192, 39–45. doi: 10.1007/BF00327644

Kay-Jackson, P. C. (2004). The CD2v protein of African swine fever virus interacts with the actin-binding adaptor protein SH3P7. *J. Gen. Virol.* 85, 119–130. doi: 10.1099/vir.0.19435-0

Khayat, R., Tang, L., Larson, E. T., Lawrence, C. M., Young, M., and Johnson, J. E. (2005). Structure of an archaeal virus capsid protein reveals a common ancestry to eukaryotic and bacterial viruses. *Proc. Natl. Acad. Sci. U.S.A.* 102, 18944–18949. doi: 10.1073/pnas.0506383102

Krupovic, M., Quemin, E. R., Bamford, D. H., Forterre, P., and Prangishvili, D. (2014). Unification of the globally distributed spindle-shaped viruses of the Archaea. *J. Virol.* 88, 2354–2358. doi: 10.1128/JVI.02941-13

Krupovic, M., White, M. F., Forterre, P., and Prangishvili, D. (2012). Postcards from the edge: structural genomics of archaeal viruses. *Adv. Virus Res.* 82, 33–62. doi: 10.1016/B978-0-12-394621-8.00012-1

Kukkaro, P., and Bamford, D. H. (2009). Virus-host interactions in environments with a wide range of ionic strengths. *Environ. Microbiol. Rep.* 1, 71–77. doi: 10.1111/j.1758-2229.2008.00007.x

Lassak, K., Ghosh, A., and Albers, S. V. (2012). Diversity, assembly and regulation of archaeal type IV pili-like and non-type-IV pili-like surface structures. *Res. Microbiol.* 163, 630–644. doi: 10.1016/j.resmic.2012.10.024

Lindas, A. C., Karlsson, E. A., Lindgren, M. T., Ettema, T. J., and Bernander, R. (2008). A unique cell division machinery in the Archaea. *Proc. Natl. Acad. Sci. U.S.A.* 105, 18942–18946. doi: 10.1073/pnas.0809467105

Luo, Y., Pfister, P., Leisinger, T., and Wasserfallen, A. (2001). The genome of archaeal prophage PsiM100 encodes the lytic enzyme responsible for autolysis of Methanothermobacter wolfeii. *J. Bacteriol.* 183, 5788–5792. doi: 10.1128/jb.183.19.5788-5792.2001

Maaty, W. S., Steffens, J. D., Heinemann, J., Ortmann, A. C., Reeves, B. D., Biswas, S. K., et al. (2012). Global analysis of viral infection in an archaeal model system. *Front. Microbiol.* 3:411. doi: 10.3389/fmicb.2012.00411

Makarova, K. S., Yutin, N., Bell, S. D., and Koonin, E. V. (2010). Evolution of diverse cell division and vesicle formation systems in Archaea. *Nat. Rev. Microbiol.* 8, 731–741. doi: 10.1038/nrmicro2406

Markine-Goriaynoff, N., Gillet, L., Van Etten, J. L., Korres, H., Verma, N., and Vanderplasschen, A. (2004). Glycosyltransferases encoded by viruses. *J. Gen. Virol.* 85, 2741–2754.

Marciano, D. K., Russel, M., and Simon, S. M. (2001). Assembling filamentous phage occlude pIV channels. *Proc. Natl. Acad. Sci. U.S.A.* 98, 9359–9364. doi: 10.1073/pnas.161170398

Martin, A., Yeats, S., Janekovic, D., Reiter, W.-D., Aicher, W., and Zillig W. (1984). SAV 1, a temperate u.v.-inducible DNA virus-like particle from the archaeabacterium *Sulfolobus acidocaldarius* isolate B12. *EMBO J.* 3, 2165–2168.

Meyer, B. H., and Albers, S. V. (2013). Hot and sweet: protein glycosylation in *Crenarchaeota*. *Biochem. Soc. Trans.* 41, 384–3892. doi: 10.1042/BST20120296

Mochizuki, T., Sako, Y., and Prangishvili, D. (2011). Provirus induction in hyperthermophilic archaea: characterization of *Aeropyrum pernix* spindle-shaped virus 1 and *Aeropyrum pernix* ovoid virus 1. *J. Bacteriol.* 193, 5412–5419. doi: 10.1128/jb.05101-11

Molineux, I. J., and Panja, D. (2013). Popping the cork: mechanisms of phage genome ejection. *Nat. Rev. Microbiol.* 11, 194–204. doi: 10.1038/nrmicro2988

Neumann, H., and Zillig, W. (1990). The TTV1-encoded viral protein TPX: primary structure of the gene and the protein. *Nucleic Acids Res.* 18, 195. doi: 10.1093/nar/18.1.195

Pelve, E. A., Lindas, A. C., Martens-Habbena, W., De La Torre, J. R., Stahl, D. A., and Bernander, R. (2011). Cdv-based cell division and cell cycle organization in the thaumarchaeon Nitrosopumilus maritimus. *Mol. Microbiol.* 82, 555–566. doi: 10.1111/j.1365-2958.2011.07834.x

Pietila, M. K., Laurinmaki, P., Russell, D. A., Ko, C. C., Jacobs-Sera, D., Butcher, S. J., et al. (2013). Insights into head-tailed viruses infecting extremely halophilic archaea. *J. Virol.* 87, 3248–3260. doi: 10.1128/jvi.03397-12

Pietila, M. K., Roine, E., Paulin, L., Kalkkinen, N., and Bamford, D. H. (2009). An ssDNA virus infecting archaea: a new lineage of viruses with a membrane envelope. *Mol. Microbiol.* 72, 307–319. doi: 10.1111/j.1365-2958.2009.06642.x

Pina, M., Basta, T., Quax, T. E., Joubert, A., Baconnais, S., Cortez, D., et al. (2014). Unique genome replication mechanism of the archaeal virus AFV1. *Mol. Microbiol.* 92, 1313–1325. doi: 10.1111/mmi.12630

Pina, M., Bize, A., Forterre, P., and Prangishvili, D. (2011). The archeoviruses. *FEMS Microbiol. Rev.* 35, 1035–1054. doi: 10.1111/j.1574-6976.2011.00280.x

Pohlschroder, M., Ghosh, A., Tripepi, M., and Albers, S. V. (2011). Archaeal type IV pilus-like structures—evolutionarily conserved prokaryotic surface organelles. *Curr. Opin. Microbiol.* 14, 357–363. doi: 10.1016/j.mib.2011.03.002

Poranen, M. M., Daugelavicius, R., and Bamford, D. H. (2002). Common principles in viral entry. *Annu. Rev. Microbiol.* 56, 521–538. doi: 10.1146/annurev.micro.56.012302.160643

Porter, K., Kukkaro, P., Bamford, J. K., Bath, C., Kivela, H. M., Dyall-Smith, M. L., et al. (2005). SH1: a novel, spherical halovirus isolated from an Australian hypersaline lake. *Virology* 335, 22–33. doi: 10.1016/j.virol.2005.01.043

Porter, K., Tang, S. L., Chen, C. P., Chiang, P. W., Hong, M. J., and Dyall-Smith, M. (2013). PH1: an archaeovirus of *Haloarcula hispanica* related to SH1 and HHIV–2. *Archaea* 2013, 456318. doi: 10.1155/2013/456318

Prangishvili, D. (2013). The wonderful world of archaeal viruses. *Annu. Rev. Microbiol.* 67, 565–585. doi: 10.1146/annurev-micro-092412-155633

Prangishvili, D., Arnold, H. P., Gotz, D., Ziese, U., Holz, I., Kristjansson, J. K., et al. (1999). A novel virus family, the Rudiviridae: structure, virus-host interactions and genome variability of the *Sulfolobus* viruses SIRV1 and SIRV2. *Genetics* 152, 1387–1396.

Prangishvili, D., Forterre, P., and Garrett, R. A. (2006a). Viruses of the Archaea: a unifying view. *Nat. Rev. Microbiol.* 4, 837–848. doi: 10.1038/nrmicro1527

Prangishvili, D., Vestergaard, G., Haring, M., Aramayo, R., Basta, T., Rachel, R., et al. (2006b). Structural and genomic properties of the hyperthermophilic archaeal virus ATV with an extracellular stage of the reproductive cycle. *J. Mol. Biol.* 359, 1203–1216. doi: 10.1016/j.jmb.2006.04.027

Prangishvili, D., and Garrett, R. A. (2005). Viruses of hyperthermophilic Crenarchaea. *Trends Microbiol.* 13, 535–542. doi: 10.1016/j.tim.2005.08.013

Prangishvili, D., Koonin, E. V., and Krupovic, M. (2013). Genomics and biology of Rudiviruses, a model for the study of virus-host interactions in Archaea. *Biochem. Soc. Trans.* 41, 443–450. doi: 10.1042/BST20120313

Prangishvili, D., and Krupovic, M. (2012). A new proposed taxon for double-stranded DNA viruses, the order "Ligamenvirales". *Arch. Virol.* 157, 791–795. doi: 10.1007/s00705-012-1229-7

Prangishvili, D., and Quax, T. E. (2011). Exceptional virion release mechanism: one more surprise from archaeal viruses. *Curr. Opin. Microbiol.* 14, 315–320. doi: 10.1016/j.mib.2011.04.006

Quax, T. E., Krupovic, M., Lucas, S., Forterre, P., and Prangishvili, D. (2010). The *Sulfolobus* rod-shaped virus 2 encodes a prominent structural component of the unique virion release system in Archaea. *Virology* 404, 1–4. doi: 10.1016/j.virol.2010.04.020

Quax, T. E., Lucas, S., Reimann, J., Pehau-Arnaudet, G., Prevost, M. C., Forterre, P., et al. (2011). Simple and elegant design of a virion egress structure in Archaea. *Proc. Natl. Acad. Sci. U.S.A.* 108, 3354–3359. doi: 10.1073/pnas.1018052108

Quax, T. E., Voet, M., Sismeiro, O., Dillies, M. A., Jagla, B., Coppee, J. Y., et al. (2013). Massive activation of archaeal defense genes during viral infection. *J. Virol.* 87, 8419–8428. doi: 10.1128/jvi.01020-13

Quemin, E. R., Lucas, S., Daum, B., Quax, T. E., Kuhlbrandt, W., Forterre, P., et al. (2013). First insights into the entry process of hyperthermophilic archaeal viruses. *J. Virol.* 87, 13379–13385. doi: 10.1128/jvi.02742-13

Quemin, E. R., Prangishvili, D., and Krupovic, M. (2014). Hard out there: understanding archaeal virus biology. *Future Virol.* 9, 703–706. doi: 10.2217/FVL.14.52

Rakonjac, J., Bennett, N. J., Spagnuolo, J., Gagic, D., and Russel, M. (2011). Filamentous bacteriophage: biology, phage display and nanotechnology applications. *Curr. Issues Mol. Biol* 13, 51–76.

Rakonjac, J., Feng, J., and Model, P. (1999). Filamentous phage are released from the bacterial membrane by a two-step mechanism involving a short C-terminal fragment of pIII. *J. Mol. Biol.* 289, 1253–1265. doi: 10.1006/jmbi.1999.2851

Redder, P., Peng, X., Brugger, K., Shah, S. A., Roesch, F., Greve, B., et al. (2009). Four newly isolated fuselloviruses from extreme geothermal environments reveal unusual morphologies and a possible interviral recombination mechanism. *Environ. Microbiol.* 11, 2849–2862. doi: 10.1111/j.1462-2920.2009.02009.x

Reddy, B. L., and Saier, M. H. Jr. (2013). Topological and phylogenetic analyses of bacterial holin families and superfamilies. *Biochim. Biophys. Acta* 1828, 2654–2671. doi: 10.1016/j.bbamem.2013.07.004

Rice, G., Tang, L., Stedman, K., Roberto, F., Spuhler, J., Gillitzer, E., et al. (2004). The structure of a thermophilic archaeal virus shows a double-stranded DNA viral capsid type that spans all domains of life. *Proc. Natl. Acad. Sci. U.S.A.* 101, 7716–7720. doi: 10.1073/pnas.0401773101

Roine, E., and Bamford, D. H. (2012). Lipids of archaeal viruses. *Archaea* 2012, 384919. doi: 10.1155/2012/384919

Roine, E., Kukkaro, P., Paulin, L., Laurinavicius, S., Domanska, A., Somerharju, P., et al. (2010). New, closely related haloarchaeal viral elements with different nucleic Acid types. *J. Virol.* 84, 3682–3689. doi: 10.1128/jvi.01879-09

Rossman, J. S., and Lamb, R. A. (2013). Viral membrane scission. *Annu. Rev. Cell Dev. Biol.* 29, 551–569. doi: 10.1146/annurev-cellbio-101011-155838

Russel, M., and Model, P. (1989). Genetic analysis of the filamentous bacteriophage packaging signal and of the proteins that interact with it. *J. Virol.* 63, 3284–3295.

Saier, M. H. Jr., and Reddy, B. L. (2015). Holins in bacteria, eukaryotes, and archaea: multifunctional xenologues with potential biotechnological and biomedical applications. *J. Bacteriol.* 197, 7–17. doi: 10.1128/jb.02046-14

Samson, R. Y., Obita, T., Freund, S. M., Williams, R. L., and Bell, S. D. (2008). A role for the ESCRT system in cell division in archaea. *Science* 322, 1710–1713. doi: 10.1126/science.1165322

Schleper, C., Kubo, K., and Zillig, W. (1992). The particle SSV1 from the extremely thermophilic archaeon *Sulfolobus* is a virus: demonstration of infectivity and of transfection with viral DNA. *Proc. Natl. Acad. Sci. U.S.A.* 89, 7645–7649. doi: 10.1073/pnas.89.16.7645

Snyder, J. C., Brumfield, S. K., Kerchner, K. M., Quax, T. E., Prangishvili, D., and Young, M. J. (2013a). Insights into a viral lytic pathway from an archaeal virus-host system. *J. Virol.* 87, 2186–2192. doi: 10.1128/jvi.02956-12

Snyder, J. C., Samson, R. Y., Brumfield, S. K., Bell, S. D., and Young, M. J. (2013b). Functional interplay between a virus and the ESCRT machinery in archaea. *Proc. Natl. Acad. Sci. U.S.A.* 110, 10783–10787. doi: 10.1073/pnas.1301605110

Snyder, J. C., Brumfield, S. K., Peng, N., She, Q., and Young, M. J. (2011). *Sulfolobus* turreted icosahedral virus c92 protein responsible for the formation of pyramid-like cellular lysis structures. *J. Virol.* 85, 6287–6292. doi: 10.1128/jvi.00379-11

Soler, N., Marguet, E., Verbavatz, J. M., and Forterre, P. (2008). Virus-like vesicles and extracellular DNA produced by hyperthermophilic archaea of the order Thermococcales. *Res. Microbiol.* 159, 390–399. doi: 10.1016/j.resmic.2008.04.015

Stedman, K. M., Deyoung, M., Saha, M., Sherman, M. B., and Morais, M. C. (2015). Structural insights into the architecture of the hyperthermophilic *Fusellovirus* SSV1. *Virology* 474, 105–109. doi: 10.1016/j.virol.2014.10.014

Suttle, C. A. (2007). Marine viruses—major players in the global ecosystem. *Nat. Rev. Microbiol.* 5, 801–812. doi: 10.1038/nrmicro1750

Torsvik, T., and Dundas, I. D. (1974). Bacteriophage of *Halobacterium salinarium*. *Nature* 248, 680–681. doi: 10.1038/248680a0

Typas, A., Banzhaf, M., Gross, C. A., and Vollmer, W. (2012). From the regulation of peptidoglycan synthesis to bacterial growth and morphology. *Nat. Rev. Microbiol.* 10, 123–136. doi: 10.1038/nrmicro2677

Vaney, M. C., and Rey, F. A. (2011). Class II enveloped viruses. *Cell. Microbiol.* 13, 1451–1459. doi: 10.1111/j.1462-5822.2011.01653.x

Veesler, D., Ng, T. S., Sendamarai, A. K., Eilers, B. J., Lawrence, C. M., Lok, S. M., et al. (2013). Atomic structure of the 75 MDa extremophile *Sulfolobus* turreted icosahedral virus determined by CryoEM and X-ray crystallography. *Proc. Natl. Acad. Sci. U.S.A.* 110, 5504–5509. doi: 10.1073/pnas.1300601110

Visweswaran, G. R., Dijkstra, B. W., and Kok, J. (2011). Murein and pseudomurein cell wall binding domains of bacteria and archaea—a comparative view. *Appl. Microbiol. Biotechnol.* 92, 921–928. doi: 10.1007/s00253-011-3637-0

Votteler, J., and Sundquist, W. I. (2013). Virus budding and the ESCRT pathway. *Cell Host Microbe* 14, 232–241. doi: 10.1016/j.chom.2013.08.012

Wais, A. C., Kon, M., Macdonald, R. E., and Stollar, B. D. (1975). Salt-dependent bacteriophage infecting *Halobacterium cutirubrum* and *H. halobium*. *Nature* 256, 314–315. doi: 10.1038/256314a0

Weissenhorn, W., Poudevigne, E., Effantin, G., and Bassereau, P. (2013). How to get out: ssRNA enveloped viruses and membrane fission. *Curr. Opin. Virol.* 3, 159–167. doi: 10.1016/j.coviro.2013.03.011

White, R., Chiba, S., Pang, T., Dewey, J. S., Savva, C. G., Holzenburg, A., et al. (2011). Holin triggering in real time. *Proc. Natl. Acad. Sci. U.S.A.* 108, 798–803. doi: 10.1073/pnas.1011921108

Young, R. (2013). Phage lysis: do we have the hole story yet? *Curr. Opin. Microbiol.* 16, 790–797. doi: 10.1016/j.mib.2013.08.008

Conflict of Interest Statement: The authors declare that the research was conducted in the absence of any commercial or financial relationships that could be construed as a potential conflict of interest.

CHAPTER 3

Unique spindle-shaped viruses in Archaea.

JVI Journals.ASM.org

Unification of the Globally Distributed Spindle-Shaped Viruses of the *Archaea*

Mart Krupovic,[a] Emmanuelle R. J. Quemin,[a] Dennis H. Bamford,[b] Patrick Forterre,[a,c] David Prangishvili[a]

Institut Pasteur, Unité Biologie Moléculaire du Gène chez les Extrêmophiles, Département de Microbiologie, Paris, France[a]; Department of Biosciences and Institute of Biotechnology, Viikki Biocenter 2, University of Helsinki, Helsinki, Finland[b]; Laboratoire de Biologie Moléculaire du Gène chez les Extrêmophiles, Institut de Génétique et Microbiologie, CNRS UMR 8621, Université Paris Sud, Orsay, France[c]

Viruses with spindle-shaped virions are abundant in diverse environments. Over the years, such viruses have been isolated from a wide range of archaeal hosts. Evolutionary relationships between them remained enigmatic, however. Here, using structural proteins as markers, we define familial ties among these "dark horses" of the virosphere and segregate all spindle-shaped viruses into two distinct evolutionary lineages, corresponding to *Bicaudaviridae* and *Fuselloviridae*. Our results illuminate the utility of structure-based virus classification and bring additional order to the virosphere.

Recent environmental studies have revealed that viruses with spindle-shaped virions are widespread and abundant in diverse habitats, including deep sea hydrothermal vents (1–3), hypersaline environments (4–7), anoxic freshwaters (8), cold Antarctic lakes (9), terrestrial hot springs (10–15), and acidic mines (16, 17), where these viruses often outnumber the ubiquitous head-tailed viruses and are likely to play an important ecological role. All spindle-shaped viruses that have been isolated so far exclusively infect archaeal hosts (18); none are associated with the two other cellular domains, the *Bacteria* or *Eukarya*. The virus species are classified by the International Committee on Taxonomy of Viruses (ICTV) into two families (*Fuselloviridae* and *Bicaudaviridae*) and one unassigned genus (*Salterprovirus*). Notably, there is certain flexibility in virion morphology among spindle-shaped viruses, even for members of the same family. For example, genetically close members of the genera *Alphafusellovirus* and *Betafusellovirus* (family *Fuselloviridae*) (19) are very different morphologically (compare Fig. 1B1 and B2). Importantly, virion flexibility might represent an inherent, biologically relevant property common to all spindle-shaped viruses. It has been demonstrated recently that under certain conditions, virions of halophilic salterprovirus His1 (5, 20) and hyperthermophilic virus *Pyrococcus abysii* virus 1 (PAV1) (2) also undergo structural transformation from regular spindles into elongated particles (2, 21, 22).

Over the years, a number of spindle-shaped viruses that could not be assigned to the existing taxa based on genome similarity have been isolated from phylogenetically distant archaeal lineages, including *Thermococcales* (*Thermococcus prieurii* virus 1 [TPV1] [3] and PAV1 [2, 23]), *Methanococcales* (*Methanococcus voltae* A3 VLP [A3-VLP] [24, 25]), *Desulfurococcales* (*Aeropyrum pernix* spindle-shaped virus 1 [APSV1] [26]), and *Sulfolobales* (*Sulfolobus tengchongensis* spindle-shaped viruses 1 and 2 [STSV1 and -2] [27, 28]). For a long time, these viruses remained "dark horses" of the archaeal virosphere, with their origins and relationships to other archaeal viruses being untraceable. Here, we assess the morphological and genomic diversity of this prominent virus group, reveal the evolutionary relationships between different spindle-shaped viruses, and refine their classification.

Viral proteins underlying the key principles of virion assembly and architecture provide a valuable marker for tracing deep evolutionary connections between distantly related viruses (29–31). Major capsid proteins (MCP) have been experimentally characterized for *Sulfolobus spindle-shaped virus 1* (SSV1), a type species of the *Fuselloviridae* (32, 33), *Acidianus two-tailed virus* (ATV), a type species of the *Bicaudaviridae* (34), and, more recently, for *His1 virus*, a type species of the genus *Salterprovirus* (22). We used this information to perform an in-depth genome analysis of all known unclassified spindle-shaped viruses.

Spindle-shaped viruses with tails. *Acidianus two-tailed virus* (ATV) is the sole member of the *Bicaudaviridae* family. A remarkable characteristic of this virus is that it can develop long tails at both pointed ends of the spindle-shaped virion outside the host cell (34, 35). The ATV virion consists of several structural proteins; high-resolution structures for two of these proteins are known (36, 37). Among the unclassified viruses, only STSV1 (27) and STSV2 (28) were found to encode homologues of the major structural protein gp131 of ATV (Fig. 2A and B). Notably, the same protein was indeed identified as the MCP of STSV1 (27). In addition, comparative genome analysis revealed that ATV has 18 genes in common with STSV1 and STSV2 (Fig. 2A), suggesting an evolutionary relationship between these viruses. Unlike ATV, STSV1 and STSV2 each have a single long tail emanating from one of the pointed ends of the virion (Fig. 1). Furthermore, extracellular morphogenesis has not been demonstrated for these viruses (27). STSV1 and STSV2 apparently possess more simple virions than ATV: (i) they do not encode homologues of the structural ATV protein gp273 (Fig. 2C), and (ii) a paralog of the ATV MCP, gp145 (Fig. 2B), also a structural component of the ATV virion, is not encoded by STSV1 or STSV2. Based on the shared gene content and similarities between their MCPs, we propose to classify STSV1 and STSV2 into a new genus, *Betabicaudavirus*, within the family *Bicaudaviridae*.

Received 7 October 2013 **Accepted** 3 December 2013

Published ahead of print 11 December 2013

Address correspondence to Mart Krupovic, krupovic@pasteur.fr, or David Prangishvili, david.prangishvili@pasteur.fr.

doi:10.1128/JVI.02941-13

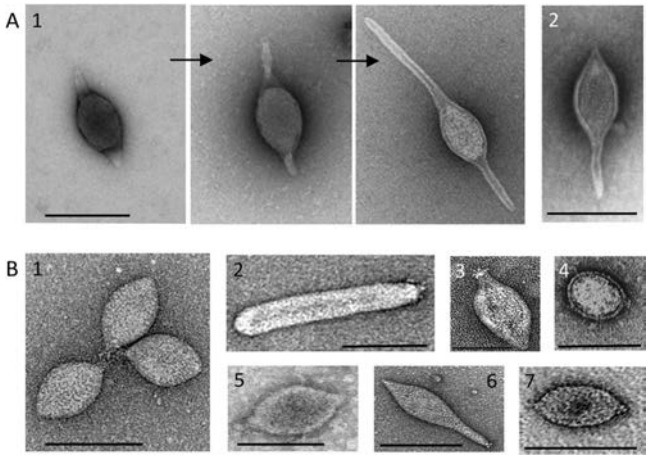

FIG 1 Negative-contrast electron micrographs of viral species with spindle-shaped virions. (A1) Three stages of extracellular tail development of ATV, the type species of the family *Bicaudaviridae* (35); (A2) STSV1 (27). (B1) SSV1, the type species of the genus *Alphafusellovirus*, family *Fuselloviridae*; (B2) *Sulfolobus spindle-shaped virus 6* (SSV6), the type species of the genus *Betafusellovirus*, family *Fuselloviridae* (19); (B3) TPV1 (3); (B4), A3-VLP (25); (B5) PAV1 (2); (B6) APSV1 (26); (B7) His1 (20), the type species of the genus *Salterprovirus*. Scale bars, 100 nm.

Tailless spindle-shaped viruses. Fuselloviruses and salterprovirus His1 typically display regular spindle-shaped morphology and build their virions using utterly different structural proteins than bicaudaviruses. Whereas MCPs of bicaudaviruses display a unique helix bundle topology (Fig. 2C) (37, 38), those of fuselloviruses and His1 are characterized by two hydrophobic domains (22, 32). Thus, it has been suggested that hyperthermophilic fuselloviruses and halophilic salterprovirus His1 might be evolutionarily related (5, 22), despite infecting hosts residing in different archaeal phyla—*Crenarchaeota* and *Euryarchaeota*, respectively. Notably, fuselloviruses encode two paralogous MCPs (VP1 and VP3), while His1 suffices with the product of a single gene (open reading frame 21 [ORF21]). We have investigated the genomes of unclassified spindle-shaped viruses for the presence of ORFs that would (i) display sequence similarity to the MCPs of fuselloviruses and His1 and (ii) share similar hydrophobicity profiles with these proteins. (Homologs were searched for using BLASTP [39], while hydrophobicity profiles were calculated with TMHMM v2 [40]). In all of the viral genomes studied, we could identify ORFs encoding proteins matching our search criteria (Fig. 3A and B). Notably, ORF121 of PAV1, which was identified as a homologue of fuselloviral MCPs (22), has been identified as the major structural component of the PAV1 virions (23), confirming the validity of our approach. Likewise, we identified homologous MCPs in TPV1, A3-VLP, and APSV1 (Fig. 3), which previously eluded functional annotation. The identification of a fusellovirus-like MCP in APSV1 is perhaps most unexpected; based on virion morphology, APSV1 was originally considered to be related to bicaudaviruses (26). However, our analysis shows that it is related to fuselloviruses instead. Although sequence identities between the MCPs of different viruses were generally low, the overall pairwise sequence similarities were typically above 50% (Fig. 3C). (Sequence identities and similarities were calculated using SIAS [http://imed.med.ucm.es/Tools/sias.html], considering the physicochemical properties of aligned amino acids.) Notably, all of the predicted MCPs contain positively charged amino acid residues in the short hydrophilic tail following the C-terminal

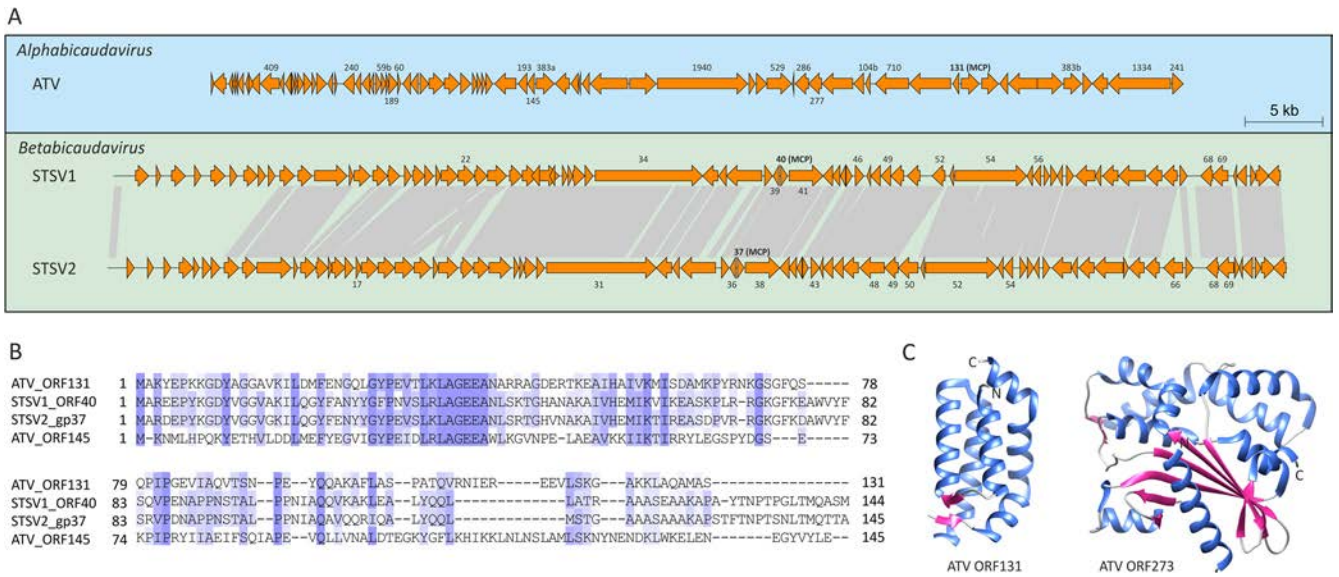

FIG 2 Evolutionary relationship between spindle-shaped viruses with tails. (A) Genome maps of *Acidianus* two-tailed virus (ATV) and *Sulfolobus tengchongensis* spindle-shaped viruses 1 and 2 (STSV1 and -2). Homologous regions shared between STSV1 and STSV2 are connected by gray shading. Names of ATV genes that have homologs in STSV1 and/or STSV2 are indicated; the names of corresponding STSV1 and STSV2 genes are also shown. The new genus "*Betabicaudavirus*" within the family *Bicaudaviridae* is proposed for classification of STSV1 and STSV2. (B) Multiple alignment of major capsid protein sequences of ATV, STSV1, and STSV2. Note that products of ATV ORF145 and ORF131 are paralogs. GenBank identification (GI) numbers: ATV ORF131, 75750454; ATV ORF145, 75750440; STSV1 ORF40, 51980166; STSV2 gp37, 448260184. (C) Available X-ray structures of two ATV structural proteins, ORF131 (PDB ID no. 3FAJ) and ORF273 (PDB ID no. 4ATS), both displaying unique folds. Whereas a homologue of ORF131 is encoded by both STSV1 and STSV2 (A and B), ORF273 is unique to ATV.

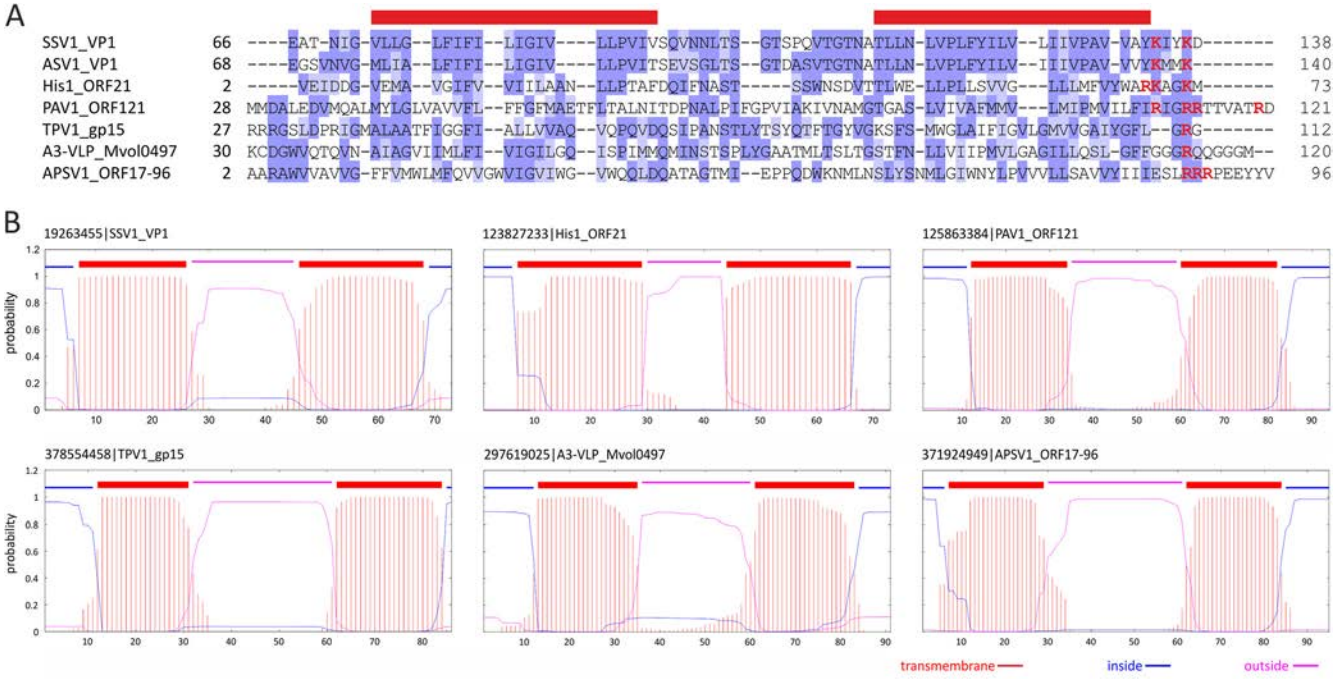

C

	SSV1	ASV1	APSV1	PAV1	TPV1	A3-VLP	His1	
SSV1	100%(100%)							*Alphafusellovirus*
ASV1	81%(95%)	100%(100%)						*Betafusellovirus*
APSV1	12%(49%)	14%(52%)	100%(100%)					*Gammafusellovirus*
PAV1	19%(56%)	18%(57%)	10%(53%)	100%(100%)				*Deltafusellovirus*
TPV1	24%(61%)	25%(63%)	15%(56%)	12%(54%)	100%(100%)			*Deltafusellovirus*
A3-VLP	22%(64%)	21%(61%)	16%(55%)	14%(65%)	28%(70%)	100%(100%)		*Deltafusellovirus*
His1	42%(77%)	40%(76%)	17%(55%)	14%(55%)	26%(64%)	22%(55%)	100%(100%)	*Epsilonfusellovirus (Salterprovirus)*

FIG 3 Evolutionary relationship between tailless spindle-shaped viruses. (A) Multiple alignment of major capsid protein sequences. Red bars above the alignment denote the positions of the two hydrophobic α-helixes. The positively charged residues (R and K) found at the hydrophilic C-terminal tail following the hydrophobic domain are highlighted in red. GenBank identification (GI) numbers: SSV1 VP1, 19263455; ASV1 VP1, 270281782; His1 ORF21, 123827233; PAV1 ORF121, 125863384; TPV1 gp15, 378554458; A3-VLP Mvol0497, 297619025; APSV1 orf17-96, 371924949. (B) Hydrophobicity profiles of the capsid proteins aligned in panel A. (C) Pairwise identity and similarity (in parentheses) values calculated from the alignment shown in panel A using SIAS (http://imed.med.ucm.es/Tools/sias.html). Sequence similarity was calculated by taking into consideration the following physicochemical properties of aligned amino acids: aromatic (F, Y, W), hydrophobic (V, I, L, M, C, A, F, Y, W), aliphatic (V, I, L), positively charged (R, K, H), negatively charged (D, E), polar (N, Q, H, K, R, D, E, T, S), or small (A, T, S, G). The proposed taxonomic classification of the tailless spindle-shaped viruses is shown on the right.

hydrophobic domain (Fig. 3A). However, the functional significance of these residues remains to be tackled experimentally.

Horizontal gene transfer plays a profound role in shaping the genomic landscape of viruses: any given gene in a viral genome, including those responsible for essential functions, such as genome replication and virion formation, can be replaced by nonhomologous counterparts (41–44). Consequently, virus classification based on a small number of shared characters does not always faithfully represent the evolutionary history of a given viral group. With this caveat in mind, we sought to further validate the grouping of tailless spindle-shaped viruses by performing an exhaustive comparative genomic analysis of spindle-shaped viruses. We found that besides the MCP genes, these viruses share an overlapping set of genes encoding various proteins involved in viral genome replication and integration (Fig. 4). For example, APSV1 encodes four other proteins with homologues in tailless spindle-

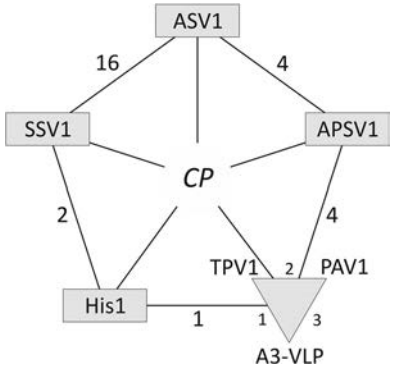

FIG 4 An overlapping gene set shared by tailless spindle-shaped viruses. The diagram shows that in addition to the capsid protein (CP) gene, the viruses share an overlapping set of genes. The numbers next to the lines connecting the viruses denote the number of shared genes. PAV1, TPV1, and A3-VLP are proposed to be grouped into a new genus "*Deltafusellovirus*," and are indicated with a triangle.

shaped viruses, including the DnaA-like AAA$^+$ ATPase believed to be involved in genome replication (45). Similarly, in addition to the MCP, PAV1 shares a three-gene cassette with A3-VLP (23, 46), while with TPV1, it shares two other genes for putative minor structural proteins (3). Notably, our analysis has shown that all spindle-shaped viruses encode AAA$^+$ ATPases. Interestingly, however, the DnaA-like ATPases typical of SSV1-like fuselloviruses apparently have been replaced in some of the lineages with nonorthologous AAA$^+$ ATPases from plasmids. Such an exchange is most explicit in the case of PAV1 and a group of *Thermococcales* plasmids (46), emphasizing the network-like process of evolution in this viral group. Based on the evidence of related capsid proteins (Fig. 3) and the shared overlapping gene content (Fig. 4), we propose to classify all tailless spindle-shaped viruses into different genera within the family *Fuselloviridae* (Fig. 3C).

Here we have addressed a long-standing, unsettled question regarding the evolutionary relationships among spindle-shaped archaeal viruses. Previous efforts failed to reveal links between spindle-shaped viruses infecting phylogenetically distant hosts. Our analysis shows that all known spindle-shaped viruses can be segregated into two distinct groups, corresponding to the families *Fuselloviridae* and *Bicaudaviridae*. Peculiarly, similarity in the overall virion morphology for the two viral groups appears to be a result of convergence, rather than divergence; notably, unlike MCPs of fuselloviruses, which are highly hydrophobic (Fig. 3B), the MCPs of bicaudaviruses are predicted to be soluble, consistent with experimental evidence (37). It is rather surprising that spindle-shaped viruses are abundant in archaea but have not been discovered in bacteria or eukaryotes. Presumably, this morphotype is well suited for interaction with archaeal cells, which often dwell in harsh habitats. Clearly, further studies on the biology and structure of spindle-shaped viruses are necessary to explain this specific association. The observation that evolutionarily related spindle-shaped viruses infect hosts thriving in extremely diverse environments and belonging to distinct phylogenetic, metabolic, and physiological groups (acidophiles, hyperthermophiles, methanogens, and halophiles) suggests that the origin of this viral lineage is likely to antedate the radiation of major archaeal groups. More generally, our results demonstrate the utility of the structure-based virus classification (29, 30) and bring additional order to the viral universe.

ACKNOWLEDGMENTS

This work was supported by the Agence Nationale de la Recherche (ANR) program BLANC, project EXAVIR (D.P.) and by the Academy Professor (Academy of Finland) funding grants 255342 and 256518 (D.H.B.). E.R.J.Q. was supported by a fellowship from the Ministère de l'Enseignement Supérieur et de la Recherche of France and the Université Pierre et Marie Curie, Paris, France.

REFERENCES

1. **Geslin C, Le Romancer M, Gaillard M, Erauso G, Prieur D.** 2003. Observation of virus-like particles in high temperature enrichment cultures from deep-sea hydrothermal vents. Res. Microbiol. **154:**303–307. http://dx.doi.org/10.1016/S0923-2508(03)00075-5.
2. **Geslin C, Le Romancer M, Erauso G, Gaillard M, Perrot G, Prieur D.** 2003. PAV1, the first virus-like particle isolated from a hyperthermophilic euryarchaeote, "*Pyrococcus abyssi*." J. Bacteriol. **185:**3888–3894. http://dx.doi.org/10.1128/JB.185.13.3888-3894.2003.
3. **Gorlas A, Koonin EV, Bienvenu N, Prieur D, Geslin C.** 2012. TPV1, the first virus isolated from the hyperthermophilic genus *Thermococcus*. Environ. Microbiol. **14:**503–516. http://dx.doi.org/10.1111/j.1462-2920.2011.02662.x.
4. **Sime-Ngando T, Lucas S, Robin A, Tucker KP, Colombet J, Bettarel Y, Desmond E, Gribaldo S, Forterre P, Breitbart M, Prangishvili D.** 2011. Diversity of virus-host systems in hypersaline Lake Retba, Senegal. Environ. Microbiol. **13:**1956–1972. http://dx.doi.org/10.1111/j.1462-2920.2010.02323.x.
5. **Bath C, Dyall-Smith ML.** 1998. His1, an archaeal virus of the *Fuselloviridae* family that infects *Haloarcula hispanica*. J. Virol. **72:**9392–9395.
6. **Porter K, Russ BE, Dyall-Smith ML.** 2007. Virus-host interactions in salt lakes. Curr. Opin. Microbiol. **10:**418–424. http://dx.doi.org/10.1016/j.mib.2007.05.017.
7. **Oren A, Bratbak G, Heldal M.** 1997. Occurrence of virus-like particles in the Dead Sea. Extremophiles **1:**143–149. http://dx.doi.org/10.1007/s007920050027.
8. **Borrel G, Colombet J, Robin A, Lehours AC, Prangishvili D, Sime-Ngando T.** 2012. Unexpected and novel putative viruses in the sediments of a deep-dark permanently anoxic freshwater habitat. ISME J. **6:**2119–2127. http://dx.doi.org/10.1038/ismej.2012.49.
9. **López-Bueno A, Tamames J, Velazquez D, Moya A, Quesada A, Alcami A.** 2009. High diversity of the viral community from an Antarctic lake. Science **326:**858–861. http://dx.doi.org/10.1126/science.1179287.
10. **Rice G, Stedman K, Snyder J, Wiedenheft B, Willits D, Brumfield S, McDermott T, Young MJ.** 2001. Viruses from extreme thermal environments. Proc. Natl. Acad. Sci. U. S. A. **98:**13341–13345. http://dx.doi.org/10.1073/pnas.231170198.
11. **Bize A, Peng X, Prokofeva M, MacLellan K, Lucas S, Forterre P, Garrett RA, Bonch-Osmolovskaya EA, Prangishvili D.** 2008. Viruses in acidic geothermal environments of the Kamchatka Peninsula. Res. Microbiol. **159:**358–366. http://dx.doi.org/10.1016/j.resmic.2008.04.009.
12. **Rachel R, Bettstetter M, Hedlund BP, Haring M, Kessler A, Stetter KO, Prangishvili D.** 2002. Remarkable morphological diversity of viruses and virus-like particles in hot terrestrial environments. Arch. Virol. **147:**2419–2429. http://dx.doi.org/10.1007/s00705-002-0895-2.
13. **Wiedenheft B, Stedman K, Roberto F, Willits D, Gleske AK, Zoeller L, Snyder J, Douglas T, Young M.** 2004. Comparative genomic analysis of hyperthermophilic archaeal *Fuselloviridae* viruses. J. Virol. **78:**1954–1961. http://dx.doi.org/10.1128/JVI.78.4.1954-1961.2004.
14. **Stedman KM, She Q, Phan H, Arnold HP, Holz I, Garrett RA, Zillig W.** 2003. Relationships between fuselloviruses infecting the extremely thermophilic archaeon *Sulfolobus*: SSV1 and SSV2. Res. Microbiol. **154:**295–302. http://dx.doi.org/10.1016/S0923-2508(03)00074-3.
15. **Zillig W, Arnold HP, Holz I, Prangishvili D, Schweier A, Stedman K, She Q, Phan H, Garrett R, Kristjansson JK.** 1998. Genetic elements in the extremely thermophilic archaeon *Sulfolobus*. Extremophiles **2:**131–140. http://dx.doi.org/10.1007/s007920050052.
16. **Baker BJ, Comolli LR, Dick GJ, Hauser LJ, Hyatt D, Dill BD, Land ML, VerBerkmoes NC, Hettich RL, Banfield JF.** 2010. Enigmatic, ultrasmall, uncultivated Archaea. Proc. Natl. Acad. Sci. U. S. A. **107:**8806–8811. http://dx.doi.org/10.1073/pnas.0914470107.
17. **Comolli LR, Baker BJ, Downing KH, Siegerist CE, Banfield JF.** 2009. Three-dimensional analysis of the structure and ecology of a novel, ultra-small archaeon. ISME J. **3:**159–167. http://dx.doi.org/10.1038/ismej.2008.99.
18. **Prangishvili D.** 2013. The wonderful world of archaeal viruses. Annu. Rev. Microbiol. **67:**565–585. http://dx.doi.org/10.1146/annurev-micro-092412-155633.
19. **Redder P, Peng X, Brugger K, Shah SA, Roesch F, Greve B, She QX, Schleper C, Forterre P, Garrett RA, Prangishvili D.** 2009. Four newly isolated fuselloviruses from extreme geothermal environments reveal unusual morphologies and a possible interviral recombination mechanism. Environ. Microbiol. **11:**2849–2862. http://dx.doi.org/10.1111/j.1462-2920.2009.02009.x.
20. **Bath C, Cukalac T, Porter K, Dyall-Smith ML.** 2006. His1 and His2 are distantly related, spindle-shaped haloviruses belonging to the novel virus group, Salterprovirus. Virology **350:**228–239. http://dx.doi.org/10.1016/j.virol.2006.02.005.
21. **Hanhijärvi KJ, Ziedaite G, Pietilä MK, Haeggström E, Bamford DH.** 2013. DNA ejection from an archaeal virus—a single-molecule approach. Biophys. J. **104:**2264–2272. http://dx.doi.org/10.1016/j.bpj.2013.03.061.
22. **Pietilä MK, Atanasova NS, Oksanen HM, Bamford DH.** 2013. Modified coat protein forms the flexible spindle-shaped virion of haloarchaeal virus His1. Environ. Microbiol. **15:**1674–1686. http://dx.doi.org/10.1111/1462-2920.12030.
23. **Geslin C, Gaillard M, Flament D, Rouault K, Le Romancer M, Prieur D,**

Erauso G. 2007. Analysis of the first genome of a hyperthermophilic marine virus-like particle, PAV1, isolated from *Pyrococcus abyssi*. J. Bacteriol. **189:**4510–4519. http://dx.doi.org/10.1128/JB.01896-06.
24. **Krupovic M, Bamford DH.** 2008. Archaeal proviruses TKV4 and MVV extend the PRD1-adenovirus lineage to the phylum *Euryarchaeota*. Virology **375:**292–300. http://dx.doi.org/10.1016/j.virol.2008.01.043.
25. **Wood AG, Whitman WB, Konisky J.** 1989. Isolation and characterization of an archaebacterial viruslike particle from *Methanococcus voltae* A3. J. Bacteriol. **171:**93–98.
26. **Mochizuki T, Sako Y, Prangishvili D.** 2011. Provirus induction in hyperthermophilic archaea: characterization of *Aeropyrum pernix* spindle-shaped virus 1 and *Aeropyrum pernix* ovoid virus 1. J. Bacteriol. **193:**5412–5419. http://dx.doi.org/10.1128/JB.05101-11.
27. **Xiang X, Chen L, Huang X, Luo Y, She Q, Huang L.** 2005. *Sulfolobus tengchongensis* spindle-shaped virus STSV1: virus-host interactions and genomic features. J. Virol. **79:**8677–8686. http://dx.doi.org/10.1128/JVI.79.14.8677-8686.2005.
28. **Erdmann S, Chen B, Huang X, Deng L, Liu C, Shah SA, Le Moine Bauer S, Sobrino CL, Wang H, Wei Y, She Q, Garrett RA, Huang L, Lin L.** 2013. A novel single-tailed fusiform *Sulfolobus* virus STSV2 infecting model *Sulfolobus* species. Extremophiles **18:**51–60. http://dx.doi.org/10.1007/s00792-013-0591-z.
29. **Krupovic M, Bamford DH.** 2010. Order to the viral universe. J. Virol. **84:**12476–12479. http://dx.doi.org/10.1128/JVI.01489-10.
30. **Krupovic M, Bamford DH.** 2011. Double-stranded DNA viruses: 20 families and only five different architectural principles for virion assembly. Curr. Opin. Virol. **1:**118–124. http://dx.doi.org/10.1016/j.coviro.2011.06.001.
31. **Prangishvili D, Krupovic M.** 2012. A new proposed taxon for double-stranded DNA viruses, the order "Ligamenvirales." Arch. Virol. **157:**791–795. http://dx.doi.org/10.1007/s00705-012-1229-7.
32. **Reiter WD, Palm P, Henschen A, Lottspeich F, Zillig W, Grampp B.** 1987. Identification and characterization of the genes encoding 3 structural proteins of the *Sulfolobus* virus-like particle SSV1. Mol. Gen. Genet. **206:**144–153. http://dx.doi.org/10.1007/BF00326550.
33. **Schleper C, Kubo K, Zillig W.** 1992. The particle SSV1 from the extremely thermophilic archaeon *Sulfolobus* is a virus—demonstration of infectivity and of transfection with viral-DNA. Proc. Natl. Acad. Sci. U. S. A. **89:**7645–7649. http://dx.doi.org/10.1073/pnas.89.16.7645.
34. **Prangishvili D, Vestergaard G, Häring M, Aramayo R, Basta T, Rachel R, Garrett RA.** 2006. Structural and genomic properties of the hyperthermophilic archaeal virus ATV with an extracellular stage of the reproductive cycle. J. Mol. Biol. **359:**1203–1216. http://dx.doi.org/10.1016/j.jmb.2006.04.027.
35. **Häring M, Vestergaard G, Rachel R, Chen L, Garrett RA, Prangishvili D.** 2005. Virology: independent virus development outside a host. Nature **436:**1101–1102. http://dx.doi.org/10.1038/4361101a.
36. **Felisberto-Rodrigues C, Blangy S, Goulet A, Vestergaard G, Cambillau C, Garrett RA, Ortiz-Lombardia M.** 2012. Crystal structure of ATV(ORF273), a new fold for a thermo- and acido-stable protein from the Acidianus two-tailed virus. PLoS One **7:**e45847. http://dx.doi.org/10.1371/journal.pone.0045847.
37. **Goulet A, Vestergaard G, Felisberto-Rodrigues C, Campanacci V, Garrett RA, Cambillau C, Ortiz-Lombardia M.** 2010. Getting the best out of long-wavelength X-rays: de novo chlorine/sulfur SAD phasing of a structural protein from ATV. Acta Crystallogr. D Biol. Crystallogr. **66:**304–308. http://dx.doi.org/10.1107/S0907444909051798.
38. **Krupovic M, White MF, Forterre P, Prangishvili D.** 2012. Postcards from the edge: structural genomics of archaeal viruses. Adv. Virus Res. **82:**33–62. http://dx.doi.org/10.1016/B978-0-12-394621-8.00012-1.
39. **Altschul SF, Madden TL, Schaffer AA, Zhang J, Zhang Z, Miller W, Lipman DJ.** 1997. Gapped BLAST and PSI-BLAST: a new generation of protein database search programs. Nucleic Acids Res. **25:**3389–3402. http://dx.doi.org/10.1093/nar/25.17.3389.
40. **Krogh A, Larsson B, von Heijne G, Sonnhammer EL.** 2001. Predicting transmembrane protein topology with a hidden Markov model: application to complete genomes. J. Mol. Biol. **305:**567–580. http://dx.doi.org/10.1006/jmbi.2000.4315.
41. **Koonin EV, Dolja VV.** 2013. A virocentric perspective on the evolution of life. Curr. Opin. Virol. **3:**546–557. http://dx.doi.org/10.1016/j.coviro.2013.06.008.
42. **Koonin EV, Wolf YI, Nagasaki K, Dolja VV.** 2009. The complexity of the virus world. Nat. Rev. Microbiol. **7:**250. http://dx.doi.org/10.1038/nrmicro2030-c2.
43. **Krupovic M.** 2013. Networks of evolutionary interactions underlying the polyphyletic origin of ssDNA viruses. Curr. Opin. Virol. **3:**578–586. http://dx.doi.org/10.1016/j.coviro.2013.06.010.
44. **Roux S, Enault F, Bronner G, Vaulot D, Forterre P, Krupovic M.** 2013. Chimeric viruses blur the borders between the major groups of eukaryotic single-stranded DNA viruses. Nat. Commun. **4:**2700. http://dx.doi.org/10.1038/ncomms3700.
45. **Koonin EV.** 1992. Archaebacterial virus SSV1 encodes a putative DnaA-like protein. Nucleic Acids Res. **20:**1143. http://dx.doi.org/10.1093/nar/20.5.1143.
46. **Krupovic M, Gonnet M, Hania WB, Forterre P, Erauso G.** 2013. Insights into dynamics of mobile genetic elements in hyperthermophilic environments from five new *Thermococcus* plasmids. PLoS One **8:**e49044. http://dx.doi.org/10.1371/journal.pone.0049044.

CHAPTER 4

One update on the architecture of SSV1 virions.

Sulfolobus spindle-shaped virus 1 contains glycosylated capsid proteins, a cellular chromatin protein and host-derived lipids

Running title: Biochemical characterization of fusellovirus SSV1

Emmanuelle R.J. Quemin[1], Maija K. Pietilä[2,*], Hanna M. Oksanen[2], Patrick Forterre[1], W. Irene C. Rijpstra[3], Stefan Schouten[3], Dennis H. Bamford[2], David Prangishvili[1], Mart Krupovic[1,#]

[1] Institut Pasteur, Unité de Biologie Moléculaire du Gène chez les Extrêmophiles, Département de Microbiologie, Paris, France

[2] Department of Biosciences and Institute of Biotechnology, University of Helsinki, Helsinki, Finland

[3] Department of Marine Organic Biogeochemistry, Royal Netherlands Institute for Sea Research, 1790, AB Den Burg, The Netherlands

* – Present address: Department of Food and Environmental Sciences, University of Helsinki, Helsinki, Finland

– Corresponding author

krupovic@pasteur.fr

Word count

Abstract: 229

Importance: 104

Text: 5,364

ABSTRACT

Geothermal and hypersaline environments are rich in virus-like particles among which spindle-shaped morphotypes dominate. Currently, viruses with spindle- or lemon-shaped virions are exclusive to Archaea and belong to two distinct viral families. The larger of the two families, the *Fuselloviridae*, comprises tail-less, spindle-shaped viruses, which infect hosts from phylogenetically distant archaeal lineages. *Sulfolobus* spindle-shaped virus 1 (SSV1) is the best known member of the family and was one of the first hyperthermophilic archaeal virus to be isolated. SSV1 is an attractive model for understanding virus-host interactions in Archaea; however, the constituents and architecture of SSV1 particles remain only partially characterized. Here, we have conducted an extensive biochemical characterization of highly purified SSV1 virions and identified four virus-encoded structural proteins, VP1-VP4, as well as one DNA-binding protein of cellular origin. The virion proteins VP1, VP3 and VP4 undergo post-translational modification by glycosylation seemingly at multiple sites. VP1 is also proteolytically processed. In addition to the viral DNA-binding protein VP2, we show that viral particles contain the *Sulfolobus solfataricus* chromatin protein Sso7d. Finally, we present evidence indicating that SSV1 virions contain glycerol dibiphytanyl glycerol tetraether (GDGT) lipids, resolving a long-standing debate on SSV1 lipid issue. Comparison of the contents of lipids isolated from the virus and its host cell suggests that GDGTs are acquired by the virus in a selective manner from the host cytoplasmic membrane, likely during the progeny egress.

IMPORTANCE

Although spindle-shaped viruses represent one of the most prominent viral groups in Archaea, structural data on their virion constituents and architecture are still scarce. The comprehensive biochemical characterization of the hyperthermophilic virus SSV1 presented here brings novel and significant insights into the organization and architecture of spindle-shaped virions. The obtained data permit the comparison between spindle-shaped viruses residing in widely different ecological niches, improving our understanding on the adaptation of viruses with unusual morphotypes to extreme environmental conditions. Our findings also pave the way for future research on the unique archaeal virosphere that will further shed light on the structure and biology of viruses.

INTRODUCTION

Viruses infecting extremophilic archaea have evolved to withstand very high temperatures, low or high pH, or near-saturating salt concentrations (1-5). Remarkably, most of these viruses do not seem to be evolutionarily related to viruses of bacteria or eukaryotes and display a considerable diversity of unique virion morphotypes (3, 4). Indeed, eleven novel viral families have been established by the International Committee for the Taxonomy of Viruses (ICTV) for classification of archaeal viruses, emphasizing the uniqueness of rod-shaped, spindle-shaped, droplet-shaped or even bottle-shaped particles that have never been observed among viruses infecting bacteria or eukaryotes (3). Functional studies proved to be highly challenging due to the lack of similarity between the protein sequences and structures of archaeal viruses and those from other viruses and cellular organisms (6-10). Among the morphotypes that are exclusively associated with archaea, spindle-shaped viruses are particularly widespread (11) and have been isolated from highly different environments, including deep sea hydrothermal vents (12-14), hypersaline environments (15-18), anoxic freshwaters (19), cold Antarctic lakes (20), terrestrial hot springs (21-23), and acidic mines (24).

Recently, we refined the evolutionary relationships among spindle-shaped viruses by assessing the morphological and genomic diversity of all available isolates infecting hosts belonging to phylogenetically distant archaeal lineages, including *Thermococcales*, *Methanococcales*, *Desulfurococcales* and *Sulfolobales* (11). The analysis has shown that spindle-shaped viruses can be broadly segregated into two evolutionarily distinct lineages. The first group includes members of the *Bicaudaviridae* family and several currently unclassified viruses. Viruses of this group have large spindle-shaped virions with one or two long tails and contain circular double-stranded (ds) DNA genomes of ~70 kb (11, 25). In the case of *Acidianus* two-tailed virus (ATV), the type species of the *Bicaudaviridae* family, the two tails develop following the release into the environment and completely independently from the host cell (26, 27). Unlike ATV, the unclassified *Sulfolobus tengchongensis* spindle-shaped viruses 1 and 2 have never been observed to undergo this kind of transformation and contain only one tail (28, 29). Nevertheless, both viruses share a number of genes with ATV, including those encoding unique four-helix bundle major capsid proteins (30, 31).

The second group includes smaller, tail-less spindle-shaped viruses, which have been tentatively classified into seven genera within the family *Fuselloviridae* (11). *Sulfolobus* spindle-shaped virus 1 (SSV1) is one of the most extensively studied members of this group and is also among the first archaeal viruses to be isolated (32). SSV1 is a temperate virus and its circular, positively-supercoiled dsDNA genome of 15.4 kb can site-specifically integrate into the host genome with the aid of a virus-encoded integrase (33-37). SSV1 has been used as a model to establish the genetic system in hyperthermophilic archaea (38, 39). As a result, the research on SSV1 has mainly focused on the

mechanism of viral genome integration into the host chromosome (34, 36, 40) and transcriptional regulation (41, 42). By contrast, only a few studies focused on the organization of SSV1 virions; it has been shown that SSV1 virion consists of three capsid protein species: two paralogous proteins VP1 and VP3, and the DNA-binding protein VP2 (32, 43). In addition, the virions were reported to contain a host-derived DNA-binding protein; however, its identity has not been determined (43). Small amounts of viral proteins C792 and D244 have also been reported based on mass spectrometry analysis of viral preparations (7, 44), but presence of the two proteins in highly purified virions remains to be confirmed. Finally, although SSV1 and fuselloviruses in general are considered to exit the host cell by budding through the cytoplasmic membrane, the actual presence of lipids in SSV1 virions is a matter of debate and has never been rigorously demonstrated (1, 32, 45). Lipids initially detected in SSV1 preparations could be derived from contaminant membrane vesicles which could co-purify with the virions (32). Recent attempts to reconstruct the SSV1 virion structure based on cryo-electron microscopy, encumbered by the heterogeneity of the viral particles, provided rather limited insight into the organization of capsid proteins in the virion, whereas the presence of a lipid-containing envelope could not be determined (46).

Although spindle-shaped particles are dominant in hypersaline environments (16, 17), only one such hyperhalophilic archaeal virus, His1, has been isolated to date (15). Recent biochemical and structural studies have shown that His1 virions are composed of one major (VP21) and a few minor capsid protein species (47, 48). Interestingly, a subset of VP21 is apparently modified by lipid moieties, although lipid bilayer could not be detected by either biochemical or structural approaches (47, 48). Furthermore, treatment of His1 virions with various compounds induced the transformation of spindle-shaped particles into tube-like structures which were devoid of the genomic DNA (47, 49). It has been suggested that such reorganization might be biologically relevant and reflects structural changes accompanying virus entry into the host (47). Although SSV1 and His1 infect widely different hosts — thermoacidophilic crenarchaea and hyperhalophilic euryarchaea, respectively — the two viruses display a very similar particle shape and their major capsid proteins share ~47% sequence identity, suggesting that they might have evolved from a common ancestor (11, 48).

To investigate the evolutionary relationships among spindle-shaped viruses residing in highly different environments, we set out to perform a rigorous biochemical characterization of SSV1 particles. We show that SSV1 virions consist of five structural protein species among which one, a DNA-binding protein, is encoded by the host. The virus-encoded proteins undergo post-translational modifications, including proteolytic cleavage and glycosylation. Finally, we put to rest the debate on the presence versus absence of lipids in SSV1 virions by showing that highly purified SSV1 virions contain tetraether lipids selectively recruited from the host cytoplasmic membrane.

MATERIALS AND METHODS

Viruses, strains and growth conditions. *Sulfolobus shibatae* strain B12 (50) and *Sulfolobus solfataricus* strain P2 (51) were used as hosts for SSV1 (32). All cultures were grown aerobically (120 rpm; Innova 44 Eppendorf) at 78°C. The *Sulfolobus* growth medium was prepared as described previously (52).

His1 (15) and its host, *Haloarcula hispanica* strain ATCC 33960, were grown in modified growth medium (MGM) at 37°C as previously described [(48) and references therein].

Virus production and purification. To induce SSV1 viruses, cultures of lysogenized *S. shibatae* B12 at an optical density [OD_{600nm}] of 0.5 were treated with UV as previously described (32). 24 hours after irradiation, cells and debris were removed by two steps of centrifugation (4,000 rpm, 30 min, 4°C and 8,000 rpm, 30 min, 4°C - Jouan BR4i rotor AB 50.10A). The cell-free supernatant was mixed with *S. solfataricus* P2 cells and added to the soft-layer of plates prepared as described in Schleper et al. (40), except that Gelzan™ CM Gelrite® (Sigma-Aldrich) was substituted with Phytagel™ (Sigma-Aldrich). After 72 h at 75°C, the top-layers of confluent plates were collected and 2 mL of medium was added per plate. The suspension was incubated with aeration (120 rpm; Innova 44 Eppendorf) at 78°C for 1 h. Cells and debris were removed by two rounds of centrifugation (8,000 rpm, 30 min, 4°C - Jouan BR4i rotor AB 50.10A, followed by 12,000 rpm, 30 min, 4°C - Avanti J-26XP rotor JLA 16.250). Virus stocks were stored at 4°C.

Virus particles were precipitated from the stocks by addition of ammonium sulfate (Sigma-Aldrich) to 50% (wt/vol) saturation at 4°C as described previously (32). The precipitate (12,000 rpm, 30 min, 4°C - Avanti J-26XP rotor JLA 16.250) was resuspended in SSV1-buffer (20 mM KH_2PO_4, 1 M NaCl, 2.14 mM $MgCl_2$, 0.43 mM $Ca(NO_3)_2$, <0.001% trace elements of *Sulfolobales* medium, pH=6; (52)). In order to remove traces of ammonium sulfate, the virus preparation was dialysed (Spectra/Por 1, SPECTRUM LABS) twice against the SSV1-buffer at 4°C.

The virus concentrate was purified in a linear 5-20% sucrose gradient (in SSV1-buffer) by rate-zonal centrifugation (24,000 rpm, 20 min, 15°C – Sorvall rotor AH629) and the light-scattering zone was collected. The virus was further concentrated and purified by equilibrium centrifugation (21,000 rpm, 20 h, 15°C – Sorvall rotor AH629) in a CsCl gradient in SSV1-buffer (mean density 1.30 g/mL). The light-scattering band was collected and diluted three-fold in SSV1-buffer, followed by concentration by differential centrifugation (21,000 rpm, 20 h, 15°C – Sorvall rotor AH629). The pellet was resuspended in a minimal volume of the SSV1-buffer. The resultant preparation is referred to as the 2x purified sample. The quality of the purification procedure was verified after each step by protein gel analysis

(see below), measurement of absorbance at 260 nm wavelength, recovery of infectivity (plaque assay) and transmission electron microscopy (TEM, see below).

Production and purification of His1 virions were performed as previously described (48).

Control of SSV1 aggregation. SSV1 preparations after ammonium sulfate precipitation were dialyzed against the SSV1-buffer containing 0.1, 0.25, 0.5, 1 or 2 M NaCl. SSV1 virions purified in the CsCl density gradient were incubated for 30 min at room temperature in the presence of 1% (vol/vol) ethanol in SSV1-buffer containing 1 M NaCl. The samples were negatively stained and processed for TEM. Virions were ascribed to three different categories: (i) single particles, (ii) rosette-like virion aggregates containing between 2 and 5 particles and (iii) aggregates with more than 5 particles. The proportion of virions in each of the three categories under the different conditions was determined by TEM. At least 1,000 viral particles from three independent biological replicates were analyzed per condition and standard deviation was calculated. Infectivity of each sample was also verified by plaque assay as previously described (40).

Protein analyses. Proteins were analyzed using modified tricine-sodium dodecyl sulphate polyacrylamide gel electrophoresis (tricine-SDS-PAGE) with 4% and 14% (wt/vol) acrylamide concentrations in the stacking and separation gels, respectively (53). After electrophoresis, gels were stained with Coomassie blue (detection limit of >7 ng) or SYPRO® Ruby (detection limit of 0.25 to 1 ng) (Life Technologies). Glycosylation of SSV1 proteins was assessed using Pro-Q® Emerald 300 glycoprotein gel stain kit according to the manufacturer's instructions (Life Technologies).

N-terminal sequencing of virion proteins was performed at the Protein Chemistry Core Facility of the Institute of Biotechnology, University of Helsinki and mass spectrometry (MS) of peptides released by in-gel trypsin digestion was done at Meilahti Clinical and Basic Proteomics Core Facility, University of Helsinki as described previously (54).

Transmembrane domains and secondary structure elements in viral proteins were predicted using TMHMM (55) and Jpred3 (56), respectively.

The relative quantification of the amount of proteins in each SDS-PAGE gel band was done using ImageJ software (National Institutes of Health). The determined value was then divided by the number of virus particle estimated from the viral DNA absorbance at 260 nm as described below.

Lipid analyses.

S. solfataricus cell pellet and 2x purified SSV1 preparation were freeze-dried and the biomass was directly acid hydrolyzed by refluxing with 5% HCl in methanol for 3 h, following Pitcher et al. (57), to release glycerol dibiphytanyl glycerol tetraether (GDGTs) lipids. A known amount (10 ng) of a C_{46} GDGT standard (58) was added to the acid hydrolyzed fraction and GDGT lipids were analyzed by high performance liquid chromatography/atmospheric pressure chemical ionization-mass spectrometry according to Schouten et al. (59). The mass spectrometer was operated in single ion mode (SIM) to monitor GDGTs with 0-8 cyclopentane moieties and the C46 GDGT standard. Relative abundances of GDGTs were determined by integrating peak areas of the SIM signal. The signal of the C_{46} GDGT standard was corrected for the difference in ionization efficiency using a 1:1 mixture of the standard and purified GDGT-0.

To establish the head groups of the GDGTs, *S. solfataricus* cells were extracted by a modified Bligh-Dyer method and analyzed for intact polar lipids as described by Pitcher et al (57).

Quantification of viral particles. The number of infectious particles was determined by plaque assay as described above. Alternatively, SSV1 particles were enumerated by determining the number of genome copies in the preparation. To this end, viral DNA was extracted from the purified virion preparation using the standard phenol:chloroform method and the number of the genome copies was estimated by measuring the absorbance at λ=260 nm and considering that the molecular weight of the SSV1 genome (15 465 bp; NC_001338) is 9,554,261.87 g/mol.

Electron microscopy. For conventional negative-stain TEM, samples were prepared as described previously (60). Briefly, 10 µL of sample was adsorbed on grids for 1 min, air dried and stained with 3% uranyl acetate pH 4.5 (EuroMedex) for 1 min. Samples were imaged using a TECNAI BIOTWIN 120 FEI transmission electron microscope operating at 100 kV in the Plateforme de Microscopie Ultrastructurale of the Institut Pasteur, Paris or JEOL JEM-1400 transmission electron microscope operating at 80 kV in the Electron Microscopy Unit of the Institute of Biotechnology, University of Helsinki.

RESULTS

Aggregation of SSV1 particles is modulated by ionic and hydrophobic interactions. Virions of SSV1 and other fuselloviruses tend to interact with each other by the terminal fibers located at one of the two pointed ends of the viral particles, forming polyvalent aggregates (22, 32, 61). Based on the aggregation state, SSV1 virions can be grouped into one of three categories: (i) individual virions, (ii) rosette-like aggregates containing between 2 and 5 particles and (iii) aggregates with more than 5 viral particles (Fig. 1A). Since large virion aggregates aggravate virion purification and prevent accurate virion enumeration, we attempted to reduce virion aggregation by varying the ionic strength conditions. Increasing the salt concentration in the "SSV1-buffer" led to the dissociation of aggregates containing more than 5 particles in a concentration-dependent manner, with concomitant increase in the proportion of single virions (Fig. 1B), implicating ionic interactions in virion aggregation. However, the portion of rosette-like viral assemblages composed of up to 5 particles remained constant (19 ± 1.5% on average) even at the highest NaCl concentration tested (Fig. 1B). It is noteworthy that SSV1 remained stable and retained infectivity for up to three months in a wide range of salt concentrations (0.1 to 2 M NaCl), highlighting the robustness of the viral particles. Considering the highly pronounced hydrophobicity of the protein implicated in the formation of terminal fibers (see below), we tested whether the smaller aggregates could be dissociated by mild treatment with organic solvents. Indeed, in the presence of 1% (vol/vol) ethanol the proportion of single particles increased to ~88%, whereas the remaining virion aggregates mainly consisted of 2 particles and no aggregates with 5 particles were observed under TEM. Such treatment reduced the infectivity by ~50%, while ethanol concentrations above 10% (vol/vol) resulted in complete dissociation of the SSV1 virions (data not shown).

Production of highly purified virions. In order to ensure high purity of the viral preparation for unambiguous determination of the SSV1 virion constituents, we developed and optimized a multistep purification protocol (see Materials and Methods). *S. shibatae* lysogens sporadically release SSV1 virions. However, even following UV irradiation, which increased SSV1 production by one order of magnitude (from ca. 10^5 to 10^6 PFU/ml), the virus titer was insufficient for robust biochemical virion characterization. To overcome this hurdle, virions were precipitated with ammonium sulfate from the virus stocks obtained by collecting the soft layer of confluent Phytagel™ plates. The virus preparation was subsequently purified using rate zonal centrifugation in a linear sucrose gradient to produce "1x" purified SSV1. However, the resultant virus preparation contained a substantial amount of impurities, as judged by SDS-PAGE analysis (not shown), necessitating an additional step of purification. The latter included equilibrium centrifugation in a CsCl gradient and concentration by differential centrifugation, resulting in the production of "2x" purified SSV1 preparation (Fig. 1C). The purification was performed under conditions minimizing aggregation of virions (1 M NaCl). Virion recovery was monitored throughout the purification procedure and the final 2x preparation corresponded to ~31% recovery of

infectious particles with a specific infectivity of ~2x10^8 PFU/mL/Abs$_{260}$ (Fig. 1C). The buoyant density of the purified SSV1 virions in CsCl was estimated to be 1.29 g/mL, which is somewhat higher than that previously reported for SSV1 (1.24 g/mL; (32)), but similar to the buoyant density of membrane-containing pleolipoviruses (1.3 g/mL; (62)).

Structural proteins of SSV1. The availability of highly purified preparation allowed us to assess the biochemical composition of the SSV1 viral particles. Hyperhalophilic spindle-shaped virus His1 was analyzed in parallel as a control and for comparison. 2x purified SSV1 and His1 virions were examined by tricine-SDS-PAGE. Following Coomassie blue staining, the migration profiles of SSV1 and His1 preparations appeared similar and displayed several major protein bands of low molecular mass (in the range of 7–17 kDa) and a minor high-molecular mass protein band (Fig. 2A); migration of His1 proteins was similar to that previously reported (48). Unexpectedly, as has also been reported for His1 virus (48), protein concentration of the purified SSV1 samples could not be determined using the Bradford method (63); it appears that the virions of SSV1 and His1 do not display sufficient reactivity with the Coomassie blue reagent, although the corresponding proteins in the tricine-SDS-PAGE gels could be detected.

The identity of SSV1 proteins was determined by a combination of N-terminal sequencing and MS techniques. Consistent with previous analysis (43), in the lower molecular mass bands we identified the proteins VP1, VP2 and VP3. Proteins VP1 and VP3 are paralogous, highly hydrophobic proteins (each contains two predicted α-helical transmembrane domains [TMDs]) (Fig. 3C). N-terminal sequencing showed that, unlike VP3, VP1 is proteolytically processed resulting in the removal of 65 N-terminal amino acids (Fig. 3B and C), as has been also shown previously (43). The high molecular mass band was identified as a product of ORF C792 (Fig. 3A). Adhering to the nomenclature used for SSV1 structural proteins (43), we denote the product of ORF C792 as VP4. The presence of VP4 in SSV1 virions has been reported previously (44). However, since the SDS-PAGE analysis of the virion preparation was not presented, the possibility of contamination could not be ruled out. Like VP1 and VP3, VP4 is highly hydrophobic; sequence analysis showed that VP4 contains three confidently-predicted (probability higher than 0.9) α-helical TMDs, but high-hydrophobicity regions are also distributed throughout the protein length (Fig. 3C). Notably, the region flanked by TMD1 and TMD2 is predicted to be β-strand-rich and is likely to adopt a β-propeller or β-barrel topology.

SSV1 virions were found to contain a considerable amount of one host-encoded protein, Sso7d (Fig. 3A and B). Sso7d is a small, basic protein, which belongs to the extensively studied Sul7d family of 7-kDa DNA-binding proteins and represents one of the major chromatin proteins of *Sulfolobus solfataricus* (64, 65). Notably, SDS-PAGE analysis of fractions collected from the CsCl gradient showed that Sso7 is

exclusively detected in the fraction containing SSV1 virions. In addition, a previous study (43) has reported the presence of an unidentified host-encoded DNA-binding protein in SSV1 virions. Consequently we assign Sso7d as a virion component. Staining of the protein gel with SYPRO® Ruby, which is eight times more sensitive compared to Coomassie brilliant blue stain (66), did not reveal any additional protein bands (Fig. 2B), strongly suggesting that incorporation of Sso7d into SSV1 particles is specific and biologically-relevant rather than accidental.

VP1, VP3 and VP4 are glycosylated. Molecular masses of SSV1 structural proteins deduced from the gel (Fig. 3A) did not coincide with those calculated from the sequence (Fig. 3B). VP1, VP2 and VP3 migrated in gels as ~11, ~13 and ~16 kDa proteins, which is considerably slower than expected based on their calculated molecular masses (i.e., 7.7, 8.6 and 9.8 kDa, respectively; Fig. 3A and B). Similarly, VP4, with predicted mass of 85 kDa, migrated as a 100 kDa protein (Fig. 3A). The discrepancy in migration pattern could not be explained by potential formation of higher-order oligomers. Thus, the possibility of post-translational modifications was considered. Since virion proteins of several archaeal viruses are known to undergo glycosylation (67-69), we tested whether this modification can be detected in the case of SSV1 virions by staining the proteins with a glycoprotein-specific stain. Indeed, VP1, VP3 and VP4 were found to be glycosylated (Fig. 2C). Unlike many crenarchaeal viruses (6, 8, 70, 71), SSV1 does not encode an identifiable glycosyltransferase; thus, glycosylation of viral proteins is likely to be performed by cellular enzymes. Protein glycosylation has been studied in several members of *Sulfolobales* (72), including *S. solfataricus* (73) which was used in this study for SSV1 production. It has been found that glycosylation in *Sulfolobus* occurs on the asparagine residue within the consensus motif N-X-S/T (where X is any amino acid except proline). All three SSV1 proteins which we found to be glycosylated (Fig. 2C) contain multiple N-X-S/T motifs: VP1 and VP3 each contain 2 such motifs located in the linker region between the TMDs, whereas VP4 possesses 20 motifs which could undergo glycosylation (Fig. 3C). The extent of glycosylation as well as detailed characterization of the glycans attached to the SSV1 proteins will be the focus of future studies.

SSV1 acquires lipids from the host cytoplasmic membrane. Membranes of organisms from the order *Sulfolobales* predominantly consist of *sn*-2,3-dibiphytanyl diglycerol tetraether lipids (also known as glycerol dibiphytanyl glycerol tetraether [GDGT]), in which the two glycerol moieties are connected by two C40 isoprenoid chains, enabling the formation of monolayer membranes (74, 75). GDGTs differ by the number of cyclopentane moieties within the isoprenoid chains, which can vary from 0 to 8 (i.e., GDGT-0 through GDGT-8).

Preliminary thin-layer chromatography analysis of the material extracted from SSV1 virions and host *S. solfataricus* cells by chloroform/methanol treatment strongly suggested the presence of phospholipids,

although in the case of SSV1 the amount detected using iodine vapor was rather low (data not shown). To determine the exact nature of SSV1 lipids and to compare it to the lipid content of the host, we analyzed GDGTs by liquid chromatography coupled with mass spectrometry on 2x purified SSV1 virions as well as *S. solfataricus* cells (see Materials and Methods). The analysis revealed that *S. solfataricus* membrane contains seven GDGT species (Fig. 4A) which are present in different amounts. Under conditions tested, GDGT-4 constituted more than half of the cellular membrane lipids (Fig. 4B). Furthermore, the lipid head groups were found to contain 2 to 3 sugar moieties. This is consistent with the previous analysis which showed that glycolipids of *Sulfolobus* contain di- and trisacharides composed of glucose, galactose or mannose moieties (76, 77).Analysis of the viral particles showed that all 7 GDGT species identified in *S. solfataricus* membrane are also present in low amounts in SSV1 virions. Interestingly, however, the ratios of different lipids in the viral particles were different when compared to the host cytoplasmic membrane. SSV1 virions were strongly enriched in GDGT-0, which represented ~68% of all viral lipids (Fig. 4B). The proportions of other lipids in the virions roughly followed those in the cellular membrane, i.e., the second most abundant lipid was GDGT-4, followed by GDGT-3 and GDGT-5. Notably, lipid analysis carried out on different SSV1 preparations showed that whereas the proportion of GDGT-0 remained constant in different experiments, the ratios of GDGT-3, -4, and -5 were more variable. Unfortunately, low abundance of lipids in viral particles precluded the detailed analysis of their head groups.

Quantification of the SSV1 virion components. To gain better understanding on SSV1 virion organization, we have performed a relative quantitation of lipids and proteins. Due to various reasons, not all virions released from the cell are infectious (i.e., plaque-forming); the ratio between non-infectious and infectious particles can vary greatly between different viruses (78). Thus, we have established the correspondence between the number of infectious SSV1 particles determined by the plaque assay and the number of genome copies estimated from the purified viral DNA absorbance at 260 nm. The particle-to-PFU ratio was estimated to be around 5, which is consistent with the values (5–10 particle/PFU) determined previously by quantitative TEM (40). Since there are more particles than PFUs (i.e., the ratio is more than 1), for subsequent calculations, we used the number of particles estimated from the number of genome copies rather than PFUs. Quantitation of virion components (see Materials and Methods) showed that each virion contains ~6 fg of lipids and ~14 fg of proteins, i.e., the two components are present in 1:2.4 ratio. Given that estimated total number of SSV1 particles might be slightly skewed due to potential artifacts (e.g., presence of empty virions, etc), these values should be considered with caution.

DISCUSSION

Large-scale production and high-level purification procedures are a prerequisite for comprehensive biochemical and structural characterization of any virus. Here, we have optimized a purification protocol for the hyperthermophilic spindle-shaped virus SSV1, which allowed its biochemical characterization. Environmental distribution of spindle-shaped viruses is particularly broad (11). Interestingly, although the natural habitats of SSV1 are characterized by very low pH and high temperatures, we found that SSV1 virions are also stable in high-salinity conditions; prolonged incubation in the presence of 2 M NaCl had no effect on virion stability or infectivity. This indicates that the design of spindle-shaped virions is inherently robust, which might explain the success of this virus group in colonizing very diverse ecological niches where their archaeal hosts are found (11, 48).

Our analyses have shown that SSV1 virion consists of four virus-encoded (VP1–4) and one host-derived protein (Sso7d) (Fig. 3). Paralogous proteins VP1 and VP3 have homologs in all spindle-shaped viruses characterized thus far (11), including hyperhalophilic virus His1 (48), and represent a signature protein in this group of viruses. Protein VP4 has been previously suggested to be involved in the formation of terminal fibers based on correlation between the fiber morphology and the presence of *vp4*-like genes in different members of the *Fuselloviridae* (22). Here we have demonstrated that VP4 is indeed a part of the virion, confirming the previous report by Menon et al (44). Electron microscopy analysis indicates that terminal fibers are implicated in virion aggregation (Fig. 1A). Two groups of virion aggregates can be defined: (i) aggregates composed of up to five virions and (ii) those containing more than five viral particles. The latter assemblages seem to be dependent on ionic interactions, whereas the former ones are not (Fig. 1B). Instead, the smaller rosette-like aggregates are apparently held together by hydrophobic interactions, presumably involving VP4, and can be dispersed by mild treatment with organic solvents. High hydrophobicity of VP4 (Fig. 3C) is in line with this conclusion.

VP2 has been previously shown to be tightly bound to dsDNA suggesting a role in organizing SSV1 genome (43). Unexpectedly, VP2 is conserved in only four (SSV1, SSV6, ASV1 and SMF1) out of ten fuselloviruses for which complete genome sequences are available. Moreover, in-frame deletion of the VP2-encoding gene had no observable effect on virion assembly or infectivity, indicating that the gene is dispensable under laboratory growth conditions (79). Interestingly, unlike other SSV1 VPs, VP2 is not specific to fuselloviruses but is also encoded by unrelated proviruses of euryarchaeon *Archaeoglobus veneficus* SNP6 (80), *Sulfolobus* turreted icosahedral virus 2 (81) as well as bacterial viruses of the recently established family *Sphaerolipoviridae* (82). Such patchy phyletic distribution of *vp2*-like genes in fuselloviruses, its conservation in other archaeal and bacterial viruses as well as dispensability of VP2 for SSV1 infectivity might indicate that *vp2* gene has been acquired relatively late in the history of fuselloviruses from a different group of viruses.

Identification of the host-encoded DNA-binding protein Sso7d in SSV1 virions suggests that Sso7d could play an important role in the organization and condensation of viral genome prior to packaging. Sso7d, a member of Sul7d family, is one of the major chromatin proteins responsible for chromosome organization in *Sulfolobus* (65). This small basic protein is known to bind dsDNA non-specifically and induces negative supercoiling (83) as well as compaction of relaxed or positively supercoiled DNA *in vitro* (64). SSV1 DNA is highly positively supercoiled in SSV1 virions (33). This positive supercoiling might result from the activity of *Sulfolobus* reverse gyrase, an enzyme that introduces positive supercoiling *in vitro* in topologically closed DNA (33). Alternatively, positive supercoiling might be induced by stoichiometric binding of a DNA-binding protein, followed by the relaxation of compensatory negative superturns by cellular DNA topoisomerases. In the latter hypothesis, this DNA binding protein cannot be SSo7d since this protein induces negative supercoiling *in vitro* (83). SSV1 DNA might be thus first positively supercoiled by reverse gyrase and later on condensed during the packaging process by interaction between Sso7d and positively supercoiled viral DNA. However, the effects of VP2 on DNA supercoiling as well as condensation of SSV1 DNA by VP2 and Sso7d remain to be investigated.

Notably, previous analysis has also suggested that viral particles contain protein D244 (44) which, however, is not essential for virion assembly and infectivity (79). X-ray structure of the D244 orthologue from *Sulfolobus* spindle-shaped virus Ragged Hills revealed that the protein is a member of the PD-(D/E)XK nuclease superfamily (84), arguing against the possibility that D244 plays a structural role in virion formation. We could not detect D244 in our virus preparation, although its presence in amounts that were below our detection limit cannot be ruled out.

Protein glycosylation is one of the most common post-translational modifications in archaeal viruses — particularly in viruses infecting hyperthermophilic hosts (67-69) — and could play an important role in virion stability and/or interaction with the host cell. Accordingly, many hyperthermophilic archaeal viruses encode their own glycosyltransferases (6, 8, 70, 71), with some viruses containing as many as five different glycosyltransferase genes per genome (8). However, this is not the case for SSV1 or any other known fusellovirus. Nevertheless, three of the SSV1 virion proteins, VP1, VP3 and VP4, are glycosylated (Fig. 2C). To the best of our knowledge, glycosylation of virion proteins has never been observed for any spindle-shaped virus. Somewhat paradoxically, hyperhalophilic spindle-shaped virus His1 encodes a putative glycosyltransferase but does not seem to glycosylate its virion proteins, at least not under the laboratory conditions (48) (Fig. 2C). In the absence of dedicated virus-encoded glycosyltransferases, glycosylation of SSV1 VPs is likely to be performed by the host enzymes. Consistently, multiple consensus glycosylation motifs (N-X-S/T; (72, 73)) are present in all three SSV1 glycoproteins; VP4 contains particularly high number of such motifs (Fig. 3C). Recent study of protein

glycosylation in *S. solfataricus* has shown that some cell surface proteins can be heavily glycosylated (73). For example, protein SSO1273 contains 20 N-X-S/T motifs and all of them were found to be modified with a glycan, which has a mass of 1,298.4 Da (73). The slower migration of VP4 in tricine-SDS-PAGE gel (as 100 kDa instead of the calculated 85 kDa), would be consistent with glycosylation on most of the theoretical glycosylation sites. Detailed characterization of the glycan structures and extent of the SSV1 VP glycosylation as well as biological significance of this modification will be an exciting area of future research.

The presence of lipids in SSV1 virions has been a matter of debate for many years (1, 32, 45). Indeed, even recent low-resolution (~32 Å) reconstruction of SSV1 virion structure provided no insight concerning this issue (46). Here we resolve this long-lasting dispute by providing evidence for the presence of lipids in highly purified SSV1 virions. Furthermore, for the first time, we determine the molecular composition of the lipid content and show that SSV1 virions contain seven different species of GDGT lipids (Fig. 4). This result is consistent with the early electron microscopic observations of SSV1 budding through the cell membrane (32). Notably, the ratio of different lipid species in the virions was different from that found in the cytoplasmic membrane of the host cells, suggesting a selective incorporation of lipids into the virion. Similarly, lipid composition of *Sulfolobus* turreted icosahedral virus, which has an internal membrane, and lipid content of membrane vesicles produced by *S. solfataricus* were found to differ considerably from that of the cellular membrane (68, 85). Interestingly, the hyperhalophilic spindle-shaped virus His1 does not appear to contain free lipids; instead its major capsid protein, homologous to VP1/VP3 of SSV1, was concluded to be covalently modified by a lipid moiety (48), suggesting that different spindle-shaped viruses use different mechanisms for lipid acquisition from the host.

The biochemical characterization of SSV1 virions presented here provides a foundation for future investigations on different aspects of biology and structure of hyperthermophilic spindle-shaped viruses. Of special interest is the role of lipids during the entry and exit stages of fusellovirus infection; comparison of these strategies with those employed by eukaryotic membrane-containing viruses might provide particularly important insights into the evolution of mechanisms mediating membrane fusion and virus budding.

ACKNOWLEDGEMENTS

This work was supported by the Agence nationale de la recherche (ANR) program BLANC, project EXAVIR (D.P.) and by Academy Professor (Academy of Finland) funding grants 256518, 283072 and 255342 (D.H.B.). E.R.J.Q. was supported by a fellowship from the Ministère de l'Enseignement

Supérieur et de la Recherche of France and the Université Pierre et Marie Curie, Paris, France as well as the European Molecular Biology Organization (ASTF 62-2014) and CIMO Fellowship, Finland (TM-13-9054). We thank Academy of Finland (grants 271413 and 272853) and University of Helsinki for the support to EU ESFRI Instruct Centre for Virus Production (ICVIR) used in this study. We would like to thank Sari Korhonen, Päivi Hannuksela and Helin Veskiväli for excellent technical assistance.

Figure legends

Figure 1. Purification of SSV1. (A) Transmission electron micrograph of negatively stained SSV1 sample. Single particles as well as different aggregates are shown. (B) Depending on the concentration of NaCl in the SSV1-buffer, different stages of aggregation were observed: single particles (white columns); rosette-like structures containing between 2 and 5 particles (grey columns), and aggregates with more than 5 particles (black columns). The number of viruses in each category was determined from negatively-stained electron micrographs obtained from three independent experiments. At least 1,000 particles were counted per condition and error bars represent standard deviations. (C) Analysis of samples taken after each step of the 2x purification procedure. Absorbance at λ=260 nm, virus titer, recovery of infectivity and specific infectivity are indicated.

Figure 2. Structural proteins of SSV1. (A) Protein profiles of 2x purified SSV1 virions compared to 2x purified His1 virions in a tricine-SDS-polyacrylamide gel stained with Coomassie blue. Molecular mass markers (M) are shown (kDa). The amount of SSV1 and His1 samples loaded are comparable based on absorbance measurements at λ=260 nm. (B-C) 2x purified SSV1 and His1 virions analyzed in a tricine-SDS-PAGE gel stained (B) with SYPRO® Ruby protein stain (detecting all proteins) and (C) with Pro-Q® Emerald 300 glycoprotein detecting reagent (detecting glycosylated proteins). Candy-Cane Glycoprotein molecular weight standard (labeled as CC) contains a mixture of non-glycosylated and glycosylated proteins. Half of the amount loaded in (A) was added to the gel shown in (B) and (C).

Figure 3. Identification of the structural proteins of SSV1. (A) Protein pattern of the 2x purified SSV1 virions in a tricine-SDS-PAGE stained with Coomassie blue. M and numbers indicate the molecular mass marker (kDa). Locations of protein bands processed for proteomic analyses are depicted with black boxes and names of proteins identified are indicated on the right. (B) Proteins identified by N-terminal sequencing (NS) and Mass Spectrometry (MS): the NCBI accession number, theoretical molecular masses, putative functions and peptide sequences determined during analysis are provided. (C) Sequence analysis of the SSV1 structural proteins VP1, VP3 and VP4. Sequences of the predicted transmembrane domains are highlighted in grey, whereas the theoretical glycosylation consensus motifs (N-X-S/T) are shown on the black background. The position of proteolytic cleavage in VP1 is indicated by a black arrowhead and the N-terminal 65 amino acid (aa) residues not shared with VP3 are boxed. Paralogous proteins VP1 and VP3 are aligned; identical and similar amino acid positions are indicated with asterisk and colon signs, respectively. At the bottom of the panel is the hydrophobicity profile of VP4. The broken line indicates the 0.9 probability threshold for the prediction of the transmembrane domains (TMD1-3). Predicted secondary structure elements are shown with green boxes (α-helixes) and blue arrows (β-strands).

Figure 4. Analysis of lipids of *Sulfolobus solfataricus* and SSV1. (A) Structures of lipids analyzed in this study: glycerol dibiphytanyl glycerol tetraethers (GDGTs). The numbers denote how many cyclopentane moieties are present within the isoprenoid chains. (B) Relative distribution of core lipid species identified by HPLC-APCI-MS in *S. solfataricus* cells and 2x purified SSV1 virions as described in Materials and Methods.

References

1. **Atanasova, N. S., A. Senčilo, M. K. Pietilä, E. Roine, H. M. Oksanen, and D. H. Bamford.** 2015. Comparison of lipid-containing bacterial and archaeal viruses. Adv Virus Res **92:**1-61.
2. **Pietilä, M. K., T. A. Demina, N. S. Atanasova, H. M. Oksanen, and D. H. Bamford.** 2014. Archaeal viruses and bacteriophages: comparisons and contrasts. Trends Microbiol **22:**334-344.
3. **Prangishvili, D.** 2013. The wonderful world of archaeal viruses. Annu Rev Microbiol **67:**565-585.
4. **Prangishvili, D.** 2015. Archaeal viruses: living fossils of the ancient virosphere? Ann N Y Acad Sci.
5. **Prangishvili, D., E. V. Koonin, and M. Krupovic.** 2013. Genomics and biology of Rudiviruses, a model for the study of virus-host interactions in Archaea. Biochem Soc Trans **41:**443-450.
6. **Krupovic, M., M. F. White, P. Forterre, and D. Prangishvili.** 2012. Postcards from the edge: structural genomics of archaeal viruses. Adv Virus Res **82:**33-62.
7. **Lawrence, C. M., S. Menon, B. J. Eilers, B. Bothner, R. Khayat, T. Douglas, and M. J. Young.** 2009. Structural and functional studies of archaeal viruses. J Biol Chem **284:**12599-12603.
8. **Prangishvili, D., R. A. Garrett, and E. V. Koonin.** 2006. Evolutionary genomics of archaeal viruses: unique viral genomes in the third domain of life. Virus Res **117:**52-67.
9. **Quemin, E. R., D. Prangishvili, and M. Krupovic.** 2014. Hard out there: understanding archaeal virus biology. Future Virol **9:**703-706.
10. **DiMaio, F., X. Yu, E. Rensen, M. Krupovic, D. Prangishvili, and E. H. Egelman.** 2015. Virology. A virus that infects a hyperthermophile encapsidates A-form DNA. Science **348:**914-917.
11. **Krupovic, M., E. R. Quemin, D. H. Bamford, P. Forterre, and D. Prangishvili.** 2014. Unification of the globally distributed spindle-shaped viruses of the Archaea. J Virol **88:**2354-2358.
12. **Geslin, C., M. Le Romancer, G. Erauso, M. Gaillard, G. Perrot, and D. Prieur.** 2003. PAV1, the first virus-like particle isolated from a hyperthermophilic euryarchaeote, "Pyrococcus abyssi". J Bacteriol **185:**3888-3894.
13. **Gorlas, A., E. V. Koonin, N. Bienvenu, D. Prieur, and C. Geslin.** 2012. TPV1, the first virus isolated from the hyperthermophilic genus *Thermococcus*. Environ Microbiol **14:**503-516.
14. **Geslin, C., M. Le Romancer, M. Gaillard, G. Erauso, and D. Prieur.** 2003. Observation of virus-like particles in high temperature enrichment cultures from deep-sea hydrothermal vents. Res Microbiol **154:**303-307.
15. **Bath, C., and M. L. Dyall-Smith.** 1998. His1, an archaeal virus of the *Fuselloviridae* family that infects *Haloarcula hispanica*. J Virol **72:**9392-9395.
16. **Oren, A., G. Bratbak, and M. Heldal.** 1997. Occurrence of virus-like particles in the Dead Sea. Extremophiles **1:**143-149.
17. **Porter, K., B. E. Russ, and M. L. Dyall-Smith.** 2007. Virus-host interactions in salt lakes. Curr Opin Microbiol **10:**418-424.
18. **Sime-Ngando, T., S. Lucas, A. Robin, K. P. Tucker, J. Colombet, Y. Bettarel, E. Desmond, S. Gribaldo, P. Forterre, M. Breitbart, and D. Prangishvili.** 2011. Diversity of virus-host systems in hypersaline Lake Retba, Senegal. Environ Microbiol **13:**1956-1972.
19. **Borrel, G., J. Colombet, A. Robin, A. C. Lehours, D. Prangishvili, and T. Sime-Ngando.** 2012. Unexpected and novel putative viruses in the sediments of a deep-dark permanently anoxic freshwater habitat. ISME J **6:**2119-2127.
20. **López-Bueno, A., J. Tamames, D. Velazquez, A. Moya, A. Quesada, and A. Alcami.** 2009. High diversity of the viral community from an Antarctic lake. Science **326:**858-861.
21. **Bize, A., X. Peng, M. Prokofeva, K. Maclellan, S. Lucas, P. Forterre, R. A. Garrett, E. A. Bonch-Osmolovskaya, and D. Prangishvili.** 2008. Viruses in acidic geothermal environments of the Kamchatka Peninsula. Res Microbiol **159:**358-366.
22. **Redder, P., X. Peng, K. Brugger, S. A. Shah, F. Roesch, B. Greve, Q. She, C. Schleper, P. Forterre, R. A. Garrett, and D. Prangishvili.** 2009. Four newly isolated fuselloviruses from extreme geothermal environments reveal unusual morphologies and a possible interviral recombination mechanism. Environ Microbiol **11:**2849-2862.

23. **Rice, G., K. Stedman, J. Snyder, B. Wiedenheft, D. Willits, S. Brumfield, T. McDermott, and M. J. Young.** 2001. Viruses from extreme thermal environments. Proc Natl Acad Sci U S A **98:**13341-13345.
24. **Baker, B. J., L. R. Comolli, G. J. Dick, L. J. Hauser, D. Hyatt, B. D. Dill, M. L. Land, N. C. Verberkmoes, R. L. Hettich, and J. F. Banfield.** 2010. Enigmatic, ultrasmall, uncultivated Archaea. Proc Natl Acad Sci U S A **107:**8806-8811.
25. **Hochstein, R., D. Bollschweiler, H. Engelhardt, C. M. Lawrence, and M. Young.** 2015. Large Tailed Spindle Viruses of Archaea: a New Way of Doing Viral Business. Journal of virology **89:**9146-9149.
26. **Häring, M., G. Vestergaard, R. Rachel, L. Chen, R. A. Garrett, and D. Prangishvili.** 2005. Virology: independent virus development outside a host. Nature **436:**1101-1102.
27. **Prangishvili, D., G. Vestergaard, M. Haring, R. Aramayo, T. Basta, R. Rachel, and R. A. Garrett.** 2006. Structural and genomic properties of the hyperthermophilic archaeal virus ATV with an extracellular stage of the reproductive cycle. J Mol Biol **359:**1203-1216.
28. **Erdmann, S., B. Chen, X. Huang, L. Deng, C. Liu, S. A. Shah, S. Le Moine Bauer, C. L. Sobrino, H. Wang, Y. Wei, Q. She, R. A. Garrett, L. Huang, and L. Lin.** 2014. A novel single-tailed fusiform *Sulfolobus* virus STSV2 infecting model *Sulfolobus* species. Extremophiles **18:**51-60.
29. **Xiang, X., L. Chen, X. Huang, Y. Luo, Q. She, and L. Huang.** 2005. *Sulfolobus tengchongensis* spindle-shaped virus STSV1: virus-host interactions and genomic features. J Virol **79:**8677-8686.
30. **Goulet, A., G. Vestergaard, C. Felisberto-Rodrigues, V. Campanacci, R. A. Garrett, C. Cambillau, and M. Ortiz-Lombardia.** 2010. Getting the best out of long-wavelength X-rays: de novo chlorine/sulfur SAD phasing of a structural protein from ATV. Acta Crystallogr D Biol Crystallogr **66:**304-308.
31. **Krupovic, M., and D. H. Bamford.** 2011. Double-stranded DNA viruses: 20 families and only five different architectural principles for virion assembly. Curr Opin Virol **1:**118-124.
32. **Martin, A., S. Yeats, D. Janekovic, W. D. Reiter, W. Aicher, and W. Zillig.** 1984. SAV 1, a temperate u.v.-inducible DNA virus-like particle from the archaebacterium *Sulfolobus acidocaldarius* isolate B12. EMBO J **3:**2165-2168.
33. **Nadal, M., G. Mirambeau, P. Forterre, W. D. Reiter, and M. Duguet.** 1986. Positively supercoiled DNA in a virus-like particle of an archaebacterium. Nature **321:**256-258.
34. **Clore, A. J., and K. M. Stedman.** 2007. The SSV1 viral integrase is not essential. Virology **361:**103-111.
35. **Muskhelishvili, G.** 1994. The archaeal SSV integrase promotes intermolecular excisive recombination *in vitro*. Syst Appl Microbiol **16:**605-608.
36. **Serre, M. C., C. Letzelter, J. R. Garel, and M. Duguet.** 2002. Cleavage properties of an archaeal site-specific recombinase, the SSV1 integrase. J Biol Chem **277:**16758-16767.
37. **Palm, P., C. Schleper, B. Grampp, S. Yeats, P. McWilliam, W. D. Reiter, and W. Zillig.** 1991. Complete nucleotide sequence of the virus SSV1 of the archaebacterium *Sulfolobus shibatae*. Virology **185:**242-250.
38. **Jonuscheit, M., E. Martusewitsch, K. M. Stedman, and C. Schleper.** 2003. A reporter gene system for the hyperthermophilic archaeon *Sulfolobus solfataricus* based on a selectable and integrative shuttle vector. Mol Microbiol **48:**1241-1252.
39. **Stedman, K. M., C. Schleper, E. Rumpf, and W. Zillig.** 1999. Genetic requirements for the function of the archaeal virus SSV1 in *Sulfolobus solfataricus*: construction and testing of viral shuttle vectors. Genetics **152:**1397-1405.
40. **Schleper, C., K. Kubo, and W. Zillig.** 1992. The particle SSV1 from the extremely thermophilic archaeon *Sulfolobus* is a virus: demonstration of infectivity and of transfection with viral DNA. Proc Natl Acad Sci U S A **89:**7645-7649.
41. **Fröls, S., P. M. Gordon, M. A. Panlilio, C. Schleper, and C. W. Sensen.** 2007. Elucidating the transcription cycle of the UV-inducible hyperthermophilic archaeal virus SSV1 by DNA microarrays. Virology **365:**48-59.
42. **Fusco, S., Q. She, S. Bartolucci, and P. Contursi.** 2013. T(lys), a newly identified *Sulfolobus* spindle-shaped virus 1 transcript expressed in the lysogenic state, encodes a DNA-binding protein interacting at the promoters of the early genes. J Virol **87:**5926-5936.

43. **Reiter, W. D., P. Palm, A. Henschen, F. Lottspeich, W. Zillig, and B. Grampp.** 1987. Identification and characterization of the genes encoding three structural proteins of the *Sulfolobus* virus-like particle SSV1. Mol Gen Genet **206:**144-153.
44. **Menon, S. K., W. S. Maaty, G. J. Corn, S. C. Kwok, B. J. Eilers, P. Kraft, E. Gillitzer, M. J. Young, B. Bothner, and C. M. Lawrence.** 2008. Cysteine usage in *Sulfolobus* spindle-shaped virus 1 and extension to hyperthermophilic viruses in general. Virology **376:**270-278.
45. **Reiter, W. D., W. Zillig, and P. Palm.** 1988. Archaebacterial viruses. Adv Virus Res **34:**143-188.
46. **Stedman, K. M., M. DeYoung, M. Saha, M. B. Sherman, and M. C. Morais.** 2015. Structural insights into the architecture of the hyperthermophilic Fusellovirus SSV1. Virology **474:**105-109.
47. **Hong, C., M. K. Pietilä, C. J. Fu, M. F. Schmid, D. H. Bamford, and W. Chiu.** 2015. Lemon-shaped halo archaeal virus His1 with uniform tail but variable capsid structure. Proc Natl Acad Sci U S A **112:**2449-2454.
48. **Pietilä, M. K., N. S. Atanasova, H. M. Oksanen, and D. H. Bamford.** 2013. Modified coat protein forms the flexible spindle-shaped virion of haloarchaeal virus His1. Environ Microbiol **15:**1674-1686.
49. **Hanhijärvi, K. J., G. Ziedaite, M. K. Pietilä, E. Haeggstrom, and D. H. Bamford.** 2013. DNA ejection from an archaeal virus--a single-molecule approach. Biophys J **104:**2264-2272.
50. **Yeats, S., P. McWilliam, and W. Zillig.** 1982. A plasmid in the archaebacterium *Sulfolobus acidocaldarius*. EMBO J **1:**1035-1038.
51. **She, Q., R. K. Singh, F. Confalonieri, Y. Zivanovic, G. Allard, M. J. Awayez, C. C. Chan-Weiher, I. G. Clausen, B. A. Curtis, A. De Moors, G. Erauso, C. Fletcher, P. M. Gordon, I. Heikamp-de Jong, A. C. Jeffries, C. J. Kozera, N. Medina, X. Peng, H. P. Thi-Ngoc, P. Redder, M. E. Schenk, C. Theriault, N. Tolstrup, R. L. Charlebois, W. F. Doolittle, M. Duguet, T. Gaasterland, R. A. Garrett, M. A. Ragan, C. W. Sensen, and J. Van der Oost.** 2001. The complete genome of the crenarchaeon *Sulfolobus solfataricus* P2. Proc Natl Acad Sci U S A **98:**7835-7840.
52. **Zillig, W., A. Kletzin, C. Schleper, I. Holz, D. Janekovic, J. Hain, M. Lanzendorfer, and J. K. Kristjansson.** 1994. Screening for *Sulfolobales*, their plasmids and their viruses in Icelandic solfataras. Syst Appl Microbiol **16:**609-628.
53. **Schägger, H., and G. von Jagow.** 1987. Tricine-sodium dodecyl sulfate-polyacrylamide gel electrophoresis for the separation of proteins in the range from 1 to 100 kDa. Anal Biochem **166:**368-379.
54. **Pietilä, M. K., E. Roine, L. Paulin, N. Kalkkinen, and D. H. Bamford.** 2009. An ssDNA virus infecting archaea: a new lineage of viruses with a membrane envelope. Mol Microbiol **72:**307-319.
55. **Krogh, A., B. Larsson, G. von Heijne, and E. L. Sonnhammer.** 2001. Predicting transmembrane protein topology with a hidden Markov model: application to complete genomes. J Mol Biol **305:**567-580.
56. **Cole, C., J. D. Barber, and G. J. Barton.** 2008. The Jpred 3 secondary structure prediction server. Nucleic Acids Res **36:**W197-201.
57. **Pitcher, A., E. C. Hopmans, A. C. Mosier, S. J. Park, S. K. Rhee, C. A. Francis, S. Schouten, and J. S. Damsté.** 2011. Core and intact polar glycerol dibiphytanyl glycerol tetraether lipids of ammonia-oxidizing archaea enriched from marine and estuarine sediments. Appl Environ Microbiol **77:**3468-3477.
58. **Huguet, C., E. C. Hopmans, W. Febo-Ayala, D. H. Thompson, J. S. Sinninghe Damsté, and S. Schouten.** 2006. An improved method to determine the absolute abundance of glycerol dibiphytanyl glycerol tetraether lipids. Org Geochem **37:**1036-1041.
59. **Schouten, S., C. Huguet, E. C. Hopmans, M. V. Kienhuis, and J. S. Damsté.** 2007. Analytical methodology for TEX86 paleothermometry by high-performance liquid chromatography/atmospheric pressure chemical ionization-mass spectrometry. Anal Chem **79:**2940-2944.
60. **Quemin, E. R., S. Lucas, B. Daum, T. E. Quax, W. Kuhlbrandt, P. Forterre, S. V. Albers, D. Prangishvili, and M. Krupovic.** 2013. First insights into the entry process of hyperthermophilic archaeal viruses. J Virol **87:**13379-13385.

61. **Wiedenheft, B., K. Stedman, F. Roberto, D. Willits, A. K. Gleske, L. Zoeller, J. Snyder, T. Douglas, and M. Young.** 2004. Comparative genomic analysis of hyperthermophilic archaeal *Fuselloviridae* viruses. J Virol **78:**1954-1961.
62. **Pietilä, M. K., N. S. Atanasova, V. Manole, L. Liljeroos, S. J. Butcher, H. M. Oksanen, and D. H. Bamford.** 2012. Virion architecture unifies globally distributed pleolipoviruses infecting halophilic archaea. J Virol **86:**5067-5079.
63. **Bradford, M. M.** 1976. A rapid and sensitive method for the quantitation of microgram quantities of protein utilizing the principle of protein-dye binding. Anal Biochem **72:**248-254.
64. **Napoli, A., Y. Zivanovic, C. Bocs, C. Buhler, M. Rossi, P. Forterre, and M. Ciaramella.** 2002. DNA bending, compaction and negative supercoiling by the architectural protein Sso7d of *Sulfolobus solfataricus*. Nucleic Acids Res **30:**2656-2662.
65. **Zhang, Z., L. Guo, and L. Huang.** 2012. Archaeal chromatin proteins. Sci China Life Sci **55:**377-385.
66. **Berggren, K., E. Chernokalskaya, T. H. Steinberg, C. Kemper, M. F. Lopez, Z. Diwu, R. P. Haugland, and W. F. Patton.** 2000. Background-free, high sensitivity staining of proteins in one- and two-dimensional sodium dodecyl sulfate-polyacrylamide gels using a luminescent ruthenium complex. Electrophoresis **21:**2509-2521.
67. **Kandiba, L., O. Aitio, J. Helin, Z. Guan, P. Permi, D. H. Bamford, J. Eichler, and E. Roine.** 2012. Diversity in prokaryotic glycosylation: an archaeal-derived N-linked glycan contains legionaminic acid. Mol Microbiol **84:**578-593.
68. **Maaty, W. S., A. C. Ortmann, M. Dlakic, K. Schulstad, J. K. Hilmer, L. Liepold, B. Weidenheft, R. Khayat, T. Douglas, M. J. Young, and B. Bothner.** 2006. Characterization of the archaeal thermophile *Sulfolobus* turreted icosahedral virus validates an evolutionary link among double-stranded DNA viruses from all domains of life. J Virol **80:**7625-7635.
69. **Mochizuki, T., T. Yoshida, R. Tanaka, P. Forterre, Y. Sako, and D. Prangishvili.** 2010. Diversity of viruses of the hyperthermophilic archaeal genus *Aeropyrum*, and isolation of the *Aeropyrum pernix* bacilliform virus 1, APBV1, the first representative of the family *Clavaviridae*. Virology **402:**347-354.
70. **Mochizuki, T., M. Krupovic, G. Pehau-Arnaudet, Y. Sako, P. Forterre, and D. Prangishvili.** 2012. Archaeal virus with exceptional virion architecture and the largest single-stranded DNA genome. Proc Natl Acad Sci U S A **109:**13386-13391.
71. **Larson, E. T., D. Reiter, M. Young, and C. M. Lawrence.** 2006. Structure of A197 from *Sulfolobus* turreted icosahedral virus: a crenarchaeal viral glycosyltransferase exhibiting the GT-A fold. J Virol **80:**7636-7644.
72. **Jarrell, K. F., Y. Ding, B. H. Meyer, S. V. Albers, L. Kaminski, and J. Eichler.** 2014. N-linked glycosylation in Archaea: a structural, functional, and genetic analysis. Microbiol Mol Biol Rev **78:**304-341.
73. **Palmieri, G., M. Balestrieri, J. Peter-Katalinic, G. Pohlentz, M. Rossi, I. Fiume, and G. Pocsfalvi.** 2013. Surface-exposed glycoproteins of hyperthermophilic *Sulfolobus solfataricus* P2 show a common N-glycosylation profile. J Proteome Res **12:**2779-2790.
74. **Villanueva, L., J. S. Damste, and S. Schouten.** 2014. A re-evaluation of the archaeal membrane lipid biosynthetic pathway. Nat Rev Microbiol **12:**438-448.
75. **Schouten, S., E. C. Hopmans, and J. S. Sinninghe Damsté.** 2013. The organic geochemistry of glycerol dialkyl glycerol tetraether lipids: a review. Org Geochem **54:**19–61.
76. **Langworthy, T. A.** 1977. Comparative lipid composition of heterotrophically and autotrophically grown Sulfolobus acidocaldarius. J Bacteriol **130:**1326-1332.
77. **Langworthy, T. A., W. R. Mayberry, and P. F. Smith.** 1974. Long-chain glycerol diether and polyol dialkyl glycerol triether lipids of Sulfolobus acidocaldarius. J Bacteriol **119:**106-116.
78. **Flint, S. J., L. W. Enquist, V. R. Racaniello, and A. M. Skalka.** 2009. Principles of Virology, 3rd edition ed. ASM Press, Washington DC.
79. **Iverson, E., and K. Stedman.** 2012. A genetic study of SSV1, the prototypical fusellovirus. Front Microbiol **3:**200.

80. **Makarova, K. S., Y. I. Wolf, P. Forterre, D. Prangishvili, M. Krupovic, and E. V. Koonin.** 2014. Dark matter in archaeal genomes: a rich source of novel mobile elements, defense systems and secretory complexes. Extremophiles **18:**877-893.

81. **Happonen, L. J., P. Redder, X. Peng, L. J. Reigstad, D. Prangishvili, and S. J. Butcher.** 2010. Familial relationships in hyperthermo- and acidophilic archaeal viruses. J Virol **84:**4747-4754.

82. **Pawlowski, A., I. Rissanen, J. K. Bamford, M. Krupovic, and M. Jalasvuori.** 2014. *Gammasphaerolipovirus*, a newly proposed bacteriophage genus, unifies viruses of halophilic archaea and thermophilic bacteria within the novel family *Sphaerolipoviridae*. Arch Virol **159:**1541-1554.

83. **López-García, P., S. Knapp, R. Ladenstein, and P. Forterre.** 1998. In vitro DNA binding of the archaeal protein Sso7d induces negative supercoiling at temperatures typical for thermophilic growth. Nucleic Acids Res **26:**2322-2328.

84. **Menon, S. K., B. J. Eilers, M. J. Young, and C. M. Lawrence.** 2010. The crystal structure of D212 from sulfolobus spindle-shaped virus ragged hills reveals a new member of the PD-(D/E)XK nuclease superfamily. J Virol **84:**5890-5897.

85. **Ellen, A. F., S. V. Albers, W. Huibers, A. Pitcher, C. F. Hobel, H. Schwarz, M. Folea, S. Schouten, E. J. Boekema, B. Poolman, and A. J. Driessen.** 2009. Proteomic analysis of secreted membrane vesicles of archaeal *Sulfolobus* species reveals the presence of endosome sorting complex components. Extremophiles **13:**67-79.

A

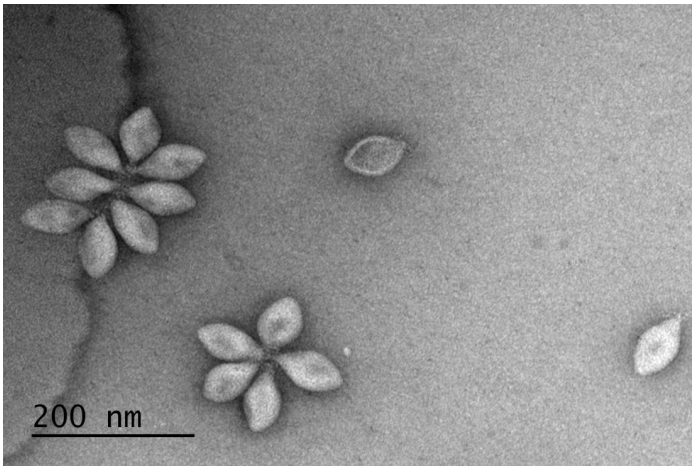

B

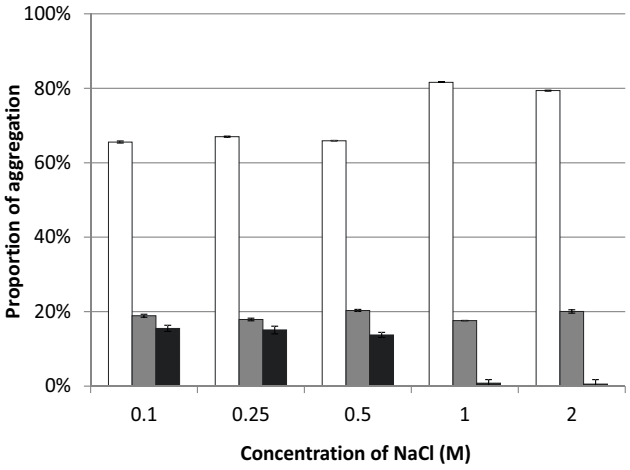

C

Purification step	Absorbance (λ=260nm)	Titer (PFU/mL)	Recovery of infectivity (%)	Specific infectivity (PFU/mL/absorbance)
Cell-free supernatant	ND	$8.5x10^6$	100	ND
Ammonium sulfate precipitate	ND	$1.6x10^8$	80.6	ND
Rate zonal centrifugation	0.6	$3x10^7$	48.3	$0.5x10^8$
Density centrifugation	0.6	$1.2x10^8$	68.4	$1.9x10^8$
2x SSV1	10.9	$2.3x10^9$	30.7	$2.1x10^8$

ND: not determined

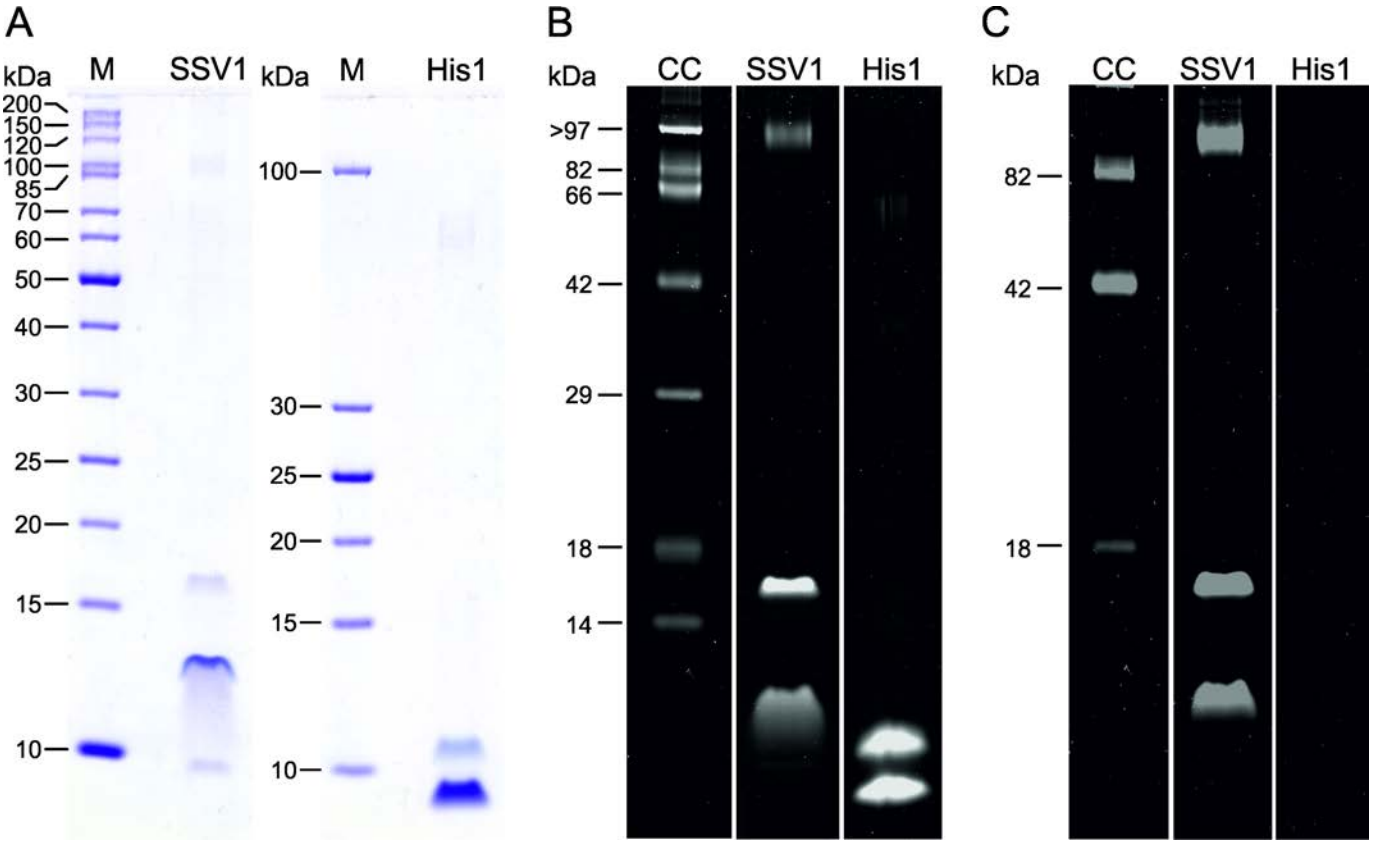

A

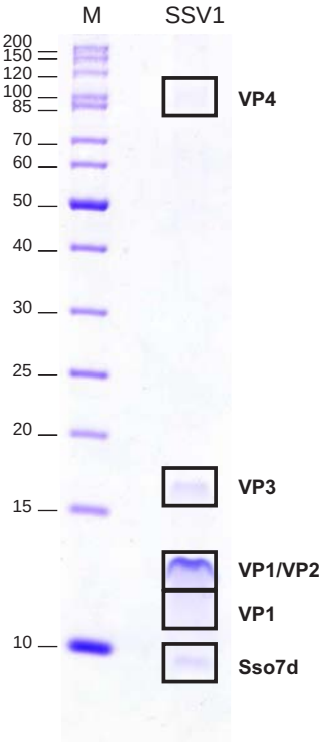

B

Protein	Accession number	Calculated mass (kDa)	Putative function	Identification[a]	Sequences determined
VP1	NP_597839	7.74[b]	Coat protein	NS MS	EATNI AVVAYKIYKD
VP2	NP_039802	8.61	DNA-binding protein	MS	RSLLSALL KRSLLSAL
VP3	NP_039801	9.8	Coat protein	NS	MEISL
VP4	NP_039798	85.658	Terminal filaments	MS	ALLIGGGG LLIGGGGPNNNGAGVY
Sso7d	NP_343300	7.279	DNA-binding protein	MS	KELLQMLE KMISFTYD

[a] - NS, N-terminal Sequencing; MS, Mass Spectrometry. [b] - calculated mass of proteolytically processed mature protein.

C

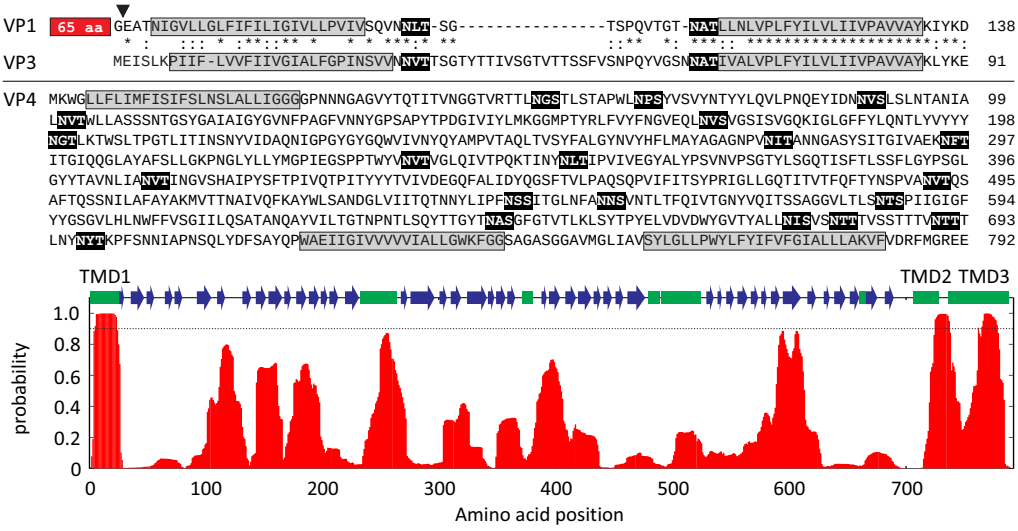

A

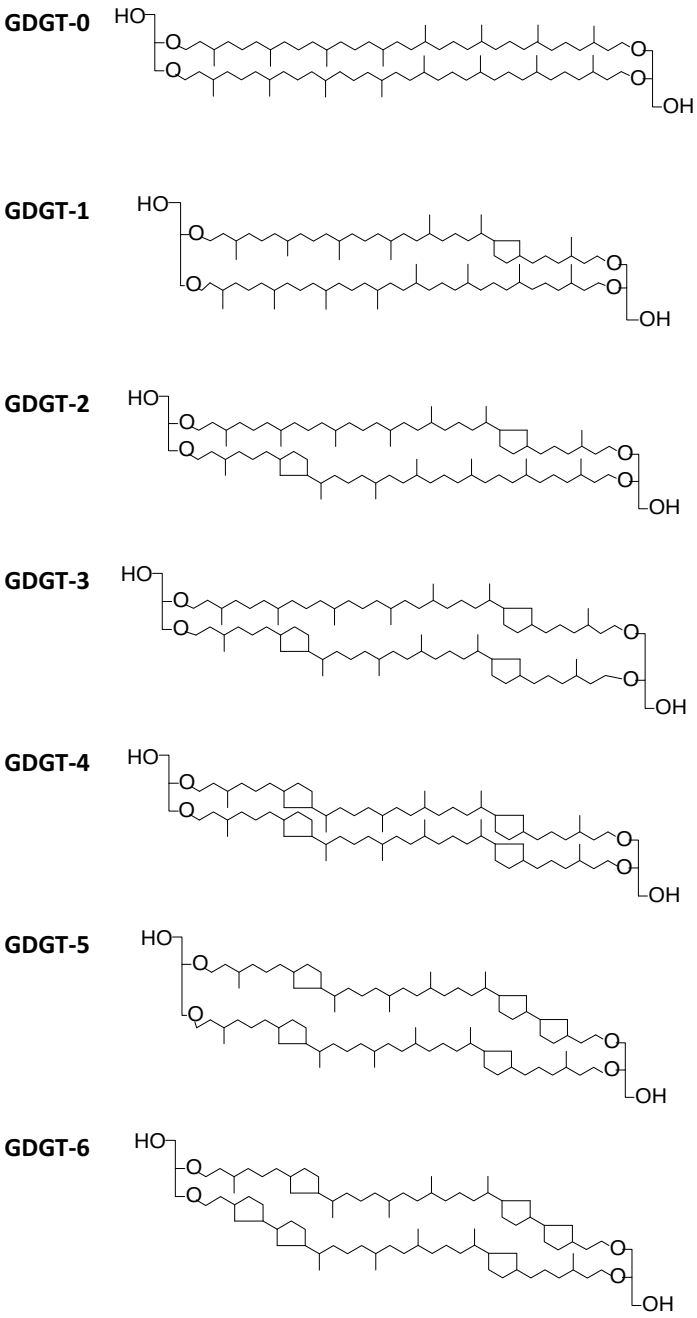

B

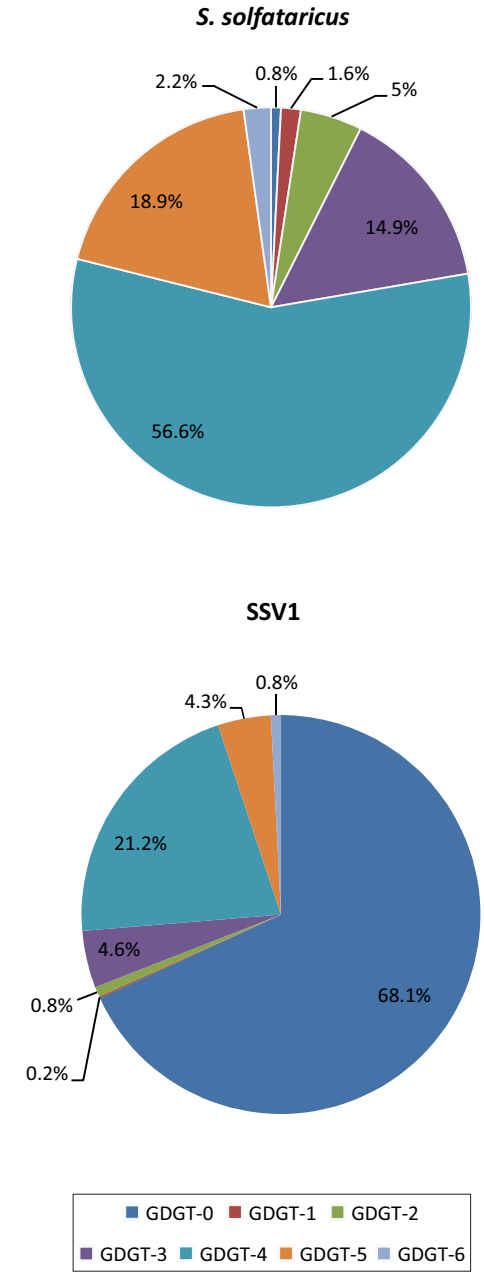

CHAPTER 5

The egress of SSV1 or how to bud from an archaeon.

How to bud from an archaeon: assembly and egress of *Sulfolobus* spindle-shaped virus 1

Quemin ER[1], Chlanda P[2], Sachse M[3], Forterre P[1], Zimmerberg J[2], Prangishvili D[1] and Krupovic M[1]

[1]Unité de Biologie Moléculaire du Gène chez les Extrêmophiles, Département de Microbiologie, Institut Pasteur, Paris, France
[2]National Institutes of Health, Eunice Kennedy Shriver National Institute of Child Health and Human Development, Bethesda, MD, USA
[3]Imagopole, Institut Pasteur, Paris, France

Running title: Egress of SSV1

Abstract

Viruses infecting archaea display a high diversity of virion morphotypes, many of which were never observed among bacterial or eukaryotic viruses. In particular, viruses with spindle-shaped, or fusiform, virions are common in geothermal and hypersaline environments dominated by archaea. Indeed, fusiform viruses represent the largest group of unique archaeal viruses and *Sulfolobus* spindle-shaped virus 1 (SSV1) serves as a model for understanding their biology. We have recently shown that SSV1 virions are composed of glycosylated proteins and host-derived lipids, which together encase the nucleoprotein filament. However, very little is known about the ways spindle-shaped viruses, and viruses of archaea in general, interact with their hosts. Here, we characterized the assembly and release of SSV1 from its natural host, the hyperthermo-acidophilic *Sulfolobus shibatae* B12. The replication of SSV1 has a pronounced effect on the subcellular organization of the host cell. At the cell periphery, the periplasmic space between the cytoplasmic membrane and the proteinaceous surface (S-) layer becomes wider, most likely as a result of modification by viral proteins. Approximately half of the cell population was deprived of any cytoplasmic content and exhibit discontinuities in the cytoplasmic membrane. Electron tomography of infected *Sulfolobus* cells revealed that assembly of SSV1 virions is concomitant with release from the host via budding through the cytoplasmic membrane and S-layer. The viral nucleoprotein complexes are extruded in the form of tube-like structures which have an envelope continuous with the cytoplasmic membrane. Subsequently, but still in association with the cell envelope, the tube-like virions appear to maturate to assume the characteristic, spindle-shaped morphology of infectious virions. Some of these spindle-shaped particles are also connected to the membrane by a dark, constricting ring-like structure which is similar to the “bud neck” involved in membrane scission during the budding of enveloped eukaryotic viruses.

Introduction

One of the most intriguing features of archaea is their capacity to thrive in nearly all conceivable environments. Members of the third domain of life are highly diversified in terms of metabolic capacities which allow them to sustain a wide range of temperature, pH, salinity, pressure, etc. (Robertson et al., 2005). Archaea are abundant in moderate environments where they can constitute a substantial fraction of the microbial biomass but their dominance over other microorganisms is particularly pronounced in hypersaline and geothermal habitats. Accordingly, recent studies have shown that archaeal species play a major role in geochemical cycles (Offre et al., 2013). Numerous environmental sampling expeditions have not only shed light on prokaryotic diversity but also provided a glimpse into the diversity of viruses present on our planet. The specific virosphere associated with archaea comprises several groups of viruses with virion morphotypes never observed for viruses that infect bacteria or eukaryotes (Prangishvili, 2013). Beside filamentous, bacilliform, spherical, droplet-shaped, bottle-shaped, etc. virus-like particles, spindle-shaped virions represent thus far the largest and probably one of the most evolutionarily successful groups of archaeal viruses (Pina et al., 2011). However, our understanding of these unique and highly diverse viruses is limited by the fact that the majority of their genes do not display any similarity to sequences in public databases (Krupovic et al., 2012).

Recently, we used structural proteins as markers and protein homology to determine the relationships between all fusiform viruses infecting archaea (Krupovic et al., 2014). It became apparent that all previously unclassified spindle-shaped viruses isolated from highly diverse habitats and infecting hosts with very different metabolic strategies belong to the family *Fuselloviridae*. All these viruses have very similar overall virion organization: the small lemon-shaped body (60x100 nm) is decorated with terminal fibers at one of the two pointed ends and encases the nucleoprotein complex. The virions are typically constructed from one major capsid protein (MCP) species which is characterized by the presence of two hydrophobic domains in the N- and C-terminus, respectively (Krupovic et al., 2014). *Sulfolobus* spindle-shaped virus 1 (SSV1) is the prototype of the *Fuselloviridae* family (Martin et al., 1984). Research up to date was aimed at characterization of (i) the infection cycle (Fusco et al., 2015, Stedman et al., 1999, Schleper et al., 1992, Palm et al., 1991); (ii) establishment of lysogeny by site-specific integration of viral genome into the host chromosome (Zhan et al., 2012, Clore and Stedman, 2007, Letzelter et al., 2004, Muskhelishvili et al., 1993, Serre et al., 2002); (iii) transcription regulation of viral and host

genes during virus replication (Frols et al., 2007, Fusco et al., 2013, Reiter et al., 1987b); (iv) architecture of virions (Iverson and Stedman, 2012, Palm et al., 1991, Quemin et al., 2015, Reiter et al., 1987a, Stedman et al., 2015).

The viral particles are composed of four virus-encoded capsid proteins, namely VP1, VP2, VP3 and VP4, as well as one host-encoded protein. The SSV1 MCP, VP1, is known to maturate through proteolytic cleavage of a precursor molecule and together with VP3 and VP4, undergo post-translational modification by glycosylation (Quemin et al., 2015, Reiter et al., 1987a). The cellular DNA-binding protein Sso7d, which is the most abundant chromatin-remodeling protein present in the host, is also found in purified virions. Glycerol dialkyl glycerol tetraether (GDGT) lipids have also been unambiguously identified in SSV1 particles. The composition and ratios of the different lipid species were different between the viral and cellular samples arguing for a selective acquisition in virions from the host cytoplasmic membrane (Quemin et al., 2015). These archaea-specific lipids are structurally distinct from their bacterial and eukaryotic counterparts and display an ether linkage between glycerol and hydrocarbon chains forming a covalently-bound monolayer (De Rosa et al., 1986). Therefore, SSV1 is a unique lipid-containing virus composed of glycosylated structural proteins and host-derived lipids which together encapsidate the nucleoprotein filament.

Several aspects of the virus biology still remain unstudied, including the way SSV1 interacts with its host (Quemin and Quax, 2015). Early reports on SSV1 featured electron micrographs of *Sulfolobus* cells from which virus-like particles were released through the cytoplasmic membrane (Martin et al., 1984). Based on these observations, it was concluded that SSV1 virions exit the host cell via budding. However, until now this finding has not been further investigated. Here, we report the detailed analysis of SSV1 assembly and egress from its natural lysogenized host, *Sulfolobus shibatae* B12. We show that virus induction by UV irradiation leads to severe modifications of the organization of the lysogenic cells. Profound reorganization was observed both at the level of cellular membrane as well as in the cytoplasm. Furthermore, electron tomography provided valuable insights into the different stages of the assembly and budding of SSV1 virions through the host cytoplasmic membrane and the S-layer.

Results

Replication of SSV1 retards the growth of its host.

Replication of the virus can be induced by UV irradiation of *S. shibatae* B12, the natural carrier of SSV1 (Martin et al., 1984, Schleper et al., 1992). As previously observed, the growth of UV-irradiated culture was retarded compared to control cells and recovered a normal growth rate only 48 hours post irradiation (hpi) (Figure 1A). Time-course analysis of viral replication using electron microscopy techniques revealed three phenotypes of *S. shibatae* cells: regular, extracted and condensed cells. The regular cells contain an evenly distributed cytoplasmic content and in all aspects do not seem to be affected by UV irradiation when analyzed by transmission electron microscopy (TEM) (Figure 1C). By contrast, the extracted cells appear to be empty, deprived of all intracellular components (Figure 1D). Other cells, which we refer to as condensed, were about half the diameter of regular cells, exhibited an irregular shape and the cytoplasmic content was denser than in regular cells (Figure 1E). Although the last two categories – extracted and small – accounted for less than 4% (n=279) of the total population in the non-irradiated control cultures, their proportion slowly increased in samples from 9 hpi (Figure 1B). By 24 hpi, the so-called extracted sub-population represented nearly half (40%; n=336) of all *S. shibatae* cells. SSV1 is a temperate virus and has been considered not to induce lysis of the host (Schleper et al., 1992). However, it has been reported recently that induction of the viral cycle by UV leads to the death of 35% of the cell population (Fusco et al., 2015). In another recent study, infection of *S. islandicus* with fusellovirus SSV9 led to the emergence of a cell sub-population which phenotypically resembles our extracted cells; it was proposed that such cells are in a dormant state but can eventually recover and resume the growth (Bautista et al., 2015). Consequently, the phenotypic changes which we observe in *S. shibatae* cells induced for virus production might represent a general effect associated with the propagation of different fuselloviruses (SSV1 and SSV9). Importantly, the fact that extracted cells are also present in SSV9-infected (rather than induced) populations suggests that the phenomenon is not a result of UV irradiation but is a genuine outcome of virus propagation.

Changes in cell morphology over time are linked to viral replication.

TEM analysis of high-pressure-frozen and thin-sectioned *S. shibatae* B12 cells revealed the presence of spherical, electron-lucent structures in the cell cytoplasm (Figure 2A). These macromolecular aggregates were also found in a small subset of cells in the control (non-

irradiated) culture. However, the proportion of cells with such structures increased in the cell population following replication of the virus (Figure 2B). Although they display an overall spherical shape, there is certain heterogeneity in their size. Their diameter was larger at 6 and 9 hpi when compared to those observed at earlier and later time points (Figure 2A). Initially, only a few of them – typically less than 5 – were present per cell but their number increased with time, and by 6 hpi they occupied most of the intracellular space, where they were tightly packed side by side (Figure 2A). *A priori* the production of these macromolecular aggregates could be a result of either SSV1 multiplication or UV treatment. Unfortunately, we failed to cure the lysogenized *S. shibatae* B12 strain from both the integrated and episomal copies of the viral genome, in agreement with the previous report (Schleper et al., 1992). Therefore, to verify if the observed increase in number and size of these cytoplasmic structures is linked with virus replication, cells of *S. solfataricus* P2, a close relative of *S. shibatae* B12 which can also be infected by SSV1, were used as a control (Schleper et al., 1992). A small proportion of *S. solfataricus* P2 cells also contained structures which were similar in their appearance to those observed in *S. shibatae* B12 cells. However, even after UV irradiation, neither their number nor their size increased in *S. solfataricus* P2 (Figure 2B). The results indicate that the dynamics of the cytoplasmic aggregates in the lysogenized strain is due to the active replication of SSV1 rather than a global stress response induced by the UV treatment.

Modifications of the cytoplasmic membrane, periplasmic space and S-layer.

The extracted cells were always present in cultures of *Sulfolobus* representing 4% of control cells that did not undergo UV treatment and 40% of UV-irradiated cells at 24 hpi (Figure 1B). Closer examination of *S. shibatae* B12 cells by electron microscopy techniques provided valuable insights into the ultrastructural differences between the different cell phenotypes. Whereas the membranes of the regular cells were continuous, those in the extracted sub-population were often fragmented (Figure 3A and D). In the latter, the cytoplasmic membrane appeared ruptured and these ruptures were particularly pronounced in the irradiated population, where the proportion of extracted cells was higher (Figure 3C and F; red arrows). The discontinuity in the cytoplasmic membrane was accompanied by the appearance of small intracellular vesicle-like structures or membrane remnants localized close to the membrane rupture points (Figure 3F; red arrows). Concerning, the regular cells, although the membrane appears intact, it is the cell envelope which is visibly modified. The periplasm, defined as the space between the cytoplasmic membrane and the protein S-layer which surrounds the cell (Albers and Meyer, 2011), was significantly wider at late time points after UV irradiation.

When compared to the non-irradiated cells, it increased from 18 nm (SD=4 nm; n=10) to 24 nm (SD=2 nm; n=10) at 24 hpi, most likely as a result of expression and accumulation of viral proteins (Figure 3B and E; blue square brackets). Furthermore, the cell surface is also extensively modified through the course of viral replication. S-layer density changes are obvious in the majority of cells (Figure 4). Whereas, under normal growth conditions the S-layer is dense and homogeneous, at late time points there is a hexagonal organization rendering its appearance spiky-like and less dense.

SSV1 assembly and budding at the cytoplasmic membrane.

Assembly and release of SSV1 virions were observed to be concomitant and occur in close proximity to the cytoplasmic membrane. Nascent tube-like structures continuous with the host cytoplasmic membrane were observed at the surface of irradiated cells at 12 hpi (Figure 5Aa and b). Notably, the inner leaflet of the bilayer appeared more contrasted by negative staining when compared to the outer leaflet. The fact that this difference was not visible in the controls, non-irradiated *S. shibatae* B12 and irradiated *S. solfataricus* P2, suggests a modification by proteins of viral origin. Interestingly, heavily stained complexes, which are likely to represent the viral nucleoprotein, were also found to be juxtaposed to the membrane and occasionally seen in the process of being encased into the tube-like structures (Figure 5Aa and b). Beside the tube-like particles, we have also observed — particularly at the latest time points after induction — spindle-shaped virions attached to the cell surface (Figure 5Ac). Unlike the situation of tube-like structures for which the lumen and envelope showed continuity with the cytoplasmic content and cellular membrane, respectively, the spindle-shaped virions were no longer continuous with the cell but rather loosely attached to its surface. Observation of two morphologically distinct particles suggests that SSV1 virion maturation occurs outside of the host cell but in association with its envelope. Consistently, the viral envelope is thinner (~4 nm) than the membrane of *Sulfolobus* cells (~5 nm), despite the fact that the former is derived from the latter. Electron tomography of infected *Sulfolobus* cells revealed additional features associated with the release of SSV1 virions. In particular, in some cases the membrane between the budded virion and the cell was constricted (Figure 5Aa, Ab and Bb; yellow arrows). Such structures are specifically located at the site of membrane constriction, suggesting a key role in the mechanism of scission between the cytoplasmic membrane and the viral envelope.

Discussion

For the first time, the assembly and egress of an enveloped virus infecting archaea has been investigated. We selected the well-characterized fusellovirus SSV1 and its natural carrier *S. shibatae* B12 as a model. After induction of viral replication by UV stimuli, the growth of the irradiated culture was slowed down and required 48h to recover a growth rate comparable to that of control cells (Figure 1A). Beside what we considered as regular and condensed phenotypes, extracted cells appeared to be empty, as if they were devoid of cytoplasmic content (Figure 1C, D and E). At late time points, the proportion of such cells increased from 4% to more than 40% which might be due to a lack of recovery from virus infection and/or UV stress for some of the growth-retarded population (Figure 1B). We hypothesize that this category represents cells in which virus replication and production have occurred. The proportion of such cells in the control cultures is negligible and likely represents the basal level of spontaneous SSV1 induction under optimal growth conditions of its host.

Analysis of the thin-sections further revealed the presence of spherical, electron-lucent aggregates in the cytoplasm of cells. They were found to increase in number and size between 3 and 9 hpi as a result of SSV1 infection (Figure 2). However, the composition and exact role of such structures during the viral cycle requires further investigation. In particular, we cannot exclude the possibility that they have a protective role in conferring immunity nor that they represent the initial stages of a phenomenon leading to the extracted phenotype. Therefore, it seems that activation of SSV1 cycle has strong effects on the subcellular organization and structure of the host cell. The so-called extracted cells are also characterized by the presence of ruptures in the cytoplasmic membrane questioning the integrity of *Sulfolobus* surface and whether the cell homeostasis is maintained (Figure 3C and F). Additional changes at the cellular membrane and surface take place in infected and irradiated *Sulfolobus* cells. Indeed, the periplasmic space which is located between the plasma membrane and the S-layer is 6 nm wider at 24 hpi when compared to non-irradiated controls (Figure 3B and E). The regular cells could represent a dormant state of the infection cycle. Following induction by UV, the viral genome will be replicated and the viral proteins synthetized (Frols et al., 2007, Fusco et al., 2013). The resulting accumulation of viral proteins and in particular of the structural components of virions would lead to modification of the cell periphery and increase in the periplasmic space. Whether the disorganization of the S-layer reported here is due to a direct (accumulation of viral membrane-binding proteins in the cytoplasmic membrane) or indirect (budding of virus leads to membrane ruptures and loss of cell turgor) effect of SSV1

replication has to be further investigated. Eventually, the production of SSV1 particles in the cell might be high, provoking the ruptures of the host cytoplasmic membrane in a way that most of the cytoplasmic content would leak out.

Furthermore, electron tomography revealed virion release from infected *Sulfolobus* cells via budding through the cytoplasmic membrane (Figure 4). Our findings suggest that the nucleoprotein filament is condensed at the cell periphery. Viral nucleoprotein appears to be extruded through the cytoplasmic membrane in the form of tube-like structures which subsequently assume the spindle-shaped morphology once membrane scission has occurred. Observation of morphologically distinct virions at different stages of virion release indicates that SSV1 needs to undergo structural rearrangement to gain the morphology of mature, infectious virions. In fact, although the viral envelope is clearly acquired from the cytoplasmic membrane during the process of egress; additional re-organization of structural components takes place within the particles, probably during or immediately after scission of the nascent virions from the parental membrane. Host-derived lipids have been identified in SSV1 virions, consistent with the observed budding mechanism(Quemin et al., 2015). These GDGT lipids are specific to archaea and differ from their bacterial and eukaryotic counterparts in that they are composed of long isoprenoid chains which are covalently linked forming a tightly-bound bilayer membrane (Albers and Meyer, 2011, De Rosa et al., 1986). Therefore, how membrane scission occurs in the case of SSV1 is intriguing and one of the main questions we are trying to address.

Assembly and exit are thus concomitant and the membrane scission events reported here as well as the presence of putative “bud neck” structures during virion release strongly suggest that SSV1 employs an egress strategy similar to that of eukaryotic enveloped viruses, such as HIV or influenza virus. Key machinery involved in the budding of enveloped eukaryotic viruses includes the ESCRT system and the ESCRT-III complex in particular (Hurley and Hanson, 2010, Marsh and Thali, 2003, Wollert et al., 2009). The role of known archaeal homologues to the ESCRT-III system (Lindas and Bernander, 2013, Moriscot et al., 2011, Samson and Bell, 2009) during SSV1 egress are the focus of ongoing research in our laboratory since several eukaryotic systems have been shown to bud through the host cytoplasmic membrane by hijacking the cellular ESCRT machinery (Hurley and Hanson, 2010).

Materials and Methods

Viruses, strains and growth conditions.

Sulfolobus shibatae strain B12 (Yeats et al., 1982) and *Sulfolobus solfataricus* strain P2 (She et al., 2001) were used as hosts for SSV1 (Martin et al., 1984). All cultures were grown aerobically (120 rpm; Innova 44 Eppendorf, Germany) at 78°C. The *Sulfolobus* growth medium was prepared as described previously (Zillig et al., 1993).

To induce SSV1 replication, cultures of lysogenized *S. shibatae* B12 at an optical density [OD_{600nm}] of 0.2-0.3 were treated with UV as previously described (Martin et al., 1984).

Growth curve

The growth of *S. shibatae* B12 cultures was followed by measuring optical density at a wavelength of 600 nm [OD_{600nm}] after UV irradiation.

Sample preparation for electron microscopy

Cultures of 50 mL of *S.shibatae* B12 at 0, 3, 6, 9, 12 and 24 hpi or *S. solfataricus* P2 at 0, 3, 6, 9 hpi were pelleted by low-speed centrifugation (4 000rpm – 15 min – 15°C ; Jouan BR4i, Thermo Scientific) and (4 000 rpm – 10 min – 15°C ; Beckmann-Coulter Alegra X-22). Cell pastes were transferred into a lecithin coated sample holder type A and frozen with a high pressure freezing machine, Bal-Tec HPM 010 (Bal-Tec Products, Middlebury, CT, USA). Following cryo-fixation, the samples were freeze-substituted with 0.5% glutaraldehyde (Electron Microscopy Sciences, Washington, PA, USA), 1% OsO_4 (Merck Millipore, Germany), 0.2% uranyl acetate (Merck, Darmstadt, Germany), 2% H_2O and 4% methanol in acetone (Electron Microscopy Sciences, Washington, PA, USA) according to the following schedule: -90°C for 40h, 5°C/h for 6h, -60°C for 8h, 5°C/h for 6h and -30°C for 8h. The cells were rinsed three times in acetone (Electron Microscopy Sciences, Washington, PA, USA) and slowly infiltrated with Agar 100 Epoxy Resin (Agar Scientific, United Kingdom). After heat polymerization, 70 nm thin sections were cut with an Ultracut R Microtome (Leica, Vienna, Austria) and collected on Formvar-coated copper grids (Electron Microscopy Sciences, Washington, PA, USA). Sections were post-stained with 4% uranyl acetate for 45 min followed by 5 min in Reynold's lead citrate. The grids were viewed using a Tecnaï™ T12 transmission electron microscope (FEI, OR, USA) operated at 120 kV.

Electron tomography

For electron tomography, embedded cells were cut into serial 200 nm thick sections with an Ultracut R Microtome (Leica, Vienna, Austria) and collected on Formvar-coated copper slot grids (Electron Microscopy Sciences, Washington, PA, USA). The sections were decorated with 10 nm protein-A gold particles (EMS, Hatfield, PA) on both sides of the section and post-stained with 2% lead citrate in water. Single or dual-axis electron tomography was performed in a FEI Tecnai^{TM} 20 transmission electron microscope (FEI, Eindhoven, Netherlands) operated at 200 kV and equipped with K2 Summit camera (Gatan, Pleasanton, CA, USA). Tomographic tilt ranges were collected, typically from +55° to -55° with an angular increment of 1° at nominal magnification of 11 500x and pixel size of 0.259 nm/pixel. Tomograms were reconstructed using the IMOD software suite (Kremer et al., 1996).

Acknowledgements

This work was supported by the Agence nationale de la recherche (ANR) program BLANC, project EXAVIR. E.R.J.Q. was supported by a fellowship from the Ministère de l'Enseigement Supérieur et de la Recherche of France and the Université Pierre et Marie Curie, Paris, France.

References

ALBERS, S. V. & MEYER, B. H. 2011. The archaeal cell envelope. *Nat Rev Microbiol,* 9**,** 414-26.

BAUTISTA, M. A., ZHANG, C. & WHITAKER, R. J. 2015. Virus-induced dormancy in the archaeon Sulfolobus islandicus. *MBio,* 6.

CLORE, A. J. & STEDMAN, K. M. 2007. The SSV1 viral integrase is not essential. *Virology,* 361**,** 103-11.

DE ROSA, M., GAMBACORTA, A. & GLIOZZI, A. 1986. Structure, biosynthesis, and physicochemical properties of archaebacterial lipids. *Microbiol Rev,* 50**,** 70-80.

FROLS, S., GORDON, P. M., PANLILIO, M. A., DUGGIN, I. G., BELL, S. D., SENSEN, C. W. & SCHLEPER, C. 2007. Response of the hyperthermophilic archaeon Sulfolobus solfataricus to UV damage. *J Bacteriol,* 189**,** 8708-18.

FUSCO, S., SHE, Q., BARTOLUCCI, S. & CONTURSI, P. 2013. T(lys), a newly identified Sulfolobus spindle-shaped virus 1 transcript expressed in the lysogenic state, encodes a DNA-binding protein interacting at the promoters of the early genes. *J Virol,* 87**,** 5926-36.

FUSCO, S., SHE, Q., FIORENTINO, G., BARTOLUCCI, S. & CONTURSI, P. 2015. Unravelling the Role of the F55 Regulator in the Transition from Lysogeny to UV Induction of Sulfolobus Spindle-Shaped Virus 1. *J Virol,* 89**,** 6453-61.

HURLEY, J. H. & HANSON, P. I. 2010. Membrane budding and scission by the ESCRT machinery: it's all in the neck. *Nat Rev Mol Cell Biol,* 11**,** 556-66.

IVERSON, E. & STEDMAN, K. 2012. A genetic study of SSV1, the prototypical fusellovirus. *Front Microbiol,* 3**,** 200.

KREMER, J. R., MASTRONARDE, D. N. & MCINTOSH, J. R. 1996. Computer visualization of three-dimensional image data using IMOD. *J Struct Biol,* 116**,** 71-6.

KRUPOVIC, M., QUEMIN, E. R., BAMFORD, D. H., FORTERRE, P. & PRANGISHVILI, D. 2014. Unification of the globally distributed spindle-shaped viruses of the Archaea. *J Virol,* 88**,** 2354-8.

KRUPOVIC, M., WHITE, M. F., FORTERRE, P. & PRANGISHVILI, D. 2012. Postcards from the edge: structural genomics of archaeal viruses. *Adv Virus Res,* 82**,** 33-62.

LETZELTER, C., DUGUET, M. & SERRE, M. C. 2004. Mutational analysis of the archaeal tyrosine recombinase SSV1 integrase suggests a mechanism of DNA cleavage in trans. *J Biol Chem,* 279**,** 28936-44.

LINDAS, A. C. & BERNANDER, R. 2013. The cell cycle of archaea. *Nat Rev Microbiol,* 11**,** 627-38.

MARSH, M. & THALI, M. 2003. HIV's great escape. *Nat Med,* 9**,** 1262-3.

MARTIN, A., YEATS, S., JANEKOVIC, D., REITER, W. D., AICHER, W. & ZILLIG, W. 1984. SAV 1, a temperate u.v.-inducible DNA virus-like particle from the archaebacterium Sulfolobus acidocaldarius isolate B12. *EMBO J,* 3**,** 2165-8.

MORISCOT, C., GRIBALDO, S., JAULT, J. M., KRUPOVIC, M., ARNAUD, J., JAMIN, M., SCHOEHN, G., FORTERRE, P., WEISSENHORN, W. & RENESTO, P. 2011. Crenarchaeal CdvA forms double-helical filaments containing DNA and interacts with ESCRT-III-like CdvB. *PLoS One,* 6**,** e21921.

MUSKHELISHVILI, G., PALM, P. & ZILLIG, W. 1993. SSV1-encoded site-specific recombination system in Sulfolobus shibatae. *Mol Gen Genet,* 237**,** 334-42.

OFFRE, P., SPANG, A. & SCHLEPER, C. 2013. Archaea in biogeochemical cycles. *Annu Rev Microbiol,* 67**,** 437-57.

PALM, P., SCHLEPER, C., GRAMPP, B., YEATS, S., MCWILLIAM, P., REITER, W. D. & ZILLIG, W. 1991. Complete nucleotide sequence of the virus SSV1 of the archaebacterium Sulfolobus shibatae. *Virology,* 185**,** 242-50.

PINA, M., BIZE, A., FORTERRE, P. & PRANGISHVILI, D. 2011. The archeoviruses. *FEMS Microbiol Rev,* 35**,** 1035-54.

PRANGISHVILI, D. 2013. The wonderful world of archaeal viruses. *Annu Rev Microbiol,* 67**,** 565-85.

QUEMIN, E. R., PIETILA, M. K., OKSANEN, H. M., FORTERRE, P., RIJPSTRA, W. I., SCHOUTEN, S., BAMFORD, D. H., PRANGISHVILI, D. & KRUPOVIC, M. 2015. Sulfolobus spindle-shaped virus 1

contains glycosylated capsid proteins, a cellular chromatin protein and host-derived lipids. *J Virol*.

QUEMIN, E. R. & QUAX, T. E. 2015. Archaeal viruses at the cell envelope: entry and egress. *Front Microbiol,* 6**,** 552.

REITER, W. D., PALM, P., HENSCHEN, A., LOTTSPEICH, F., ZILLIG, W. & GRAMPP, B. 1987a. Identification and characterization of the genes encoding three structural proteins of the Sulfolobus virus-like particle SSV1. *Mol Gen Genet,* 206**,** 144-153.

REITER, W. D., PALM, P., YEATS, S. & ZILLIG, W. 1987b. Gene expression in archaebacteria: physical mapping of constitutive and UV-inducible transcripts from the Sulfolobus virus-like particle SSV1. *Mol Gen Genet,* 209**,** 270-5.

ROBERTSON, C. E., HARRIS, J. K., SPEAR, J. R. & PACE, N. R. 2005. Phylogenetic diversity and ecology of environmental Archaea. *Curr Opin Microbiol,* 8**,** 638-42.

SAMSON, R. Y. & BELL, S. D. 2009. Ancient ESCRTs and the evolution of binary fission. *Trends Microbiol,* 17**,** 507-13.

SCHLEPER, C., KUBO, K. & ZILLIG, W. 1992. The particle SSV1 from the extremely thermophilic archaeon Sulfolobus is a virus: demonstration of infectivity and of transfection with viral DNA. *Proc Natl Acad Sci U S A,* 89**,** 7645-9.

SERRE, M. C., LETZELTER, C., GAREL, J. R. & DUGUET, M. 2002. Cleavage properties of an archaeal site-specific recombinase, the SSV1 integrase. *J Biol Chem,* 277**,** 16758-67.

SHE, Q., SINGH, R. K., CONFALONIERI, F., ZIVANOVIC, Y., ALLARD, G., AWAYEZ, M. J., CHAN-WEIHER, C. C., CLAUSEN, I. G., CURTIS, B. A., DE MOORS, A., ERAUSO, G., FLETCHER, C., GORDON, P. M., HEIKAMP-DE JONG, I., JEFFRIES, A. C., KOZERA, C. J., MEDINA, N., PENG, X., THI-NGOC, H. P., REDDER, P., SCHENK, M. E., THERIAULT, C., TOLSTRUP, N., CHARLEBOIS, R. L., DOOLITTLE, W. F., DUGUET, M., GAASTERLAND, T., GARRETT, R. A., RAGAN, M. A., SENSEN, C. W. & VAN DER OOST, J. 2001. The complete genome of the crenarchaeon Sulfolobus solfataricus P2. *Proc Natl Acad Sci U S A,* 98**,** 7835-40.

STEDMAN, K. M., DEYOUNG, M., SAHA, M., SHERMAN, M. B. & MORAIS, M. C. 2015. Structural insights into the architecture of the hyperthermophilic Fusellovirus SSV1. *Virology,* 474**,** 105-9.

STEDMAN, K. M., SCHLEPER, C., RUMPF, E. & ZILLIG, W. 1999. Genetic requirements for the function of the archaeal virus SSV1 in Sulfolobus solfataricus: construction and testing of viral shuttle vectors. *Genetics,* 152**,** 1397-405.

WOLLERT, T., YANG, D., REN, X., LEE, H. H., IM, Y. J. & HURLEY, J. H. 2009. The ESCRT machinery at a glance. *J Cell Sci,* 122**,** 2163-6.

YEATS, S., MCWILLIAM, P. & ZILLIG, W. 1982. A plasmid in the archaebacterium Sulfolobus acidocaldarius. *EMBO J,* 1**,** 1035-8.

ZHAN, Z., OUYANG, S., LIANG, W., ZHANG, Z., LIU, Z. J. & HUANG, L. 2012. Structural and functional characterization of the C-terminal catalytic domain of SSV1 integrase. *Acta Crystallogr D Biol Crystallogr,* 68**,** 659-70.

ZILLIG, W., KLETZIN, A., SCHLEPER, C., HOLZ, I., JANEKOVIC, D., HAIN, J., LANZENDÖRFER, M. & KRISTJANSSON, J. K. 1993. Screening for Sulfolobales, their Plasmids and their Viruses in Icelandic Solfataras. *Systematic and Applied Microbiology,* 16**,** 609-628.

Figure legends

Figure 1:

Induction of SSV1 retards the growth of *S. shibatae* cultures. (A) Growth curves of control (circles, dark grey line) and irradiated (squares, light grey line). Optical density measured at a wavelength of 600 nm is shown. (B) Proportion in percentage of each phenotype of cells observed in cultures at different time points after irradiation with UV: dark grey bars represent regular; light grey, extracted and grey, condensed cells. Electron micrographs of 200 nm thick sections of *S. shibatae* representative of each of the phenotypes are shown: regular (C); extracted (D) and condensed (E). Scale bars = 1 000 nm.

Figure 2:

Changes in cell morphology through the course of SSV1 replication are linked with viral replication. (A) Electron micrograph of thin-sections of *S. shibatae* at 6 hpi showing spherical, electron-lucent aggregates in the cytoplasm of condensed and extracted cells. (B) Proportion of cells containing cytoplasmic structures (light grey) or characteristic of regular (dark grey) and extracted phenotypes (grey) for controls and UV irradiated *S. shibatae* and *S. solfataricus* cultures at different time points after induction. Scale bar = 500 nm.

Figure 3:

Subcellular location of viral components leads to modification of the plasma membrane and periplasmic space. Electron tomogram of sections of non-irradiated controls (A) or *S. shibatae* at 24 hpi (D) displaying regular – R – and extracted – E – cells. The area defined by dark squares in (A) and (D) are shown in (B) and (E) for regular or (C) and (F) for extracted cells, respectively. Blue square brackets represent the periplasmic space located between the plasma membrane and the S-layer. Red arrows indicate ruptures in the cytoplasmic membrane (C) or membrane remnants (F). Scale bar = 50 nm.

Figure 4:

Modification of the S-layer. Representative electron micrographs of thin-sections of *S. shibatae* at 24 hpi (A), (B) and (C). Scale bar = 200 nm.

Figure 5:

Assembly and budding of SSV1 progeny occur at the cytoplasmic membrane. Electron tomograms of SSV1 virions being assembled at the cytoplasmic membrane or budding through the S-layer. The yellow arrows indicate ring-shaped, dark structures at the base of the constriction of SSV1 virions (A and B). The green stars indicate ruptures of the S-layer after budding of SSV1 virions (C). Scale bar = 50 nm.

Figure 1

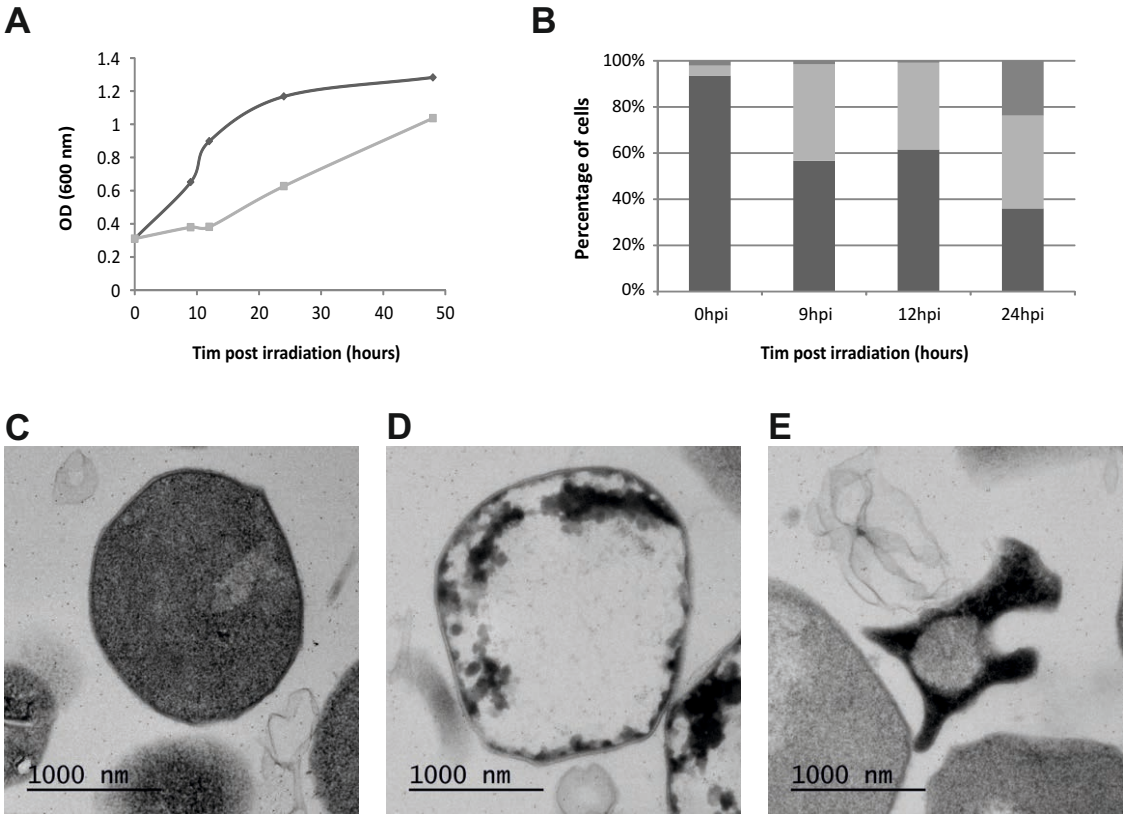
A
1.4
1.2
1
0.8
0.6
0.4
0.2
0
OD (600 nm)
0
10
20
30
40
50
Tim post irradiation (hours)
B
100%
80%
60%
40%
20%
0%
Percentage of cells
0hpi
9hpi
12hpi
24hpi
Tim post irradiation (hours)
C
1000 nm
D
1000 nm
E
1000 nm

Figure 2

A

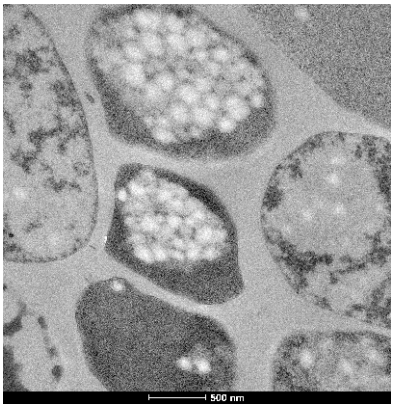
500 nm

B

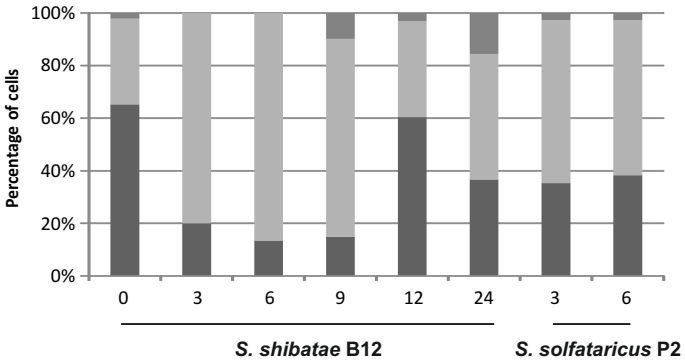
100%
80%
60%
40%
20%
0%
Percentage of cells
0
3
6
9
12
24
3
6
S. shibatae B12
S. solfataricus P2

Figure 3

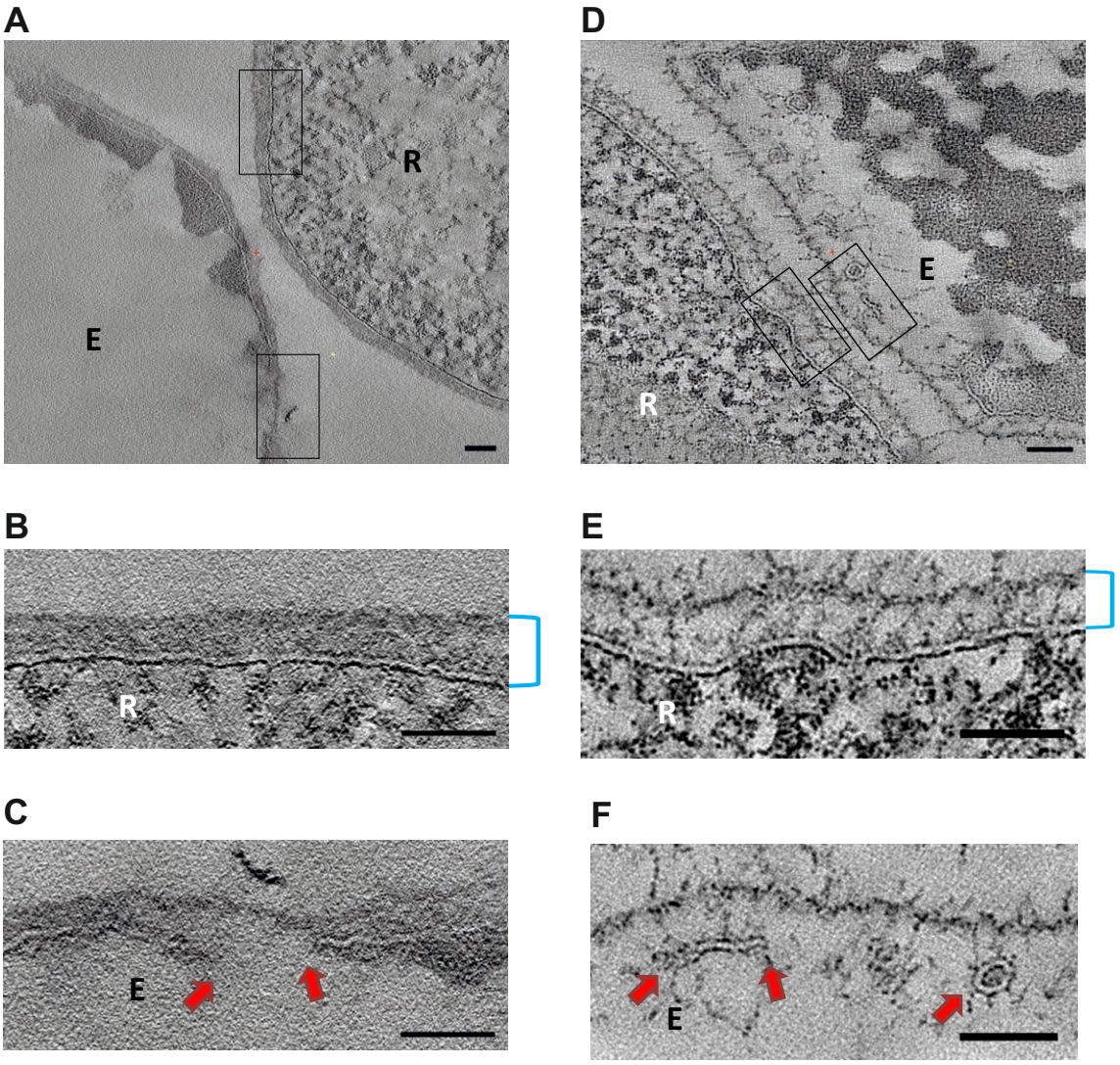

Figure 4

A

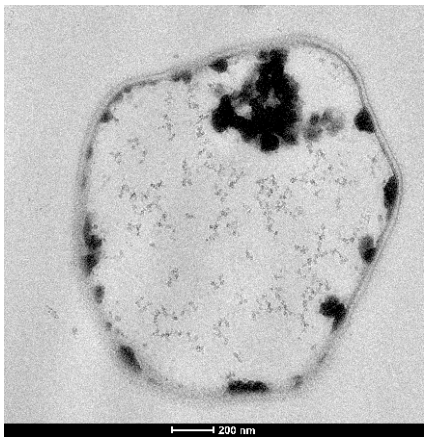

B

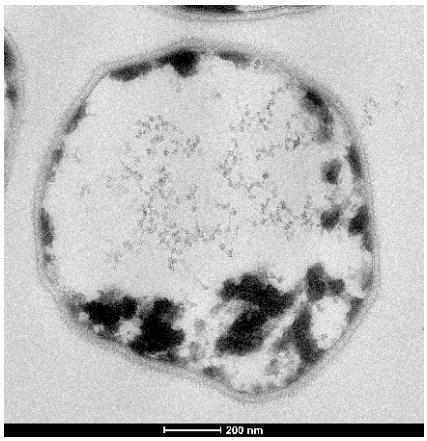

C

Figure 5

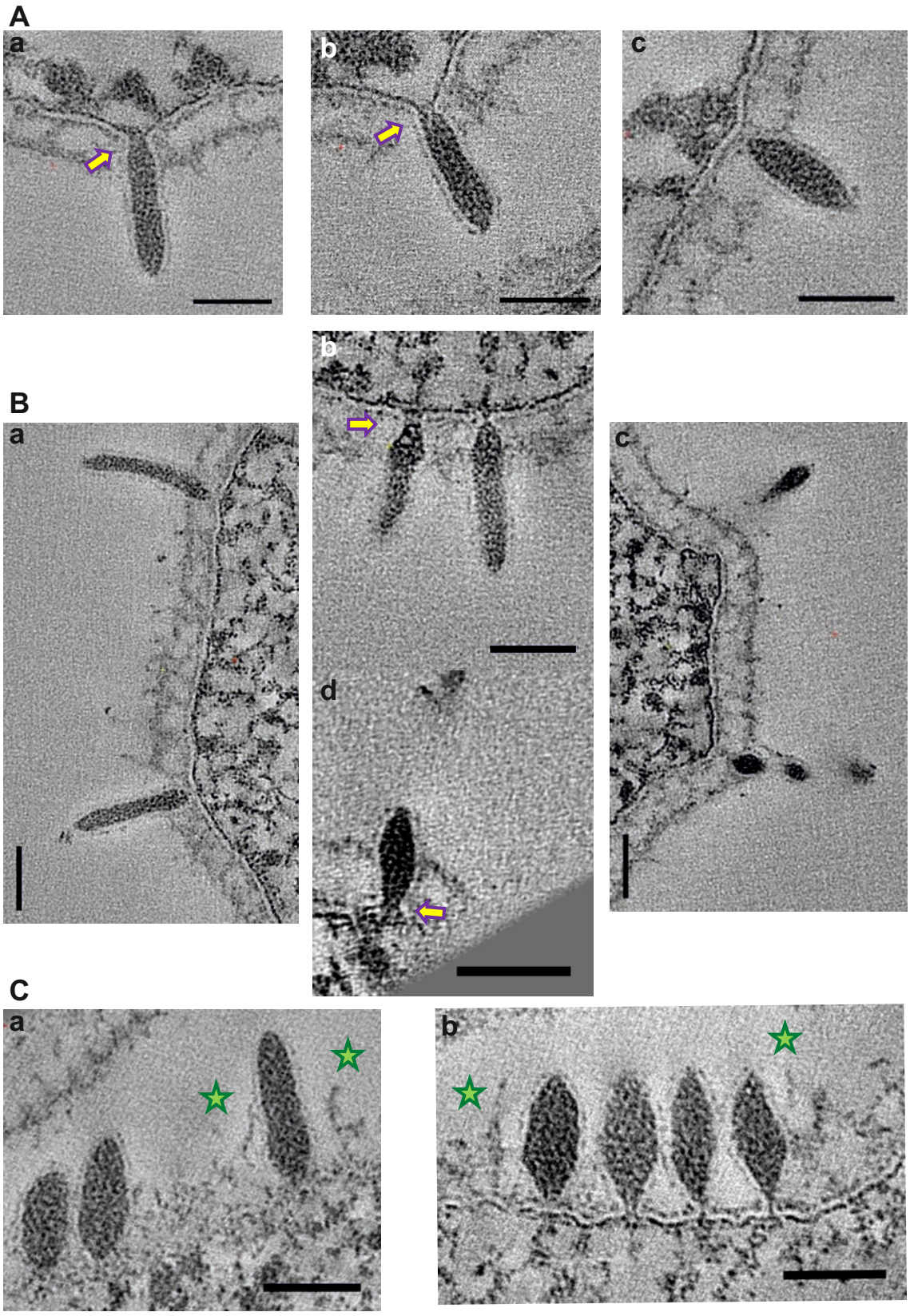

CHAPTER 6

Unravelling the early stages of SIRV2 infection.

JVI Journals.ASM.org

First Insights into the Entry Process of Hyperthermophilic Archaeal Viruses

Emmanuelle R. J. Quemin,[a] Soizick Lucas,[a] Bertram Daum,[b] Tessa E. F. Quax,[a] Werner Kühlbrandt,[b] Patrick Forterre,[a] Sonja-Verena Albers,[c] David Prangishvili,[a] Mart Krupovic[a]

Institut Pasteur, Unité Biologie Moléculaire du Gène chez les Extrêmophiles, Département de Microbiologie, Paris, France[a]; Department of Structural Biology, Max Planck Institute of Biophysics, Frankfurt am Main, Germany[b]; Molecular Biology of Archaea, Max-Planck Institute for Terrestrial Microbiology, Marburg, Germany[c]

A decisive step in a virus infection cycle is the recognition of a specific receptor present on the host cell surface, subsequently leading to the delivery of the viral genome into the cell interior. Until now, the early stages of infection have not been thoroughly investigated for any virus infecting hyperthermophilic archaea. Here, we present the first study focusing on the primary interactions between the archaeal rod-shaped virus *Sulfolobus islandicus rod-shaped virus 2* (SIRV2) (family *Rudiviridae*) and its hyperthermoacidophilic host, *S. islandicus*. We show that SIRV2 adsorption is very rapid, with the majority of virions being irreversibly bound to the host cell within 1 min. We utilized transmission electron microscopy and whole-cell electron cryotomography to demonstrate that SIRV2 virions specifically recognize the tips of pilus-like filaments, which are highly abundant on the host cell surface. Following the initial binding, the viral particles are found attached to the sides of the filaments, suggesting a movement along these appendages toward the cell surface. Finally, we also show that SIRV2 establishes superinfection exclusion, a phenomenon not previously described for archaeal viruses.

Viruses infecting Archaea constitute an integral, yet unique part of the virosphere. In particular, a significant portion of the viruses infecting hyperthermophilic archaea display morphotypes—bottle shaped, lemon shaped, droplet shaped, etc.—not known to be associated with the other two cellular domains, Bacteria and Eukarya (1–3). Furthermore, the distinctiveness of archaeal viruses extends to their genome sequences (4, 5) and the structure of proteins that they encode (1). The ways these viruses interact with their hosts are therefore also likely to be unique. However, until now, the studies on archaeal viruses were mostly confined to biochemical and genetic characterization of their virions, and the knowledge on virus-host interplay in Archaea is minuscule compared to the wealth of data available on bacterial and eukaryotic systems. In particular, insights are lacking into the entry process of hyperthermophilic archaeal viruses.

Recognition of a suitable host cell is an essential first step in the infection cycle of any virus. This is typically achieved by specific interactions between a receptor-binding protein exposed on the virion and a receptor present on the host cell surface, which subsequently leads to cell envelope penetration, accompanied by internalization of the viral genome (6). A variety of cell surface structures are known to be targeted by viruses. For example, in the case of bacterial viruses, nearly all components of the cell envelope are known to serve as receptors (7), including lipopolysaccharide (8–10), pili (11–13), flagella (14–17), (lipo-)teichoic acids (18–20), peptidoglycan (21), or various integral membrane proteins (22–24). The only archaeal virus for which a potential cellular receptor has been identified is ϕCh1, infecting the hyperhalophilic host *Natrialba magadii* (25). Notably, ϕCh1 is a member of the viral order *Caudovirales* (26), sharing clear evolutionary history with tailed double-stranded DNA (dsDNA) bacteriophages (27). Similarly to bacterial viruses, ϕCh1 utilizes tail fibers to bind to its cellular receptor. Galactose moieties were found to be important for ϕCh1 adsorption; however, the exact nature of the receptor remains to be identified (25).

Sulfolobus islandicus rod-shaped virus 2 (SIRV2) (28) and its host, *Sulfolobus islandicus* LAL14/1 (29), represent a valuable model system to study virus-host interactions in Archaea (30). SIRV2 is a member of the family *Rudiviridae*, within the recently established order *Ligamenvirales* (31). It has a nonenveloped, stiff, rod-shaped virion composed of four structural proteins encasing a linear dsDNA genome of 35 kb (28). Both termini of the virion are decorated with three fibers composed of the minor structural protein P1070 (32) and thought to be involved in host recognition. At the end of the infection cycle, SIRV2 induces the formation of large pyramidal structures on the surface of infected cells that serve as portals for the release of progeny viruses (33–35). A similar egress mechanism has been also demonstrated for the unrelated icosahedral archaeal virus STIV (36, 37), indicating that mechanisms underlying virus-host interactions in a particular virus-host system are sometimes applicable to a wider range of archaeal viruses. In contrast to the egress mechanism, which has been characterized to some detail, almost nothing is known about the entry process of SIRV2. Here, we investigate the SIRV2-*S. islandicus* interaction, focusing on the early stages of infection.

MATERIALS AND METHODS

Strain cultivation and virus purification. *Sulfolobus islandicus* strain LAL14/1 (29) was used as a host for SIRV2 in all experiments. The cells were cultivated with aeration (150 rpm) in a water bath shaker, Innova 3100 (Eppendorf), filled with silicon oil, in 50-ml flasks at 75°C, pH 3.5. The rich medium was prepared as described previously (38). SIRV2 was

Received 24 September 2013 Accepted 25 September 2013
Published ahead of print 2 October 2013
Address correspondence to Mart Krupovic, krupovic@pasteur.fr.
Supplemental material for this article may be found at http://dx.doi.org/10.1128/JVI.02742-13.

doi:10.1128/JVI.02742-13

purified by CsCl density gradient centrifugation and the virus titer determined by plaque assay as described previously (28).

Adsorption assay. For adsorption assays, LAL14/1 cells (optical density at 600 nm [OD_{600}] = 0.15; 10^8 CFU/ml) were infected using a multiplicity of infection (MOI) of 0.1. At defined time intervals, a sample of infected culture was removed and the adsorption stopped by immediate centrifugation (10,000 × *g*, 5 min, room temperature [RT]). The number of remaining PFU was determined by the plaque assay and compared to the amount of virus present in a cell-free control incubated at 75°C. The adsorption rate constant was calculated as described previously (39).

Receptor saturation assay. For the receptor saturation assay, a constant number of LAL14/1 cells (grown to a cell density of 10^8 CFU/ml) were infected using MOIs between 0.1 and 370. At 30 min postinfection, the cells were removed by centrifugation (10,000 × *g*, 5 min, RT) and the number of nonadsorbed viral particles in the supernatants was determined using the plaque assay and compared to the amount of virus present in a cell-free control incubated at 75°C.

Superinfection assay. LAL14/1 cells were infected at an MOI of 10 for 1 h. Cells were washed twice with fresh rich medium in two rounds of gentle centrifugation (Jouan BR4i, rotor AB 50.10A [Thermo Scientific]; 3,500 rpm, 10 min, 20°C). Infected cells were subjected to a second round of infection using an MOI of 0.1, and the number of unadsorbed particles remaining in the supernatant was determined as described above.

Filament purification. *S. islandicus* filaments were purified as described previously (40) with minor modifications. Briefly, 3 liters of LAL14/1 cells were grown to an OD_{600} of 0.3, collected (Avanti J-26XP, rotor JLA 16.250 [Beckman Coulter]; 3,500 rpm, 15 min, 15°C) and resuspended in 15 ml of Brock's basal salt medium. Filaments were mechanically sheared from the cells by vortexing at maximum speed for 15 min. Cells and debris were removed by two steps of centrifugation (Jouan BR4i rotor AB 50.10A; Thermo Scientific): 8,000 rpm for 30 min at 15°C, followed by 6,000 rpm for 1 h at 15°C. The filaments were pelleted (Beckman rotor 70.1Ti at 65,000 rpm, 1 h, 15°C) and further purified on a CsCl gradient (Beckman rotor SW60, 55,000 rpm, 48 h, 15°C). Gradient fractions containing filaments were collected and processed for transmission electron microscopy (TEM).

Interaction of SIRV2 with cellular appendages. SIRV2 virions were incubated with either *S. islandicus* LAL14/1 cells (MOI = 10) or purified filaments in a thermoblock (Fisher Scientific) at 75°C for 1 to 2 or 5 to 10 min, respectively, and immediately prepared for TEM.

TEM. For conventional negative-stain TEM, 10 μl of sample was added on Formvar-coated grids (Eloïse Instruments Service SARL) for 2 min, air dried, and stained with 2% uranyl acetate (EuroMedex) for 30 s. Samples were imaged in a JEOL 1200EX-II transmission electron microscope at 80 kV.

Electron cryotomography. A suspension of LAL14/1 cells infected with SIRV2 was mixed (1 min postinfection) with an equal amount of 10 nm gold fiducial markers (Aurion). Three microliters of this mixture was added to a glow-discharged R2/2 Quantifoil grid and rapidly plunged into liquid ethane.

Samples were transferred into a FEI TITAN Krios transmission electron microscope at liquid nitrogen temperature. The microscope was equipped with a field emission gun operated at 300 kV. Zero-loss filtered tilt series were collected on a 4x4k Gatan charge-coupled-device (CCD) camera in a range of −60° to + 60° in steps of 1.5° or 2° and a defocus of 8 to 9 μm. The magnification was chosen to give a pixel size of 0.477 nm in the final image. Tomograms were generated with the IMOD software (41) and denoised by nonlinear anisotropic diffusion (NAD) (42). Tomograms were segmented and surface rendered using Amira (Mercury systems).

RESULTS AND DISCUSSION

SIRV2 adsorption is very rapid. To gain insights into the initial stages of SIRV2 entry, we followed the kinetics of SIRV2 adsorption to LAL14/1 cells. The adsorption was very efficient, with

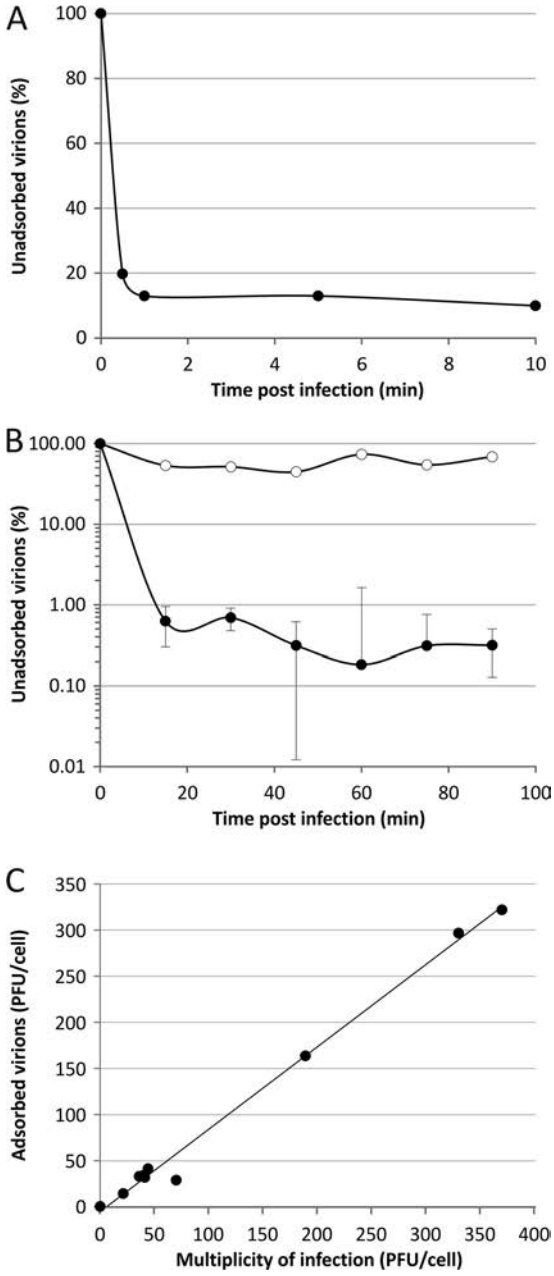

FIG 1 Adsorption of SIRV2 to cells of *S. islandicus* LAL14/1. (A) Kinetics of SIRV2 adsorption. Cells were infected with SIRV2 using an MOI of 0.1 at 75°C. The number of unbound virus particles was determined at different time points postinfection as described in Materials and Methods. (B) SIRV2-mediated superinfection exclusion. Cells were infected at an MOI of 10 for 1 h, washed twice with rich medium, and subjected to a second round of infection using an MOI of 0.1. The number of unadsorbed particles remaining in the supernatant was determined. The kinetics of adsorption to noninfected, control cells is shown by closed circles, while open circles represent adsorption to preinfected cells. All experiments were conducted in triplicate, and error bars represent standard deviations. When error bars are not visible, the deviation was below 5%. (C) Receptor saturation. Cells were infected with SIRV2 using MOIs ranging from 0.1 to 370. At 30 min postinfection, the number of unadsorbed viral particles present in the supernatant was determined by plaque assay and compared to that of the cell-free control.

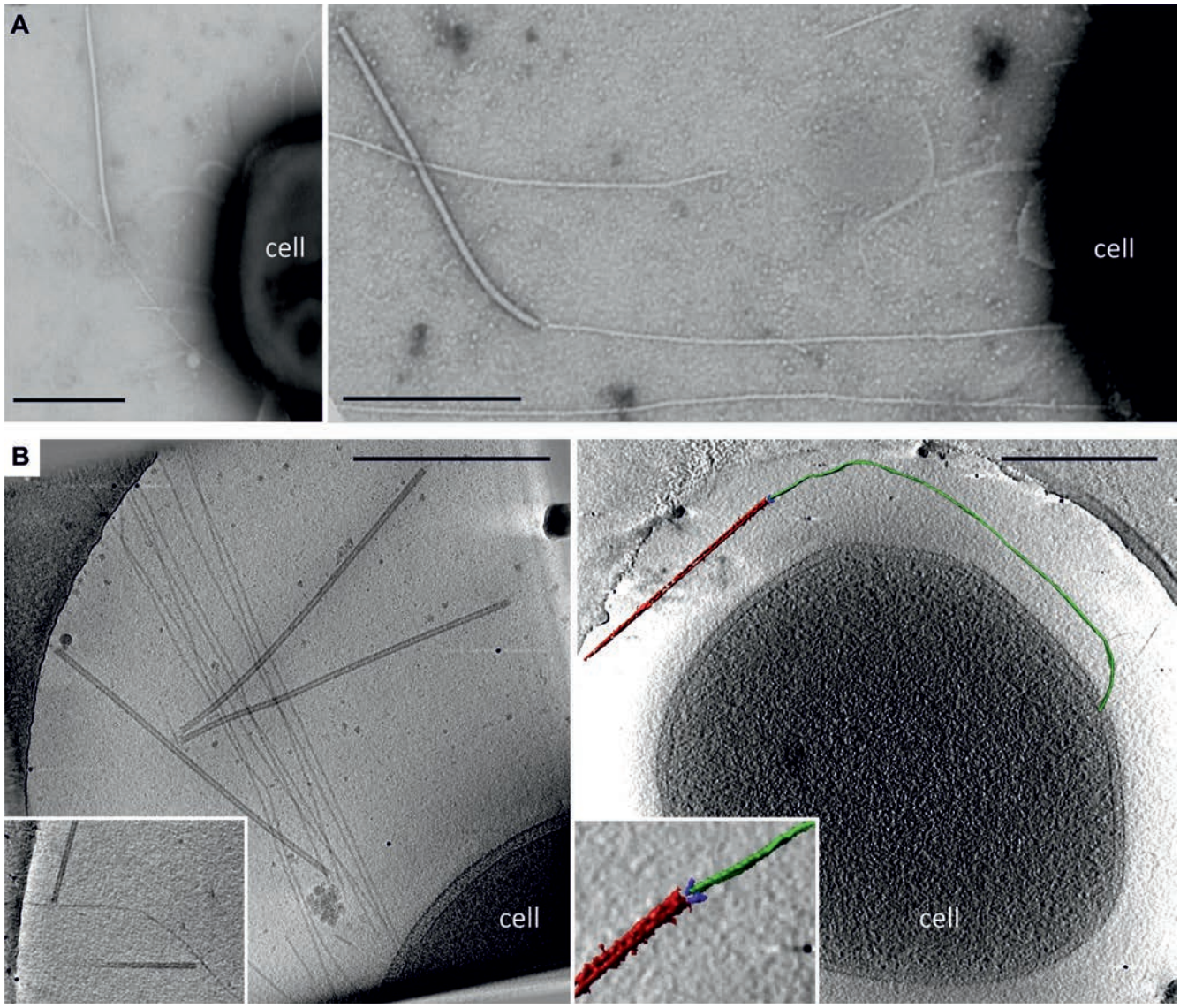

FIG 2 Electron micrographs of SIRV2 interaction with *S. islandicus* LAL14/1 cells. Samples were collected 1 min postinfection and negatively stained for TEM (A) or plunge-frozen for electron cryotomography (cryo-ET) (B). The virions interact both at the filament tips (right panels) and along the length of the filaments (left panels). The inset in the lower left panel depicts two virions bound to the sides of a single filament. The lower right panel shows a segmented tomographic volume of the SIRV2 virion (red) attached to the tip of an *S. islandicus* filament (green). The three terminal virion fibers that appear to mediate the interaction are shown in blue (the inset depicts a magnified view of the interaction between the virion fibers and the tip of the filament). A complete tomogram of the cell depicted in the lower right panel can be found in the supplemental material. Scale bars, 500 nm.

~80% of virions being bound to cells within the first 30 s of infection (Fig. 1A). Further incubation of the virus in the presence of the host cells resulted in additional virion binding; ~99% of virions were bound within 20 to 30 min postinfection (p.i.). All adsorption assays were conducted under the conditions optimal for the growth of *S. islandicus* cells, i.e., at high temperature (75°C) and in acidic pH (pH 3.5). The possibility that the observed effects were due to high-temperature- and/or acid-induced virion inactivation rather than adsorption was eliminated by performing a cell-free control in which the same amount of SIRV2 as used for the infection was incubated at 75°C in the LAL14/1 growth medium.

Upon the first encounter of a susceptible host, many bacterial viruses initially bind reversibly to the structures on the cell surface and only then commit to the infection by attaching to the cell irreversibly, a stage subsequently followed by delivery of the viral genome into the cell interior (8, 21, 43–45). To test the reversibility of the SIRV2 adsorption, we investigated whether viral particles could be washed off from the host cell surface. However, no virus particles could be released at any of the time points tested (starting with 1 min postinfection), suggesting that SIRV2 binding very quickly becomes irreversible and the reversible step, if it occurs, is transient.

Such a rapid adsorption rate (calculated as 2×10^{-8} ml min^{-1} at 1 min p.i.) is surprising, given that viruses of halophilic archaea—the only group of archaeal viruses for which adsorption has been studied—often bind to their hosts extremely slowly (46). For example, only 30% of salterprovirus His1 (47, 48) and *Halo-*

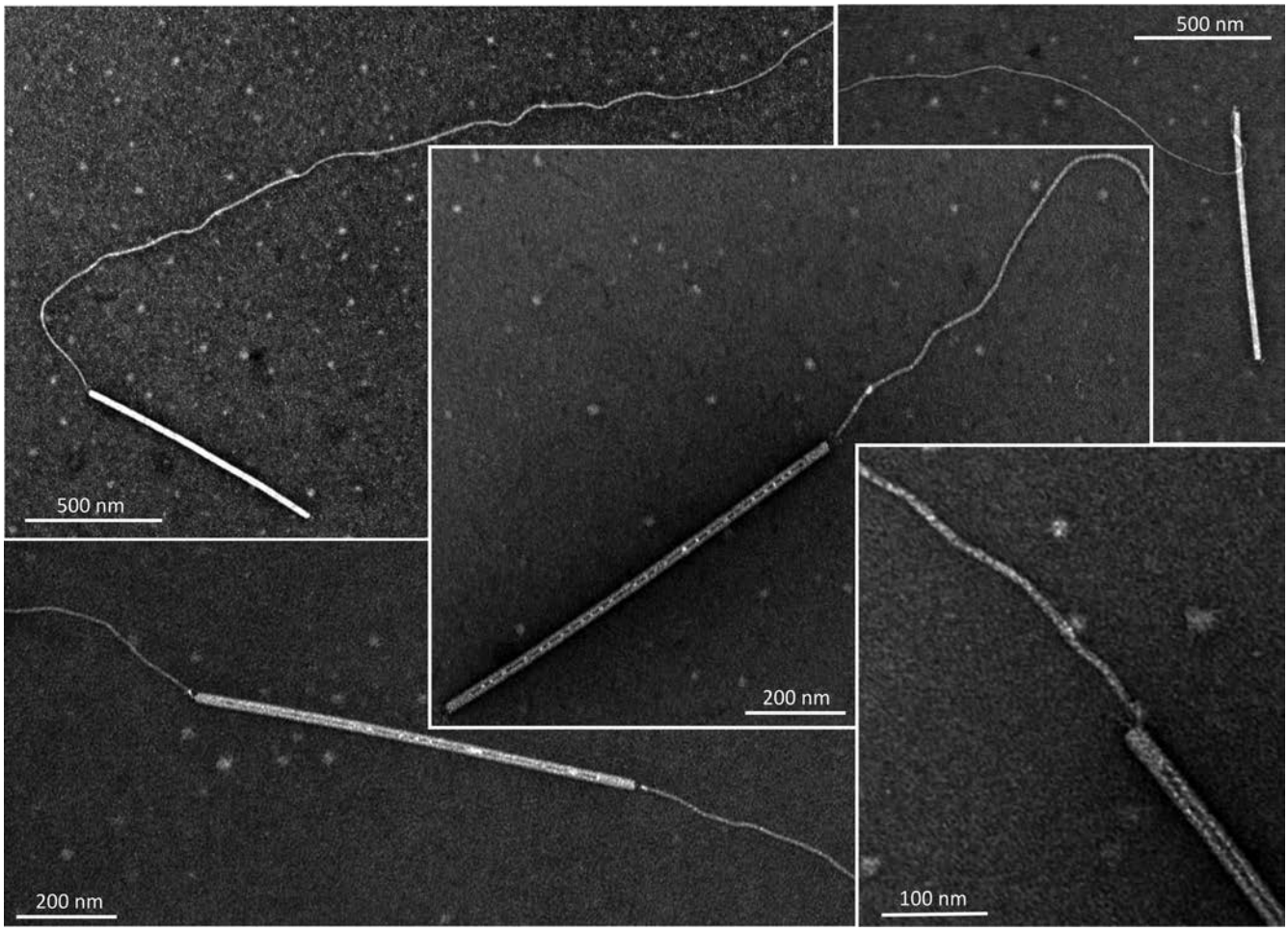

FIG 3 Transmission electron micrographs of SIRV2 interaction with purified cellular filaments. The filaments were removed from *S. islandicus* LAL14/1 cells as described in Materials and Methods.

arcula hispanica tailed virus 1 (HHTV-1; *Siphoviridae*) (46) virions adsorb in 3 h. The fast adsorption of SIRV2 is consistent with recent transcriptomics data revealing that transcription of the early SIRV2 genes starts within 1 min of infection (49). Despite the fact that SIRV2 adsorption is quick, the intracellular phase of the viral cycle is fairly long (~10 to 15 h). We hypothesize that the duration of both stages has been fine-tuned during SIRV2's evolution to minimize the time spent by the virus in the hostile extracellular environment, i.e., high temperature and acidic pH.

SIRV2 establishes superinfection exclusion. In the case of many bacterial virus-host systems, virus infection of a cell renders it resistant to subsequent infections by related viruses—a phenomenon known as superinfection exclusion (50). Although relatively widespread among bacterial viruses, to the best of our knowledge, superinfection exclusion has not been described for any archaeal virus. We investigated whether SIRV2 infection modulates the susceptibility of its host to subsequent infections. For this purpose, LAL14/1 cells were preinfected with SIRV2 at an MOI of 10 for 1 h, to ensure that infection was established in all cells. After removing the unadsorbed viral particles, the cells were challenged with a second course of infection at an MOI of 0.1. We observed a dramatic decrease in the amount of virions bound to preinfected cells compared to the noninfected control cells (Fig. 1B). Infected cells were no longer able to efficiently adsorb the virus even after 90 min of incubation. This result suggests that upon infection SIRV2 establishes superinfection exclusion; the exact mechanism underlying this phenomenon remains to be elucidated.

SIRV2 receptor is highly abundant. The abundance and nature of cell surface molecules that serve as receptors for virions are specific for each virus-host system. The receptor saturation assay is a classical experiment used to determine the approximate number of receptors present on the host cell surface (39). For this purpose, *S. islandicus* cells were infected with SIRV2 at various MOI values ranging from 0.1 to 370 and the number of free particles remaining in the supernatant was determined and compared to the initial number of virions added into the cell-free control (Fig. 1C). Remarkably, even at the highest MOI tested, 95% of virions were bound 30 min p.i., indicating that the receptor mediating the primary interaction between SIRV2 and LAL14/1 is highly abundant, consistently with the high adsorption rate.

SIRV2 binds to long filaments on *S. islandicus* cells. To gain more-detailed insight into the interaction of SIRV2 with LAL14/1 cells, we followed the initial stages of infection by transmission electron microscopy and whole-cell electron cryotomography (cryo-ET). The surface of noninfected LAL14/1 cells was covered

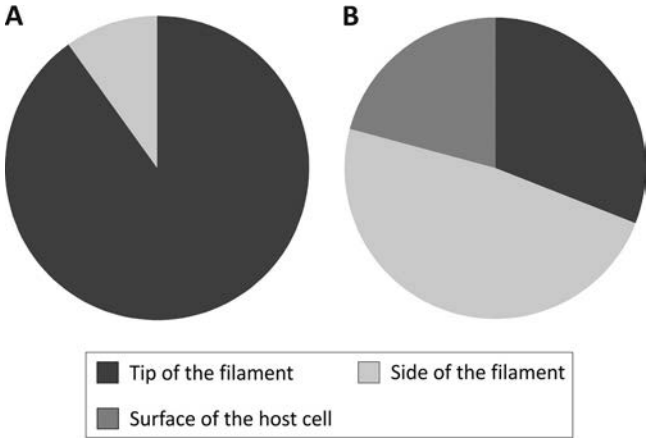

FIG 4 Interactions between SIRV2 and purified filaments (A) or *S. islandicus* LAL14/1 cells (B). SIRV2 virions were incubated with purified filaments for 5 to 10 min or LAL14/1 cells for 1 to 2 min at 75°C and prepared for TEM (see Materials and Methods). Binding of viral particles to the tips, the sides of LAL14/1 filaments, or the cell surface was counted in electron micrographs of negatively stained samples.

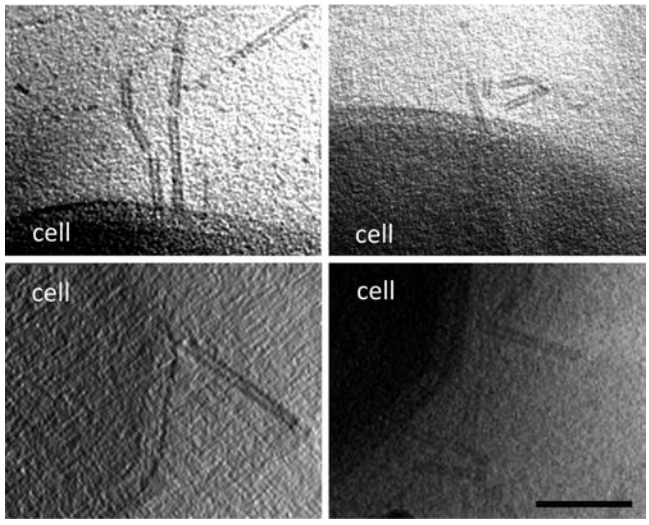

FIG 5 A tomographic slice through *S. islandicus* LAL14/1 cells 1 min after infection with SIRV2 reveals partially disassembled SIRV2 virions at the cell surface. Scale bar, 100 nm.

with pilus-like filaments. The number of filaments varied between individual cells. With negative staining, the filament diameter was close to 10 nm but the length was highly variable. In cryo-ET, the filaments appeared thinner, with a diameter of 5 nm. Negative staining involves dehydration and flattening of the sample on the carbon support film, which may cause the filaments to appear thicker in projection. In contrast, for cryo-ET the filaments are rapidly frozen in their native, fully hydrated state. Cryo-ET thus shows the actual *in situ* structure and dimensions of the filaments. The exact nature of the filaments remains to be determined.

It has been previously observed that SIRV2 virions copurify with filamentous structures (51). To verify whether the structures on the surface of *S. islandicus* cells might be involved in SIRV2 binding, the cells were infected at an MOI of 10 and observed by TEM and cryo-ET. Indeed, an interaction between SIRV2 virions and the cellular filaments was observed (Fig. 2). The interaction involved the terminal fibers of the SIRV2 virion. Typically, a single filament accommodated several SIRV2 virions (Fig. 2B). This is consistent with the receptor saturation experiment, which indicated that nearly 370 particles could adsorb per one LAL14/1 cell.

SIRV2 specifically interacts with the tips of the cellular filaments. To verify that the filaments indeed represent SIRV2 receptors, the fibers were removed from noninfected LAL14/1 cells by vortexing and purified on CsCl density gradient (see Materials and Methods). The filament preparations were then tested for SIRV2 binding. TEM analysis revealed that virions preferentially interact with the tip of the filaments (Fig. 3); of the 202 observed interactions (in 4 independent experiments), only 9.9% (20 interactions) occurred along the length of a filament (Fig. 4A). In some cases, the two termini of a rod-shaped virion were bound to two different filaments (Fig. 3), indicating that the two ends of the virion are functionally equivalent. Unexpectedly, this preference was not observed with filaments attached to LAL14/1 cells, where the virions typically bound not only to the tip but also to the sides of the filaments (Fig. 2) and were also observed at the cell surface. Of the 629 observed cases of virus-host interactions (in 6 independent experiments), 31% (195) occurred with the tips and 48.2% (303) with the sides of the LAL14/1 filaments, while the remaining 20.8% (131) of virions were found to interact directly with the cell surface (Fig. 4B).

Concluding remarks. Collectively, our data provide valuable insight into the entry process of SIRV2 and suggest the following sequence of events. SIRV2 binds to the tip of the filament with its three terminal fibers (Fig. 2 and 3) and subsequently progresses along the filaments toward the cell surface. Interestingly, in one case we observed virions bound to the tip of a 12.5-μm-long filament, which raises the question of how the virus overcomes such a long distance to reach the cell body. Once the SIRV2 virion reaches the cell surface, it disassembles, presumably as the viral DNA is delivered to the cell interior. Although the last step remains enigmatic, partially disassembled virions that we observed by cryo-ET at the cell surface postinfection (Fig. 5) are consistent with such a process. Many bacterial viruses utilize filamentous cellular appendages, such as pili or flagella, as primary receptors (7). Superficially, the adsorption of SIRV2 to LAL14/1 filaments resembles the interaction of filamentous Ff inoviruses with F-pili. The pIII protein of Ff phages binds to the tip of the F-pilus; subsequent retraction of the pilus brings the virion close to the cell surface, where upon binding the secondary receptor, TolA, the viral genome is translocated into the cytoplasm (12). A similar F-pilus retraction-driven entry has been also described for certain single-stranded RNA (ssRNA) phages of the family *Leviviridae* (13). However, the apparent translocation of SIRV2 virions along the LAL14/1 filaments, as judged from the differential binding of the virions to purified filaments (Fig. 4A) and filaments attached to LAL14/1 cells (Fig. 4B), implies that the mechanism of SIRV2 entry might differ from that employed by pilus-specific bacterial viruses. Indeed, no retracting pili have been identified in archaea so far, which is also consistent with the apparent lack of genes encoding typical retraction ATPases in the archaeal pilus operons (52, 53). A retraction-independent mechanism is utilized by flagellotrophic bacteriophages, which instead harness the energy of

flagellar rotation to move along the flagellum toward the cell surface (14, 16, 17). Notably, the flagella (called archaella in archaea) of *Sulfolobus* are considerably thicker (~14 nm in diameter [54]) than the LAL14/1 filaments to which SIRV2 binds. Whether the mechanism of SIRV2 translocation along the filaments is related to that of flagellotrophic bacteriophages is under investigation. The work described here provides the basis for future studies, which should illuminate the mechanistic details of SIRV2 cell entry.

ACKNOWLEDGMENTS

This work was supported by the Agence Nationale de la Recherche (ANR) program BLANC, project EXAVIR. E.R.J.Q. was supported by a fellowship from the Ministère de l'Enseignement Supérieur et de la Recherche of France and the Université Pierre et Marie Curie, Paris, France.

REFERENCES

1. **Krupovic M, White MF, Forterre P, Prangishvili D.** 2012. Postcards from the edge: structural genomics of archaeal viruses. Adv. Virus Res. **82:**33–62.
2. **Pina M, Bize A, Forterre P, Prangishvili D.** 2011. The archeoviruses. FEMS Microbiol. Rev. **35:**1035–1054.
3. **Prangishvili D.** 2013. The wonderful world of archaeal viruses. Annu. Rev. Microbiol. **67:**565–585.
4. **Krupovic M, Prangishvili D, Hendrix RW, Bamford DH.** 2011. Genomics of bacterial and archaeal viruses: dynamics within the prokaryotic virosphere. Microbiol. Mol. Biol. Rev. **75:**610–635.
5. **Prangishvili D, Garrett RA, Koonin EV.** 2006. Evolutionary genomics of archaeal viruses: unique viral genomes in the third domain of life. Virus Res. **117:**52–67.
6. **Poranen MM, Daugelavicius R, Bamford DH.** 2002. Common principles in viral entry. Annu. Rev. Microbiol. **56:**521–538.
7. **Vinga I, São-José C, Tavares P, Santos MA.** 2006. Bacteriophage entry in the host cell, p 163–203. *In* Wêgrzyn G (ed), Modern bacteriophage biology and biotechnology. Research Signpost, Kerala, India.
8. **Daugelavičius R, Cvirkaitė V, Gaidelytė A, Bakienė E, Gabrėnaitė-Verkhovskaya R, Bamford DH.** 2005. Penetration of enveloped double-stranded RNA bacteriophages phi13 and phi6 into *Pseudomonas syringae* cells. J. Virol. **79:**5017–5026.
9. **Inagaki M, Kawaura T, Wakashima H, Kato M, Nishikawa S, Kashimura N.** 2003. Different contributions of the outer and inner R-core residues of lipopolysaccharide to the recognition by spike H and G proteins of bacteriophage phiX174. FEMS Microbiol. Lett. **226:**221–227.
10. **Molineux IJ.** 2001. No syringes please, ejection of phage T7 DNA from the virion is enzyme driven. Mol. Microbiol. **40:**1–8.
11. **Bamford DH, Palva ET, Lounatmaa K.** 1976. Ultrastructure and life cycle of the lipid-containing bacteriophage phi 6. J. Gen. Virol. **32:**249–259.
12. **Rakonjac J, Bennett NJ, Spagnuolo J, Gagic D, Russel M.** 2011. Filamentous bacteriophage: biology, phage display and nanotechnology applications. Curr. Issues Mol. Biol. **13:**51–76.
13. **Shiba T, Miyake T.** 1975. New type of infectious complex of *E. coli* RNA phage. Nature **254:**157–158.
14. **Yen JY, Broadway KM, Scharf BE.** 2012. Minimum requirements of flagellation and motility for infection of *Agrobacterium* sp. strain H13-3 by flagellotropic bacteriophage 7-7-1. Appl. Environ. Microbiol. **78:**7216–7222.
15. **Choi Y, Shin H, Lee JH, Ryu S.** 2013. Identification and characterization of a novel flagellum-dependent *Salmonella*-infecting bacteriophage, iEPS5. Appl. Environ. Microbiol. **79:**4829–4837.
16. **Guerrero-Ferreira RC, Viollier PH, Ely B, Poindexter JS, Georgieva M, Jensen GJ, Wright ER.** 2011. Alternative mechanism for bacteriophage adsorption to the motile bacterium *Caulobacter crescentus*. Proc. Natl. Acad. Sci. U. S. A. **108:**9963–9968.
17. **Samuel AD, Pitta TP, Ryu WS, Danese PN, Leung EC, Berg HC.** 1999. Flagellar determinants of bacterial sensitivity to chi-phage. Proc. Natl. Acad. Sci. U. S. A. **96:**9863–9866.
18. **Young FE, Smith C, Reilly BE.** 1969. Chromosomal location of genes regulating resistance to bacteriophage in *Bacillus subtilis*. J. Bacteriol. **98:**1087–1097.
19. **Xia G, Corrigan RM, Winstel V, Goerke C, Grundling A, Peschel A.** 2011. Wall teichoic acid-dependent adsorption of staphylococcal siphovirus and myovirus. J. Bacteriol. **193:**4006–4009.
20. **Raisanen L, Schubert K, Jaakonsaari T, Alatossava T.** 2004. Characterization of lipoteichoic acids as *Lactobacillus delbrueckii* phage receptor components. J. Bacteriol. **186:**5529–5532.
21. **Gaidelytė A, Cvirkaite-Krupovic V, Daugelavičius R, Bamford JK, Bamford DH.** 2006. The entry mechanism of membrane-containing phage Bam35 infecting *Bacillus thuringiensis*. J. Bacteriol. **188:**5925–5934.
22. **Jakutytė L, Baptista C, São-José C, Daugelavičius R, Carballido-Lopez R, Tavares P.** 2011. Bacteriophage infection in rod-shaped gram-positive bacteria: evidence for a preferential polar route for phage SPP1 entry in *Bacillus subtilis*. J. Bacteriol. **193:**4893–4903.
23. **Letellier L, Boulanger P, Plancon L, Jacquot P, Santamaria M.** 2004. Main features on tailed phage, host recognition and DNA uptake. Front. Biosci. **9:**1228–1339.
24. **Randall-Hazelbauer L, Schwartz M.** 1973. Isolation of the bacteriophage lambda receptor from *Escherichia coli*. J. Bacteriol. **116:**1436–1446.
25. **Klein R, Rossler N, Iro M, Scholz H, Witte A.** 2012. Haloarchaeal myovirus phiCh1 harbours a phase variation system for the production of protein variants with distinct cell surface adhesion specificities. Mol. Microbiol. **83:**137–150.
26. **Klein R, Baranyi U, Rossler N, Greineder B, Scholz H, Witte A.** 2002. Natrialba magadii virus phiCh1: first complete nucleotide sequence and functional organization of a virus infecting a haloalkaliphilic archaeon. Mol. Microbiol. **45:**851–863.
27. **Krupovic M, Forterre P, Bamford DH.** 2010. Comparative analysis of the mosaic genomes of tailed archaeal viruses and proviruses suggests common themes for virion architecture and assembly with tailed viruses of bacteria. J. Mol. Biol. **397:**144–160.
28. **Prangishvili D, Arnold HP, Gotz D, Ziese U, Holz I, Kristjansson JK, Zillig W.** 1999. A novel virus family, the *Rudiviridae*: structure, virus-host interactions and genome variability of the *Sulfolobus* viruses SIRV1 and SIRV2. Genetics **152:**1387–1396.
29. **Jaubert C, Danioux C, Oberto J, Cortez D, Bize A, Krupovic M, She Q, Forterre P, Prangishvili D, Sezonov G.** 2013. Genomics and genetics of *Sulfolobus islandicus* LAL14/1, a model hyperthermophilic archaeon. Open Biol. **3:**130010. doi:10.1098/rsob.130010.
30. **Prangishvili D, Koonin EV, Krupovic M.** 2013. Genomics and biology of Rudiviruses, a model for the study of virus-host interactions in Archaea. Biochem. Soc. Trans. **41:**443–450.
31. **Prangishvili D, Krupovic M.** 2012. A new proposed taxon for double-stranded DNA viruses, the order "Ligamenvirales". Arch. Virol. **157:**791–795.
32. **Steinmetz NF, Bize A, Findlay KC, Lomonossoff GP, Manchester M, Evans DJ, Prangishvili D.** 2008. Site-specific and spatially controlled addressability of a new viral nanobuilding block: *Sulfolobus islandicus* rod-shaped virus 2. Adv. Funct. Mater. **18:**3478–3486.
33. **Bize A, Karlsson EA, Ekefjard K, Quax TE, Pina M, Prevost MC, Forterre P, Tenaillon O, Bernander R, Prangishvili D.** 2009. A unique virus release mechanism in the Archaea. Proc. Natl. Acad. Sci. U. S. A. **106:**11306–11311.
34. **Quax TE, Krupovic M, Lucas S, Forterre P, Prangishvili D.** 2010. The *Sulfolobus* rod-shaped virus 2 encodes a prominent structural component of the unique virion release system in Archaea. Virology **404:**1–4.
35. **Quax TE, Lucas S, Reimann J, Pehau-Arnaudet G, Prevost MC, Forterre P, Albers SV, Prangishvili D.** 2011. Simple and elegant design of a virion egress structure in Archaea. Proc. Natl. Acad. Sci. U. S. A. **108:**3354–3359.
36. **Brumfield SK, Ortmann AC, Ruigrok V, Suci P, Douglas T, Young MJ.** 2009. Particle assembly and ultrastructural features associated with replication of the lytic archaeal virus *Sulfolobus* turreted icosahedral virus. J. Virol. **83:**5964–5970.
37. **Snyder JC, Brumfield SK, Peng N, She Q, Young MJ.** 2011. *Sulfolobus* turreted icosahedral virus c92 protein responsible for the formation of pyramid-like cellular lysis structures. J. Virol. **85:**6287–6292.
38. **Zillig W, Kletzin A, Schleper C, Holz I, Janekovic D, Hain J, Lanzendorfer M, Kristjansson JK.** 1994. Screening for *Sulfolobales*, their plasmids and their viruses in Icelandic solfataras. Syst. Appl. Microbiol. **16:**609–628.
39. **Adams MH.** 1959. Bacteriophages. Interscience Publishers, Inc., New York, NY.
40. **Lassak K, Neiner T, Ghosh A, Klingl A, Wirth R, Albers SV.** 2012.

Molecular analysis of the crenarchaeal flagellum. Mol. Microbiol. **83:**110–124.
41. **Kremer JR, Mastronarde DN, McIntosh JR.** 1996. Computer visualization of three-dimensional image data using IMOD. J. Struct. Biol. **116:**71–76.
42. **Frangakis AS, Hegerl R.** 2001. Noise reduction in electron tomographic reconstructions using nonlinear anisotropic diffusion. J. Struct. Biol. **135:** 239–250.
43. **Cvirkaite-Krupovic V, Krupovic M, Daugelavičius R, Bamford DH.** 2010. Calcium ion-dependent entry of the membrane-containing bacteriophage PM2 into its *Pseudoalteromonas* host. Virology **405:**120–128.
44. **Hu B, Margolin W, Molineux IJ, Liu J.** 2013. The bacteriophage T7 virion undergoes extensive structural remodeling during infection. Science **339:**576–579.
45. **Jakutytė L, Lurz R, Baptista C, Carballido-Lopez R, São-José C, Tavares P, Daugelavičius R.** 2012. First steps of bacteriophage SPP1 entry into *Bacillus subtilis*. Virology **422:**425–434.
46. **Kukkaro P, Bamford DH.** 2009. Virus-host interactions in environments with a wide range of ionic strengths. Environ. Microbiol. Rep. **1:**71–77.
47. **Pietilä MK, Atanasova NS, Oksanen HM, Bamford DH.** 2013. Modified coat protein forms the flexible spindle-shaped virion of haloarchaeal virus His1. Environ. Microbiol. **15:**1674–1686.
48. **Bath C, Dyall-Smith ML.** 1998. His1, an archaeal virus of the *Fuselloviridae* family that infects *Haloarcula hispanica*. J. Virol. **72:**9392–9395.
49. **Quax TE, Voet M, Sismeiro O, Dillies MA, Jagla B, Coppee JY, Sezonov G, Forterre P, van der Oost J, Lavigne R, Prangishvili D.** 2013. Massive activation of archaeal defense genes during viral infection. J. Virol. **87:** 8419–8428.
50. **Lu MJ, Henning U.** 1994. Superinfection exclusion by T-even-type coliphages. Trends Microbiol. **2:**137–139.
51. **Zillig W, Prangishvilli D, Schleper C, Elferink M, Holz I, Albers S, Janekovic D, Gotz D.** 1996. Viruses, plasmids and other genetic elements of thermophilic and hyperthermophilic Archaea. FEMS Microbiol. Rev. **18:**225–236.
52. **Albers SV, Driessen AJ.** 2005. Analysis of ATPases of putative secretion operons in the thermoacidophilic archaeon Sulfolobus solfataricus. Microbiology **151:**763–773.
53. **Albers SV, Pohlschroder M.** 2009. Diversity of archaeal type IV pilin-like structures. Extremophiles **13:**403–410.
54. **Albers SV, Meyer BH.** 2011. The archaeal cell envelope. Nat. Rev. Microbiol. **9:**414–426.

DISCUSSION

DISCUSSION

Successful spindle-shaped archaeal viruses.

Archaea-specific virosphere exhibits a rich diversity of viruses which display unique virion morphotypes and uncommon genomic properties (Krupovic et al., 2012; Prangishvili et al., 2013). Viruses infecting hyperthermophilic archaea are particularly diverse in terms of their morphologies, including bottle-shaped, droplet-shaped, spindle-shaped, bacilliform, etc. which have never been associated with the other two cellular domains (Pina et al., 2011). Research on archaeal viruses has focused on the isolation of new members and their characterization led to the establishment of novel viral families by the ICTV (Prangishvili, 2015). However, a number of isolates have thus far remained unclassified including a vast majority of spindle-shaped viruses.

Despite the fact that there is some pleomorphicity, the viral particles display an overall similar lemon-shaped body which is either tail-less, single-tailed or two-tailed. They are known to infect a broad range of hosts which rely on very diverse metabolisms and belong to phylogenetically distant groups. Using structural proteins as markers, we defined two viral lineages: the *Bicaudaviridae* and the *Fuselloviridae* depending on the fold of the MCP (Krupovic et al., 2014) (**Chapter 3**). The two-tailed bicaudavirus ATV was shown to be related to single-tailed STSV1 and STSV2 based upon the helix-bundle fold of their MCPs and shared gene content with 18 genes in common. On the other hand, His1, former 'Salterprovirus', and other tail-less fusiform viruses display similar hydrophobicity profiles with two transmembrane domains present in the N- and C-terminal parts of the MCP. In addition, some of these viruses share an overlapping set of genes for viral genome replication and integration into the host chromosome and are proposed to represent the subgroups α-, β-, γ-, δ- and ε-fuselloviruses.

Our in-depth comparative analysis between all the spindle-shaped viruses infecting archaea has permitted to retrieve a global network of relationships between distantly-related viruses. The *Fuselloviridae* appears as the most prominent and potentially evolutionarily successful family of viruses infecting archaea. Fuselloviruses and spindle-shaped viruses in general are particularly abundant in ecosystems where archaea outnumber bacterial species such as geothermal and hypersaline habitats which suggest that they might play an important ecological role. Unfortunately, the information on the organization of spindle-shaped virions

and the ways these viruses interact with their hosts is limited (Quemin and Quax, 2015) (**Chapter 2**).

Architecture of spindle-shaped virions: the case-study of SSV1.

SSV1 has been one of the first archaeal viruses to be isolated and is the prototypical member of the *Fuselloviridae* family (Martin et al., 1984; Pina et al., 2011). Like most fuselloviruses, SSV1 virions are lemon-shaped and possess short filamentous appendages at one end. In order to improve our understanding on the architecture of spindle-shaped archaeal viruses, we carried out a comprehensive biochemical characterization of SSV1 virions (Quemin et al., 2015) (**Chapter 4**). As a prerequisite, we established large-scale virus production and purification methods which were not available before. Indeed, recent structural analysis by cryo-EM and 3D reconstruction could not conclude on the organization of SSV1 virions being limited in the resolution by the number of particles considered and heterogeneity within sample (Stedman et al., 2015). In addition, the presence of lipids and/or viral envelope could not be addressed and has remained controversial up to now (Martin et al., 1984; Reiter et al., 1987).

In agreement with previous reports, the virions were found to contain four virus-encoded structural proteins: VP1, VP2, VP3 and VP4 – formerly known as C792 (Reiter et al., 1987; Redder et al., 2009). The MCP VP1 maturates through proteolytic cleavage of a precursor molecule and together with VP3 and VP4 undergo post-translational glycosylation. Notably, the viral DNA-binding protein VP2 is not essential for virus infectivity and for most of the fuselloviruses, no homologous ORF has been identified in the viral genome (Redder et al., 2009; Iverson and Stedman, 2012). For the first time, our findings suggest that another cellular DNA-binding protein included in the viral particles, Sso7d, can replace VP2. Sso7d is the most abundant chromatin remodeling protein in the host and a member of the 7-kDa protein superfamily (Koster et al., 2015). Hence, it is likely that the viral and cellular DNA-binding proteins play a similar function in condensing the circular dsDNA genome in SSV1 virions. Furthermore, we could unambiguously resolve the controversy concerning the viral architecture and specifically the presence of lipids in the viral particles. We identified GDGT lipids in highly purified SSV1 virions using mass spectrometry techniques. These lipids are specific to archaea and structurally distinct from their bacterial and eukaryotic counterparts.

They display an ether linkage between the glycerol moiety and the hydrocarbon chains forming a covalently-bound monolayer (De Rosa et al., 1986).

Collectively our data showed that SSV1 is a unique lipid-containing virus composed of glycosylated structural proteins encapsidating the nucleoprotein filaments made of circular dsDNA genome either bound to viral VP2 and/or cellular Sso7d. The detailed understanding of the structural components and the architecture of SSV1 virions is a prerequisite for subsequent studies targeting SSV1-*Sulfolobus* interactions. In particular, the spindle-shaped body is decorated at one of the two pointed ends by thin terminal fibres which mediate interactions with cell-derived vesicles or even between the particles themselves (Figure 6). It has been shown that aggregates of SSV1 virions rely on ionic and most importantly hydrophobic interactions (Quemin et al., 2015) (**Chapter 4**). Hence, the terminal appendages must be involved in adsorption to the host cell surface. Based on the fact that SSV1 is a lipid-containing virus, we propose a mechanism for entry by fusion between the viral envelope and the cytoplasmic membrane of the host which would be mediated by the terminal fibres. In analogy with eukaryotic enveloped viruses, the viral progeny might bud through the cytoplasmic membrane thereby acquiring lipids while exiting the cell without apparent lysis (Martin et al., 1984; Schleper et al., 1992).

SSV1 as a model for lipid-containing viruses infecting archaea.

Apart from transcriptomic analyses of viral and host gene expression levels through the course of the viral cycle (Frols et al., 2007b; Fusco et al., 2013; Fusco et al., 2015), the interactions between SSV1 and *Sulfolobu*s, as well as other fuselloviruses and their hosts, remain poorly characterized. In particular, the entry mechanism has never been studied and there has been only one report concerning the egress of this virus. Based on negatively-stained electron micrographs of infected *Sulfolobus* cells, it was concluded that SSV1 virions are released from the host via budding through the cytoplasmic membrane without lysis of the cell (Martin et al., 1984). In order to gain more detailed understanding into the late stages of SSV1 infection and particularly into the mechanism of virion egress, we analyzed the infection cycle of SSV1 in its natural host, *S. shibatae* B12 (Quemin et al., in preparation) (**Chapter 5**).

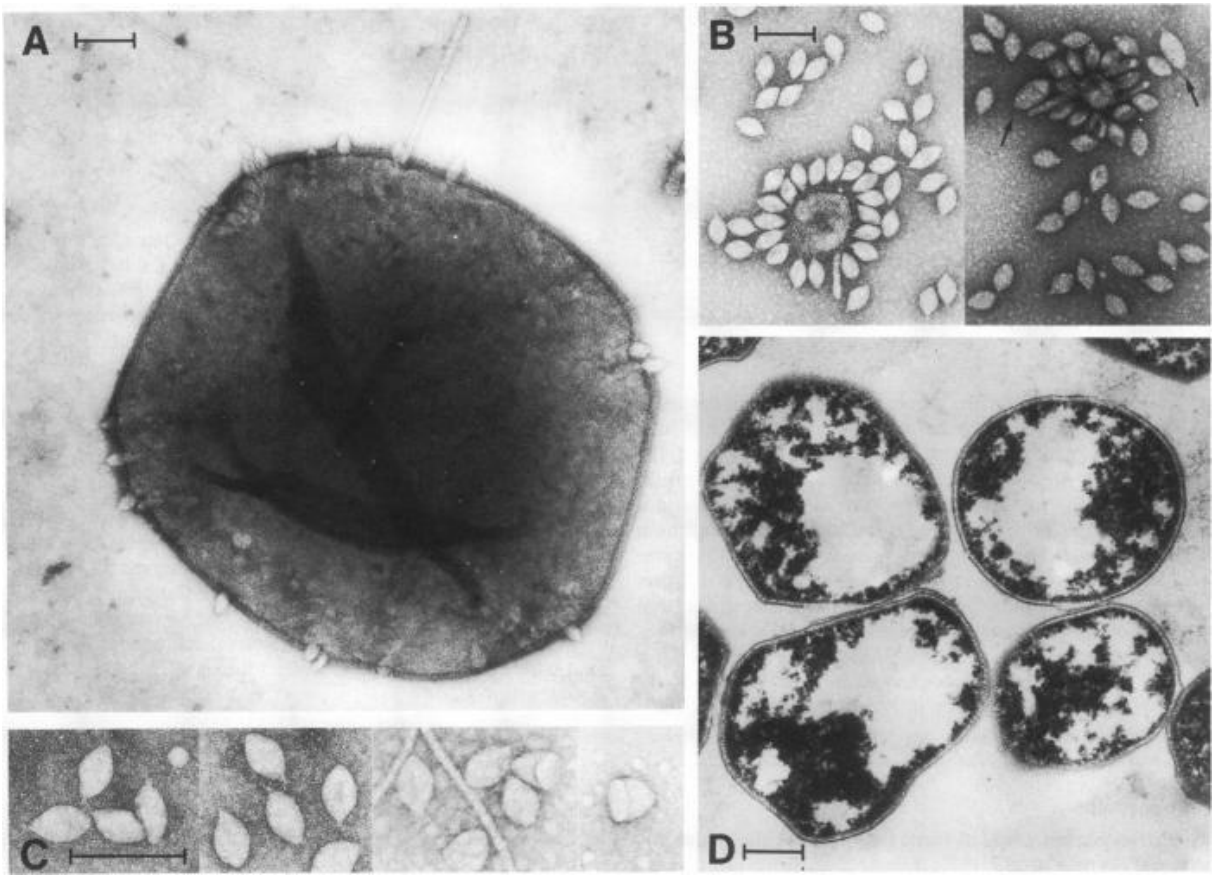

Figure 6: Electron micrographs of virus particles. (A) Cell apparently extruding virus. (B) Free virus and virus particles attached to cellular material. Two large particles are arrowed. (C) Purified free virus particles exhibiting tail structures. Three bullet-shaped particles are seen on the right. (D) Thin sections of cells sampled 6 h after u.v. irridation showing three cell -cell contacts. The bars represent 0.2 Imn.

Reproduced with permission from Martin et al., 1984: *SAV 1, a temperate u.v.-inducible DNA virus-like particle from the archaebacterium Sulfolobus acidocaldarius isolate B12*.

Electron tomography showed that the exit of SSV1 progeny from the host occurs via budding through the cytoplasmic membrane and the S-layer. The virions are initially assembled at the cell periphery in a tubular form piercing through the membrane towards the extracellular environment. They encase the viral nucleoprotein filaments which are presumably accumulating in close proximity to the cytoplasmic membrane. Interestingly, the inner leaflet of the membrane is differentially stained than the outer one, most likely as a consequence of the presence of viral structural proteins. Although the tube-like intermediates exhibit an extra-layer originating from and continuous with the plasma membrane of *Sulfolobus*, this viral envelope is always thinner than the cellular membrane (~4 versus ~5 nm). Subsequently, the virions assume the lemon-shaped morphology representing the mature form of SSV1 virions. Although the possibility that the different morphotypes observed in our samples are aberrant products of assembly, they are more likely to be intermediates depending on whether

membrane scission and structural rearrangements have occurred or not. In particular, ring-shaped, dark structures are often located at the junction between the enveloped virions protruding through the S-layer and the parental membrane from the host cell. The constriction of membranes observed in the case of SSV1 resembles the scission mechanism of eukaryotic enveloped viruses. One hypothesis is that the maturation of SSV1 virions involves the ESCRT proteins in a similar manner as described during infection by HIV for example (Morita et al., 2011).

Membrane budding is an essential step of the life cycle of eukaryotic enveloped viruses and most, but not all, of them exit the host cell by co-opting the ESCRT machinery of their host (Hurley, 2010; Votteler and Sundquist, 2013). The ESCRT is a conserved cellular machinery involved in cell division, multi-vesicular body (MVB) formation and virus budding (Figure 7) (Raiborg and Stenmark, 2009; Babst, 2011). It performs three distinct but connected functions orchestrated by four ESCRT protein complexes. ESCRT-0 first recognizes and forms a network around the ubiquitylated cargo preventing its recycling and retrograde trafficking (Mayers et al., 2011). Then, ESCRT-I serves as a signal for sorting the ubiquitylated cargo into the MVB pathway (Katzmann et al., 2001). Together, ESCRT-I and ESCRT-II drive endosomal invagination and membrane budding (Gill et al., 2007). Finally, ESCRT-III recruitment leads to stabilization of the budding neck, vesicle abscission and is dissociated upon the action of the ATPase Vps4 (Obita et al., 2007; Lata et al., 2008). In archaea, a number of species encode homologues to the eukaryotic ESCRT-III proteins although no similarity has been detected for components of the ESCRT-0, ESCRT-I and ESCRT-II complexes (Makarova et al., 2010; Lindas and Bernander, 2013). In *Sulfolobus*, there are four homologs of ESCRT-III and one for Vps4 (Hobel et al., 2008; Samson et al., 2008; Samson and Bell, 2009). Such a simplified version of the system is also encountered in protozoan parasites in which ESCRT-III complex is assembled without the upstream machinery on the neck of spontaneously forming vesicles (Babst, 2011). Notably, the archaeal homologs to ESCRT-III are up-regulated during infection by STIV (Maaty et al., 2012a; Maaty et al., 2012b) and have even been identified in STIV virions (Maaty et al., 2006). However, they were found to be down-regulated upon exposure of *Sulfolobus* cells to UV irradiation in two independent studies (Frols et al., 2007a; Gotz et al., 2007) and have never been reported to be part of SSV1 virions (Reiter et al., 1987; Quemin et al., 2015) (**Chapter 4**). Whether the ESCRT-III homologues present in *Sulfolobus* are involved in the structural rearrangements which are required for the assembly and release of SSV1 virions remains to be confirmed.

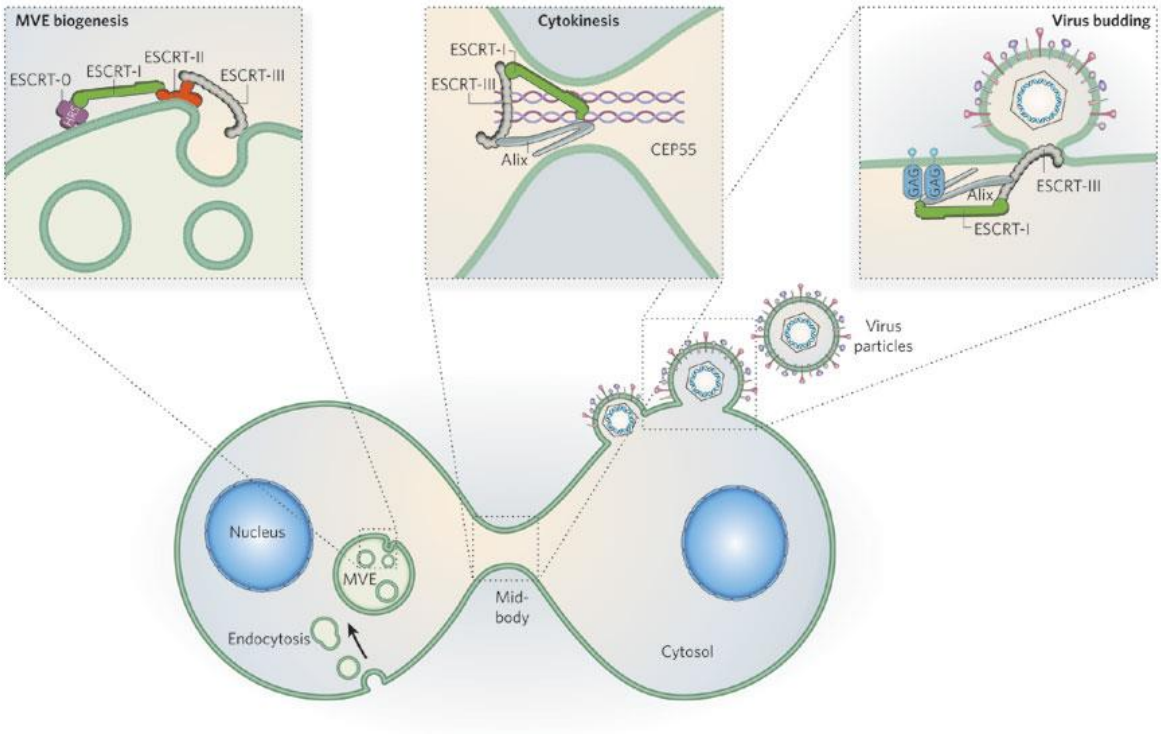

Figure 7: ESCRT-III is a conserved machinery for the abscission of narrow membrane stalks filled with cytosol. In MVE biogenesis (left), ESCRT-III is recruited by ESCRT-0, -I and -II. In cytokinesis (middle), ESCRT-III is recruited by the centrosome/midbody protein CEP55 and Alix (and, to a lesser extent, by ESCRT-I). In HIV budding (right), ESCRT-III is recruited by the viral GAG protein and ESCRT-I (and, to a lesser extent, by Alix).

Reproduced with permission from Raibord and Stenmark, 2009: *The ESCRT machinery in endosomal sorting of ubiquitylated membrane proteins*.

The terminal fibres which are located at one of the two pointed ends could be involved in the budding process serving as an encapsidation signal for example or alternatively, they might also take part in the scission of membranes at late stages. Indeed, VP4 – the supposedly sole component of the terminal fibres – might play a pivotal role by mediating ionic and, most importantly, hydrophobic interactions (Quemin et al., 2015) (**Chapter 4**). It is well-known that SSV1 virions spontaneously bind to host-derived vesicles and this interaction specifically involves the virus appendages (Figure 6) (Martin et al., 1984). Based on this property of virions and the fact that they contain lipids, it has also been proposed that SSV1 virions reach the cell interior by fusion between the host cytoplasmic membrane and the viral envelope. To the best of our knowledge, the entry mechanism of SSV1 hasn't been investigated so far and no similarity has been detected between VP4 and any of the described eukaryotic viral fusion proteins.

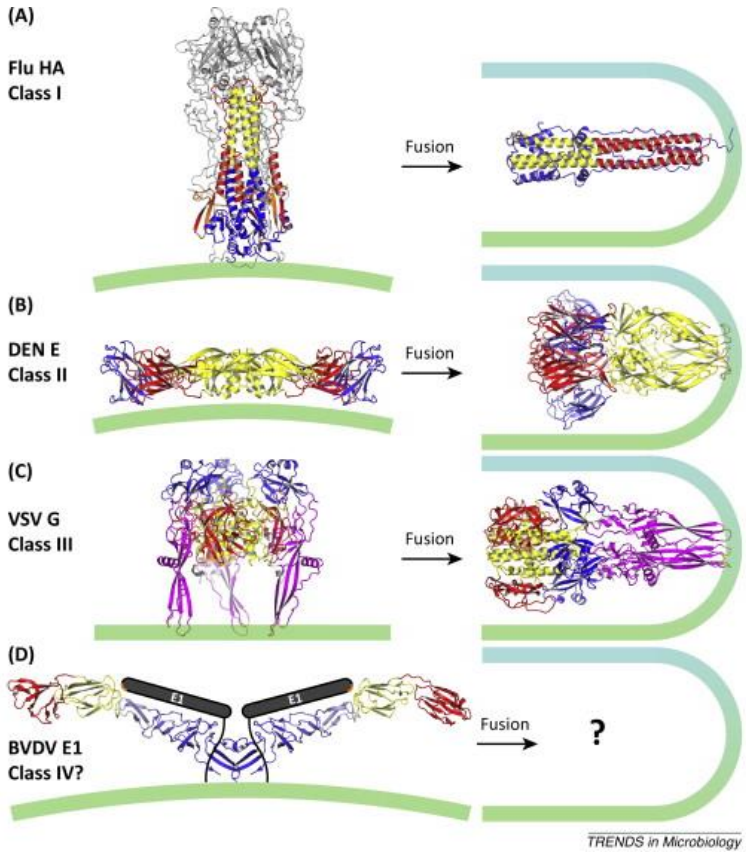

Figure 8: Conformational changes associated with membrane fusion in the different structural classes of membrane fusion proteins. In all classes, a fusion motif (orange) that is shielded from the solvent in the prefusion conformation (left column) becomes exposed in response to environmental cues (e.g., low pH or coreceptor binding). The fusion motif inserts into the cell membrane and the protein folds back on itself, forcing the fusion motif and the C-terminal transmembrane domain (not shown) anchored in the viral membrane towards each other. The proteins are trimeric in their postfusion conformations (right column). (A) In class I fusion proteins, such as influenza A virus hemagglutinin (Flu HA) shown here, membrane fusion is catalyzed by extensive refolding and secondary structure rearrangements of prefusion trimers to form a six-helix bundle [Protein Data Bank (PDB) codes 2HMG, 1HTM, 1QU1]. (B) Class II proteins usually form icosahedral shells in infectious virions. The envelope proteins respond to the reduced pH of an endosome with a repositioning of the three domains with only minor changes in secondary structure. The proteins form trimers during the fusion transition and the fusion loop in the central domain is directed towards the viral transmembrane anchor. The pre- and postfusion conformations of dengue type 2 virus E (DEN E) are shown here (PDB codes 1OKE, 1OK8). (C) Class III proteins are trimeric before and after fusion and undergo extensive refolding during the fusion transition like class I fusion proteins, but they contain internal fusion loops like class II proteins. The pre- and postfusion structures of vesicular stomatitis virus G (VSV G) are shown here (PDB codes 2J6J, 2CMZ). (D) The structure of envelope glycoprotein E2 from the pestivirus bovine viral diarrhea virus (BVDV) has been proposed to serve as a molecular scaffold for E1, which may define a new structural class of fusion machinery (PDB code 4JNT). The structure of envelope protein E1 (gray) and the nature of the fusogenic conformational change remain unknown. The outer leaflets of the viral and cellular membranes are represented in green and cyan, respectively.

Reproduced with permission from Li and Modis, 2014: *A novel membrane fusion protein family in Flaviviridae?*

In eukaryotes, viral proteins which mediate fusion belong to four classes depending on the structural hallmarks of their pre- and post-fusion conformations (Figure 8) (White et al., 2008; Li and Modis, 2014). The class I fusion proteins (Influenza, HIV, Ebola, etc.) exhibit a proteolytically generated N-terminal fusion peptide and a core composed of three central α-

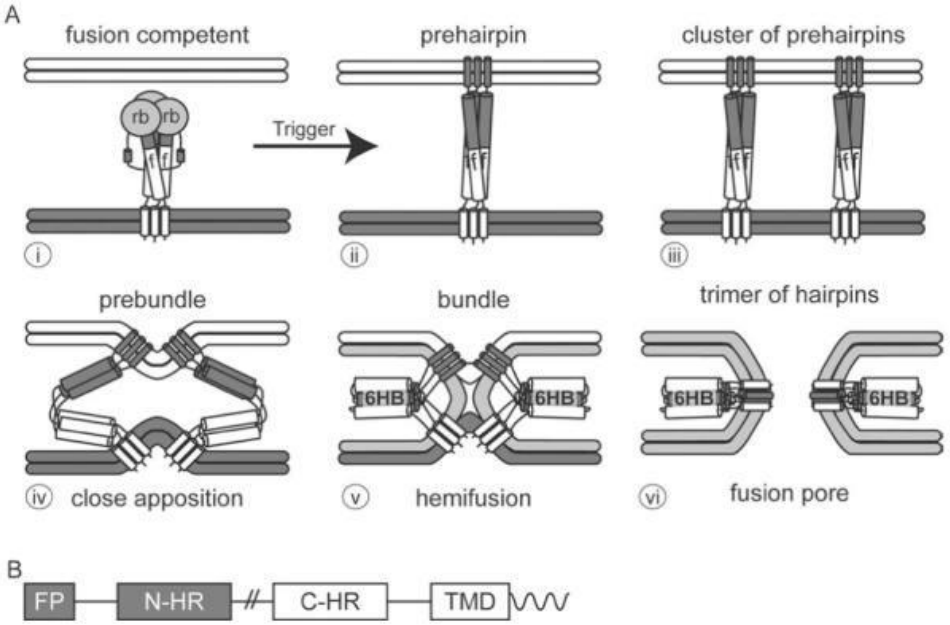

Figure 9: The common trimer-of-hairpins pathway of membrane fusion. (A) The model depicts a Class I fusion protein, but related structures (e.g., prehairpins and trimers-of-hairpins) form for Class II and III proteins, which also promote membrane merger through stages of close apposition (iv), hemifusion (v), small fusion pores (not shown), and large fusion pores (vi). See Table 2 and text for comparisons among the different classes of viral fusion proteins. The depicted Class I fusion protein is one that does not require any other viral surface proteins for fusion (e.g., influenza HA or a retroviral Env); it contains both a receptor binding subunit (labeled rb in image i) and a fusion subunit (labeled f in images i to iii). The target and viral membranes are, respectively, at the top and bottom of the images. The receptor binding subunit (rb) is not shown beyond image i as its location at the later stages is not known; in all cases studied, however, the rb subunit of this type of class I fusion protein must move out of the way, thus unclamping the fusion subunit in the metastable fusion competent state and allowing fusion to proceed. For Class I fusion proteins six helix bundles (6HBs) are seen in their bundle (v) and trimer-of-hairpins (vi) forms; the length and position of the 6HB varies for different proteins. The starting (i) and final (vi) images represent structures that are known for several viral fusion proteins; high level structural information is currently lacking on the intermediates. (B) The key features of a class I fusion protein from N- to C-terminus: a fusion peptide (FP) at or near the N-terminus, an N-heptad repeat (N-HR aka HR1 or HRA), a C-heptad repeat (C-HR aka HR2 or HRB), a transmembrane domain (TMD), and a cytoplasmic tail (squiggle). Linkers of variable lengths are indicated as straight lines. (The // between the N- and C-heptad repeats indicates that the length of these linkers varies considerably). Peptide analogs of the N-HR and C-HR helices can inhibit fusion and infection.

Reproduced with permission from White et al., 2008: *Structures and Mechanisms of Viral Membrane Fusion Proteins. Multiple Variations on a Common Theme.*

helices in the pre-fusion conformation, which refolds into a six-helix bundle after fusion (Skehel and Wiley, 2000). The class II fusion proteins (Dengue virus, Semliki Forest virus, Tick-Borne Encephalitis virus, etc.) consist primarily of β-sheet structures with internal fusion peptides formed as loops at the tips of the β-strands. They are often associated with a chaperone protein which is cleaved during or soon after viral assembly (Modis, 2013). The third class of fusion proteins (Herpes Simplex virus 1, Vesicular Stomatitis virus, Rabies virus, etc.) shares features of both class I and class II fusion proteins. Like the former they possess core helical bundles but the central β-stranded domain contains one or more fusion

loops resembling those of the latter (Backovic and Jardetzky, 2011). Recently, the envelope proteins from Hepatitis C virus and a pestivirus were found to have two novel folds, distinct from each other, which have been suggested to define a new structural class IV for viral fusion proteins (Li and Modis, 2014). The fusion proteins encoded by viruses not only belong to different classes which are genetically and structurally unrelated but also vary in their mode of activation: receptor-binding, acidification, a mix between the two factors, etc. Despite these differences, common principles behind the action of fusion proteins have emerged (Figure 9). In response to the activating trigger, the metastable fusion protein found on virion surface converts to an extended structure which inserts into the target membrane via its fusion peptide. A subsequent conformational change causes the fusion loop to fold back upon itself, thereby bringing its fusion peptide and its transmembrane domain into close contact, together with the attached target and viral membranes. Fusion ensues as the initial lipid stalk progresses through local hemifusion, and then there is opening and enlargement of the fusion pore (Earp et al., 2005). Hemifusion is a key intervening step during which small regions of the outer contacting monolayers merge while the inner ones remain intact (White et al., 2008). However, in *Sulfolobus* and SSV1, the membrane exclusively contains GDGTs. These lipid species are completely different from the lipids of eukaryotes or bacteria and form a monolayer-like membrane (De Rosa et al., 1986). If fusion of the envelope of SSV1 virions with the cytoplasmic membrane of the archaeon occurs, it would rather happen directly without any hemifusion stage. Therefore, if and how fusion of membranes can be completed at once and how the energy required is provided are intriguing questions that remain unanswered. These key aspects of the life cycle of enveloped viruses infecting archaea require further investigation in order to reveal fundamental principles of virus biology in the different domains of life.

SIRV2 as a model for non-enveloped viruses infecting archaea.

Beside fusiform viruses, filamentous VLPs are the other morphotypes encountered in abundance in archaea-dominated ecosystems such as geothermal environments. To date, all the filamentous viruses isolated encase linear dsDNA genomes and are unique to Archaea (linear viruses with dsDNA genomes are not known in Bacteria or Eukarya). They belong to the *Rudiviridae* and *Lipothrixviridae* families within the order *Ligamenvirales* (Prangishvili and Krupovic, 2012). The rudiviruses display stiff, rod-shaped, non-enveloped virions and

have recently emerged as virus model systems in archaea (Prangishvili et al., 2013). While studying SIRV2-*Sulfolobus* interactions, a new mechanism of virion release has been described. At the end of the infection cycle, virus-encoded pyramidal structures are formed on the cell surface. Eventually, these pyramids open up leading to virion escape from the cell interior (Bize et al., 2009). In addition, data have been accumulating on virion architecture, replication of viral genome and transcription regulation upon infection (Prangishvili et al., 2013; Quax et al., 2013; DiMaio et al., 2015). As opposed to the egress mechanism of SIRV2 which has been extensively studied (Quax et al., 2010; Quax et al., 2011; Daum et al., 2014), nothing was known about the early stages of the infection cycle, i.e. adsorption to the host cell surface and entry of the viral genome into the cell cytoplasm (Quemin et al., 2013) (**Chapter 6**).

To gain insights into the entry of SIRV2 virions, we have utilized a number of different assays to assess the binding kinetics, reversible and irreversible adsorption, receptor saturation, etc. which were initially developed to study the interaction of bacteriophages with their hosts (Hyman and Abedon, 2009). As a result, we have determined that adsorption is rapid and more than 80% of the viral particles are irreversibly bound to the host cells within the first minute of infection. Thus, it appears that host recognition and adsorption of SIRV2 virions is much more efficient than that of halophilic viruses which require several hours to bind to the surface of their hosts (Kukkaro and Bamford, 2009). The receptor present on the host cell surface is abundant since more than 370 viral particles are able to bind to a single cell. Furthermore, transmission electron microscopy and whole-cell electron tomography strongly suggest that SIRV2 virions specifically attach to the tip of pili-like filaments allowing a strong and irreversible interaction between the viral and cellular determinants. Subsequently, viral particles are found on the side of the appendages indicating a progression along these appendages to reach the cell surface. At the cell surface, there is the delivery of the viral genome into the cell interior which seems to be concomitant with disassembly of particles lying outside. The next step towards understanding the entry mechanism of SIRV2 will be to identify the cellular and viral determinants responsible for the different interactions observed. The two ends of the viral particles are equivalent in their capacity of binding to pili-like filaments and specifically involve the three terminal fibers; whether the virion body also plays a role has to be determined. On the host side, the nature of the filaments and the presence of a secondary receptor at the cell surface are under investigation. Another question which also

needs to be addressed is how SIRV2 virions move along the pilus-like cellular receptor and reach the cell surface.

Receptor recognition and binding are key steps and typically induce a cascade of events that starts with structural reorganization of virion leading to viral genome penetration through the cell envelope. In general, non-enveloped prokaryotic viruses rely on two strategies: (i) genome injection into the cell interior while leaving the empty capsid associated with the cell envelope (e.g., tailed dsDNA bacteriophages); (ii) disassembly of the virion at the cell envelope concomitantly with genome delivery (e.g., filamentous bacteriophages) (Poranen et al., 2002). Interestingly, partially broken viral particles were observed at the cell membrane following the course of adsorption by electron microscopy techniques suggesting a genome delivery mechanism similar to filamentous bacteriophages. In particular, filamentous Ff inoviruses interact with the F-pili of their host and utilize the retraction system to reach the cell surface and finally bind the secondary receptor in order to deliver their genome into the host cytoplasm (Rakonjac et al., 2011). The interaction of SIRV2 with *Sulfolobus* filaments appears similar although retraction of the latter was never observed either during infection or under normal growth conditions (Lassak et al., 2012a; Lassak et al., 2012b). On the other hand, flagellotrophic bacteriophages bind the host flagella and harness the energy of rotation to reach the host cell surface (Guerrero-Ferreira et al., 2011). Notably, flagella (called archaella in archaea) of *Sulfolobus* are considerably thicker, ~14 nm in diameter (Ghosh and Albers, 2011) than the filaments to which SIRV2 binds, arguing against the possibility that flagella serves as an entry receptor during SIRV2 infection. Whether the mechanism of SIRV2 translocation along the filaments is related to that of Ff inoviruses, flagellotrophic bacteriophages or is completely novel is one of the open questions that remain to be adressed.

Concluding remarks and future perspectives.

The work undertaken during my PhD thesis aims to provide a better understanding on virus-host interplay in Archaea. Typical environments where archaea outnumber bacteria are geothermal ecosystems. In such environments, the vast majority of the encountered VLPs are fusiform and filamentous in shape. As models of these two viral groups, we selected: (i) the temperate, spindle-shaped SSV1 – the best-known member of the family *Fuselloviridae* – and (ii) the lytic, non-enveloped, rod-shaped SIRV2 – the type-species of the family *Rudiviridae*. Both viruses infect members of the genus *Sulfolobus*, contain dsDNA genomes and were among the first hyperthermophilic archaeal viruses to be isolated (Martin et al., 1984; Prangishvili et al., 1999). Our findings provide insights into the entry, assembly and egress stages of these viruses throughout the course of infection cycle. The obtained information is not only improving our comprehension of two different virus-host systems but also empowers more general comparisons with the corresponding mechanisms employed by bacterial and eukaryotic viruses. However, further research is required to fully appreciate the properties which are exclusive to archaeal viruses as well as the viral strategies which are reminiscent to those employed by viruses of the other two domains.

Many spindle-shaped viruses which are thus far unique to archaea, have been isolated from diverse hosts. The relationships between these viruses are mainly established based on comparative genomics studies which have revealed a set of genes conserved in fuselloviruses. These genes are supposedly involved in viral genome replication and integration although the exact roles of encoded proteins during the viral cycle remain to be demonstrated experimentally. Even though bioinformatic approaches provide valuable information on the evolutionary relationships between distant isolates and could retrieve potential capsid proteins that previously eluded annotation (Krupovic et al., 2014), complementary comprehensive biochemical characterization of virions is often lacking. More importantly, no high-resolution structure has been solved for any spindle-shaped virus. In the case of SSV1 virions (Quemin et al., 2015; Stedman et al., 2015), information regarding the organization of viral particles is particularly scarce. It is not clear what is the exact location and arrangement of the structural proteins in SSV1 virion; does it contain an internal or external lipid membrane; how is the genome packed and condensed by viral and/or cellular proteins? Cryo-EM and 3D-reconstruction have been used to determine the structure of SSV1 virions and resulted in a model with limited resolution due to the pleomorphic nature of viral particles (Stedman et al., 2015). Thus, alternative approaches to study viral architecture should be explored. For

example, controlled dissociation of structural components composing SSV1 virions by treatments with detergents could be used, as it has been done in the case of the other spindle-shaped His1 virions (Hong et al., 2015). Such systematic biochemical dissociation would provide valuable information on the organization of viral particles which might also be relevant to the life cycle of the virus. Based on the results of various treatments, an *in vitro* system has been established to study DNA ejection from His1 virions helping to shed light on the potential entry process of spindle-shaped viruses (Hanhijarvi et al., 2013).

The analysis of SSV1 egress by electron tomography provided significant insights into the budding and assembly of enveloped viruses in Archaea (Quemin et al., in preparation). We thus proposed a model for the assembly and egress of SSV1 virions which will have to be confirmed using a combination of molecular biology, biochemical, genetics and microscopy approaches. In particular, the following questions should be addressed: where each of the capsid proteins is located, in the cytoplasm or at the membrane? What is their role during building of viral capsids? How is the dissymmetry of the virion with two different pointed ends determined? Is the surface of the host cell modified as a result of capsid proteins anchoring? Does the composition of the cytoplasmic membrane change through the course of the viral cycle? What is scission machinery utilized? How does it assemble and bend the membrane to form spindle-shaped virions? How budding of viral progeny is controlled? What is the effect of viral budding on cell viability?

Previous research focused on the assembly and exit of SIRV2 and our study of the entry process completed the available picture of the viral cycle (Quemin et al., 2013). However, several aspects of the primary interactions between the virus and its host remain unraveled. Until now, the nature of cellular appendages to which SIRV2 virions are binding, the energy requirement for their movement along the filaments or else, the presence of a secondary receptor at the cell surface have not been investigated. Therefore, additional work is needed to understand the entry mechanism of rudiviruses in greater detail and identify the molecular players involved. Although the infection cycle of SIRV2 is one of the best characterized among archaeal viruses, there are still unanswered questions, e.g. concerning the dependence of the viral life cycle on environmental factors like high temperature, acidic pH, etc.

When compared to the wealth of data available on bacterial and eukaryotic viral systems, the knowledge on archaea-specific virosphere is minuscule. Various lines of research proposed hereinabove should not only illuminate the molecular mechanisms underlying virus-host

interactions but are also expected to reveal the parallels between the corresponding processes in Bacteria and Eukarya. Therefore, functional studies targeting molecular processes and players involved throughout the viral life cycle might also permit to tackle questions regarding the emergence and evolution of viruses from the three domains of life.

REFERENCES

ACKERMANN, H.W., AND PRANGISHVILI, D. (2012). PROKARYOTE VIRUSES STUDIED BY ELECTRON MICROSCOPY. *ARCH VIROL* 157, 1843-1849.

AHN, D.G., KIM, S.I., RHEE, J.K., KIM, K.P., PAN, J.G., AND OH, J.W. (2006). TTSV1, A NEW VIRUS-LIKE PARTICLE ISOLATED FROM THE HYPERTHERMOPHILIC CRENARCHAEOTE THERMOPROTEUS TENAX. *VIROLOGY* 351, 280-290.

AJON, M., FROLS, S., VAN WOLFEREN, M., STOECKER, K., TEICHMANN, D., DRIESSEN, A.J., GROGAN, D.W., ALBERS, S.V., AND SCHLEPER, C. (2011). UV-INDUCIBLE DNA EXCHANGE IN HYPERTHERMOPHILIC ARCHAEA MEDIATED BY TYPE IV PILI. *MOL MICROBIOL* 82, 807-817.

ALBERS, S.V., FORTERRE, P., PRANGISHVILI, D., AND SCHLEPER, C. (2013). THE LEGACY OF CARL WOESE AND WOLFRAM ZILLIG: FROM PHYLOGENY TO LANDMARK DISCOVERIES. *NAT REV MICROBIOL* 11, 713-719.

ALBERS, S.V., AND MEYER, B.H. (2011). THE ARCHAEAL CELL ENVELOPE. *NAT REV MICROBIOL* 9, 414-426.

ALVES, R.J., WANEK, W., ZAPPE, A., RICHTER, A., SVENNING, M.M., SCHLEPER, C., AND URICH, T. (2013). NITRIFICATION RATES IN ARCTIC SOILS ARE ASSOCIATED WITH FUNCTIONALLY DISTINCT POPULATIONS OF AMMONIA-OXIDIZING ARCHAEA. *ISME J* 7, 1620-1631.

ARNOLD, H.P., ZILLIG, W., ZIESE, U., HOLZ, I., CROSBY, M., UTTERBACK, T., WEIDMANN, J.F., KRISTJANSON, J.K., KLENK, H.P., NELSON, K.E., AND FRASER, C.M. (2000). A NOVEL LIPOTHRIXVIRUS, SIFV, OF THE EXTREMELY THERMOPHILIC CRENARCHAEON SULFOLOBUS. *VIROLOGY* 267, 252-266.

ATANASOVA, N.S., DEMINA, T.A., BUIVYDAS, A., BAMFORD, D.H., AND OKSANEN, H.M. (2015). ARCHAEAL VIRUSES MULTIPLY: TEMPORAL SCREENING IN A SOLAR SALTERN. *VIRUSES* 7, 1902-1926.

ATANASOVA, N.S., ROINE, E., OREN, A., BAMFORD, D.H., AND OKSANEN, H.M. (2012). GLOBAL NETWORK OF SPECIFIC VIRUS-HOST INTERACTIONS IN HYPERSALINE ENVIRONMENTS. *ENVIRON MICROBIOL* 14, 426-440.

BABST, M. (2011). MVB VESICLE FORMATION: ESCRT-DEPENDENT, ESCRT-INDEPENDENT AND EVERYTHING IN BETWEEN. *CURR OPIN CELL BIOL* 23, 452-457.

BACKOVIC, M., AND JARDETZKY, T.S. (2011). CLASS III VIRAL MEMBRANE FUSION PROTEINS. *ADV EXP MED BIOL* 714, 91-101.

BANERJEE, A., GHOSH, A., MILLS, D.J., KAHNT, J., VONCK, J., AND ALBERS, S.V. (2012). FLAX, A UNIQUE COMPONENT OF THE CRENARCHAEAL ARCHAELLUM, FORMS OLIGOMERIC RING-SHAPED STRUCTURES AND INTERACTS WITH THE MOTOR ATPASE FLAI. *J BIOL CHEM* 287, 43322-43330.

BANG, C., AND SCHMITZ, R.A. (2015). ARCHAEA ASSOCIATED WITH HUMAN SURFACES: NOT TO BE UNDERESTIMATED. *FEMS MICROBIOL REV*.

BARNS, S.M., DELWICHE, C.F., PALMER, J.D., AND PACE, N.R. (1996). PERSPECTIVES ON ARCHAEAL DIVERSITY, THERMOPHILY AND MONOPHYLY FROM ENVIRONMENTAL RRNA SEQUENCES. *PROC NATL ACAD SCI U S A* 93, 9188-9193.

BARNS, S.M., FUNDYGA, R.E., JEFFRIES, M.W., AND PACE, N.R. (1994). REMARKABLE ARCHAEAL DIVERSITY DETECTED IN A YELLOWSTONE NATIONAL PARK HOT SPRING ENVIRONMENT. *PROC NATL ACAD SCI U S A* 91, 1609-1613.

BATH, C., CUKALAC, T., PORTER, K., AND DYALL-SMITH, M.L. (2006). HIS1 AND HIS2 ARE DISTANTLY RELATED, SPINDLE-SHAPED HALOVIRUSES BELONGING TO THE NOVEL VIRUS GROUP, SALTERPROVIRUS. *VIROLOGY* 350, 228-239.

BELAY, N., MUKHOPADHYAY, B., CONWAY DE MACARIO, E., GALASK, R., AND DANIELS, L. (1990). METHANOGENIC BACTERIA IN HUMAN VAGINAL SAMPLES. *J CLIN MICROBIOL* 28, 1666-1668.

BERNANDER, R., AND POPLAWSKI, A. (1997). CELL CYCLE CHARACTERISTICS OF THERMOPHILIC ARCHAEA. *J BACTERIOL* 179, 4963-4969.

BERTANI, G., AND BARESI, L. (1987). GENETIC TRANSFORMATION IN THE METHANOGEN METHANOCOCCUS VOLTAE PS. ***J BACTERIOL*** **169, 2730-2738.**

BETTSTETTER, M., PENG, X., GARRETT, R.A., AND PRANGISHVILI, D. (2003). AFV1, A NOVEL VIRUS INFECTING HYPERTHERMOPHILIC ARCHAEA OF THE GENUS ACIDIANUS. ***VIROLOGY*** **315, 68-79.**

BIZE, A., KARLSSON, E.A., EKEFJARD, K., QUAX, T.E., PINA, M., PREVOST, M.C., FORTERRE, P., TENAILLON, O., BERNANDER, R., AND PRANGISHVILI, D. (2009). A UNIQUE VIRUS RELEASE MECHANISM IN THE ARCHAEA. ***PROC NATL ACAD SCI U S A*** **106, 11306-11311.**

BIZE, A., PENG, X., PROKOFEVA, M., MACLELLAN, K., LUCAS, S., FORTERRE, P., GARRETT, R.A., BONCH-OSMOLOVSKAYA, E.A., AND PRANGISHVILI, D. (2008). VIRUSES IN ACIDIC GEOTHERMAL ENVIRONMENTS OF THE KAMCHATKA PENINSULA. ***RES MICROBIOL*** **159, 358-366.**

BROCHIER-ARMANET, C., BOUSSAU, B., GRIBALDO, S., AND FORTERRE, P. (2008). MESOPHILIC CRENARCHAEOTA: PROPOSAL FOR A THIRD ARCHAEAL PHYLUM, THE THAUMARCHAEOTA. ***NAT REV MICROBIOL*** **6, 245-252.**

BROCHIER, C., GRIBALDO, S., ZIVANOVIC, Y., CONFALONIERI, F., AND FORTERRE, P. (2005). NANOARCHAEA: REPRESENTATIVES OF A NOVEL ARCHAEAL PHYLUM OR A FAST-EVOLVING EURYARCHAEAL LINEAGE RELATED TO THERMOCOCCALES? ***GENOME BIOL*** **6, R42.**

BROCK, T.D., BROCK, K.M., BELLY, R.T., AND WEISS, R.L. (1972). SULFOLOBUS: A NEW GENUS OF SULFUR-OXIDIZING BACTERIA LIVING AT LOW PH AND HIGH TEMPERATURE. ***ARCH MIKROBIOL*** **84, 54-68.**

BRUM, J.R., SCHENCK, R.O., AND SULLIVAN, M.B. (2013). GLOBAL MORPHOLOGICAL ANALYSIS OF MARINE VIRUSES SHOWS MINIMAL REGIONAL VARIATION AND DOMINANCE OF NON-TAILED VIRUSES. ***ISME J*** **7, 1738-1751.**

CHONG, P.L. (2010). ARCHAEBACTERIAL BIPOLAR TETRAETHER LIPIDS: PHYSICO-CHEMICAL AND MEMBRANE PROPERTIES. ***CHEM PHYS LIPIDS*** **163, 253-265.**

CLORE, A.J., AND STEDMAN, K.M. (2007). THE SSV1 VIRAL INTEGRASE IS NOT ESSENTIAL. ***VIROLOGY*** **361, 103-111.**

COHEN-KRAUSZ, S., AND TRACHTENBERG, S. (2008). THE FLAGELLAR FILAMENT STRUCTURE OF THE EXTREME ACIDOTHERMOPHILE SULFOLOBUS SHIBATAE B12 SUGGESTS THAT ARCHAEABACTERIAL FLAGELLA HAVE A UNIQUE AND COMMON SYMMETRY AND DESIGN. ***J MOL BIOL*** **375, 1113-1124.**

CRAIG, L., PIQUE, M.E., AND TAINER, J.A. (2004). TYPE IV PILUS STRUCTURE AND BACTERIAL PATHOGENICITY. ***NAT REV MICROBIOL*** **2, 363-378.**

DAUM, B., QUAX, T.E., SACHSE, M., MILLS, D.J., REIMANN, J., YILDIZ, O., HADER, S., SAVEANU, C., FORTERRE, P., ALBERS, S.V., KUHLBRANDT, W., AND PRANGISHVILI, D. (2014). SELF-ASSEMBLY OF THE GENERAL MEMBRANE-REMODELING PROTEIN PVAP INTO SEVENFOLD VIRUS-ASSOCIATED PYRAMIDS. ***PROC NATL ACAD SCI U S A*** **111, 3829-3834.**

DE ROSA, M., AND GAMBACORTA, A. (1988). THE LIPIDS OF ARCHAEBACTERIA. ***PROG LIPID RES*** **27, 153-175.**

DE ROSA, M., GAMBACORTA, A., AND GLIOZZI, A. (1986). STRUCTURE, BIOSYNTHESIS, AND PHYSICOCHEMICAL PROPERTIES OF ARCHAEBACTERIAL LIPIDS. ***MICROBIOL REV*** **50, 70-80.**

DELONG, E.F. (2005). MICROBIAL COMMUNITY GENOMICS IN THE OCEAN. ***NAT REV MICROBIOL*** **3, 459-469.**

DELONG, E.F., WU, K.Y., PREZELIN, B.B., AND JOVINE, R.V. (1994). HIGH ABUNDANCE OF ARCHAEA IN ANTARCTIC MARINE PICOPLANKTON. ***NATURE*** **371, 695-697.**

DIMAIO, F., YU, X., RENSEN, E., KRUPOVIC, M., PRANGISHVILI, D., AND EGELMAN, E.H. (2015). VIROLOGY. A VIRUS THAT INFECTS A HYPERTHERMOPHILE ENCAPSIDATES A-FORM DNA. ***SCIENCE*** **348, 914-917.**

DRIDI, B., RAOULT, D., AND DRANCOURT, M. (2011). ARCHAEA AS EMERGING ORGANISMS IN COMPLEX HUMAN MICROBIOMES. ***ANAEROBE*** **17, 56-63.**

DYALL-SMITH, M., TANG, S.L., AND BATH, C. (2003). HALOARCHAEAL VIRUSES: HOW DIVERSE ARE THEY? ***RES MICROBIOL*** **154, 309-313.**

EARP, L.J., DELOS, S.E., PARK, H.E., AND WHITE, J.M. (2005). THE MANY MECHANISMS OF VIRAL MEMBRANE FUSION PROTEINS. ***CURR TOP MICROBIOL IMMUNOL*** **285, 25-66.**

Elkins, J.G., Podar, M., Graham, D.E., Makarova, K.S., Wolf, Y., Randau, L., Hedlund, B.P., Brochier-Armanet, C., Kunin, V., Anderson, I., Lapidus, A., Goltsman, E., Barry, K., Koonin, E.V., Hugenholtz, P., Kyrpides, N., Wanner, G., Richardson, P., Keller, M., and Stetter, K.O. (2008). A korarchaeal genome reveals insights into the evolution of the Archaea. *Proc Natl Acad Sci U S A* 105, 8102-8107.

Ellen, A.F., Zolghadr, B., Driessen, A.M., and Albers, S.V. (2010). Shaping the archaeal cell envelope. *Archaea* 2010, 608243.

Eme, L., Reigstad, L.J., Spang, A., Lanzen, A., Weinmaier, T., Rattei, T., Schleper, C., and Brochier-Armanet, C. (2013). Metagenomics of Kamchatkan hot spring filaments reveal two new major (hyper)thermophilic lineages related to Thaumarchaeota. *Res Microbiol* 164, 425-438.

Erdmann, S., Chen, B., Huang, X., Deng, L., Liu, C., Shah, S.A., Le Moine Bauer, S., Sobrino, C.L., Wang, H., Wei, Y., She, Q., Garrett, R.A., Huang, L., and Lin, L. (2014). A novel single-tailed fusiform Sulfolobus virus STSV2 infecting model Sulfolobus species. *Extremophiles* 18, 51-60.

Frols, S., Ajon, M., Wagner, M., Teichmann, D., Zolghadr, B., Folea, M., Boekema, E.J., Driessen, A.J., Schleper, C., and Albers, S.V. (2008). UV-inducible cellular aggregation of the hyperthermophilic archaeon Sulfolobus solfataricus is mediated by pili formation. *Mol Microbiol* 70, 938-952.

Frols, S., Gordon, P.M., Panlilio, M.A., Duggin, I.G., Bell, S.D., Sensen, C.W., and Schleper, C. (2007a). Response of the hyperthermophilic archaeon Sulfolobus solfataricus to UV damage. *J Bacteriol* 189, 8708-8718.

Frols, S., Gordon, P.M., Panlilio, M.A., Schleper, C., and Sensen, C.W. (2007b). Elucidating the transcription cycle of the UV-inducible hyperthermophilic archaeal virus SSV1 by DNA microarrays. *Virology* 365, 48-59.

Fusco, S., Liguori, R., Limauro, D., Bartolucci, S., She, Q., and Contursi, P. (2015). Transcriptome analysis of Sulfolobus solfataricus infected with two related fuselloviruses reveals novel insights into the regulation of CRISPR-Cas system. *Biochimie*.

Fusco, S., She, Q., Bartolucci, S., and Contursi, P. (2013). T(lys), a newly identified Sulfolobus spindle-shaped virus 1 transcript expressed in the lysogenic state, encodes a DNA-binding protein interacting at the promoters of the early genes. *J Virol* 87, 5926-5936.

Galand, P.E., Fritze, H., Conrad, R., and Yrjala, K. (2005). Pathways for methanogenesis and diversity of methanogenic archaea in three boreal peatland ecosystems. *Appl Environ Microbiol* 71, 2195-2198.

Garrett, R.A., Prangishvili, D., Shah, S.A., Reuter, M., Stetter, K.O., and Peng, X. (2010). Metagenomic analyses of novel viruses and plasmids from a cultured environmental sample of hyperthermophilic neutrophiles. *Environ Microbiol* 12, 2918-2930.

Geslin, C., Le Romancer, M., Gaillard, M., Erauso, G., and Prieur, D. (2003). Observation of virus-like particles in high temperature enrichment cultures from deep-sea hydrothermal vents. *Res Microbiol* 154, 303-307.

Ghosh, A., and Albers, S.V. (2011). Assembly and function of the archaeal flagellum. *Biochem Soc Trans* 39, 64-69.

Gill, D.J., Teo, H., Sun, J., Perisic, O., Veprintsev, D.B., Emr, S.D., and Williams, R.L. (2007). Structural insight into the ESCRT-I/-II link and its role in MVB trafficking. *EMBO J* 26, 600-612.

Gittel, A., Barta, J., Kohoutova, I., Schnecker, J., Wild, B., Capek, P., Kaiser, C., Torsvik, V.L., Richter, A., Schleper, C., and Urich, T. (2014). Site- and horizon-specific patterns of microbial community structure and enzyme activities in permafrost-affected soils of Greenland. *Front Microbiol* 5, 541.

Gotz, D., Paytubi, S., Munro, S., Lundgren, M., Bernander, R., and White, M.F. (2007). Responses of hyperthermophilic crenarchaea to UV irradiation. *Genome Biol* 8, R220.

GROGAN, D.W., OZARZAK, M.A., AND BERNANDER, R. (2008). VARIATION IN GENE CONTENT AMONG GEOGRAPHICALLY DIVERSE SULFOLOBUS ISOLATES. *ENVIRON MICROBIOL* 10, 137-146.

GUERRERO-FERREIRA, R.C., VIOLLIER, P.H., ELY, B., POINDEXTER, J.S., GEORGIEVA, M., JENSEN, G.J., AND WRIGHT, E.R. (2011). ALTERNATIVE MECHANISM FOR BACTERIOPHAGE ADSORPTION TO THE MOTILE BACTERIUM CAULOBACTER CRESCENTUS. *PROC NATL ACAD SCI U S A* 108, 9963-9968.

GUO, L., BRUGGER, K., LIU, C., SHAH, S.A., ZHENG, H., ZHU, Y., WANG, S., LILLESTOL, R.K., CHEN, L., FRANK, J., PRANGISHVILI, D., PAULIN, L., SHE, Q., HUANG, L., AND GARRETT, R.A. (2011). GENOME ANALYSES OF ICELANDIC STRAINS OF SULFOLOBUS ISLANDICUS, MODEL ORGANISMS FOR GENETIC AND VIRUS-HOST INTERACTION STUDIES. *J BACTERIOL* 193, 1672-1680.

GUY, L., AND ETTEMA, T.J. (2011). THE ARCHAEAL 'TACK' SUPERPHYLUM AND THE ORIGIN OF EUKARYOTES. *TRENDS MICROBIOL* 19, 580-587.

HANHIJARVI, K.J., ZIEDAITE, G., PIETILA, M.K., HAEGGSTROM, E., AND BAMFORD, D.H. (2013). DNA EJECTION FROM AN ARCHAEAL VIRUS--A SINGLE-MOLECULE APPROACH. *BIOPHYS J* 104, 2264-2272.

HAPPONEN, L.J., REDDER, P., PENG, X., REIGSTAD, L.J., PRANGISHVILI, D., AND BUTCHER, S.J. (2010). FAMILIAL RELATIONSHIPS IN HYPERTHERMO- AND ACIDOPHILIC ARCHAEAL VIRUSES. *J VIROL* 84, 4747-4754.

HARING, M., PENG, X., BRUGGER, K., RACHEL, R., STETTER, K.O., GARRETT, R.A., AND PRANGISHVILI, D. (2004). MORPHOLOGY AND GENOME ORGANIZATION OF THE VIRUS PSV OF THE HYPERTHERMOPHILIC ARCHAEAL GENERA PYROBACULUM AND THERMOPROTEUS: A NOVEL VIRUS FAMILY, THE GLOBULOVIRIDAE. *VIROLOGY* 323, 233-242.

HARING, M., RACHEL, R., PENG, X., GARRETT, R.A., AND PRANGISHVILI, D. (2005A). VIRAL DIVERSITY IN HOT SPRINGS OF POZZUOLI, ITALY, AND CHARACTERIZATION OF A UNIQUE ARCHAEAL VIRUS, ACIDIANUS BOTTLE-SHAPED VIRUS, FROM A NEW FAMILY, THE AMPULLAVIRIDAE. *J VIROL* 79, 9904-9911.

HARING, M., VESTERGAARD, G., BRUGGER, K., RACHEL, R., GARRETT, R.A., AND PRANGISHVILI, D. (2005B). STRUCTURE AND GENOME ORGANIZATION OF AFV2, A NOVEL ARCHAEAL LIPOTHRIXVIRUS WITH UNUSUAL TERMINAL AND CORE STRUCTURES. *J BACTERIOL* 187, 3855-3858.

HARING, M., VESTERGAARD, G., RACHEL, R., CHEN, L., GARRETT, R.A., AND PRANGISHVILI, D. (2005C). VIROLOGY: INDEPENDENT VIRUS DEVELOPMENT OUTSIDE A HOST. *NATURE* 436, 1101-1102.

HJORT, K., AND BERNANDER, R. (1999). CHANGES IN CELL SIZE AND DNA CONTENT IN SULFOLOBUS CULTURES DURING DILUTION AND TEMPERATURE SHIFT EXPERIMENTS. *J BACTERIOL* 181, 5669-5675.

HOBEL, C.F., ALBERS, S.V., DRIESSEN, A.J., AND LUPAS, A.N. (2008). THE SULFOLOBUS SOLFATARICUS AAA PROTEIN SSO0909, A HOMOLOGUE OF THE EUKARYOTIC ESCRT VPS4 ATPASE. *BIOCHEM SOC TRANS* 36, 94-98.

HONG, C., PIETILA, M.K., FU, C.J., SCHMID, M.F., BAMFORD, D.H., AND CHIU, W. (2015). LEMON-SHAPED HALO ARCHAEAL VIRUS HIS1 WITH UNIFORM TAIL BUT VARIABLE CAPSID STRUCTURE. *PROC NATL ACAD SCI U S A* 112, 2449-2454.

HUBER, H., BURGGRAF, S., MAYER, T., WYSCHKONY, I., RACHEL, R., AND STETTER, K.O. (2000). IGNICOCCUS GEN. NOV., A NOVEL GENUS OF HYPERTHERMOPHILIC, CHEMOLITHOAUTOTROPHIC ARCHAEA, REPRESENTED BY TWO NEW SPECIES, IGNICOCCUS ISLANDICUS SP NOV AND IGNICOCCUS PACIFICUS SP NOV. AND IGNICOCCUS PACIFICUS SP. NOV. *INT J SYST EVOL MICROBIOL* 50 PT 6, 2093-2100.

HURLEY, J.H. (2010). THE ESCRT COMPLEXES. *CRIT REV BIOCHEM MOL BIOL* 45, 463-487.

HYMAN, P., AND ABEDON, S.T. (2009). PRACTICAL METHODS FOR DETERMINING PHAGE GROWTH PARAMETERS. *METHODS MOL BIOL* 501, 175-202.

IVERSON, E., AND STEDMAN, K. (2012). A GENETIC STUDY OF SSV1, THE PROTOTYPICAL FUSELLOVIRUS. *FRONT MICROBIOL* 3, 200.

JAAKKOLA, S.T., ZERULLA, K., GUO, Q., LIU, Y., MA, H., YANG, C., BAMFORD, D.H., CHEN, X., SOPPA, J., AND OKSANEN, H.M. (2014). HALOPHILIC ARCHAEA CULTIVATED FROM SURFACE STERILIZED MIDDLE-LATE EOCENE ROCK SALT ARE POLYPLOID. *PLOS ONE* 9, E110533.

JAIN, S., CAFORIO, A., FODRAN, P., LOLKEMA, J.S., MINNAARD, A.J., AND DRIESSEN, A.J. (2014). IDENTIFICATION OF CDP-ARCHAEOL SYNTHASE, A MISSING LINK OF ETHER LIPID BIOSYNTHESIS IN ARCHAEA. *CHEM BIOL* 21, 1392-1401.

JARRELL, K.F., DING, Y., MEYER, B.H., ALBERS, S.V., KAMINSKI, L., AND EICHLER, J. (2014). N-LINKED GLYCOSYLATION IN ARCHAEA: A STRUCTURAL, FUNCTIONAL, AND GENETIC ANALYSIS. *MICROBIOL MOL BIOL REV* 78, 304-341.

JAUBERT, C., DANIOUX, C., OBERTO, J., CORTEZ, D., BIZE, A., KRUPOVIC, M., SHE, Q., FORTERRE, P., PRANGISHVILI, D., AND SEZONOV, G. (2013). GENOMICS AND GENETICS OF SULFOLOBUS ISLANDICUS LAL14/1, A MODEL HYPERTHERMOPHILIC ARCHAEON. *OPEN BIOL* 3, 130010.

JORDAN, M., MEILE, L., AND LEISINGER, T. (1989). ORGANIZATION OF METHANOBACTERIUM THERMOAUTOTROPHICUM BACTERIOPHAGE PSI M1 DNA. *MOL GEN GENET* 220, 161-164.

JORGENSEN, S.L., HANNISDAL, B., LANZEN, A., BAUMBERGER, T., FLESLAND, K., FONSECA, R., OVREAS, L., STEEN, I.H., THORSETH, I.H., PEDERSEN, R.B., AND SCHLEPER, C. (2012). CORRELATING MICROBIAL COMMUNITY PROFILES WITH GEOCHEMICAL DATA IN HIGHLY STRATIFIED SEDIMENTS FROM THE ARCTIC MID-OCEAN RIDGE. *PROC NATL ACAD SCI U S A* 109, E2846-2855.

JORGENSEN, S.L., THORSETH, I.H., PEDERSEN, R.B., BAUMBERGER, T., AND SCHLEPER, C. (2013). QUANTITATIVE AND PHYLOGENETIC STUDY OF THE DEEP SEA ARCHAEAL GROUP IN SEDIMENTS OF THE ARCTIC MID-OCEAN SPREADING RIDGE. *FRONT MICROBIOL* 4, 299.

KASHEFI, K., AND LOVLEY, D.R. (2003). EXTENDING THE UPPER TEMPERATURE LIMIT FOR LIFE. *SCIENCE* 301, 934.

KATZMANN, D.J., BABST, M., AND EMR, S.D. (2001). UBIQUITIN-DEPENDENT SORTING INTO THE MULTIVESICULAR BODY PATHWAY REQUIRES THE FUNCTION OF A CONSERVED ENDOSOMAL PROTEIN SORTING COMPLEX, ESCRT-I. *CELL* 106, 145-155.

KEOUGH, B.P., SCHMIDT, T.M., AND HICKS, R.E. (2003). ARCHAEAL NUCLEIC ACIDS IN PICOPLANKTON FROM GREAT LAKES ON THREE CONTINENTS. *MICROB ECOL* 46, 238-248.

KESSLER, A., BRINKMAN, A.B., VAN DER OOST, J., AND PRANGISHVILI, D. (2004). TRANSCRIPTION OF THE ROD-SHAPED VIRUSES SIRV1 AND SIRV2 OF THE HYPERTHERMOPHILIC ARCHAEON SULFOLOBUS. *J BACTERIOL* 186, 7745-7753.

KLEIKEMPER, J., POMBO, S.A., SCHROTH, M.H., SIGLER, W.V., PESARO, M., AND ZEYER, J. (2005). ACTIVITY AND DIVERSITY OF METHANOGENS IN A PETROLEUM HYDROCARBON-CONTAMINATED AQUIFER. *APPL ENVIRON MICROBIOL* 71, 149-158.

KNITTEL, K., LOSEKANN, T., BOETIUS, A., KORT, R., AND AMANN, R. (2005). DIVERSITY AND DISTRIBUTION OF METHANOTROPHIC ARCHAEA AT COLD SEEPS. *APPL ENVIRON MICROBIOL* 71, 467-479.

KOGA, Y., AND MORII, H. (2005). RECENT ADVANCES IN STRUCTURAL RESEARCH ON ETHER LIPIDS FROM ARCHAEA INCLUDING COMPARATIVE AND PHYSIOLOGICAL ASPECTS. *BIOSCI BIOTECHNOL BIOCHEM* 69, 2019-2034.

KOSTER, M.J., SNEL, B., AND TIMMERS, H.T. (2015). GENESIS OF CHROMATIN AND TRANSCRIPTION DYNAMICS IN THE ORIGIN OF SPECIES. *CELL* 161, 724-736.

KRISHNAN, L., AND SPROTT, G.D. (2008). ARCHAEOSOME ADJUVANTS: IMMUNOLOGICAL CAPABILITIES AND MECHANISM(S) OF ACTION. *VACCINE* 26, 2043-2055.

KRUPOVIC, M., QUEMIN, E.R., BAMFORD, D.H., FORTERRE, P., AND PRANGISHVILI, D. (2014). UNIFICATION OF THE GLOBALLY DISTRIBUTED SPINDLE-SHAPED VIRUSES OF THE ARCHAEA. *J VIROL* 88, 2354-2358.

KRUPOVIC, M., WHITE, M.F., FORTERRE, P., AND PRANGISHVILI, D. (2012). POSTCARDS FROM THE EDGE: STRUCTURAL GENOMICS OF ARCHAEAL VIRUSES. *ADV VIRUS RES* 82, 33-62.

KUKKARO, P., AND BAMFORD, D.H. (2009). VIRUS-HOST INTERACTIONS IN ENVIRONMENTS WITH A WIDE RANGE OF IONIC STRENGTHS. *ENVIRON MICROBIOL REP* 1, 71-77.

KULIK, E.M., SANDMEIER, H., HINNI, K., AND MEYER, J. (2001). IDENTIFICATION OF ARCHAEAL RDNA FROM SUBGINGIVAL DENTAL PLAQUE BY PCR AMPLIFICATION AND SEQUENCE ANALYSIS. *FEMS MICROBIOL LETT* 196, 129-133.

Langworthy, T.A. (1977). Comparative lipid composition of heterotrophically and autotrophically grown Sulfolobus acidocaldarius. *J Bacteriol* 130, 1326-1332.

Langworthy, T.A., Mayberry, W.R., and Smith, P.F. (1974). Long-chain glycerol diether and polyol dialkyl glycerol triether lipids of Sulfolobus acidocaldarius. *J Bacteriol* 119, 106-116.

Langworthy, T.A., Mayberry, W.R., and Smith, P.F. (1976). A sulfonolipid and novel glucosamidyl glycolipids from the extreme thermoacidophile Bacillus acidocaldarius. *Biochim Biophys Acta* 431, 550-569.

Lassak, K., Ghosh, A., and Albers, S.V. (2012a). Diversity, assembly and regulation of archaeal type IV pili-like and non-type-IV pili-like surface structures. *Res Microbiol* 163, 630-644.

Lassak, K., Neiner, T., Ghosh, A., Klingl, A., Wirth, R., and Albers, S.V. (2012b). Molecular analysis of the crenarchaeal flagellum. *Mol Microbiol* 83, 110-124.

Lata, S., Schoehn, G., Jain, A., Pires, R., Piehler, J., Gottlinger, H.G., and Weissenhorn, W. (2008). Helical structures of ESCRT-III are disassembled by VPS4. *Science* 321, 1354-1357.

Leininger, S., Urich, T., Schloter, M., Schwark, L., Qi, J., Nicol, G.W., Prosser, J.I., Schuster, S.C., and Schleper, C. (2006). Archaea predominate among ammonia-oxidizing prokaryotes in soils. *Nature* 442, 806-809.

Lepp, P.W., Brinig, M.M., Ouverney, C.C., Palm, K., Armitage, G.C., and Relman, D.A. (2004). Methanogenic Archaea and human periodontal disease. *Proc Natl Acad Sci U S A* 101, 6176-6181.

Letzelter, C., Duguet, M., and Serre, M.C. (2004). Mutational analysis of the archaeal tyrosine recombinase SSV1 integrase suggests a mechanism of DNA cleavage in trans. *J Biol Chem* 279, 28936-28944.

Li, Y., and Modis, Y. (2014). A novel membrane fusion protein family in Flaviviridae? *Trends Microbiol* 22, 176-182.

Lindas, A.C., and Bernander, R. (2013). The cell cycle of archaea. *Nat Rev Microbiol* 11, 627-638.

Lipp, J.S., Morono, Y., Inagaki, F., and Hinrichs, K.U. (2008). Significant contribution of Archaea to extant biomass in marine subsurface sediments. *Nature* 454, 991-994.

Luo, Y., Pfister, P., Leisinger, T., and Wasserfallen, A. (2001). The genome of archaeal prophage PsiM100 encodes the lytic enzyme responsible for autolysis of Methanothermobacter wolfeii. *J Bacteriol* 183, 5788-5792.

Maaty, W.S., Ortmann, A.C., Dlakic, M., Schulstad, K., Hilmer, J.K., Liepold, L., Weidenheft, B., Khayat, R., Douglas, T., Young, M.J., and Bothner, B. (2006). Characterization of the archaeal thermophile Sulfolobus turreted icosahedral virus validates an evolutionary link among double-stranded DNA viruses from all domains of life. *J Virol* 80, 7625-7635.

Maaty, W.S., Selvig, K., Ryder, S., Tarlykov, P., Hilmer, J.K., Heinemann, J., Steffens, J., Snyder, J.C., Ortmann, A.C., Movahed, N., Spicka, K., Chetia, L., Grieco, P.A., Dratz, E.A., Douglas, T., Young, M.J., and Bothner, B. (2012a). Proteomic analysis of Sulfolobus solfataricus during Sulfolobus Turreted Icosahedral Virus infection. *J Proteome Res* 11, 1420-1432.

Maaty, W.S., Steffens, J.D., Heinemann, J., Ortmann, A.C., Reeves, B.D., Biswas, S.K., Dratz, E.A., Grieco, P.A., Young, M.J., and Bothner, B. (2012b). Global analysis of viral infection in an archaeal model system. *Front Microbiol* 3, 411.

Makarova, K.S., Yutin, N., Bell, S.D., and Koonin, E.V. (2010). Evolution of diverse cell division and vesicle formation systems in Archaea. *Nat Rev Microbiol* 8, 731-741.

Martin, A., Yeats, S., Janekovic, D., Reiter, W.D., Aicher, W., and Zillig, W. (1984). SAV 1, a temperate u.v.-inducible DNA virus-like particle from the archaebacterium Sulfolobus acidocaldarius isolate B12. *EMBO J* 3, 2165-2168.

Mayers, J.R., Fyfe, I., Schuh, A.L., Chapman, E.R., Edwardson, J.M., and Audhya, A. (2011). ESCRT-0 assembles as a heterotetrameric complex on membranes and binds multiple ubiquitinylated cargoes simultaneously. ***J Biol Chem*** **286, 9636-9645.**

Meyer, B.H., and Albers, S.V. (2013). Hot and sweet: protein glycosylation in Crenarchaeota. ***Biochem Soc Trans*** **41, 384-392.**

Miller, T.L., Wolin, M.J., Conway De Macario, E., and Macario, A.J. (1982). Isolation of Methanobrevibacter smithii from human feces. ***Appl Environ Microbiol*** **43, 227-232.**

Mochizuki, T., Krupovic, M., Pehau-Arnaudet, G., Sako, Y., Forterre, P., and Prangishvili, D. (2012). Archaeal virus with exceptional virion architecture and the largest single-stranded DNA genome. ***Proc Natl Acad Sci U S A*** **109, 13386-13391.**

Mochizuki, T., Sako, Y., and Prangishvili, D. (2011). Provirus induction in hyperthermophilic archaea: characterization of Aeropyrum pernix spindle-shaped virus 1 and Aeropyrum pernix ovoid virus 1. ***J Bacteriol*** **193, 5412-5419.**

Mochizuki, T., Yoshida, T., Tanaka, R., Forterre, P., Sako, Y., and Prangishvili, D. (2010). Diversity of viruses of the hyperthermophilic archaeal genus Aeropyrum, and isolation of the Aeropyrum pernix bacilliform virus 1, APBV1, the first representative of the family Clavaviridae. ***Virology*** **402, 347-354.**

Modis, Y. (2013). Class II fusion proteins. ***Adv Exp Med Biol*** **790, 150-166.**

Moissl, C., Rachel, R., Briegel, A., Engelhardt, H., and Huber, R. (2005). The unique structure of archaeal 'hami', highly complex cell appendages with nano-grappling hooks. ***Mol Microbiol*** **56, 361-370.**

Morita, E., Sandrin, V., Mccullough, J., Katsuyama, A., Baci Hamilton, I., and Sundquist, W.I. (2011). ESCRT-III protein requirements for HIV-1 budding. ***Cell Host Microbe*** **9, 235-242.**

Muskhelishvili, G., Palm, P., and Zillig, W. (1993). SSV1-encoded site-specific recombination system in Sulfolobus shibatae. ***Mol Gen Genet*** **237, 334-342.**

Ng, S.Y., Zolghadr, B., Driessen, A.J., Albers, S.V., and Jarrell, K.F. (2008). Cell surface structures of archaea. ***J Bacteriol*** **190, 6039-6047.**

Nolling, J., Van Eeden, F.J., and De Vos, W.M. (1993). Distribution and characterization of plasmid-related sequences in the chromosomal DNA of different thermophilic Methanobacterium strains. ***Mol Gen Genet*** **240, 81-91.**

Nunoura, T., Oida, H., Nakaseama, M., Kosaka, A., Ohkubo, S.B., Kikuchi, T., Kazama, H., Hosoi-Tanabe, S., Nakamura, K., Kinoshita, M., Hirayama, H., Inagaki, F., Tsunogai, U., Ishibashi, J., and Takai, K. (2010). Archaeal diversity and distribution along thermal and geochemical gradients in hydrothermal sediments at the Yonaguni Knoll IV hydrothermal field in the Southern Okinawa trough. ***Appl Environ Microbiol*** **76, 1198-1211.**

Obita, T., Saksena, S., Ghazi-Tabatabai, S., Gill, D.J., Perisic, O., Emr, S.D., and Williams, R.L. (2007). Structural basis for selective recognition of ESCRT-III by the AAA ATPase Vps4. ***Nature*** **449, 735-739.**

Ochsenreiter, T., Selezi, D., Quaiser, A., Bonch-Osmolovskaya, L., and Schleper, C. (2003). Diversity and abundance of Crenarchaeota in terrestrial habitats studied by 16S RNA surveys and real time PCR. ***Environ Microbiol*** **5, 787-797.**

Offre, P., Spang, A., and Schleper, C. (2013). Archaea in biogeochemical cycles. ***Annu Rev Microbiol*** **67, 437-457.**

Okutan, E., Deng, L., Mirlashari, S., Uldahl, K., Halim, M., Liu, C., Garrett, R.A., She, Q., and Peng, X. (2013). Novel insights into gene regulation of the rudivirus SIRV2 infecting Sulfolobus cells. ***RNA Biol*** **10, 875-885.**

Pawlowski, A., Rissanen, I., Bamford, J.K., Krupovic, M., and Jalasvuori, M. (2014). Gammasphaerolipovirus, a newly proposed bacteriophage genus, unifies viruses of halophilic archaea and thermophilic bacteria within the novel family Sphaerolipoviridae. ***Arch Virol*** **159, 1541-1554.**

Peng, X., Blum, H., She, Q., Mallok, S., Brugger, K., Garrett, R.A., Zillig, W., and Prangishvili, D. (2001). Sequences and replication of genomes of the archaeal rudiviruses SIRV1 and SIRV2: relationships to the archaeal lipothrixvirus SIFV and some eukaryal viruses. *Virology* 291, 226-234.

Pester, M., Schleper, C., and Wagner, M. (2011). The Thaumarchaeota: an emerging view of their phylogeny and ecophysiology. *Curr Opin Microbiol* 14, 300-306.

Peyfoon, E., Meyer, B., Hitchen, P.G., Panico, M., Morris, H.R., Haslam, S.M., Albers, S.V., and Dell, A. (2010). The S-layer glycoprotein of the crenarchaeote Sulfolobus acidocaldarius is glycosylated at multiple sites with chitobiose-linked N-glycans. *Archaea* 2010.

Pfister, P., Wasserfallen, A., Stettler, R., and Leisinger, T. (1998). Molecular analysis of Methanobacterium phage psiM2. *Mol Microbiol* 30, 233-244.

Pietila, M.K., Atanasova, N.S., Manole, V., Liljeroos, L., Butcher, S.J., Oksanen, H.M., and Bamford, D.H. (2012). Virion architecture unifies globally distributed pleolipoviruses infecting halophilic archaea. *J Virol* 86, 5067-5079.

Pietila, M.K., Laurinavicius, S., Sund, J., Roine, E., and Bamford, D.H. (2010). The single-stranded DNA genome of novel archaeal virus halorubrum pleomorphic virus 1 is enclosed in the envelope decorated with glycoprotein spikes. *J Virol* 84, 788-798.

Pietila, M.K., Roine, E., Paulin, L., Kalkkinen, N., and Bamford, D.H. (2009). An ssDNA virus infecting archaea: a new lineage of viruses with a membrane envelope. *Mol Microbiol* 72, 307-319.

Pina, M., Bize, A., Forterre, P., and Prangishvili, D. (2011). The archeoviruses. *FEMS Microbiol Rev* 35, 1035-1054.

Poranen, M.M., Daugelavicius, R., and Bamford, D.H. (2002). Common principles in viral entry. *Annu Rev Microbiol* 56, 521-538.

Prangishvili, D. (2015). Archaeal viruses: living fossils of the ancient virosphere? *Ann N Y Acad Sci* 1341, 35-40.

Prangishvili, D., Arnold, H.P., Gotz, D., Ziese, U., Holz, I., Kristjansson, J.K., and Zillig, W. (1999). A novel virus family, the Rudiviridae: Structure, virus-host interactions and genome variability of the sulfolobus viruses SIRV1 and SIRV2. *Genetics* 152, 1387-1396.

Prangishvili, D., Koonin, E.V., and Krupovic, M. (2013). Genomics and biology of Rudiviruses, a model for the study of virus-host interactions in Archaea. *Biochem Soc Trans* 41, 443-450.

Prangishvili, D., and Krupovic, M. (2012). A new proposed taxon for double-stranded DNA viruses, the order "Ligamenvirales". *Arch Virol* 157, 791-795.

Prangishvili, D., Vestergaard, G., Haring, M., Aramayo, R., Basta, T., Rachel, R., and Garrett, R.A. (2006). Structural and genomic properties of the hyperthermophilic archaeal virus ATV with an extracellular stage of the reproductive cycle. *J Mol Biol* 359, 1203-1216.

Probst, A.J., Auerbach, A.K., and Moissl-Eichinger, C. (2013). Archaea on human skin. *PLoS One* 8, e65388.

Quax, T.E., Krupovic, M., Lucas, S., Forterre, P., and Prangishvili, D. (2010). The Sulfolobus rod-shaped virus 2 encodes a prominent structural component of the unique virion release system in Archaea. *Virology* 404, 1-4.

Quax, T.E., Lucas, S., Reimann, J., Pehau-Arnaudet, G., Prevost, M.C., Forterre, P., Albers, S.V., and Prangishvili, D. (2011). Simple and elegant design of a virion egress structure in Archaea. *Proc Natl Acad Sci U S A* 108, 3354-3359.

Quax, T.E., Voet, M., Sismeiro, O., Dillies, M.A., Jagla, B., Coppee, J.Y., Sezonov, G., Forterre, P., Van Der Oost, J., Lavigne, R., and Prangishvili, D. (2013). Massive activation of archaeal defense genes during viral infection. *J Virol* 87, 8419-8428.

Quemin, E.R., Chlanda, P., Sachse, M., Forterre, P., Zimmerberg, J., Prangishvili, D., and Krupovic, M. (in preparation). How to bud from an archaeon: assembly and release of *Sulfolobus* spindle-shaped virus 1.

Quemin, E.R., Lucas, S., Daum, B., Quax, T.E., Kuhlbrandt, W., Forterre, P., Albers, S.V., Prangishvili, D., and Krupovic, M. (2013). First insights into the entry process of hyperthermophilic archaeal viruses. *J Virol* 87, 13379-13385.

Quemin, E.R., Pietila, M.K., Oksanen, H.M., Forterre, P., Rijpstra, W.I., Schouten, S., Bamford, D.H., Prangishvili, D., and Krupovic, M. (2015). Sulfolobus spindle-shaped virus 1 contains glycosylated capsid proteins, a cellular chromatin protein and host-derived lipids. *J Virol*.

Quemin, E.R., Prangishvili, D., and Krupovic, M. (2014). Hard out there: understanding archaeal virus biology. *Future Virol.* 9, 703-706.

Quemin, E.R., and Quax, T.E. (2015). Archaeal viruses at the cell envelope: entry and egress. *Front Microbiol* 6, 552.

Rachel, R., Bettstetter, M., Hedlund, B.P., Haring, M., Kessler, A., Stetter, K.O., and Prangishvili, D. (2002). Remarkable morphological diversity of viruses and virus-like particles in hot terrestrial environments. *Arch Virol* 147, 2419-2429.

Raiborg, C., and Stenmark, H. (2009). The ESCRT machinery in endosomal sorting of ubiquitylated membrane proteins. *Nature* 458, 445-452.

Rakonjac, J., Bennett, N.J., Spagnuolo, J., Gagic, D., and Russel, M. (2011). Filamentous bacteriophage: biology, phage display and nanotechnology applications. *Curr Issues Mol Biol* 13, 51-76.

Raymann, K., Brochier-Armanet, C., and Gribaldo, S. (2015). The two-domain tree of life is linked to a new root for the Archaea. *Proc Natl Acad Sci U S A* 112, 6670-6675.

Redder, P., Peng, X., Brugger, K., Shah, S.A., Roesch, F., Greve, B., She, Q., Schleper, C., Forterre, P., Garrett, R.A., and Prangishvili, D. (2009). Four newly isolated fuselloviruses from extreme geothermal environments reveal unusual morphologies and a possible interviral recombination mechanism. *Environ Microbiol* 11, 2849-2862.

Reindl, S., Ghosh, A., Williams, G.J., Lassak, K., Neiner, T., Henche, A.L., Albers, S.V., and Tainer, J.A. (2013). Insights into FlaI functions in archaeal motor assembly and motility from structures, conformations, and genetics. *Mol Cell* 49, 1069-1082.

Reiter, W.D., Palm, P., Henschen, A., Lottspeich, F., Zillig, W., and Grampp, B. (1987). Identification and characterization of the genes encoding three structural proteins of the Sulfolobus virus-like particle SSV1. *Mol Gen Genet* 206, 144-153.

Reiter, W.D., Palm, P., and Yeats, S. (1989). Transfer RNA genes frequently serve as integration sites for prokaryotic genetic elements. *Nucleic Acids Res* 17, 1907-1914.

Reiter, W.D., Zillig, W., and Palm, P. (1988). Archaebacterial viruses. *Adv Virus Res* 34, 143-188.

Rice, G., Stedman, K., Snyder, J., Wiedenheft, B., Willits, D., Brumfield, S., Mcdermott, T., and Young, M.J. (2001). Viruses from extreme thermal environments. *Proc Natl Acad Sci U S A* 98, 13341-13345.

Rice, G., Tang, L., Stedman, K., Roberto, F., Spuhler, J., Gillitzer, E., Johnson, J.E., Douglas, T., and Young, M. (2004). The structure of a thermophilic archaeal virus shows a double-stranded DNA viral capsid type that spans all domains of life. *Proc Natl Acad Sci U S A* 101, 7716-7720.

Rieger, G., Rachel, R., Hermann, R., and Stetter, K.O. (1995). Ultrastructure of the hyperthermophilic archaeon *Pyrodictium abyssi*. *J Struct Biol* 11, 578-587.

Roine, E., Kukkaro, P., Paulin, L., Laurinavicius, S., Domanska, A., Somerharju, P., and Bamford, D.H. (2010). New, closely related haloarchaeal viral elements with different nucleic acid types. *J Virol* 84, 3682-3689.

Samson, R.Y., and Bell, S.D. (2009). Ancient ESCRTs and the evolution of binary fission. *Trends Microbiol* 17, 507-513.

SAMSON, R.Y., OBITA, T., FREUND, S.M., WILLIAMS, R.L., AND BELL, S.D. (2008). A ROLE FOR THE ESCRT SYSTEM IN CELL DIVISION IN ARCHAEA. *SCIENCE* 322, 1710-1713.

SANTOS, F., YARZA, P., PARRO, V., MESEGUER, I., ROSSELLO-MORA, R., AND ANTON, J. (2012). CULTURE-INDEPENDENT APPROACHES FOR STUDYING VIRUSES FROM HYPERSALINE ENVIRONMENTS. *APPL ENVIRON MICROBIOL* 78, 1635-1643.

SCHLEPER, C., KUBO, K., AND ZILLIG, W. (1992). THE PARTICLE SSV1 FROM THE EXTREMELY THERMOPHILIC ARCHAEON SULFOLOBUS IS A VIRUS: DEMONSTRATION OF INFECTIVITY AND OF TRANSFECTION WITH VIRAL DNA. *PROC NATL ACAD SCI U S A* 89, 7645-7649.

SERRE, M.C., LETZELTER, C., GAREL, J.R., AND DUGUET, M. (2002). CLEAVAGE PROPERTIES OF AN ARCHAEAL SITE-SPECIFIC RECOMBINASE, THE SSV1 INTEGRASE. *J BIOL CHEM* 277, 16758-16767.

SIMON, H.M., DODSWORTH, J.A., AND GOODMAN, R.M. (2000). CRENARCHAEOTA COLONIZE TERRESTRIAL PLANT ROOTS. *ENVIRON MICROBIOL* 2, 495-505.

SPANG, A., SAW, J.H., JORGENSEN, S.L., ZAREMBA-NIEDZWIEDZKA, K., MARTIJN, J., LIND, A.E., VAN EIJK, R., SCHLEPER, C., GUY, L., AND ETTEMA, T.J. (2015). COMPLEX ARCHAEA THAT BRIDGE THE GAP BETWEEN PROKARYOTES AND EUKARYOTES. *NATURE* 521, 173-179.

STEDMAN, K.M., DEYOUNG, M., SAHA, M., SHERMAN, M.B., AND MORAIS, M.C. (2015). STRUCTURAL INSIGHTS INTO THE ARCHITECTURE OF THE HYPERTHERMOPHILIC FUSELLOVIRUS SSV1. *VIROLOGY* 474, 105-109.

STEDMAN, K.M., SCHLEPER, C., RUMPF, E., AND ZILLIG, W. (1999). GENETIC REQUIREMENTS FOR THE FUNCTION OF THE ARCHAEAL VIRUS SSV1 IN SULFOLOBUS SOLFATARICUS: CONSTRUCTION AND TESTING OF VIRAL SHUTTLE VECTORS. *GENETICS* 152, 1397-1405.

STEDMAN, K.M., SHE, Q., PHAN, H., ARNOLD, H.P., HOLZ, I., GARRETT, R.A., AND ZILLIG, W. (2003). RELATIONSHIPS BETWEEN FUSELLOVIRUSES INFECTING THE EXTREMELY THERMOPHILIC ARCHAEON SULFOLOBUS: SSV1 AND SSV2. *RES MICROBIOL* 154, 295-302.

STETTER, K.O. (1999). EXTREMOPHILES AND THEIR ADAPTATION TO HOT ENVIRONMENTS. *FEBS LETT* 452, 22-25.

THAUER, R.K. (2011). ANAEROBIC OXIDATION OF METHANE WITH SULFATE: ON THE REVERSIBILITY OF THE REACTIONS THAT ARE CATALYZED BY ENZYMES ALSO INVOLVED IN METHANOGENESIS FROM CO2. *CURR OPIN MICROBIOL* 14, 292-299.

TRINGE, S.G., VON MERING, C., KOBAYASHI, A., SALAMOV, A.A., CHEN, K., CHANG, H.W., PODAR, M., SHORT, J.M., MATHUR, E.J., DETTER, J.C., BORK, P., HUGENHOLTZ, P., AND RUBIN, E.M. (2005). COMPARATIVE METAGENOMICS OF MICROBIAL COMMUNITIES. *SCIENCE* 308, 554-557.

URBIETA, M.S., RASCOVAN, N., CASTRO, C., REVALE, S., GIAVENO, M.A., VAZQUEZ, M., AND DONATI, E.R. (2014). DRAFT GENOME SEQUENCE OF THE NOVEL THERMOACIDOPHILIC ARCHAEON ACIDIANUS COPAHUENSIS STRAIN ALE1, ISOLATED FROM THE COPAHUE VOLCANIC AREA IN NEUQUEN, ARGENTINA. *GENOME ANNOUNC* 2.

URICH, T., LANZEN, A., STOKKE, R., PEDERSEN, R.B., BAYER, C., THORSETH, I.H., SCHLEPER, C., STEEN, I.H., AND OVREAS, L. (2014). MICROBIAL COMMUNITY STRUCTURE AND FUNCTIONING IN MARINE SEDIMENTS ASSOCIATED WITH DIFFUSE HYDROTHERMAL VENTING ASSESSED BY INTEGRATED META-OMICS. *ENVIRON MICROBIOL* 16, 2699-2710.

VEITH, A., KLINGL, A., ZOLGHADR, B., LAUBER, K., MENTELE, R., LOTTSPEICH, F., RACHEL, R., ALBERS, S.V., AND KLETZIN, A. (2009). ACIDIANUS, SULFOLOBUS AND METALLOSPHAERA SURFACE LAYERS: STRUCTURE, COMPOSITION AND GENE EXPRESSION. *MOL MICROBIOL* 73, 58-72.

VILLANUEVA, L., DAMSTE, J.S., AND SCHOUTEN, S. (2014). A RE-EVALUATION OF THE ARCHAEAL MEMBRANE LIPID BIOSYNTHETIC PATHWAY. *NAT REV MICROBIOL* 12, 438-448.

VOTTELER, J., AND SUNDQUIST, W.I. (2013). VIRUS BUDDING AND THE ESCRT PATHWAY. *CELL HOST MICROBE* 14, 232-241.

WHITAKER, R.J., GROGAN, D.W., AND TAYLOR, J.W. (2003). GEOGRAPHIC BARRIERS ISOLATE ENDEMIC POPULATIONS OF HYPERTHERMOPHILIC ARCHAEA. *SCIENCE* 301, 976-978.

White, J.M., Delos, S.E., Brecher, M., and Schornberg, K. (2008). Structures and mechanisms of viral membrane fusion proteins: multiple variations on a common theme. *Crit Rev Biochem Mol Biol* 43, 189-219.

Wiedenheft, B., Stedman, K., Roberto, F., Willits, D., Gleske, A.K., Zoeller, L., Snyder, J., Douglas, T., and Young, M. (2004). Comparative genomic analysis of hyperthermophilic archaeal Fuselloviridae viruses. *J Virol* 78, 1954-1961.

Woese, C.R., and Fox, G.E. (1977). Phylogenetic structure of the prokaryotic domain: the primary kingdoms. *Proc Natl Acad Sci U S A* 74, 5088-5090.

Woese, C.R., Kandler, O., and Wheelis, M.L. (1990). Towards a natural system of organisms: proposal for the domains Archaea, Bacteria, and Eucarya. *Proc Natl Acad Sci U S A* 87, 4576-4579.

Wood, A.G., Whitman, W.B., and Konisky, J. (1989). Isolation and characterization of an archaebacterial viruslike particle from Methanococcus voltae A3. *J Bacteriol* 171, 93-98.

Xiang, X., Chen, L., Huang, X., Luo, Y., She, Q., and Huang, L. (2005). Sulfolobus tengchongensis spindle-shaped virus STSV1: virus-host interactions and genomic features. *J Virol* 79, 8677-8686.

Yeats, S., Mcwilliam, P., and Zillig, W. (1982). A plasmid in the archaebacterium Sulfolobus acidocaldarius. *EMBO J* 1, 1035-1038.

Zhan, Z., Ouyang, S., Liang, W., Zhang, Z., Liu, Z.J., and Huang, L. (2012). Structural and functional characterization of the C-terminal catalytic domain of SSV1 integrase. *Acta Crystallogr D Biol Crystallogr* 68, 659-670.

Zillig, W., Kletzin, A., Schleper, C., Holz, I., Janekovic, D., Hain, J., Lanzendörfer, M., and Kristjansson, J.K. (1993). Screening for Sulfolobales, their Plasmids and their Viruses in Icelandic Solfataras. *Systematic and Applied Microbiology* 16, 609-628.

Zolghadr, B., Weber, S., Szabo, Z., Driessen, A.J., and Albers, S.V. (2007). Identification of a system required for the functional surface localization of sugar binding proteins with class III signal peptides in Sulfolobus solfataricus. *Mol Microbiol* 64, 795-806.

ACKNOWLEDGMENTS

One jury

I would like to acknowledge the reviewers of my PhD thesis as well as all the other members of my jury for their time, involvement and consideration.

Bosses are like… well, you know…

I wish to thank Patrick Forterre for allowing me to perform my PhD in his laboratory and for being such a knowledgeable and friendly boss. My profund gratitude goes to my PhD directors, Mart and David, for their supervision during the past three years. Thank you for the confidence, support, guidance and freedom in conducting my own projects (based on your ideas of course!).

Ana also has to be acknowledged for her patience, organization and amiability among other marvelous qualities.

Sweet colleagues

My PhD would not have been that pleasant without my great colleagues. Special thanks go to Elena for her expertise that she is always willing to share, for her highly professional behavior in the laboratory, for her particular humor and more importantly friendship and support! I would also like to thank Soizick for teaching me all when I started and for always taking care of our lab. I have to acknowledge my students as well, Guillaume and Lorenzo in particular. Both of them have done a great piece of work carrying projects, mastering techniques, optimizing protocols and providing reliable data; I definitely enjoyed working with these two excellent students. I would also like to thank Virginija who has recently joined our group and wish her the best of luck with the projects. I surely do not forget all the former members of our laboratory from whom it's always a pleasure to have news.

The unit *Biologie Moléculaire du Gène chez les Extrêmophiles* is also a very nice place to work in. I would like to thank all the members, past and present, for their kindness, friendship, advices, support and pleasant atmosphere. In particular, I am really glad for the help I received from Chantal and Estelle which has been highly appreciated and saved me a lot of time through these years.

Fruitful collaborations

On campus, I have to acknowledge the members of the *Ultrapole* and Martin Sachse, in particular, who has dedicated a certain amount of time to teach me electron microscopy. Together, we started collaborating with Petr Chlanda on the assembly and exit of SSV1 which has been a very successful collaboration. During my PhD, I have also had the unique opportunity to visit the laboratory of Dennis Bamford for a few months allowing me to improve my knowledge and acquire relevant skills. I must acknowledge Dennis for our weekly meetings with Hanna Oksanen and Maija Pietila as well as Sari Korhonen, Pälvi Hannuksela and Helvin Veskiväli for excellent technical assistance.

In a few words, it has been a real pleasure to work with all of you. I wish you all the best for the future and hope to hear from you. I have definitely learnt a lot both professionally and

personally. It has been a wonderful experience and although there have been some harsh moments, they were always rewarding and I only keep nice memories. Many thanks to all the people I have met for the last three years, at the Institut Pasteur in Paris, in Helsinki or in Heidelberg.

Meilleure famille au Monde

Pour finir, je tiens à remercier mes parents et l'ensemble de ma famille pour leur affection et leur soutien qui me sont indispensables. Merci à mes parents de m'avoir encouragé jusqu'ici à faire mes propres choix et à suivre mes envies tout en prenant en compte mes responsabilités ; mais aussi pour être parfaits tout simplement.

Un énorme merci à tous mes proches, famille et amis, pour leur amour inconditionnel qui me porte chaque jour !

MEMBERS OF THE JURY

PhD supervised by:

Mart Krupovic, PhD

Unité BMGE – Département de Microbiologie
Institut Pasteur
25, rue du Dr. Roux
75015, Paris
France
mart.krupovic@pasteur.fr

David Prangishvili, PhD

Unité BMGE – Département de Microbiologie
Institut Pasteur
25, rue du Dr. Roux
75015, Paris
France
david.prangishvili@pasteur.fr

PhD thesis reviewed by:

Christa Schleper, PhD

Room: 1.093
Wien, Althanstraße 14 (UZA I)
Austria
christa.schleper@univie.ac.at

Paulo Tavares, PhD

UMR CNRS 2472 INRA 1157
Bât. 14B
1 Avenue de la Terrasse
91198 Gif-sur-Yvette Cedex
France
Paulo.TAVARES@vms.cnrs-gif.fr

PhD thesis examined by:

Claire Geslin, PhD

IUEM
Technopôle Brest-Iroise
29280 Plouzané
France
Claire.Geslin@univ-brest.fr

Jacomine Krijnse-Locker, PhD

Equipe Ultrapôle – Département de Biologie Structurale
Institut Pasteur
28, rue du Dr. Roux
75015, Paris
France
jacomine.krinjse-locker@pasteur.fr

President of the PhD committee:

Guennadi Sezonov, PhD

Cassan, bâtiment A, étage 2, porte 222
Case courrier 5
7 quai Saint Bernard
75 252 PARIS CEDEX
France
guennadi.sezonov@upmc.fr